University of Southampton

Faculty of Engineering

School of Engineering Science

Doctor of Philosophy

# Pressure Distribution Beneath the Foot in Sideslope Walking

by Stephen Robert Urry

Pressure Distribution beneath the Foot in Sideslope Walking

Abstract

Dynamic loading profiles beneath the human foot during sideslope walking were determined and differences to level walking established. The contact area of the foot was measured, and the arch index derived from the footprint. Thirty healthy adults walked on a tiltable walkway which had a polymer sensor pressure platform mounted at the mid-point. The sideways tilt could be adjusted in 2° increments from level to 8°. By walking in both directions on the sideslope, volunteers placed their right foot in either the upslope or downslope position. Loading profiles and contact areas were recorded for upslope and downslope foot placements at each angle of tilt.

The characteristics of the electrically resistive polymer sensors were determined prior to the walking trials. The sensor output was non-linear, mean within-sensor variation ≈3% (maximum 8%), mean hysteresis ≈9% (maximum 13%), pressure threshold sensitivity ≈35 kPa, and mean between-sensor variation ≈8% (maximum 18%) over the surface of the platform. The dynamic behaviour was reliable to 26Hz. The sensor was found to be sensitive to shear. The impact of this characteristic was assessed by comparison with a similar platform incorporating capacitive transducers that were not shear sensitive. The polymer sensor system indicated increased pressures beneath the heel with upslope foot placement, and similar increases beneath the central metatarsals with downslope placement. These features were not apparent in the profiles returned by the second platform. For both platforms, however, the first metatarsal showed increased pressures with downslope placement but decreased pressures with upslope placement. In addition, the initial contact time and duration of loading for the first metatarsal altered significantly. The contact area of the foot changed systematically with sideslope walking, such that the arch index increased with upslope placement and decreased with downslope placement.

This study demonstrated that the conventional approach of assessing level walking would fail to identify the increased foot pressures that occur on sideslopes. This may have crucial implications for ulceration risk assessment. The systematic changes in arch index and first metatarsal loading indicate that sideslope walking might be beneficial in revealing aspects of the mechanical behaviour of the human foot if combined with a simultaneous kinematic analysis. Potentially, the method offers a new approach to assessing the functional capacity of the foot for both clinical and research purposes.

## Acknowledgements

I wish to thank my two supervisors for their patient support. First, Professor John Turner, who encouraged me to start, second, but with equal gratitude, Professor John McBride, who persuaded me to finish. Slightly before either of them, Professor Lindsay McLellan convinced me that Southampton University was the right place for me, thank you. All of the technicians in the Engineering Faculty were helpful, and I thank them and their team leader Bob Peach. Special thanks, however, go to Peter Wheeler, who obtained it for me when I needed it, fixed it if it broke, and always had a contact when he couldn't provide the solution himself. Martyn Hill helped tidy up loose ends in the closing stages.

Thanks to my colleagues, especially Lloyd Reed for giving me marvellous feedback and being an enduring source of enthusiasm, and Scott Wearing for tricking me back into the fray and then being the most tenaciously constructive critic ever. Thanks also to Dr Diana Battistutta, who somehow enabled me to handle the statistical analyses.

For the production of the thesis, and for the conference presentations, I had the nicest support team anyone could hope for. Pam Koger, presentation whiz, Vivienne Wilson, great graphics, Sonja DeSterke, the best photographer ever. Ian Hutson generated the amazing images of the sensors. Thank you all.

Thanks go also to my close friends for their support, encouragement and favours, in times good and bad. Dr Alan Borthwick, Chris and Jo Griffith, Judy Legon, Nick Graffy, Dr Fiona Wylie, Lisa Simms, Hugh and Carolyn Peterken, Dr Russ Sion, Lalitaratna and Siddhartha Gautama. My younger sister lost her kitchen table while I wrote my literature review but still fed me, thanks Jackie. My mother and father gave me opportunities they never had, thank you Stella and Bob.

Last, but certainly not least, thanks to Annette, my wife, staunch supporter and loyal friend. This is for you, with all my love.

# CONTENTS

## TABLES

## FIGURES

## Glossary

**Abduction**: movement of the foot, parallel with the transverse plane, such that the distal end moves away from the midline of the body.

**Adduction**: movement of the foot, parallel with the transverse plane, such that the distal end moves towards the midline of the body.

**Ankle**: the anatomical region at the junction between the foot and leg. Used specifically, it sometimes refers to the talo-crural joint. Some authors use it to refer to both the talo-crural (upper ankle)joint and or the subtalar (lower ankle) joint.

**Arch index (AI)**: a geometrically derived parameter indicating the proportion of the contact area that is made up by the midfoot region of a footprint.

**Cadence**: the number of steps taken per minute.

**Calcaneo-cuboid**: the articulation between the calcaneum and the cuboid bones (see diagram of foot skeleton).

**Calcaneum**: the heel bone (see diagram of foot skeleton).

**Centre of pressure (CoP)**: the point beneath the foot where the ground reaction force acts, and about which the sum of the moments equals zero.

$C_{max}$: the maximum count method used to derive contact area of the foot (each peripheral element of the footprint was counted as contributing its full area to the sum total).

**Coefficient of variation (cv)**: an indicator of variability derived as the division of the standard deviation by the mean. It has the advantage of being unit-less.

**Compensation**: an adjustment by one part of the body for a change in position, structure or function at another part of the body.

**Contact duration (CD, or Dur)**: the period of time that a region of the foot is in contact with the weight bearing surface.

**Cuboid**: a bone of the tarsus (see diagram of foot skeleton).

**Cuneiform**: a bone of the tarsus (see diagram of foot skeleton).

$C_{wt}$: the weighted count method used to derive contact area of the foot (each peripheral element of the footprint was counted as contributing half its area to the sum total).

**Distal**: towards the peripheries of the body (toes, fingers, head).

**Dorsiflexion**: movement of the foot, parallel with the sagittal plane, such that the toes and sole move up towards the leg, or a similar movement by a part of the foot.

**Downslope**: when the weight bearing foot, during sideslope walking, is lower on the sideslope than the non-weight bearing foot.

**Eccentric contraction**: muscle contraction with lengthening.

**Electromyography**: technique used to investigate muscle function the basis of the electrical activity of the muscle.

**Eversion**: movement of the foot or a part of the foot, parallel with the frontal plane, such that the sole moves to face away from the midline of the body (see figure 1.7).

**Extensor digitorum longus**: a muscle in the anterior compartment of the leg that acts to produce relative dorsiflexion of the toes and or foot.

**External rotation**: a rotation about the longitudinal (vertical) axis of the limb or leg such that the forefoot would move away from the midline of the body.

**Flexor digitorum longus**: a muscle in the posterior compartment of the leg that acts to produce relative flexion of the toes and or foot.

**Foot contact area (FCA)**: the contact area of the foot excluding the toes.

**Foot placement angle**: synonymous with foot progression angle (FPA).

**Foot progression angle (FPA)**: the angle formed between a long axis of the foot, commonly the midline, and the line of progression in walking.

**Foot tilt strategy**: a sideways tilting strategy by the foot to assist with the control of balance. The tilt occurs predominantly at the subtalar joint in the rearfoot.

**Force sensing resistor (FSR)**: polymer sensors that demonstrate a decrease in electrical resistance when subjected to physical pressure.

**Forefoot**: the anterior part of the foot, usually considered to comprise of the metatarsals and toes (see diagram of foot skeleton).

**Frontal plane**: an imaginary plane, used to aid anatomical descriptions, that divides the body, or body part, into anterior and posterior portions.

**FTI**: the force time integral (impulse).

**Full scale output (FSO)**: The maximum output amplitude demonstrated by a sensor when fully loaded.

**Gait angle (angle of gait)**: the angle formed by the long axis of the foot and the line of progression during walking (see foot placement angle, FPA).

**Gait cycle**: the repetitive cycle of events that occurs during walking. It is comprised of a swing phase and a stance phase.

**General linear model (GLM)**: a statistical model in which the equations connecting the variates or variables are in a linear form.

**Hallux**: the first, or big toe.

**Hallux valgus**: a foot deformity where the hallux deviates towards the lesser toes.

**Heel**: the posterior part of the foot.

**Hl**: heel.

**Initial contact time (ICT)**: the instant a which a part of the foot, or foot site, is registered as contacting the supporting surface. It is expressed as a percentage of the stance phase time.

**Internal rotation**: a rotation about the longitudinal (vertical) axis of the limb or leg such that the forefoot would tend to move towards the midline of the body.

**In-toe (toe-in)**: a walking style where the foot is angled so that the toes point in from the midline of the body.

**Inversion**: movement of the foot or a part of the foot, parallel to the frontal plane, such that the sole moves to face towards the midline of the body (see figure 1.6).

**Kinematic**: a method of describing function in terms of displacement, velocity or acceleration without reference to associated forces.

**Kinetic**: a method of describing function in terms of forces without reference to any associated displacement, velocity or acceleration.

**Lateral**: to the side or edge of the body, or body part.

**Lateral arch**: the arch of the outer (lateral) side of the foot, comprised of the calcaneum, cuboid and fourth and fifth metatarsals (see diagram of foot skeleton).

**Lattice template**: a paper template printed with a grid, or lattice, pattern that was dimensionally identical to the polymer array of the pressure platform.

**Longitudinal arch**: the arch of the inner (medial) side of the foot, comprised of the calcaneum, navicular, cuneiforms, and first, second and third metatarsals (see diagram of foot skeleton).

**M1**: first metatarsal, the metatarsal at the medial side of the foot.

**M5**: fifth metatarsal, the metatarsal at the lateral side of the foot.

**Mask**: a geometric outline superimposed on a footprint to define and separate an area or areas of interest.

**Maximum-count**: the maximum count method used to derive contact area of the foot (each peripheral element of the footprint was counted as contributing its full area to the sum total).

**Mc**: the central metatarsal site, comprised of metatarsals two, three and four.

**MdFt**: the middle part of the foot, often defined as the central third of the footprint (excluding the toes).

**Medial**: the middle of the body, or body part. It is also used to refer to the side of the foot that is closest to the midline of the body.

**Medial arch**: the arch of the inner (medial) side of the foot, comprised of the calcaneum, talus, navicular, cuneiforms and metatarsals one, two and three (see diagram of foot skeleton).

**Medialisation**: redistribution of load towards the medial side of the foot, can occur with and increase in walking speed.

**Metatarsal**: one of five long bones in the forefoot (see diagram of foot skeleton).

**Midfoot**: the middle part of the foot, often defined as the central third of the footprint (excluding the toes).

**Mid-gait method**: method of acquiring foot pressure data when a constant walking speed is reached, thereby avoiding the acceleration and deceleration phases.

**Navicular**: a bone of the tarsus (see diagram of foot skeleton).

**Osteoligamentous**: ligamentous attachment between two or more bones (osteo).

**Out-toe (toe-out)**: a walking style where the foot is angled so that the toes point away from the midline of the body.

**Pascal (Pa)**: The preferred unit for the measurement of foot pressure ($Pa=Nm^{-2}$). Generally expressed as kilopascals (kPa).

**Pathology**: a disease state.

**Peripheral element ratio (PER)**: the relative number of peripheral elements observed in either an electronic footprint, or an ink footprint on a latticed template.

**Peroneus longus**: a muscle in the lateral compartment of the leg that acts to produce relative eversion of the foot. It crosses the sole of the foot beneath the cuboid and attaches to the base of the first metatarsal.

**Plantar**: pertaining to the sole.

**Plantarflexion**: movement of the foot such that the toes and sole move down away from the leg, or a similar movement by a part of the foot.

**Pronation**: a tri-planar movement comprising of simultaneous eversion, abduction and dorsiflexion. Used by some authors interchangeably with eversion (see figure 1.7).

**Proximal**: towards the centre of the body.

**PTI**: pressure time integral.

**Rearfoot**: used to identify the posterior part of the foot, particularly the talus and calcaneum, or the posterior third of the footprint image (see diagram of foot skeleton).

**Sagittal plane**: an imaginary plane, used to aid anatomical descriptions, that divides the body, or body part, into right and left portions.

**Stance phase**: the period of time in the gait cycle when the foot has some contact with the underlying surface.

**Subtalar**: the joint complex linking the talus and calcaneum, and facilitating foot tilt, pronation-supination, inversion-eversion movements.

**Supination**: a tri-planar movement comprising of simultaneous inversion, adduction and plantarflexion. Used by some authors interchangeably with inversion (see figure 1.6).

**Swing phase**: the period of time in the gait cycle when the foot has no contact with the underlying surface and is swinging forwards.

**T1**: toe 1, or the hallux.

**Talo-calcaneal**: the articulation between the talus and the calcaneum, effectively the subtalar joint (see figure 1.5).

**Talo-crural**: the articulation between the talus and the leg bones (tibia and fibula).

**Talo-navicular** the articulation between the talus and the navicular bones (see diagram of foot skeleton).

**Talus**: a bone of the tarsus (see diagram of foot skeleton).

**Tarsal mechanism**: the coupling mechanism in the tarsus that transmits transverse plane rotations of the leg to frontal plane rotations in the foot.

**Tarsus**: the irregular bones of the rearfoot and midfoot (talus, calcaneum, cuboid, navicular, cuneiforms).

**Tibialis posterior**: a muscle in the posterior compartment of the leg that acts to produce relative inversion of the foot. It crosses the sole of the foot beneath the medial arch and attaches to the bones of the tarsus, excluding the talus. A crucial muscle for maintaining the integrity of the medial longitudinal arch.

**Time to peak force (TPF)**: the time at which the force profile peaks, expressed as a percentage of the stance phase.

**Time to peak pressure (TPP)**: the time at which the pressure profile peaks, expressed as a percentage of the stance phase.

**Transverse plane**: an imaginary plane, used to aid anatomical descriptions, that divides the body, or body part, into upper and lower portions.

**Triplanar**: pertaining to the three body planes simultaneously. A triplanar joint axis is angled to all three body planes.

**Ulcer**: an open wound or break in the skin, usually associated with delayed healing - relatively common on weight bearing sites of the feet of individuals with diabetes or similar diseases causing poor tissue vitality.

**Upslope**: when the weight bearing foot, during sideslope walking, is higher on the sideslope than the non-weight bearing foot.

**Weighted-count**: the weighted count method used to derive contact area of the foot (each peripheral element of the footprint was counted as contributing half its area to the sum total).

**Bones of the foot**

(shown without the toes)

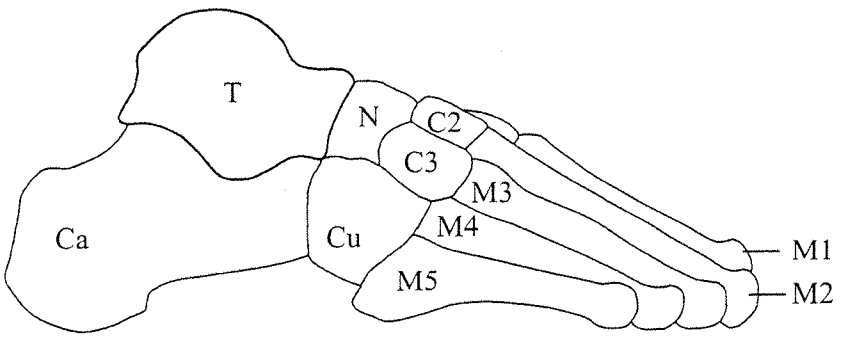


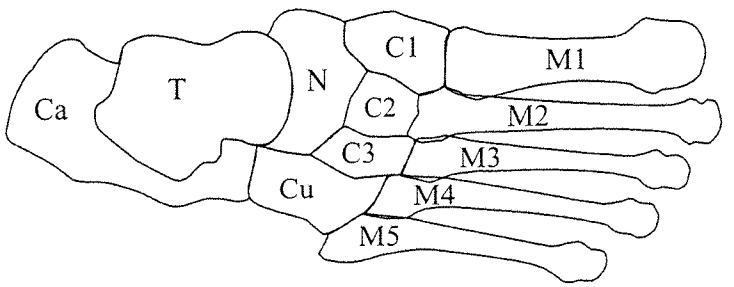


| | | | |
|---|---|---|---|
| Ca | calcaneum | T | talus |
| N | navicular | Cu | cuboid |
| C1 | medial cuneiform | C2 | intermediate cuneiform |
| C3 | lateral cuneiform | M | metatarsal (1 to 5) |

**Axes of the joints of the foot**

Schematic representation of principal joint axes referred to in the text.

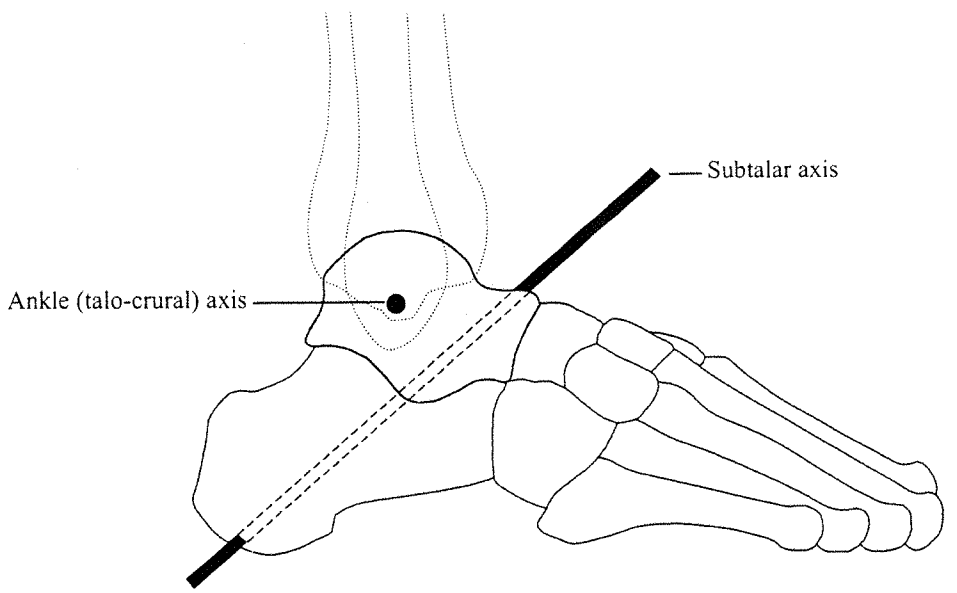


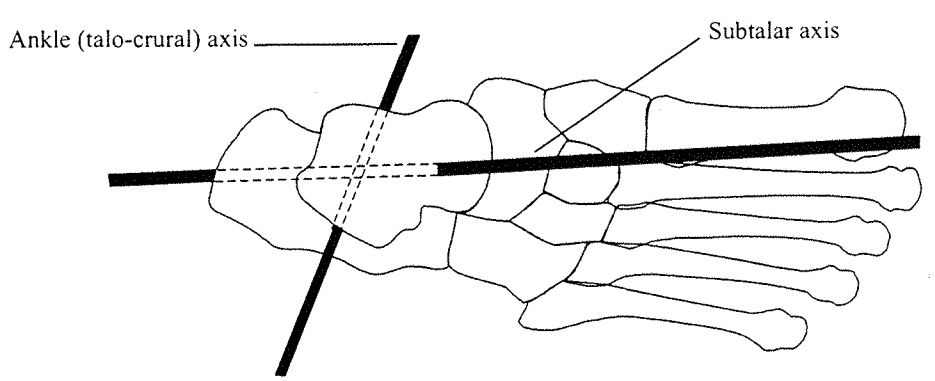

# 1. Introduction

'It has been emphasised that function is the key word which must be understood and fully appreciated whenever we examine a patient with a foot problem, and that the primary function of the foot is locomotion. Therefore, in the examination of the foot by pressure measurement, dynamic measurements taken during walking have a rightfully prominent place. Where the function of the foot is disturbed by disease or trauma, then this can be expected to reflect in abnormal pressure during gait.'

This quotation, from a 1986 review by Lord *et al.* [1], reflects a commonly held expectation that there may be some discernible relationship between foot function and load distribution under the sole. If the mechanisms underlying such a relationship could be clarified then dynamic pressure analysis might become a useful tool for the clinical assessment of feet. Despite considerable advances over the last fifty years however, a predominant relationship has yet to be identified. Indeed, one recent substantial study revealed that combined analysis of both structural and functional characteristics of the foot could at best account for only approximately fifty percent of the variance in peak pressure across the sole [2]. These findings indicate clearly that there are additional factors yet to be explored. Investigations of foot pressure are generally limited to level walking[3,4] but this constraint might exclude potentially useful information that may only be apparent with other activities. Since level walking is relatively undemanding of foot function, it may produce loading profiles that are restricted or attenuated, making a relationship between function and loading difficult to discern. By depicting aspects of the loading profile that may be latent during level walking, a more complete description could be achieved and this may facilitate a clearer understanding of the weightbearing activities of the foot.

This study adopted the novel approach of investigating load distribution associated with walking on a sideslope. Loading profiles were measured beneath discrete regions of the feet of healthy adults while they walked on an inclined walkway, figure 1.1. Loading profiles for level walking were obtained for comparison. The intention was to detect and quantify significant differences

between level and sideslope loading profiles. No previous study of the distribution of load beneath the foot for sideslope walking could be found in the literature, although a few studies have investigated foot pressures with both uphill and downhill walking[5-8]. The findings from these studies have been inconsistent, but typically they have demonstrated minimal alterations in the loading profiles. While the inconsistent findings casts some doubt on their reliability, and this is worsened by the overall paucity of effect, it should not be concluded that walking on all inclined surfaces will have insignificant effects on foot loading. On the contrary, it may be argued that up or downhill walking is not representative of sideslope walking, and that the findings of the former are not applicable to the latter. Perhaps the most pertinent evidence in support of this argument lies in the anatomical mechanisms that endow the foot with its capacity for movement.

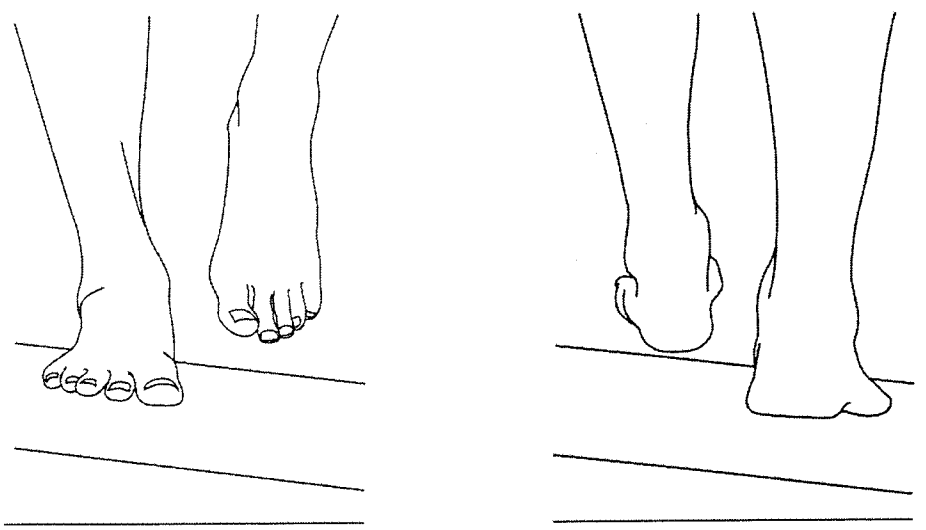


**Figure 1:1 Sideslope walking**

The positions of the weight bearing foot as referred to in the text. Upslope position (a), and downslope position (b).

While the functional capability of the foot has not been completely documented in the literature, there is a consensus of opinion that it has a well developed capacity for tilting. With the foot firmly planted on the ground, the leg can be

inclined either forwards or backwards. The forward-backward motion occurs primarily at the ankle, or talo-crural joint, and the leg leans through the sagittal plane, figure 1.2a. Similarly, the leg can be inclined sideways over the weight bearing foot, with motion occurring at the subtalar joint while the leg is displaced through the frontal plane[9], figure 1.2b. These tilting actions usually occur as part of an overall change in body posture and are associated with activities such as standing, leaning or walking. Tilting of the foot also occurs when uneven or sloping terrain is encountered. Walking uphill on a gradient, the leg leans forwards so that dynamic balance is least compromised[10]. With downhill walking, the leg may lean either forwards or backwards relative to the weight bearing foot, depending on whether an acceleration or deceleration strategy of descent is adopted[6], figure 1.3. Similarly, when a sideslope is encountered the leg leans sideways relative to the supporting foot to assist the maintenance of balance, figure 1.4. While the principle of foot-tilt is fundamentally the same, regardless of whether it occurs in response to a postural demand from the body or an environmental demand from the surface, there are substantial differences between the sagittal and frontal plane tilt mechanisms.

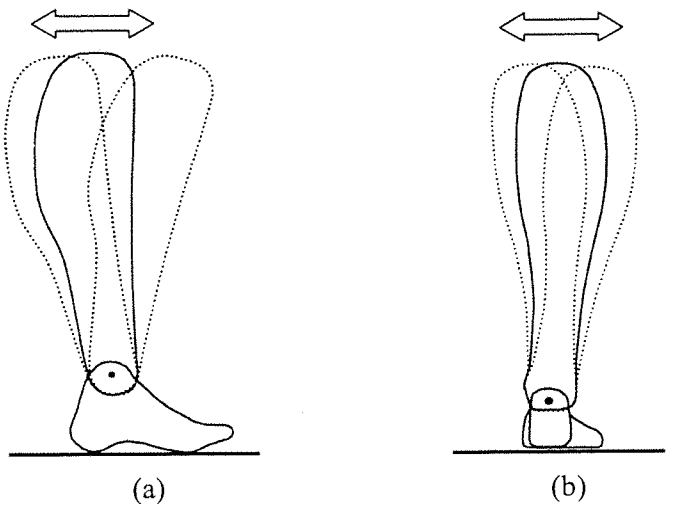


**Figure 1:2 Tilting of the leg on a level surface**

Forward and backward tilting of the leg occurs at the ankle and facilitates motion in the sagittal plane (a). Sideways tilting occurs at the subtalar joint and facilitates frontal plane motion (b).

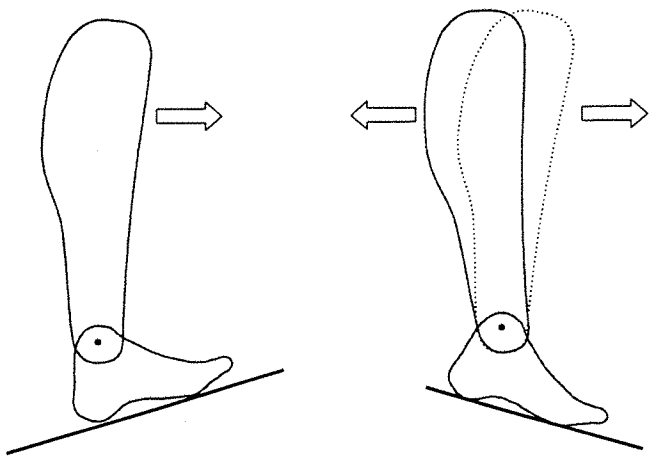

**Figure 1:3 Sagittal plane adjustments on inclined surfaces**

Walking uphill the leg leans forward over the foot to assist balance. Walking downhill the inclination of the leg is adjusted to help control the rate of descent

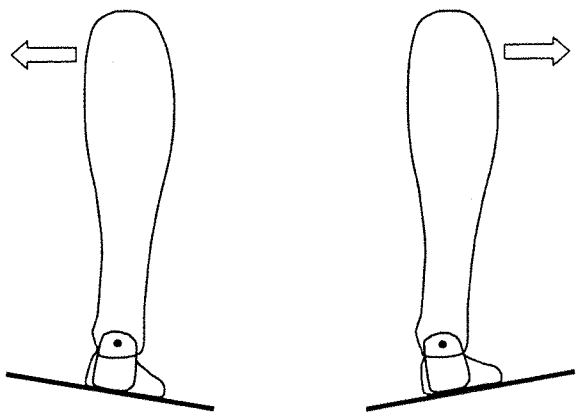

**Figure 1:4 Frontal plane adjustments on inclined surfaces**

Walking on a sideslope the leg leans over the foot to assist balance.

Sideways tilting through the frontal plane occurs primarily at the subtalar (talo-calcaneal) joint. Anatomically, this joint is directly linked with the talo-navicular and calcaneo-cuboid articulations, and together they form a major functional component of the foot, the tarsal mechanism [11-13], figure 1.5.

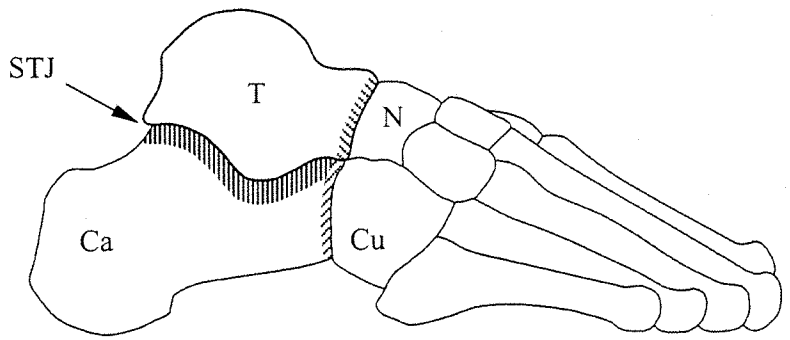


**Figure 1:5 Tarsal mechanism**

Relative movement between the talus (T) and the calcaneus (Ca), occurring at the subtalar joint (STJ), causes displacement of the navicular (N) and the cuboid (Cu). In the weight bearing foot, close mechanical coupling through the tarsal mechanism (shaded) ensures that a reorientation of all four bones occurs simultaneously.

When weight bearing, frontal plane tilting of the heel is accompanied by a simultaneous change in the medial long arch of the foot as a result of the closed kinematic chain function of the tarsal mechanism. When the heel inverts then the arch height increases, and when the heel everts the arch lowers, figures 1.6 and 1.7. Because of these alterations in arch height, the first metatarsal must simultaneously either depress or elevate if the forefoot is to maintain its contact with the underlying surface, figures 1.6 and 1.7. Frontal plane foot tilt is therefore accompanied by a marked realignment of the bones of the foot because of the direct mechanical coupling between the heel and the midfoot. Sagittal plane adjustments, in contrast, can occur without substantial transmission of motion to the tarsal mechanism[14]. This is because the adjustments occur at the periphery of the foot, where the leg articulates with the talus, rather than deeply within the structure of the foot, figure 1.8. Since the coupling mechanism directly involves only one foot bone, motion does not have to be transmitted through the foot as is the case with frontal plane tilt.

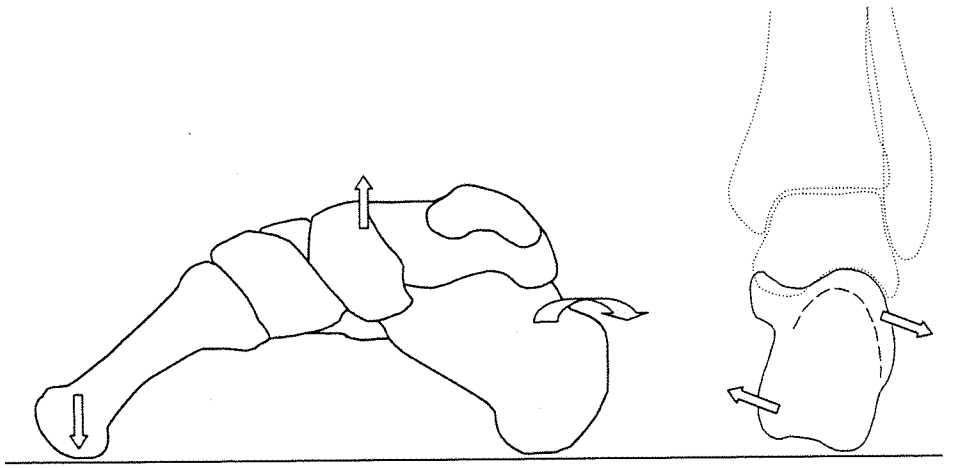

**Figure 1:6 Heel inversion and arch elevation**

When the heel inverts, closed kinematic chain function of the tarsal mechanism necessitates relative plantarflexion (depression) of the first metatarsal if ground contact is to be maintained beneath the forefoot.

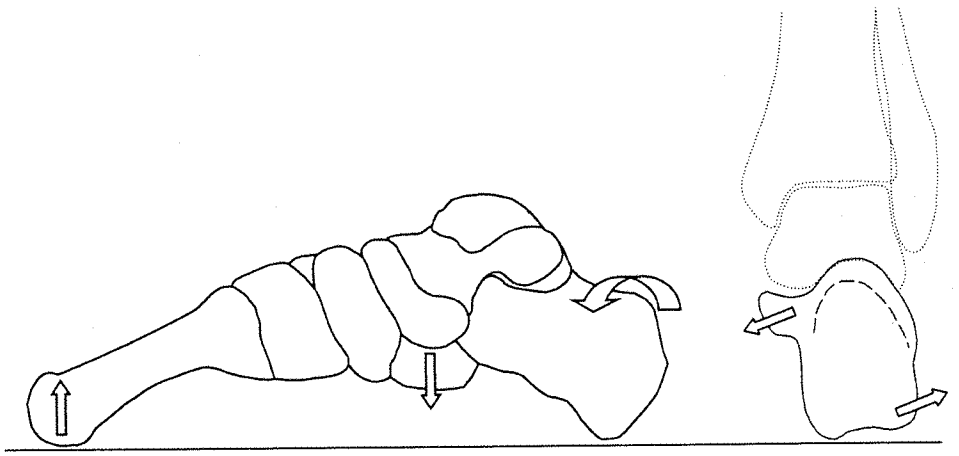

**Figure 1:7 Heel eversion and arch depression**

When the heel everts, closed kinematic chain function of the tarsal mechanism necessitates relative dorsiflexion (elevation) of the first metatarsal if ground contact is to be maintained beneath the forefoot.

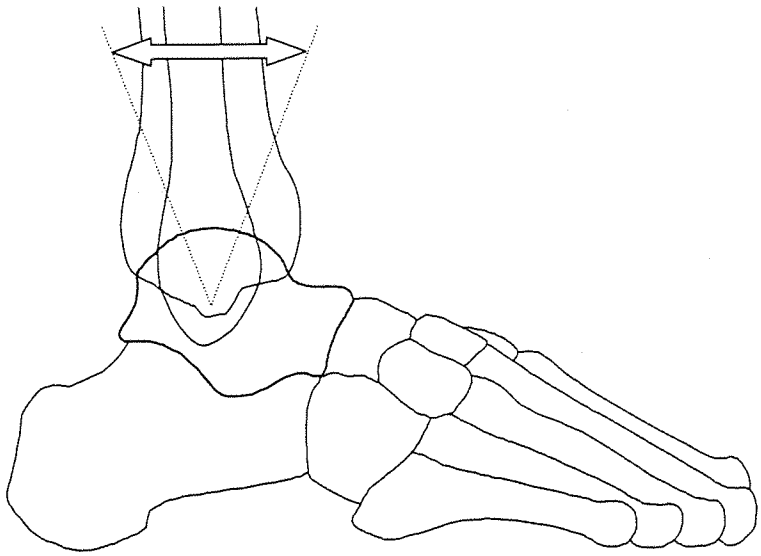

**Figure 1:8 Sagittal plane tilt mechanism**

Sagittal plane adjustments occur mainly at the talocrural articulation of the ankle. The leg rotates about an articulation that is at the periphery of the foot, and there is minimal transmission of motion through the bones of the foot.

While the two tilt mechanisms clearly facilitate different actions they are not entirely independent[12]. Furthermore, neither mechanism is purely uniplanar, rather both are triplanar, and small amounts of movement will always occur simultaneously in the three anatomical planes[12]. However, the clinical significance of the frontal plane component of foot tilt is considered to be particularly important. Abnormal frontal plane tilting has been cited as a key factor in many foot disorders because unrestrained motion of the tarsal mechanism is believed to be a cause of structural instability of the foot[15]. For this reason many of the kinematic studies of foot motion have focused their attention on frontal plane tilt. However, comparatively few kinetic studies have measured loading of the tilted foot and all of these, without exception, have investigated sagittal plane tilting only[5-8, 16-19]. Therefore, the prominence given to frontal plane function in kinematic studies is not reflected in kinetic studies and this inequality should be redressed.

While the functional anatomy of the foot indicates that frontal plane tilting could cause redistribution of load, certain incidental studies point to the same conclusion. When the weight bearing foot is tilted sideways, large, rapid displacements of the centre of pressure occur indicating a simultaneous redistribution of load [20]. Furthermore, the possibility of a relationship between foot tilt and load redistribution was raised in an early investigation using cadaver limbs[21]. Alterations of metatarsal load were found to occur when amputated legs were tilted under load. The effect was observed to be more striking when the leg was tilted sideways than when it was angled either forwards or backwards. The redistribution of load was attributed wholly to the architecture of the bones and ligaments of the foot and ankle because no tension had been applied to the dissected tendons of the legs while they were being tilted. At the time, it was conjectured that the bony adjustments of the foot that enabled the leg to tilt would occur while walking on uneven terrain, and would bring about a redistribution load. The indirect evidence from these incidental studies supports the idea of load redistribution with sideways tilt. In addition, a predominant influence by frontal plane tilting could account for the generally insignificant findings reported from foot loading studies of sagittal plane tilting.

While previous studies have already demonstrated that feet adjust to sideslope walking by tilting[22,23], and the primary objective of this investigation was the measurement of the loading profiles, additional signs of adaptation by the foot were sought. Assessment of the motion of the joints of the foot is particularly problematic because the bones are small and irregularly shaped. In fact, the compact and complex anatomical structure that endows the foot with its remarkable versatility also presents the greatest challenge to quantitative analysis of intrinsic adjustments. The use of surface mounted markers or electrogoniometers for kinematic analysis has been questioned because of the likelihood of unrepresentative motion of the soft tissues[24]. Footprint analysis was selected as an alternative approach because, in the opinion of some investigators, footprint parameters such as the arch index may be indicators of arch height or foot function[25-29]. If the tarsal mechanism enables the foot to adjust for sideslope walking, then the arch height or shape may alter and subsequent changes should be apparent in the footprint. Since electronic images

of the foot contact area are easily obtained from pressure platforms, this approach is particularly advantageous for this study. Footprints for both level and sideslope walking were therefore analysed. The footprints were also used to determine the foot progression angle, or angle of gait, which is the relative in-toe or out-toe attitude of the weight bearing foot. Changes in the foot progression angle may give some indication of gait alterations that are necessary to facilitate sideslope walking. As a prerequisite to the main study it was therefore necessary to determine the accuracy of the footprint images produced by the pressure platform and to establish the factors that influenced them.

The need to obtain acceptable images of the footprint indicated that a foot pressure platform with high spatial resolution be used to measure the loading profiles beneath the sole of the foot. Instrumented insoles were considered as an alternative method of measurement but they were rejected because they would have imposed the need to wear shoes and could have confounded the findings[30]. Furthermore, in-shoe pressure measurement is technically more demanding than pressure measurement on a flat surface, and this potentially increases both measurement error and the risk of device failure[31]. The pressure platform was large enough to capture an impression of the entire foot without the need for overt targeting, and thereby minimised any potential disruption of the natural walking style. Monitoring the entire contact area of the sole of the foot was important because it removed the need, prior to the study, for any decision to identify anatomical regions most likely to demonstrate significant changes in loading. The detailed footprint images from the pressure platform were subdivided graphically - a process known as masking - to facilitate a regional analysis of the distribution of foot load, figure 1.9. For a single step, the maximum value returned by an individual sensor within a region was identified, recorded, and referred to as the peak pressure for that site, figure 1.9. While elevated pressures contribute to ulcer formation[32,33] and pressure is therefore worthy of measurement, it is influenced by additional factors such as bony protuberances[2] and as a result does not necessarily reflect the magnitude of load experienced at a foot site. Regional ground reaction forces, in contrast to pressures, give more insight into the mechanical function of the foot[34], and are known to be significantly altered with abnormal foot function[35,36] and fatigue[37].

Estimates of regional force were therefore obtained to complement the pressure data. They were derived by summing the individual values returned by all of the sensors within a region, figure 1.9.

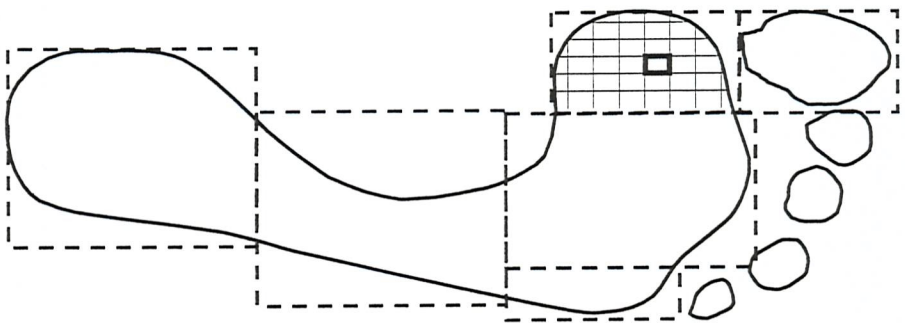

**Figure 1:9 Footprint mask for regional analysis of load**

The footprint was masked to give six sites for the regional analysis of load distribution. Local force was derived from the sum of the values returned by all sensors within a site (latticed example for first metatarsal site). Local peak pressure was identified as the maximum value returned from a single sensor element within a site (bold example for first metatarsal site).

Regional forces cannot be measured directly from pressure platforms and must be estimated on the assumption that the distribution of load over the active surface of individual sensors is uniform[38]. This assumption is necessary because the transducers used in contemporary pressure platforms are sensitive to magnitude of force and area of contact, independently[39,40]. Thus, if a force is unevenly or only partially distributed over the active surface of a sensor, then the output of that sensor will deviate from the expected or calibrated value. Despite the compromise imposed by force estimation, the pressure platform provided the best combination of features for the purpose of measuring the selected spatial and temporal parameters.

The performance of the polymer sensor array in the pressure platform had not been reported previously, although the characteristics of individual sensors of similar design and construction were known[39-49]. Therefore, the performance of the transducer array was determined prior to the study of sideslope walking. Sensor elements were tested in order to determine their response to static and

dynamic loading conditions. Two test rigs were designed and constructed for the purposes of the tests. The main rig could be configured to allow either static loading with calibrated weights, or dynamic loading via an elctromechanical shaker. The second rig allowed a shear force to be applied concurrent with vertical load. Through these tests, the ability of each sensor to repeatedly measure a known input - the within sensor repeatability - was to be determined, as was the variation in sensor performance over the surface of the platform. The pressure threshold, full-scale measurement range, hysteresis, dynamic fidelity and sensitivity to shear were also to be established. A second pressure platform, using alternative sensor technology, was subsequently acquired for comparison so that the practical implications of the sensor characteristics could be evaluated.

An investigation of foot loading during sideslope walking serves several purposes. First, it addresses a substantial omission in the literature. Second, it brings kinetic studies of foot loading into alignment with both kinematic studies of foot function and aspects of contemporary clinical thinking. In addition, knowledge of pressure redistribution provides information of immediate and direct clinical significance. High pressure is a recognised factor in the initiation and progression of foot ulceration[32,33], particularly when associated with diabetes. Ulceration may lead to gangrene amputation and, in some cases, death[50]. The cost in both personal terms and to the health care system is substantial. To minimise risk, foot pressures are routinely screened. Conventionally, however, screening assesses level walking, and could fail to identify latent high pressures that may manifest only during sideslope walking. This investigation aimed to return the first estimates of such pressure changes so as to determine whether a reassessment of the current situation regarding issues of risk is necessary. Overall, the study addresses several issues of immediate concern while establishing a fresh direction for new research. Potentially, this approach may offer a way for overcoming the problems associated with current techniques for the clinical assessment of the mechanical function of the foot[51].

## 1.1. Aims of the investigation

- To determine the characteristics of individual elements of the polymer array of the main pressure platform and compare them with those established previously for discrete polymer sensors.
- To determine the accuracy of contact area measurements derived from footprints obtained with the pressure platform, and to identify factors influencing the measurement of contact area.
- To determine the level of similarity between the arch index parameter as derived from ink and electronic footprints.
- To establish a method for the investigation of foot loading during sideslope walking that may be incorporated into subsequent kinematic studies, or investigations of foot pathology.

### 1.1.1. Hypotheses of the investigation

The contact area of the sole of the foot in sideslope walking will differ from that in level walking, and differences will be reflected in the arch index parameter.
The distribution of load beneath the foot during sideslope walking will differ to that beneath the foot during level walking.
Changes in both the contact area and the distribution of load will be systematic with the angle of the sideslope.
Redistribution of load with sideslope walking will be dependent on anatomical site.

# 2. Literature Review

## 2.1. Introduction

This chapter reviews literature relevant to the overall investigation. Initially, an overview of previous studies of gait on non-level (inclined) surfaces is given. Because this work is not extensive, additional literature regarding the tilting function of the foot in standing and walking is reviewed. This emphasises the importance of foot tilt for the maintenance of balance and posture, and the simultaneous internal readjustments that are likely to accompany sideways tilting. Data collection protocols, along with factors that might influence the quality of the collected data, are then appraised. This is followed by a synopsis of the key measurement variables, indicating the relevance of the variables along with the values reported by previous investigators. Finally, a review of the relevant types of equipment is given, identifying the performance strengths and weaknesses of the various devices. Polymer sensors are reviewed in detail towards the end of the chapter.

## 2.2. Locomotor function on inclined surfaces

There is little information relating to standing or walking on slopes, gradients or cambers in the previously published literature. In total sixteen reports were located, fourteen of which relate to standing or walking on uphill or downhill gradients and three describe sideslope activities. Analyses of up and downhill walking are, in effect, investigations into sagittal plane behaviour [10]. Of the fourteen, four report on kinematic changes [10,18,19,52] three on muscle activity as revealed by electromyography [53,54], four give estimates of ground reaction force [16-19], four measured foot pressures [5-8], and one was limited to an analysis of standing and lifting [56]. Three papers report investigations of gait on a sideslope or camber [22,23,57]. These undertook kinematic rather than kinetic analyses. Only two papers report any findings concerning foot function [22,23]on a sideslope. One was limited by the size of the subject population [22]. The second, while primarily intended as an investigation of post-operative function, quantified the compensatory behaviour of normal feet in sideslope walking [13].

### 2.2.1. Locomotor function on uphill and downhill inclines

Walking up or downhill has been shown to influence the patterns of joint motion, the associated activity of the lower limb muscles, the components of the ground reaction force, and the foot pressures. There are some conflicting results but this may be due to the limited size of investigations and the variety of methods that have been employed. There is, however, general agreement that subjects adopt accommodative walking styles and that the compensatory joint motions are most substantial in the sagittal plane [10], indicating that joint adjustments occur in line with the slope. No compensations in the transverse plane have been demonstrated [10] but it has been revealed that subjects commonly lean backwards and shorten their step length when walking downhill [10,52]. This strategy results in a decrease in the forward-backward shear component of the ground reaction force and is thought to reduce the increased friction demand, thereby minimising the risk of slipping [52,16]. When walking uphill, subjects seemed to shorten their step length and reduce their cadence, the combined effect of which was a reduction in their walking speed [52,17]. Significant phasic changes in muscle activity have been shown to occur [53] on uphill slopes over 6° and downhill slopes over 3°, demonstrating considerable postural sensitivity to small changes. It was suggested that the altered muscle behaviour increased the stability of the ankle and knee joints [53], improved the precision of the control of the distal segments [54], and provided additional power to raise [53,54], or lower [53], the body. Further, when walking downhill, increased activity of the intrinsic muscles of the foot may have reduced its sagittal plane compliance so that it could act as a rigid segment to counteract the moment about the ankle joint created by the accelerating body [55].

The reported effects on foot pressure when walking up or downhill are inconclusive. Kastenbauer *et al.* [5], investigated peak pressures for diabetic patients and a normal control group, and found a significant change only beneath the first toe for patients with sensory loss when walking downhill. However, a maximum gradient of only 5° was used and the walking speed, which is known to influence foot pressures, was not reported. It was concluded that the gradient induced only a minor redistribution of foot pressure and that this was clinically

insignificant. Simpson *et al.* [6], used a larger downhill gradient of about 9° and reported that the peak pressure beneath the fifth metatarsal increased significantly while the pressure beneath the medial metatarsals decreased, although not significantly. The decreased loading of the medial side of the forefoot contradicted the findings of Kastenbauer *et al.* [5] but this may have been because Simpson *et al.* used a treadmill rather than a fixed walkway. Simpson *et al.* [6], reported two downhill walking strategies. The subjects either leaned forwards or remained more upright, and it was suggested that this may have been influential on foot pressures. Some subjects, who chose to walk fast when going downhill, adopted a forward leaning attitude which increased the peak pressures under their heels and this may have reduced the forefoot pressures on their opposite foot. Milani and Hennig [7], also found increased pressures beneath the heel during downhill running but reported that the pressure beneath the hallux only increased when running uphill. With the exception of Kastenbauer *et al.* [5] research has been conducted using treadmills and this may have influenced the gait. Studies of foot loading on sagittal plane inclines demonstrate minimal changes and the findings are inconsistent.

### 2.2.2. Locomotor function on sideslopes

There are few investigations primarily concerned with gait on sideslopes, however, all have reported accommodative styles of locomotion [22,23,57]. Gehlsen *et al.*[57], found that knee joint motion altered in all three body planes when running, with substantial changes occurring in both the support and the swing phases of gait. Most of the significant changes occurred on slopes less than 5°. Transverse plane rotation showed the most statistically significant change, and it was speculated that this might have been related to the tilt of the foot although no measurements of foot motion were obtained. Foot joint motion was measured by Kitaoka *et al.* [23] on both level and 10° sideslopes. Although this was primarily a clinical study of post-surgical cases, the data from the normal control group revealed that the total range of frontal plane motion increased from 11° on the level to 16° with the foot in the upslope position. There was a decrease to 9° when the foot was in the downslope position. The clinical group showed a similar pattern of response but their ranges of motion were generally smaller (8°,

13° and 9°, level, upslope and downslope respectively). Wright *et al.* [22] demonstrated that motion at the subtalar joint was displaced from its neutral (level walking) position during sideslope walking on an incline of about 10°. When the foot was in the upslope position the motion was displaced into eversion, whereas downslope positioning caused inversion. However, the study reported results for only two subjects. There are no reports giving details of ground reaction forces or foot pressure distribution for sideslope walking.

### 2.2.3. The role of foot tilt in standing and walking

In an attempt to gain some understanding of the relationship between posture, body sway and foot pressure Koles and Castelein [58] compared the movement of the centre of pressure (CoP) with the angular motion of the joints at the ankle, hip and shoulder levels. The investigation was limited to the sagittal plane only and the CoP was selected since it had previously gained popularity as an indicator of postural instability. Increased sway, which was observed when postural stability was poor, had been correlated with greater displacements of the CoP. Koles and Castelein [58], demonstrated that the movement of the CoP was most sensitive to the rotation at the ankles although influences from the hips and spine were clear. The authors commented on the complexity of the interplay and suggested that the horizontal components of the ground reaction force, which they had not measured, would be influenced more by hip rotation than by ankle rotation.

A subsequent investigation by Horak [59] corroborated the earlier results of Koles and Castelein [58] and confirmed the influence of the horizontal component of force. Volunteers stood on support surfaces of various lengths, allowing their feet either complete or very limited purchase with the ground, and this caused them to adopt different postural movement strategies in order to maintain their balance whenever an attempt was made to disturb them. Standing on a normal support surface and being subjected to a brief forward and backward horizontal perturbation force elicited reflex activity in the ankle joint muscles and produced compensatory torques about the ankle joints to restore equilibrium. Although muscle activity subsequently radiated to the thigh and trunk, the pattern was

termed the *ankle strategy* because it restored equilibrium by moving the body primarily around the ankle joints. When the experiment was repeated with the subjects standing on a support surface that was short in relation to their foot length, muscle activity commenced in the trunk and thigh and radiated downwards but the ankle muscles remained unresponsive. This pattern produced a compensatory horizontal shear force at the support surface but little, if any, ankle torque. It was termed the *hip strategy*. This study was limited by being an analysis of the sagittal plane behaviour only, and it served in some ways to reinforce the idea that the CoP was related to changes in body posture.

Not all researchers accepted that displacement of the CoP reflected body sway and could thus be interpreted as an indicator of postural stability, even though there had been numerous reports using the CoP as such. Winter [60], stated that the CoP merely reflected the response of the neuromuscular system to correct the centre of mass of the body, and cited the finding that amputees have significantly less sway, as measured by the excursions of their CoP, than normal individuals. These studies retained the emphasis on sagittal plane analysis of function, in part because of the perceived importance of the ankle and hip strategies, until postural control of single-limb stance became a focus for research [61].

Tropp [61], investigated single-limb stance from a frontal plane perspective in an attempt to reveal the underlying mechanism behind lateral ankle sprain injuries. The sprains seemed to arise from sudden, uncontrolled lateral tilts of the foot. The findings from this study indicated that sideways equilibrium was maintained, in the first instance, by frontal plane corrections at the subtalar joint. It was demonstrated that the frequency at which the CoP displaced depended largely on the frequency of the subtalar corrections and reflected the electromyographic patterns of the peroneus longus muscle, thereby suggesting a process of active correction. This strategy was effective when body sway amplitude was small, indicating that the subject was reasonably stable. However, with progressive instability, the sway amplitude increased and corrections, when possible, were brought about by large rapid movements of the trunk over the hip

joint. This strategy was similar to the sagittal plane hip strategy and produced large inertial forces with reactive shear forces at the sole of the foot.

A follow-up study [62], with an improved methodology, postulated that the axis of the subtalar joint was shifted laterally, as was the CoP, when the heel inverted in response to an inverting torque by the muscles. If the lateral displacement of the joint axis exceeded the lateral position of the CoP then the external everting torque generated by the ground reaction force suddenly reversed to become an inverting torque. If the sudden reversal was not counteracted quickly, then an ankle sprain injury might result. Furthermore, the likelihood of an ankle sprain injury would be greater in situations where large amplitude sway corrections at the hip occurred simultaneously with lateral displacement of the subtalar joint axis because the external torque acting on the foot would be erratic and subject to rapid but brief increases. Gauffin *et al.* [62], demonstrated clearly that subtalar joint torque preceded subtalar joint motion by about one to two tenths of a second and concluded that active corrections of posture were therefore occurring at this joint.

Most recently Hoogvliet *et al.* [20], developed a model demonstrating more effectively the relationship of frontal plane foot tilt and the frontal plane displacement of the CoP during single-limb stance. They described a model, known as the *Rocker Shaped Interface*, which defined the rearfoot as having a curved plantar surface such that every angle of foot tilt was exclusively linked with only one position of the CoP. Foot tilt without displacement of the CoP was not possible. This model predicted that the foot tilt would counteract body tilt (sway) by displacing the CoP towards the line of action of the destabilising gravitational force acting through the centre of gravity of the body. Such a manoeuvre would generate a stabilising moment and would assist in controlling dynamic equilibrium. This mechanism for balance control was termed the *Foot Tilt Strategy* because, according to the model, foot tilt was imperative for displacement of the CoP. Since the frontal plane movements of the CoP were predominantly the result of the foot tilt strategy, an increase in the amplitude or velocity of the CoP could be interpreted as an increase in the activity for balance control and would occur in situations where balance control was more arduous.

Therefore, because balance is believed to be more demanding with sideslope walking [23], especially in the frontal plane, a vigorous implementation of the foot tilt strategy would be anticipated.

The two strategies that are available for frontal plane postural control in single-limb stance, the foot tilt strategy and the hip strategy, have been found to have their counterparts in normal walking [63]. In walking, a state of dynamic imbalance is maintained towards the centreline of the plane of progression as weight is cyclically transferred from limb-to-limb with each step. The most important factor affecting frontal plane whole body balance was the relative medio-lateral placement of the foot, with respect to the centre of mass, that was determined at initial contact. Once the foot had been placed on the ground and its position firmly established, two levels of control were available to fine tune the medial acceleration of the centre of mass (CoM). The first level of control was at the subtalar joint of the foot. Alterations in the magnitude and direction of subtalar joint movement, in response to relevant muscle contraction, created a rocking of the foot. The rock was either in the direction of eversion or inversion as appropriate. Subtalar eversion moments were generated to correct the large medial accelerations of the CoM created by overly lateral placement of the foot. The subtalar eversion moment reduced the magnitude of the destabilising gravitational moment and generated an eversion acceleration moment. Subtalar inversion moments were generated when the foot was placed more medially and had the opposite effects to the eversion moments. In walking, as in single-limb stance, alterations in the magnitude and direction of the subtalar moments changed the mediolateral location of the CoP. The authors suggested that this process facilitated a greater variety and range of responses to aid postural stability.

The second level of body balance control while walking, as in standing, was at the supporting hip. Covariance analysis revealed that a close interaction occurred between the moments at the subtalar and hip joints and the destabilising gravitational moment. The coupling between these three factors suggested that an interactive link existed between the whole body balance system relative to the support surface, and the musculature that controlled the

balance and posture of the trunk and head. The authors concluded that hierarchical strategies may be utilised during gait, as in single-limb stance, whereby small errors are corrected distally by the subtalar muscles and large errors are corrected at the hip by the hip muscles.

Further insight into the muscle activity associated with foot tilt while walking can be gained from the work of Matsusaka [64], who investigated the electromyographic patterns for eight of the muscles of the lower limb and trunk. Additionally, Matsusaka [64] recorded the components of the ground reaction force and the motion of the subtalar joint. Two main electromyographic patterns were clearly identified. An intermediate electromyographic pattern, which overlapped the two main types, also occurred, and indicated that a continuum of response existed between two extremes. In one pattern the subtalar joint eversion was relatively large. With reference to the work of Mackinnon [63], this could indicate that the foot had been placed rather wide (lateral placement error). The medio-lateral component of the ground reaction force was small and electrical activity was recorded in the tibialis posterior, flexor digitorum longus and extensor digitorum longus muscles. The author interpreted the muscle activity as an attempt to control the position of the leg. However, it is also possible that an eccentric contraction may facilitate controlled eversion of the subtalar joint. In the second pattern, which may have occurred with medial placement errors, there was little subtalar joint eversion, the medio-lateral component of the ground reaction force was larger and the peroneus longus muscle was active. The author suggested that, because of its insertion into the first metatarsal bone, the peroneus longus held the head of the first metatarsal in contact with the ground in addition to controlling the displacement of the leg from the vertical.

The findings of Matsusaka [64] indicate that muscular control of the rearfoot may contribute significantly to frontal plane postural control of the leg via the inversion-eversion foot tilt mechanism of the subtalar joint. These findings reinforce those derived from investigations of single-limb stance and other studies of walking. It is evident that an inversion response incorporates different patterns of muscle activity to an eversion response. However, since all of these

muscles insert into bones of the midfoot and forefoot it is likely that the whole foot rather, than just the rearfoot, will be involved in frontal plane postural control.

### 2.2.4. Intrinsic adjustments of the foot

The notion that the rearfoot, midfoot and forefoot can behave in an organised and coordinated manner was demonstrated clearly by Olerud [14]. Although the investigation was limited to the study of ten dissected osteoligamentous specimens obtained from fresh cadavers, the findings were clear and unequivocal. The rearfoot had a torque transmitting capacity that translated transverse plane rotations of the leg into frontal plane rotations of the foot. The translation of rotation occurred by means of the subtalar joint pronation-supination mechanism, which is the same mechanism responsible for the inversion-eversion foot tilt. The use of the pronation-supination terminology made explicit the fact that the motions occurred with respect to all three anatomical planes, whereas eversion-inversion refers only to the frontal plane component of the motions. Olerud [14] found a linear relationship between external rotation of the tibia and supination of the foot, reporting that the leg rotated an average of 0.44° for each degree of supination. Displacements of the bones of the arches of the foot were also measured. The bones in the midfoot (navicular and cuboid) were constrained by their ligamentous attachments to follow the motion of the bones of the rearfoot (talus and calcaneum). However, the amplitudes of the frontal plane rotational displacements were unequal and demonstrated a ratio of about 2:1, midfoot to rearfoot. Thus when the subtalar joint was supinated by external rotation of the leg, the consequential motion of the midfoot bones was amplified causing an elevation of the medial side of the foot and a depression of the lateral side. This behaviour alters the morphology and height of the medial arch of the foot, and the underlying osseous mechanism is generally referred to as the tarsal mechanism [11]. Olerud [14] also observed that when the ankle joint was placed in a range of positions from 10° of dorsiflexion to 30° of plantarflexion, the frontal plane rotations of the bones of the midfoot were essentially unaffected. This indicates that frontal plane rotations are transmitted through the foot in a consistent manner that is largely independent of

ankle joint motion. These observations are important. Up and downhill walking require sagittal plane adjustments at the ankle, but this may have no substantial effect on frontal plane foot tilt, therefore, distribution of load beneath the foot might remain essentially unaltered. In stark contrast, frontal plane rotations are transmitted from the rearfoot to the forefoot, bringing about a realignment of the bones of the arch, and could facilitate redistribution of load as a result.

The strong functional link between the rearfoot and the forefoot may account for some of the unexpected observations reported in a recent study of foot tilt [65]. Hoogvliet *et al.* [65], argued that the width of the foot would influence the efficiency with which the mediolateral displacement of the CoP was controlled. A small tilt of a wide foot would produce a large, rapid displacement of the CoP and could, therefore, efficiently counteract a destabilising gravitational moment. When body weight was shifted away from the wider forefoot and towards the narrower rearfoot, by leaning backwards, the subjects increased both the amplitude and velocity of their foot tilt in an attempt to maintain their balance. As predicted, they were less efficient. When body weight was shifted towards the forefoot, however, a decrease in the amplitude of foot tilt did occur but it was accompanied by an unexpected increase in the velocity of the foot tilt. The displacement of the CoP similarly showed a mixed response with a decrease in its amplitude but an increase in its velocity. This contradicted the predictions of the rocker shaped interface model, which indicated that amplitude and velocity should increase or decrease together. It is possible, however, that the forefoot has a more substantial role in balance when body weight is shifted forwards. If so, then the rapid, small amplitude displacements may be a reflection of fluctuating muscle activity needed to swiftly control adjustments of the smaller joints of the midfoot and forefoot. This explanation would also accord well with the variety of muscle activity patterns associated with foot tilt in walking, as reported by Matsusaka [64].

Other investigations have noted relationships between forefoot behaviour and the tilt of the rearfoot. When torsionally stiff shoes are worn, restricted motion of the midfoot can bring about compensatory pronation of the subtalar joint, demonstrating that, at least in some circumstances, the forefoot can influence

rearfoot tilt [66]. Furthermore, transverse plane conduct of the forefoot appears to be related to rearfoot tilt. Two distinct configurations of transverse plane foot alignment have been described [67,68]. In one, the forefoot was relatively abducted with respect to the rearfoot and was termed an *open* foot configuration, while in the other the forefoot was relatively adducted and was termed a *closed* foot configuration. Correlation was demonstrated between the peak vertical ground reaction force and the configuration of the foot, and it was speculated that the relative forefoot alignment might have been associated with the compliance of the foot. The open configuration was thought to be flexible while the closed appeared stiffer. Since the transverse plane configurations were shown to correlate with the frontal plane angle of the rearfoot, it was suggested that foot tilt might be associated with transverse plane adjustments of the forefoot [69].

### 2.2.5. Summary: Role of foot tilt in postural control of standing and walking

The foot plays an important role in assisting the maintenance of postural control and balance for both standing and walking. The ankle joint contributes significantly to control in the sagittal plane by allowing the leg to tilt forward or backward on the weight bearing foot. When sagittal plane motion occurs at the ankle, internal readjustment of the foot is minimal. The subtalar joint contributes to control in the frontal plane and, in contrast to the ankle joint, induces a change in the alignment of the bones of the arch as rotations are transmitted from the rearfoot through the midfoot. Frontal plane function of the foot becomes apparent when the rearfoot inverts or everts, and the foot tilts from side-to-side. When these movements are used to assist balance, the activity is referred to as the foot tilt strategy. For relaxed standing, this strategy accounts for 15% of the control of the CoP and body balance [70]. In addition to inducing a realignment of the foot bones, tilt of the rearfoot is associated with specific patterns of muscle activity. Since the involved muscles attach to the bones of the midfoot and forefoot then those structures may cooperate with foot tilt and extend the role of the foot in postural control. In walking, first metatarsal function in particular appears complementary to tilting of the foot. The foot tilt manoeuvre causes rapid lateral displacements of the centre of pressure which are indicative of a redistribution of the load over the sole of the foot. Because sideslope walking

induces change in frontal plane foot tilt it could be accompanied by significant alteration of the loading profile. In contrast, sagittal plane adjustments at the ankle require minimal realignment of the foot bones, and alterations to the loading profile may be negligible or absent.

In summary, tilt of the rearfoot influences the function of the midfoot [14] and forefoot [66-68], and an active response of the first metatarsal can occur [64]. Because no alternative controlling mechanism has been identified, it is suggested that the behaviour of the forefoot is constrained predominantly by the tilting action of the rearfoot [14]. The position of the centre of pressure is strongly influenced by the frontal plane tilt of the rearfoot, in both single-limb stance [20,61,62], and walking [63]. Therefore, the pressure distribution over the sole of the foot must be influenced by the tilt of the foot. Redistribution of load may be affected not only by the tilt of the rearfoot but also by accompanying movements of the forefoot, especially the first metatarsal. Previous foot pressures studies have revealed that the first metatarsal is frequently out of phase with the other metatarsals, suggesting that it can function independently [71,72]. Furthermore, the importance of the first toe for dynamic balance has been demonstrated [73], and its loss by amputation is known to cause difficulty in coping with uneven terrain [74].

Kastenbauer *et al.* [5], commented on the rarity of literature relating to the study of walking on gradients, and Sun *et al.* [52]concluded that more complete studies of walking on inclined surfaces are needed. A substantial gap in knowledge has therefore been identified with respect to walking on inclines in general and sideslopes in particular.

### 2.3. Clinical relevance of the study

Knowledge of pressure redistribution during sideslope walking will provide information of immediate and direct clinical significance. High pressure is a recognised contributory factor of foot ulceration, especially when associated with poor tissue vitality, and can be particularly detrimental in diabetes [32,33]. Ulceration may lead to gangrene amputation and, in some cases, death. The personal and financial costs are substantial. To minimise risk, foot pressures are

routinely screened. Conventional screening, however, assesses level walking only and could fail to identify latent high pressures that may manifest during sideslope walking only. This investigation will provide the first estimates of pressure changes with sideslope walking, and will therefore facilitate an initial reassessment of the current situation regarding issues of risk.

The flexibility of the foot, as determined by its joints and their soft tissue constraints, varies remarkably through the population. Individuals may therefore differ considerably in their ability to adapt, or compensate, when walking over uneven terrain. Despite the fact that this aspect of foot function has been the subject of considerable clinical interest for at least seventy years [75], only one attempt to quantify compensatory mechanisms of the foot [76] could be located in the literature. Olerud [76] assessed subtalar joint pronation in ten cadaver specimens finding that, while all were capable of the same compensatory strategy, there was marked variation in the capacity of response. The average pronation response was 9.5° (± 7°). In two specimens, however, the capacity was less than 1°. Olerud [76] postulated that in situations where a deformity exceeded the compensatory mechanism then the joints would be stressed in an extreme position, with overloading consequences to other foot structures. The closest in vivo approach to this problem seems to be the work of Kitaoka *et al.* [23]. Their study investigated patients with restricted motion of the joints of the rearfoot in an attempt to demonstrate consequential compensatory limitations. Sideslope walking was used to stress the feet into eversion or inversion and the resulting joint motion was measured, demonstrating the restricted kinematic response of the joints. However, they were unable to show any associated stress concentrations because loading profiles were not measured. The impacts of restricted compensations therefore remain unknown and will do so until a suitable method for measuring loading profiles on inclined surfaces has been developed. This study aimed to establish a reliable method for measuring the foot loading profiles during sideslope walking in order to facilitate future work regarding the compensatory behaviour of the foot.

## 2.4. Foot pressure data collection

Pressure platforms are commonly used for the collection of pressure data since they offer an acceptable compromise between temporal and spatial resolutions, are efficient in use and readily available. They are restricted to the analysis of the unshod foot and data can only be collected from a single step, unlike in-shoe sensors that can collect data from sequential steps. However, the technical difficulties associated with in-shoe pressure measurements are greater [31].

### 2.4.1. Data collection protocols

A variety of data collection protocols have been reported in the literature for gathering foot pressure data from pressure platforms, These include the mid-gait, one-step, two-step and two-step-stop methods [77-79]. All of the techniques require that a subject walks along a walkway, steps on to the pressure platform and continues forward until clear of the equipment. With the mid-gait method the subject approaches the platform from some distance, usually several meters, while most other methods deliberately start closer to the platform. The one-step protocol positions the individual only a single step from the platform, and the two-step methods use two approach or departure steps. A close starting position minimises the demands on the subject and maximises the likelihood of successfully striking the platform on each walk. Protocols that use a shorter walking distance can be used on shorter walkways when space is limited. However, a short approach distance is thought to limit the speed of gait and the subject may still be in a phase of acceleration. Protocols with a short approach may therefore reduce the pressure levels beneath the feet [77], but not all investigators [78] have reported this effect.

When the predominant mid-gait method is employed, ensuring that the platform is contacted cleanly and repeatedly over several successive trials can be difficult. Two alternative methods are available for use. In the first, the platform is positioned in the walkway and hidden from view by a cover. The subject is then instructed to walk the length of the walkway repeatedly until sufficient random strikes have been recorded on the platform. This technique is time consuming, and can be inappropriately fatiguing [80]. Also, repetitive barefoot walking on hard

surfaces, such as those found on most walkways, may be damaging to fragile soft tissues of the sole of the foot, especially for diabetics and similarly compromised individuals [77]. The alternative approach is to establish, by iteration, an appropriate starting position for each subject so that the nominated foot will strike the platform. With this method some subjectivity is required so that any step which shows obvious targeting, adjustment of gait, loss of balance, or side-to-side deviation be excluded.

### 2.4.2. Targeting

A platform that is clearly visible may enhance targeting and be beneficial to some subjects, especially those with impaired vision such as diabetics. Targeting uses vision in order to attain specific placement of the foot [81] and is therefore likely to necessitate the adjustment of the stride or step. The effect of such adjustments on the ground reaction force has previously been cause for concern. Patla *et al.* [82] and Grabiner *et al.*[83] have reported the ground reaction force parameters to be independent of visual guidance. Martin and Marsh [84], however, found that step length changes as small as 10% altered both the magnitude and timing of the ground reaction force. A recent study by Wearing *et al.* [85], showed that there was a two-fold increase in the variability of the length of the step prior to a target (the target step) in comparison to the same step in a non-targeting condition. This confirmed that adjustments to step length do occur in order to contact a specific target of the size of most pressure platforms, and corroborates the similar findings of Hirokawa [86]. However, the average length of the target step, over five trials, was not significantly effected. Furthermore, the study found no significant differences in either stance phase duration times or ground reaction force parameters as measured in the time-domain between the targeting and non-targeting conditions. It was concluded that targeting does result in small changes to step parameters, but these are minimised by averaging over several trials. Changes in the target step, however, are insufficient to cause significant alterations to time domain ground reaction force parameters. The only identified report of the effects of targeting on foot pressures [80], similarly concluded that they were insignificant and that the advantage gained by reducing the number of inappropriate trials was preferable. Targeting does not seem to bring about

significant alterations in ground reaction force or foot pressure data collected from a single platform, although this conclusion cannot be extended to those situations where multiple platforms are arranged sequentially

### 2.4.3. Walking speed

While the effects of targeting are insignificant, those associated with walking speed are not. Andriacchi *et al.* [87] observed cadence and step length to vary linearly with walking speed, while the stance and swing phase durations were inversely proportional to the walking speed. In addition, of the nine ground reaction force parameters that were measured, six were found to vary linearly with velocity. Although the investigation was undertaken with an orthodox force plate, similar observations have been reported with segmented force plates and pressure platforms. Stott *et al.* [88] found that when the cadence was in the range of 100-116 steps $min^{-1}$ the pattern of loading across the forefoot remained reasonably constant, but that if subjects walked slowly (92 steps $min^{-1}$) then the forefoot distributed more load to its lateral side. Conversely, higher speeds, such as those in sprint running, resulted in almost one hundred percent of body weight being transferred to the force plate through the segment beneath the first metatarsal. These observations were later verified [89] in a more methodologically sound study in which cadence was controlled at 84, 112, and 114 steps $min^{-1}$. The results reinforced the opinion that force and pressure changes appeared to be linear with walking speed. The increased force was again observed to shift to the medial forefoot with a simultaneous decrease of force on the lateral forefoot. However, the study reported that, in association with the changes in the magnitude of force, there was a decrease in the duration of loading.

The interplay between the speed of walking, and the duration and magnitude of loading was investigated further in two studies that used discrete pressure sensors placed in the shoes of normal volunteers. This method allowed for the analysis of multiple sequential footsteps. Zhu *et al.* [90] controlled the cadence from 70 to 120 steps $min^{-1}$, in increments of 10 steps $min^{-1}$, to match the range reported previously for a general pedestrian population [91]. With increasing cadence, the mean contact duration continuously decreased (a reduction to 64%

at 120 steps $min^{-1}$ with respect to 70 steps $min^{-1}$). The mean pressure-time integrals at all sensor sites also reduced (45% at 120 steps $min^{-1}$). However, in support of earlier findings, mean peak pressures continuously increased at all sensor sites (up to 119% at 120 steps $min^{-1}$). The peak pressures beneath the medial metatarsals increased by 60% while those beneath the lateral metatarsals only increased by 26%. In a further study, Zhu *et al.*[92] instructed volunteers to simulate a slow (0.51 $ms^{-1}$), shuffling gait for comparison with their usual (1.29 $ms^{-1}$) walking style. The shuffling gait succeeded in reducing the peak pressures at 130 of the 140 sensor sites (14 sensors, 10 subjects). The peak pressures beneath the medial metatarsal reduced by 55% while those beneath the lateral metatarsals only reduced by 30%. Although these studies used an in-shoe technique, the findings support those of earlier barefoot measurements and confirm that peak pressures generally increase with faster walking but decrease with slower walking. While all metatarsals showed the same general response to changes in walking speed, the magnitude of response varied from metatarsal-to-metatarsal. Overall the load on the forefoot appears to shift medially when walking faster.

The term medialisation has been adopted for the shift of load to the medial side of the forefoot, and the subsequent local increase of pressure, that occurs with faster walking. It has been suggested that medialisation is the result of increased eversion of the rearfoot and or increased velocity of eversion of the rearfoot [93]; both of which occur with faster walking. Rosenbaum *et al.*[93] postulated that the entire foot would tilt further and or faster so that the medial forefoot would be pushed towards the ground while the lateral forefoot lifted away. A study to test this hypothesis [93], measured the angular displacements and velocities of the heels of subjects who walked over a pressure platform at speeds of 0.8, 1.2 and 1.7 $ms^{-1}$. The findings demonstrated medialisation of loading with increased speed and found that both the total range of eversion and the angular velocity of eversion increased simultaneously. The subjects for this study were grouped according to their foot type as having a high, normal or low arch. Each group revealed a general medialisation response, but in the low arched group the rearfoot angular motion was significantly more pronounced and this was taken as an indication that these feet were more flexible. One surprising finding was

an increase of peak pressure beneath the first metatarsal of the low arched group when walking slowly even though the rearfoot angular displacement and velocity were both reduced. This observation suggests that other factors, such as instability of the foot or postural imbalance, may influence load distribution or interact with walking speed. The medialisation phenomenon has, however, also been reported in children[94].

The influence of walking speed on the magnitude and distribution of load beneath the foot has been clearly shown. Several studies have reported that many of the parameters of gait, including the ground reaction force components, exhibit an almost linear change with speed of walking. These findings indicate that knowledge of walking speed is important for the interpretation of pressure distribution patterns and that observations may be needed over a complete range of speeds to characterise fully a particular gait parameter [87]. When the objective of a study is to make comparisons between groups, or when an individual is to be compared with normal values, then it is preferable that they have been measured at similar walking speeds. However, while the control of walking speed can be advantageous it can also bring about undesirable effects by increasing the variability in the gait pattern. Gait studies that have used the coefficient of variation as a dependent variable [86,95], demonstrated that the best consistency or repeatability occurs when subjects self-select their walking speed or self-select other factors, such as cadence, that determine the walking speed. The reduction in temporal variability that occurred with self-selected gait has been interpreted as an indicator of optimal energy efficiency and stability of performance, and is believed to be a useful measure of motor skill [95]. Tasks that are more demanding of motor skills may therefore exhibit greater variation, particularly when the activity is artificially constrained, as in control of walking speed. A dilemma therefore exists as to whether the walking speed should be controlled or not. By controlling the speed, the effect on pressure is standardised but the motor skill performance may be marred causing increased variability. A compromise may be reached, however, by monitoring the stance phase duration and using it as an indicator of consistency of walking, since it is known to correlate highly with walking velocity [86,87,93].

### 2.4.4. Reliability

The reliability of measurements obtained from a single step on a pressure platform has been shown to be poor. Stehr [96] compared single step values with mean values obtained from four other steps by the same subject and in 60 out of 154 (39%) comparisons the single step estimates were beyond the range determined by the mean $\pm$ 1 standard deviation. High levels of reliability can be achieved by using data from three or more steps [89]. Holmes [97], recommended that the three steps should be obtained on the same day rather than on different days, because of differences between day-to-day step-to-step variability. The findings of Gross and Bunch [98], who used discrete in-shoe sensors, also indicate that the between-day variability is greater than the within-day variability. Their results, however, were probably influenced by alterations in the re-positioning of the sensors. Measurements from a matrix insole [99] that was not subject to positional change were in close agreement with the findings from pressure platforms. In order to obtain reliable estimates of pressure from platforms it is essential to record multiple steps. Previous reports [89,90] indicate that measurements from three steps gives measurement reliability without excessive burden on the participant.

### 2.4.5. Summary of the data collection procedure

The literature indicates that, for a subject group whose walking is not limited by disease or discomfort, the mid-gait protocol is preferable and that data from three steps should be obtained to ensure good reliability. The general recommendations for the mid-gait method would be that each subject begins walking from predetermined starting position at least 3 or 4 full steps prior to the platform. They are instructed to walk across the platform and continue to the far end of the walkway. The starting position is iteratively adjusted for each subject until they contact the platform in a relaxed and consistent manner while looking straight ahead rather than down. Even if it does occur, targeting is unlikely to distort the data. Participants should be allowed to practice until they feel comfortable. Contact time rather than the walking speed may be monitored until a predetermined level of walking consistency is achieved ($\leq$30 ms [77]). Data are

rejected when the subject shows signs of instability or uncertainty when walking, or when the contact time is outside the predetermined limits.

## 2.5. Dependent variables

The findings from previous studies are usually reported in terms of peak (maximum) pressure, peak force or impulse. It is common for the measured values to relate to specific sites of the foot and they are then referred to as the regional pressure or force. Unfortunately, terminology is not always used precisely. Pressure and force have been used synonymously in some instances, which makes the interpretation of some results difficult. Peak pressure is the most commonly reported variable, possibly because of its important association with plantar ulceration. Peak pressure values are influenced by the instrumentation used, with sensor size exerting a strong effect [100,101], and comparisons between results from different measurement systems is therefore difficult. Results differ according to the activity under investigation, and reference values for both standing and walking are available.

### 2.5.1. Normal standing pressures

The mean peak pressures beneath the normal static foot as determined with an optical pedobarograph have been reported [102,103] to be about 50-100 kPa. However, maximum peak pressures were in the region of 120-170 kPa. Cavanagh [104], assessed 107 feet using a capacitance mat and reported the mean peak pressure as 140.5 kPa with a coefficient of variation of 21% indicating considerable variation between individuals. The distribution of peak pressures in standing showed the largest (100-140 kPa) to be in the heel while those in the forefoot were about half this magnitude. Pressure under the 1st metatarsal was about 27% less than the peak under the other metatarsals and only 15% of the feet had the maximum peak under the 1st metatarsal. The distribution of load was given as rearfoot (60.5%), midfoot (7.8%), forefoot (28.1%), toes (3.6%).

### 2.5.2. Normal walking pressures

Normal dynamic peak pressures determined with an optical pedobarograph have been reported to be <980 kPa[102]. Bennett and Duplock [105], used a polymer

pressure sensor platform to establish values for 75 normal adults. They reported the mean peak pressures to be about 412, 304, 225 kPa for the central, first and fifth metatarsals respectively, while that for the hallux was 343 kPa. The results are in close agreement to those collected using a capacitance based system with comparable specifications, and obtained from a similar subject group [93], tables 2.1 and 2.2.

**Table 2:1 Normal foot pressures (walking)**

Normal pressures kPa (sd), derived from large array pressure platforms.

| | Heel (med) | Heel (lat) | Mets (2-4) | Met (1) | Met (5) | Toe (1) |
|---|---|---|---|---|---|---|
| FSR [105] | 314 (49) | 284 (49) | 412 (98) | 304 (88) | 226 (98) | 343 (108) |
| Capacitance [93] | 322 (116) | 210 (58) | 358 (87) | 299 (137) | 142 (61) | 317 (116) |

**Table 2:2 Comparison of pressure platform characteristics**

For systems referred to in table 2.1. Stance phase duration estimated * from Hughes *et al.* [41]

| | Frequency (Hz) | Sensor ($cm^2$) | Subjects (N) | Mean Age (years) | Stance Phase (ms) |
|---|---|---|---|---|---|
| FSR [105] | 64 | 0.372 | 74 | 21 | 700* |
| Capacitance [93] | 70 | 0.5 | 30 | 26.7 | 715 |

A capacitance system was also used to establish normal values from a sample of 111 adults [94] (mean age of 27.4 years) and fifteen children (age unspecified), table 2.3. Although the walking speed was not controlled, the results for the adult group are comparable with those in table 2.1.

**Table 2:3 Peak foot pressures for adults and children (walking)**

Pressure values according to foot site.

| | Heel (med) | Heel (lat) | Met (3) | Met (1) | Met (5) | Toe (1) | Midfoot |
|---|---|---|---|---|---|---|---|
| Adults [94] | 312 | 277 | 380 | 314 | 215 | 416 | 59 |
| kPa (sd) | (101) | (79) | (170) | (185) | (126) | (187) | (77) |
| Children [94] | 119 | 99 | 99 | 95 | 87 | 141 | 41 |
| kPa (sd) | (61) | (39) | (32) | (38) | (45) | (72) | (20) |

### 2.5.3. Peak Force

In comparison to peak pressure, peak force values are poorly represented in the literature. Regional force data provides useful information regarding foot function[34], with changes in the distribution of ground reaction forces reported for both foot pathology [35,36] and fatigue [37]. One early study [106], that used a medium resolution matrix force plate, presented peak force results as a proportion of body weight rather than in newtons. This was considered as an acceptable method of normalising values in order to make comparisons between subjects. Approximations, derived from the graphs, are given in table 2.4. The findings demonstrated that the force on the heel and hallux decreased with age from mid-life. Walking speed was not controlled and the slower walking that occurs with aging may have contributed to the decreased values. However, it might be argued that a decrease in the walking speed should have similarly reduced the force on the central metatarsals but this was not found. Indeed, the force on the midfoot and lateral metatarsals increased. The authors concluded that the feet functioned less effectively with age, as indicated by the collapse of the longitudinal arch and the reduced loading of the hallux. The assessment of regional force was hampered in early studies because of the relatively low spatial resolution of the measurement systems, however, contemporary platforms reduce this difficulty. The most recent study indicates that, for healthy young adults, the heel and central metatarsals are the primary load bearing structures [38].

**Table 2:4 Peak force as a percentage of body weight**

| **Force values by foot site** | | | | | | |
|---|---|---|---|---|---|---|
| | Heel | Midfoot | Met 1 | Met 2 | Met 3/4/5 | Toe 1 |
| % body wt [66] | 75% | 10% | 25% | 25% | 12% (each) | 20% |

### 2.5.4. Force-time integral and pressure-time integral

The impulse has been defined as the force-time integral (FTI) [94], and regional impulses are believed to be useful indicators of foot function [93]. The pressure-time integral (PTI) has also been reported in the literature [93,107]. The PTI is similar to the FTI, but reflects the impulse acting on a particular sensor rather

than an anatomical region of the foot. Soames [107], found the PTI accentuated the functional importance of the 1st metatarsal and toe in a way that neither pressure nor time did as separate variables. The impulse data of Schaff [108] also showed most clearly the way in which a rocker soled shoe affected the function of the foot. Bransby-Zackary [109], commented that the PTI often showed changes where a simple measurement of peak pressure showed no change. However, Hennig [94], comparing loading patterns in children and adults found the impulse patterns almost identical although the peak pressure patterns differed. Rodgers [110], assessed Morton's foot type and found differences in peak pressures but not impulses beneath the 1st and 2nd metatarsals. These results suggest that impulse, which represents change in the momentum of the individual [109], may be more indicative of the mechanical function of a foot.

### 2.5.5. Summary of dependent variables

The peak pressure is derived from individual sensors while regional forces can be estimated by summing the output from groups of sensors at defined sites. In addition, the impulse can be determined when the loading history is known. There is little consensus within the literature as to the importance of each variable. The usefulness probably depends upon the type of investigation. Pressure has relevance to ulceration and soft tissue pathology whereas force, and the FTI may be more useful when the mechanical function of the foot is of interest. Temporal parameters are required if the FTI is to be determined. Temporal parameters may also indicate alterations in function and change when foot pathology is present [111].

## 2.6. Foot pressure measurement techniques

Attempts to assess the distribution of load over the sole of the foot date back to the latter part of the nineteenth century. Efforts by Marey and Carlet, cited by Alexander *et al.* [3], involved the use of an ingenious pneumatic shoe system, while Beely, cited by Elftman [112], simply used a thin sack filled with Plaster of Paris. These early attempts demonstrate that such investigations can be undertaken with the foot either shod or unshod. While in-shoe measurement techniques are developing rapidly, the majority of studies have used pressure

mats or platforms to investigate barefoot walking. This review focuses on techniques using mats or platforms because of their relevance to the current study.

The methods of pressure measurement adopted over the last seventy years show three broad phases of development, each reflecting the technology of the time. Initially, the distribution of pressure was judged from ink footprints obtained by using textured rubber mats, and this technique was quickly modified by the incorporation of still and cinephotography. Optical imaging and recording techniques evolved to include transduction methods based on refraction and photoelasticity. While both refractive and photoelastic methods are still used, the most recent period of development has given attention to electromechanical transducers, as these are particularly suitable for digital data handling procedures. Measurement systems of this sort of have utilised resistive strain gauges, piezoelectric ceramics, and capacitive or resistive sensors constructed from elastomers or polymers.

### 2.6.1. Pressure measurement with textured mats

Textured rubber mats were used initially by Elftman [112] and later by Harris and Beath [113]. Elftman's method was simple but the effect was highly visual. The textured surface of the rubber mat was viewed through a glass plate so that the distortion of its pyramidal projections could be observed. Load applied to the top surface of the mat increased the area of contact between the pyramids and the underlying glass, while the introduction of a white fluid into the spaces between the pyramids enhanced the contrast of the image for filming [112]. Elftman's analysis was subjective but the technique was enhanced by Miura *et al.* [114], to give a quantitative output scale subdivided into six colour zones. Even so, the amplitude of this system was limited and fell short of the range of pressures encountered in walking.

The Harris and Beath mat [113] had fine ridges on one surface rather than pyramidal projections. The ridges ran at right angles to each other and were at different levels. The mat was inked and covered with a sheet of paper to obtain a

footprint on which areas of high pressure appeared dark. The mat had a useful range of approximately 25-500 kPa and would therefore fail to identify the higher pressures that can occur beneath the foot. Footprint images have also been produced using microcapsules [115] that release coloured dye when ruptured. The rupture thresholds varied between 1000 and 10000 kPa which is above foot pressure levels but, by placing the pressure sensitive sheet between a mat of small ball bearings and a hard acrylic substrate, a working pressure range of 50-350 kPa was achieved. This range was still inadequate for general use.

A novel variation in the use of textured mats was reported by Grieve and Rashdi [116], who sandwiched aluminium foil between the pyramidal projections of a rubber mat and a sheet of low density foam plastic. Loading produced permanent distortions in [116] the ductile foil and these were measured to give an estimate of the applied pressure. As with the other mat based methods, the sensitive range of 0-600 kPa was less than desirable. Furthermore, the incorporation of the low density foam sheet was thought to attenuate the pressures.

### 2.6.2. Pressure measurement with optical devices

The optical pedobarograph [117] (PBG) was a major development in the field of foot pressure sensing. It consisted of a glass plate covered by a thin mat[118] of a material such as plastic, rubber or paper. The plate was illuminated from its side edges and the light internally reflected as long as the angle of incidence at the internal surface was larger than a certain critical angle. If the angle of incidence was less than the critical angle then the light was transmitted through the surface. The difference between the refractive index of the carrier (glass) and that of the outside contact medium (air) determined the critical angle. As the difference became less the critical angle became larger. When pressure was applied to the top surface the interface mat was pushed into close contact with the glass by deformation of the microscopic surface-asperities, the critical angle increased, less light internally reflected and a greater proportion was transmitted through the surface[119]. When viewed from below, a pressure profile was seen where light intensity was proportional to the applied pressure. The monochrome

image was converted to colour[120], and captured by photography or video. Early machines were restricted to seven colours and the pressure amplitude resolution was therefore limited. Consequently, each colour zone represented a relatively broad range of pressure and a reasonable estimate of peak pressure could only be achieved by adjusting the threshold values between zones. This could be done during static stance evaluations but was not possible during dynamic analysis. Furthermore, the re-setting of the threshold was undesirable because it made comparisons between subjects difficult. Later machines used a video frame grabber (768 x 512 pixels, 256 levels)[101] and, with appropriate software, measured the image intensity of each pixel to give an estimate of the local pressure. The very high spatial resolution afforded by this technique is advantageous, particularly for the investigation of soft tissue problems where peak pressure estimation and the local spatial distribution of pressure appear to be important clinical factors. The physical properties and behaviour of the top mat is most influential on the performance of such a system[118,119]. A relatively thick, deformable mat such as foam plastic will redistribute and attenuate pressure partly by virtue of its vertical compression and reshaping. Additionally, such materials suffer from restrictions of dynamic response and linearity. A thin, hard mat[101] would therefore appear to be the logical alternative. However, the additional factor of mechanical crosstalk cannot be disregarded because, although each pixel is displayed as an individual element, the transducer surface (mat) is a continuous sheet. The sensors are not, therefore, mechanically isolated elements. Although a detailed analysis of all mat materials has not been published the estimates of pressure derived from the optical pedobarograph are useful as reference values since they indicate higher magnitudes than most other methods, and high peak pressure has clinical implications. The system does have the disadvantage of requiring a built up walkway and its dynamic performance is limited.

Arcan and Brull [121] first proposed the use of polarised light photoelasticity for foot pressure measurement in 1976. Initially, applied load was transmitted to a photoelastic sheet by an array of hemispheres attached to the undersurface of a thin leather sheet but later designs used independent vertical plungers[122,123] in order to eliminate mechanical cross-talk between elements. The pressure

distribution beneath the foot was represented by discrete sharply defined, circular interference patterns. These interference stress patterns were thus a function of the contact pressure, with the diameter of each circular fringe being proportional to the applied load. The images were recorded using still or cine photography (48 frames per second). Some images were digitised and used to produce what were possibly the earliest computer generated graphic displays [124] of foot pressure, however the process had to be manually completed and proved too laborious to be suitable for clinical use.

Static calibration of the photoelastic system by step-loading[121] produced a non-linear curve showing greater sensitivity to lower loads, and dynamic calibration was undertaken by applying load via a damped pendulum[125]. Using this technique the force-time variation could be controlled in the range of 0-20N over a time interval of 18-80 ms. The upper load limit of 20N produced pressures below that to be expected in practise. However, impulse loading[124] with loads upto100 N was used to investigate the transducer response within a pressure range of about 0-1000 kPa. Synchronous filming of the optical interference pattern at 500 Hz indicated an attenuation of approximately 15% of the peak value and it was concluded that the optical device would give best estimates during the rising phase of a slowly applied force[124].

### 2.6.3. Pressure measurement with electromechanical devices

The next stage in the evolution of platforms focused predominantly on the development of designs that used strain gauges as transducers. These systems incorporated load cells with some form of bending element, such as a beam or ring, as the sensor mechanism. The top surface of the platform was sub-divided and each segment was individually instrumented. The need for discrete instrumentation usually limited the overall number of segments to between twelve and sixteen, although Dhanendran [126] produced a platform with one hundred and twenty-eight load cells. The overall surface area of the platforms was therefore restricted and small plates had difficulty in accommodating an adult foot, figure 2.1, and table 2.5.

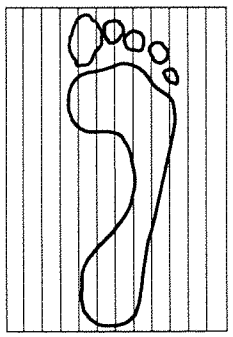

250x170 mm
Stott 1973
12 beams

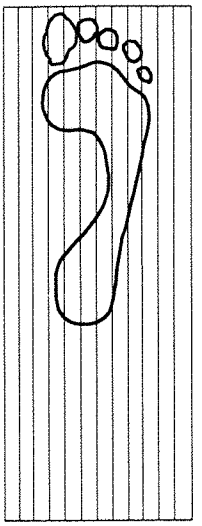

400x144 mm
Stokes 1974
12 beams

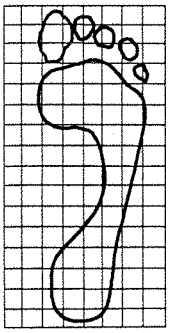

250x125 mm
Dhanendran 1978
128 load cells

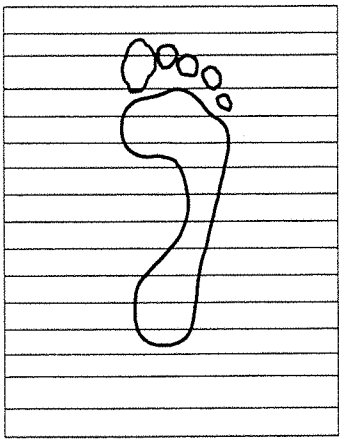

335x260 mm
Manley 1979
16 transparent beams

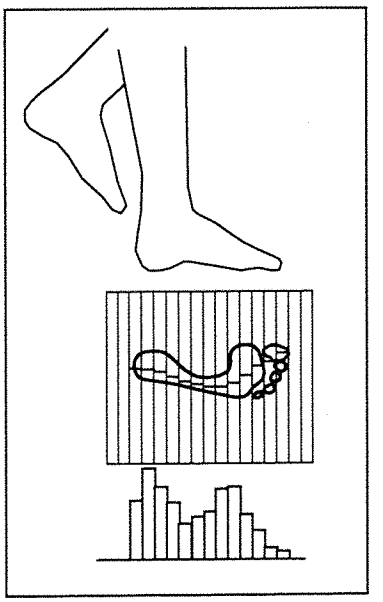

Transparent beam plate:
Schematic representation
of video output

**Medium resolution plates**

All plates drawn to scale
showing an adult foot,
size 42 Eur (25 cm long)

**Figure 2:1 Medium resolution platforms**

Dimensions and specifications of systems given in table 2.5.

Also, the position and shape of the foot usually had to be recorded by simultaneously obtaining an ink footprint from the surface of the plate, although this restriction was overcome in one design [127] that used transparent beams and video recording. The use of video in conjunction with quantitative measurement produced an intelligible display and formed the basis of a system suitable for efficient clinical use. Segmented force plates were under trial for about ten years from 1973. They had many desirable characteristics such as near linear response to loading, low hysteresis, high natural frequency and fast frequency response, small errors to offset loading and good repeatability. Unfortunately, the spatial resolution was poor, especially in the larger plates, and they were eventually superseded by other designs.

**Table 2:5 Characteristics of medium resolution segmented force plates**

Where sufficient information has allowed (*), a schematic representation to scale is given in figure 2.1.

| Authors | Fig 2.1 | Plate Area (cm) | Segment Size (cm) | Sensor Element | Natural Frequency (Hz) | Sampling Frequency |
|---|---|---|---|---|---|---|
| Stott *et al.* [88] | * | 25 x 17 | 25 x 1.4 | Beam | 400 | |
| Stokes *et al.* [128] | * | 40 x 14.4 | 40 x 1.14 | Beam | | |
| Dhanendran *et al.* [126] | * | 25 x 12.5 | 1.5 x 1.5 | Ring | 6000 | 85 Hz |
| Manley & Solomon [127] | * | 33.5 x 26 | 26 x 2 | Beam | > 30 | 50 Hz |
| Arvikar & Seirig [129] | | | | Ring | | |

The need to improve the spatial resolution of the systems while maintaining or increasing the overall surface area brought about a move away from strain gauge technology. Alternative techniques were developed using materials that allowed large arrays of small sensors to be easily and inexpensively fabricated, figure 2.2. Capacitive sensors can be produced in large arrays[130] almost as easily as a single sensor. One array of this type was made from a rubber mat each side of which was covered by conducting strips, the strips on one side being placed orthogonally to the strips on the other side. The arrangement of strips in rows and columns allowed any point on the array to be sampled by selecting one appropriate strip on each surface. The capacitance of the transducer increased as the rubber dielectric was compressed [131]. The physical behaviour of early elastomers was poor [131] although if suitable rubbers were chosen [132] then sensors could be constructed for a variety of applications.

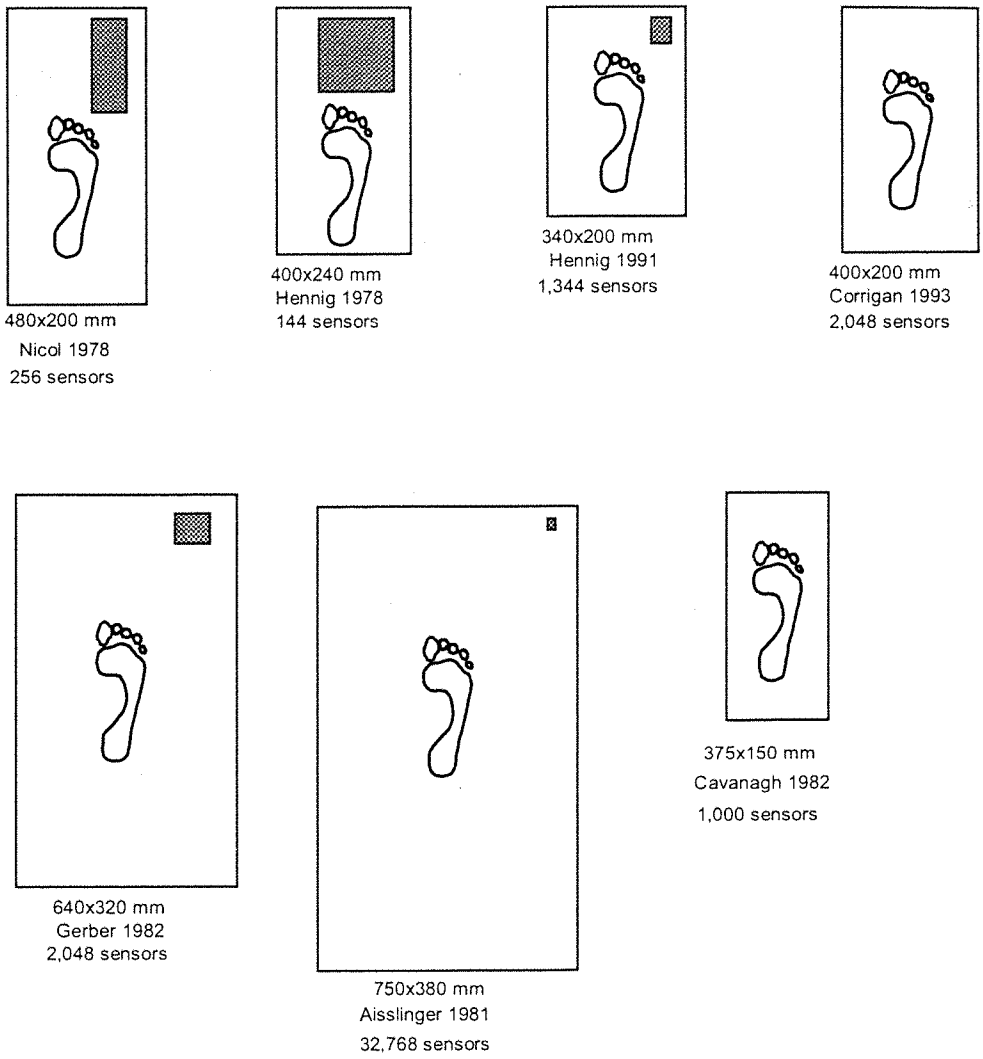


**Figure 2:2 High resolution platforms**

Dimensions and specifications of capacitance plates are given in table 2.6.

Table 2.6 shows the various configurations of capacitance based systems that have been reported in the literature. Gerber [133], achieved a practical compromise between spatial and temporal resolution [133] with a system comprising of 2048 transducers each 10 x 10 mm (1cm$^2$), a total area of 640 x 320 mm and a scanning frequency 160 Hz per channel, figure 2.2. This was possibly the first system with spatial and temporal resolutions that allowed detailed analysis of foot function. Even so, with a sensor size of 1cm$^2$, peak pressure could have been underestimated by between 17%[100] and 70%[101].

A variety of problems have been reported with capacitance mats including substantial crosstalk between adjacent capacitors, although Gerber [133] reported this as less than 3%. They may also suffer from a restricted frequency response, non-linear stress-strain relationship and hysteresis, while the measurement range can be limited by the thickness of the capacitive material [131]. Moreover, because some elastomers have a very low Young's modulus (decreasing in thickness by about 30% under a compressive stress of 100 kPa) they may significantly attenuate the peak pressure.

**Table 2:6 Characteristics of capacitance systems**

Where sufficient information has allowed (*), a schematic representation to scale is given in figure 2.2.

| Authors | Year | Fig 2.2 | No of Sensors | Resolution (Spatial cm$^2$) | Area (cm) | Scanning Frequency (Hz) |
|---|---|---|---|---|---|---|
| Nicol & Hennig[130] | 1978 | * | 256 | 2.6 | 48 x 24 | 200 |
| Hennig & Nicol[131] | 1978 | * | 144 | 4.83 | 40 x 20 | 25 |
| Aisslinger *et al.*[134] | 1981 | * | 32,768 | 0.09 | 75 x 38 | 3.05 |
| Aisslinger *et al.*[134] | 1981 | | 2,048 | 4.88 | 100 x 100 | 100 |
| Gerber[133] | 1982 | * | 2,048 | 1.00 | 64 x 32 | 160 |
| Cavanagh & Rodgers[135] | 1984 | | | 1.00 | | |
| Cavanagh *et al.*[104] | 1987 | | | 1.00 | | |
| Janssen *et al.*[136] | 1990 | | 1,984 | 0.5 | 62 x 32 | 70 |
| Mittlmeier *et al.*[137] | 1990 | | | 0.5 | | 70 |
| Samnegard *et al.*[138] | 1990 | | 1,300 | 0.5 | | 25 |
| Hennig & Rosenbaum[94] | 1991 | * | 1,344 | 0.5 | 34 x 20 | 20 |
| Hughes *et al.*[89] | 1991 | | 1,344 | 0.5 | 34 x 20 | 20 |

Cavanagh *et al.* used ceramics to fabricate small (5 x 5 mm) piezoelectric sensors and constructed a 1000 element platform with good spatial resolution[139], figure 2.2. The platform was relatively narrow, with a sensitive area of 15 x 37.5 cm, and could only fully accommodate a foot that was placed in close alignment with its long axis. The use of the stiff ceramic substrate, in preference to the elastomers used in capacitive systems, gave the platform a very high frequency response. However, the system was mechanically fragile and individual charge amplifiers had to be used for each element making it unsuitable as a commercial or clinical system. A scanning frequency of about 33 Hz was initially used for data collection but this was subsequently increased [111] to 50 Hz. Prior to data analysis, a moving average process, that effectively replaced each raw element value with the value of the eight neighbouring elements, smoothed the pressure values. This process, performed due to the presence of noise, probably resulted in an under estimation of peak pressure.

Maalej [40] introduced a thin polymer, resistive-effect sensor, or force sensitive resistor (FSR), for measuring plantar pressures. The manufacturing process for FSR sensors includes screen-printing of conductive electrodes onto a polymer film substrate. The printing is inexpensive and efficient once the artwork for the design is complete. By simply altering the artwork a single sensor design can be reconfigured to form the fundamental element of a large array. One polymer sensor pressure platform system had 2048 elements in a 64x32 array (figure 2.2, Corrigan *et al.*) with a single sensor area of 0.3 $cm^2$ and a scanning frequency up to 65Hz [140,141] . The high resolution polymer array superseded an alternative resistive technique[142,143] that used a carbon loaded elastomer to bridge annular gaps etched in copper foil - a technique similar to that adopted later for in-shoe sensors[144].

Apart from the platforms described already, conventional multicomponent force plates have been customised by the addition of contact area transducer arrays[145-148]. This combination has enabled the simultaneous measurement of the component forces and the contact area of the plantar surface of the foot. Thus, at any instant, the average contact stress may be derived. Because all three components of the ground reaction force are measured, estimates of both the

normal and shear stresses [145-148] have been made. Draganich *et al.*[146] observed that the force and contact area curves increased and decreased in similar manners and suggested that the average pressure under the foot remained relatively constant. Subsequent studies with high resolution pressure plates show that subjects may have highly individualistic patterns.

### 2.6.4. Summary of pressure measurement techniques

The earliest forms of pressure assessment, such as footprinting with textured rubber mats, offered reasonable spatial resolution but gave no indication of the temporal features of foot loading. Local sites of concentrated pressure could usually be determined but even if the magnitudes of the loads were derived they were equivocal because of the restricted measurement ranges associated with these techniques. Evaluation of the temporal characteristics of loading was achieved a little later by using cinephotography. The combination of cinephotography with optical pedobarography and photoelasticity then produced some of the earliest quantitative dynamic profiles of load distribution beneath the foot. Digital methods of image capture and analysis have removed the manual effort that was once required with these techniques, and both are still in use. In addition, the optical pedobarograph offers a spatial resolution greater than other contemporary methods. However, in general, optical techniques have given way to electromechanical methods, especially since small platforms, when linked to personal computers, have produced portable systems capable of real-time quantitative analysis.

The evolution of electromechanical techniques illustrates the struggle to develop a measurement system with a refined combination of spatial and temporal performance characteristics. The single load cells of the earlier segmented force platforms demonstrated excellent performance characteristics. Repeatability was good (±2% Stokes [128]) with only small errors to offset loading (<2% Stokes [128], <5% Dhanendran [126]). Their almost linear output (±2% Stokes [128]) enabled easy calibration, while their combination of high natural frequency (400 Hz Stott [88], 600 Hz Dhanendran [126]), fast frequency response and low hysteresis would induce minimal distortion of the force-time output signal. However, the use of

segmented force platforms was restricted because of the small size of the sensing areas, low spatial resolutions, or both. The demand for platforms with larger sensing areas and greater spatial resolution brought about a move away from traditional strain gauge technology. Unfortunately, the resulting sensors, such as those incorporating elastic dielectrics or polymer substrates, exhibit non-linear responses, and are subject to time dependent effects. In addition, because of the flexible nature of these types of sensors, offset, partial or non-uniform loading may cause considerable measurement errors. The use of stiffer materials, such as piezoelectric ceramics, has demonstrated that high spatial resolution can be achieved in conjunction with excellent response characteristics, although such systems are both fragile and expensive. Currently two high resolution electromechanical systems are available commercially. While some information regarding the sensor types incorporated in contemporary systems is available in the literature, no comprehensive evaluation of performance characteristics has been published. There is a need, therefore, to determine the operational limitations of contemporary systems.

## 2.7. Polymer pressure sensors

The term force sensing resistor (FSR) is commonly used to refer to the two types of conductive polymer sensors (Interlink FSR™ and Tecscan Fscan™) that are employed for foot pressure measurement. Both sensors are lamelliform in construction and appear outwardly similar. However, the designs are different and Tecscan use conductive ink [149] while Interlink organically dope one polymer layer to facilitate electrical flow [150]. The sensors demonstrate decreasing electrical resistance when subjected to increasing pressure. Conductive polymer sensors have become popular for foot pressure measurement because they are thin, robust, inexpensive and require relatively simple electronics [151-154]. Discrete, or individual, sensors are most frequently used and are generally incorporated within insoles for in-shoe pressure measurements [151-153]. While several reports give details about discrete Interlink FSR™ sensors, very little information is available regarding the large arrays. A large Interlink FSR™ transducer array formed the sensor matrix of the primary pressure platform used in this investigation.

Discrete Interlink FSR™ sensors were first used for foot pressure measurement in 1988 [40]. They have subsequently been used in a variety of sizes and shapes from 9.5 to 16mm in diameter and 5x5mm square. They vary in thicknesses between 0.25 – 0.5mm. While some designs use two polymer membranes [42] others have three [44], the middle one acting as a spacer to separate the outer two.

**Table 2:7 Characteristics of FSR™ polymer sensors**

| Author | Pressure (MPa) | Hysteresis % | Repeatability % | Polymer | Temperature drift /°C |
|---|---|---|---|---|---|
| Maalej *et al.*[40] | 0-2 | 8 (a) | <7 | Mylar | -0.5% |
| Maalej *et al.*[41] | | 6 (a) | <7 | UItem | |
| Knudson & White[42] | 0-2 | <5 (d) | | Mylar | |
| Hedman[39] | 0-5.6 | ≈5 (c) | <10 | | |
| Wertsch *et al.*[44] | 0-1.2 | 8 (b) | <7 | Ultem | |

(a) 2MPa full scale output; (b) 1.2MPa full scale output;
(c) 400N full scale output, loading rates ≤ 2.5 Hz (complete cycle);
(d) not defined in original text.

Previously reported characteristics of discrete FSR™ sensors are given in table 2.7. The sensors exhibit hysteresis, along with a non-linear response that results in a change in sensitivity through their working range [39,48] causing low sensitivity to high pressures (>1Mpa). Despite these imperfections, they have become well established for foot pressure measurement [46,47,90,92,155-157]. The variety of FSR™ designs that have been reported in the literature is a reflection of the relative ease with which they are produced. The conductive tracks are screen printed onto one of the polymer membranes while the other is chemically doped to render it electrically conductive. This process enables the construction of the large array used in some pressure platforms[141].

Bench tests of FSR™ polymer arrays have been reported in brief [158]. The tests were restricted to groups of twenty-five sensors. Static accuracy over fifteen pressure levels to 1.5 MPa was determined on two separate occasions as 3.5% and 3.8% full scale error. Also, the repeatability for each sensor was determined

from ten trials and the mean variation was reported to be 5.2%. While these results demonstrate agreement with those for discrete sensors, table 2.7, several characteristics of large arrays have yet to be determined. Furthermore, the degree of uniformity between elements throughout the array is also unknown. Operational trials of polymer platform systems have, however, indicated that the method of calibration has a significant effect on accuracy [159,160]. Despite the limited information regarding the performance of the arrays, the results produced through clinical trials show consistency with those obtained using other technologies [141,161].

Rapid repetitive load-unload cycles, encountered when polymer sensors are used within a shoe, can lead to mechanical failure in the form of delamination [162]. Undesirable time-dependent behaviour of Fscan™ sensors has been exposed by both bench tests [154,163,164] and controlled clinical trials [165,166]. The time-dependent behaviour manifests as an increasing sensitivity to pressure, with repeated cyclical or sustained loading giving progressively higher values (an average increase of 15%). When subjected to a pressure of 500 kPa for 15 minutes the output exhibited 19% creep, and after a load-unload cycle to a pressure of 1200 kPa hysteresis of 21% was found. It was postulated that these responses were the result of a combination of recoverable (rapid viscoelastic) and irrecoverable (slow creep) components [154], both of which were primarily influenced by the duration of loading rather than the cyclical history.

Design, material and construction differences between Fscan™ and FSR™ sensors could influence performance characteristics significantly. Therefore, conclusions derived from the tests of Fscan™ may not be fully applicable to FSR™ sensors. While time dependent effects, particularly creep, are unlikely to be problematic with pressure platforms because of the relatively long interval between loading cycles, additional tests are required to establish the response characteristics of FSR™ polymer arrays.

## 2.8. Dynamic performance of sensors

Attempts have been made to determine the frequency characteristics of the ground reaction force signal and relate them to the design requirements for foot-pressure transducers. Antonsson & Mann [167], concluded that 98% of the spectral power of the normal walking force signal was contained below 10 Hz and over 90% was below 5 Hz. These results were obtained by using a rigid force plate capable of registering the transient impulse associated with heel strike. Archarya *et al.* [168], used discrete sensors, individually located within an insole beneath the foot, and reported similar findings. Nevill *et al.* [169], developed an in-shoe transducer with a frequency response up to 200 Hz and then used a low pass filter to demonstrate that no significant change in signal morphology occurred until the filter frequency was reduced to about 10 Hz. These studies show that most of the spectral power of the normal gait signal is contained below 10 Hz. However, transient forces with higher frequency components can occur during heel impact or forefoot impact. Zhu *et al.* [170], sampled discrete polymer sensors at rates between 5 and 200 Hz and then undertook a time domain comparison of the signals. It was reported that the signal sampled at 20 Hz was not significantly different from that at 200 Hz. While this method indicates that the sampling frequency may be kept low without any detrimental effect, it gives no indication of the frequency response of the sensor. The dynamic behaviour of FSR™ polymer transducers is therefore unknown and requires investigation.

# 3. Equipment and Instrumentation

## 3.1. Introduction

Two pressure platforms were used in the investigation. The primary platform incorporated a conductive polymer sensor array, described at the start of the chapter, with transducers utilising the electrical resistance principle. Two rigs were designed and constructed to test the sensor elements. The main rig allowed both static and dynamic tests to be conducted within one frame. The frame could be reconfigured according to the needs of the test. A proving ring reference transducer was constructed, and its design details are described in an appendix. The operational characteristics of the main rig were assessed and are reported, along with the results for the calibration of the proving ring. Details of a second rig, designed to allow the assessment of shear effects, are also described. Shear testing was also conducted on a second platform. A tiltable walkway was constructed for the main study of sideslope walking.

## 3.2. Conductive polymer sensor array

Conductive polymer pressure sensors are produced as discrete sensor units and as arrays comprising of multiple elements. The sensor used in these tests was of the large array type, and was constructed from two transparent polymer membranes, the lower one of which had been chemically doped [150] to render it electrically conductive. In the array, multiple conductive tracks were orthogonally arranged, figure 3.1, requiring that the longitudinal and transverse tracks crossed each other. At each intersection, or node, the tracks were separated by a small insulation component (pad). Because of the multilaminate construction, each node was relatively thick in comparison with other parts of the sensor, figure 3.2. The nodes therefore supported the upper polymer membrane and separated it from the lower one. The upper membrane sagged slightly between nodes and gave a dimpled appearance to the surface of the array, figure 3.3. The sagging of the upper membrane was referred to as hammocking. Pressure applied to the upper membrane deflected it downwards until it contacted the conductive lower membrane, thereby completing an electrical circuit. As the applied pressure increased, the electrical resistance decreased.

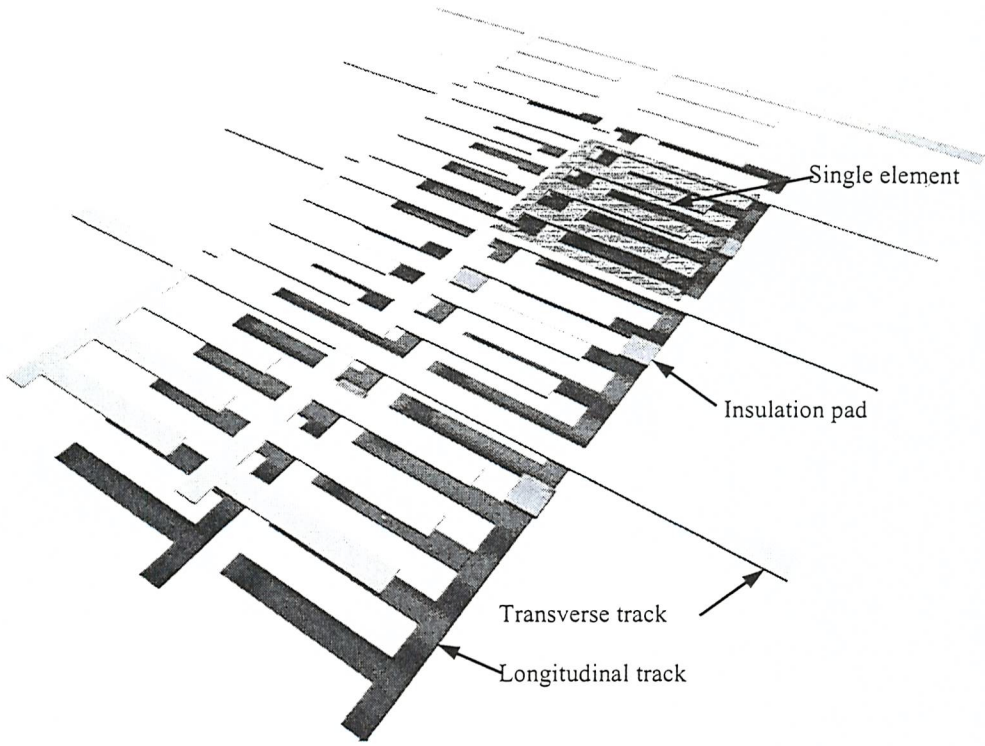


**Figure 3:1 Schematic illustration of a section of the polymer array**

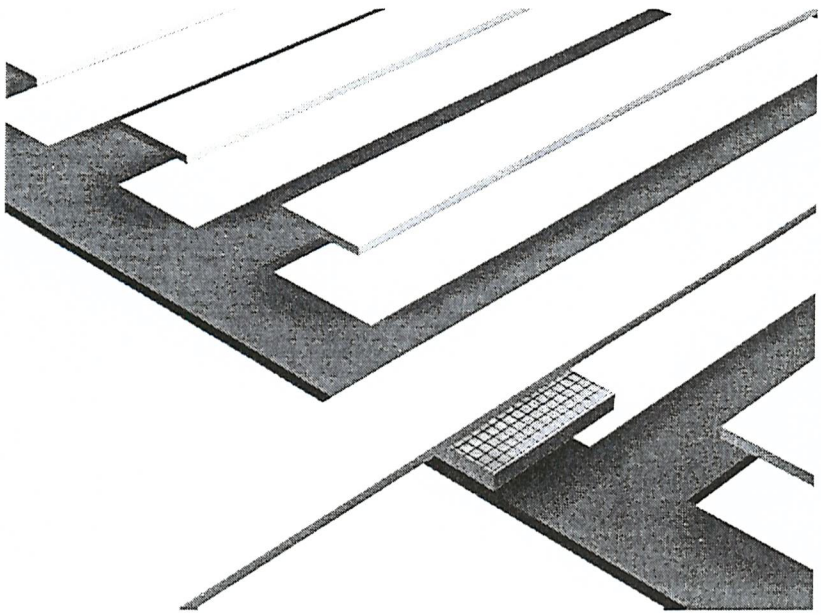

**Figure 3:2 Conductive track intersection and insulation pad detail**

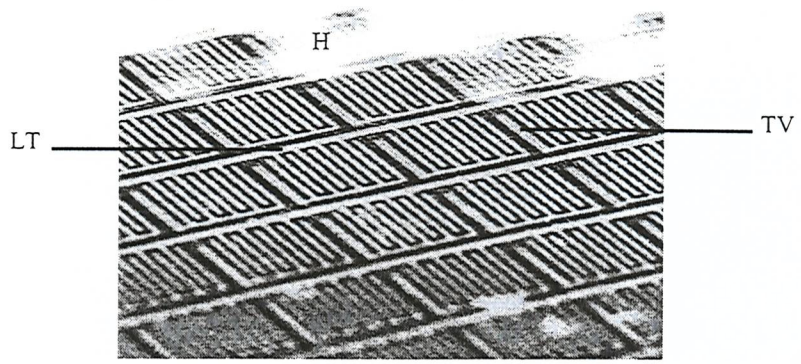


(a)

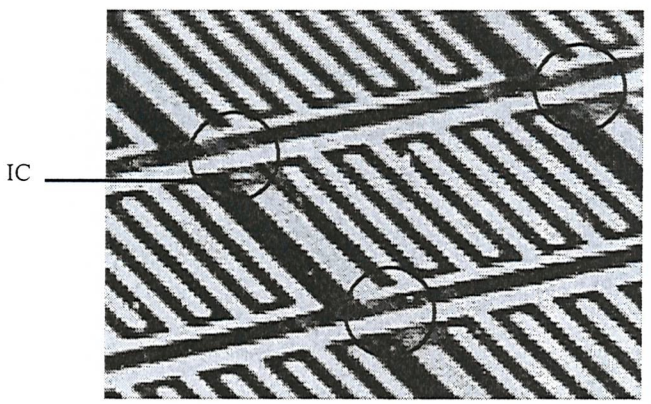


(b)

**Figure 3:3Conductive polymer array**

(a) Overview of polymer array illustrating longitudinal (LT) and transverse (TV) arrangement of conductive tracks. Hammocking (H) of the upper membrane over individual elements was seen as a dimpled appearance of the surface.
(b) Cross-over nodes, circled, were formed by the combined thickness of the orthogonal tracks (LT and TV) and their intervening insulation component. One insulation component (pad) is faintly visible and indicated (IC).

### 3.3. Primary pressure platform

The polymer sensor was of the commercially available Interlink FSR™ type, and was incorporated in a Musgrave Footprint™ foot pressure platform system. There were 2048 sensor elements, each ≈5x6 mm in size, covering an overall area of approximately 450x200 mm. The polymer array was removed from the casing of the platform for testing, but the 6 mm aluminium substrate to which it was bonded was kept in place to prevent bending. Individual elements were isolated by their appropriate conductive tracks, incorporated into a voltage stabilised LS743 operational amplifier circuit, and their output was recorded directly rather than through the accompanying computer system. However, for the walkway study, the array was replaced in the housing and was scanned at a frequency of 50 Hz using the on-board circuitry.

### 3.4. Secondary pressure platform

An Emed SF™ pressure platform was used for a component part of the study. The sensors in the second pressure platform utilised the capacitive principle of transduction. The platform had a matrix of 2736 transducers, with a density of four sensors per square centimetre, and a sampling frequency of 50Hz. Its general characteristics were therefore very similar to those of the primary pressure platform.

### 3.5. Main test rig design

A rig was designed to facilitate the testing of selected individual elements of the large array polymer foil in the pressure platform. Both static and dynamic loads could be applied to the polymer sensor through the test rig mechanism. For walking, frequencies below 10 Hz dominate the ground reaction force signal, while frequencies beyond about 20 Hz account for less than 1% of the spectral power. A desirable test frequency range of 30 Hz was therefore specified, and an electromechanical shaker (Ling Dynamic Systems model 403) was selected to form the basis of the test rig. Alternative methods for applying known load-time profiles were considered, including standard material testing machines and pneumatic actuators, but these did not offer sufficiently rapid cycling rates.

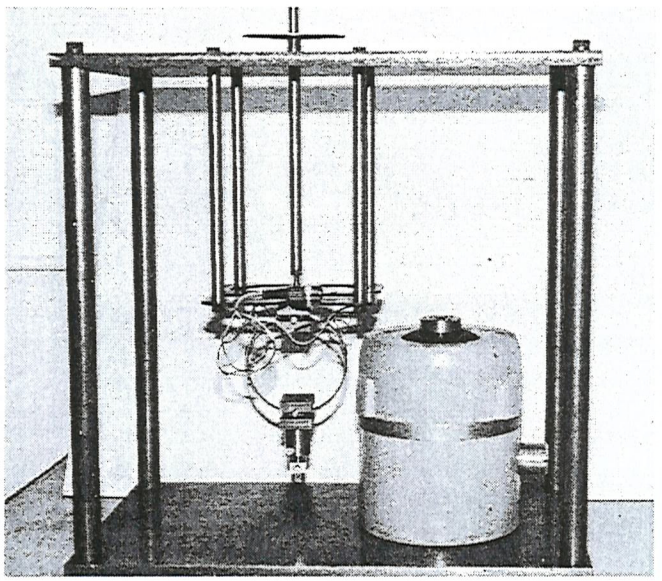

**Figure 3:4 Test rig with static load mechanism in-situ**

The central spindle mechanism could be replaced by the electromechanical shaker, shown on the right, for dynamic testing.

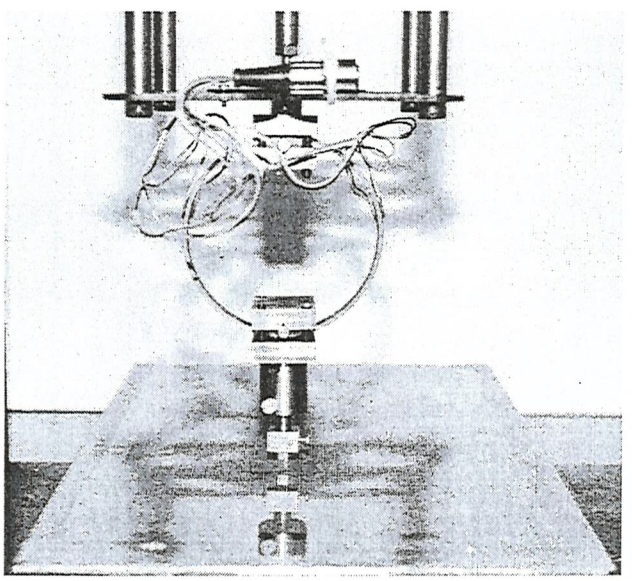

**Figure 3:5 Proving ring and adjustment mechanism**

Small anvil aligned over polymer array.

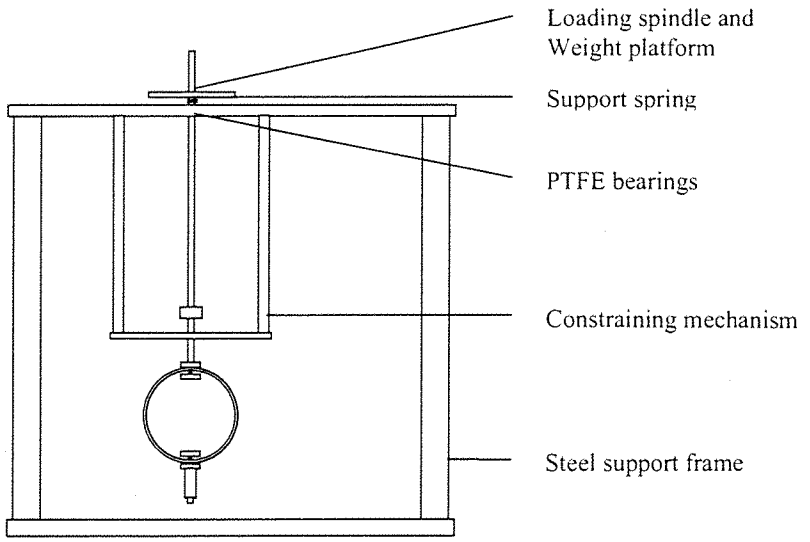


**Figure 3:6 Test rig: static test configuration**

Load applied to weight platform and transmitted to polymer sensor via central spindle, proving ring and adjustment mechanism.

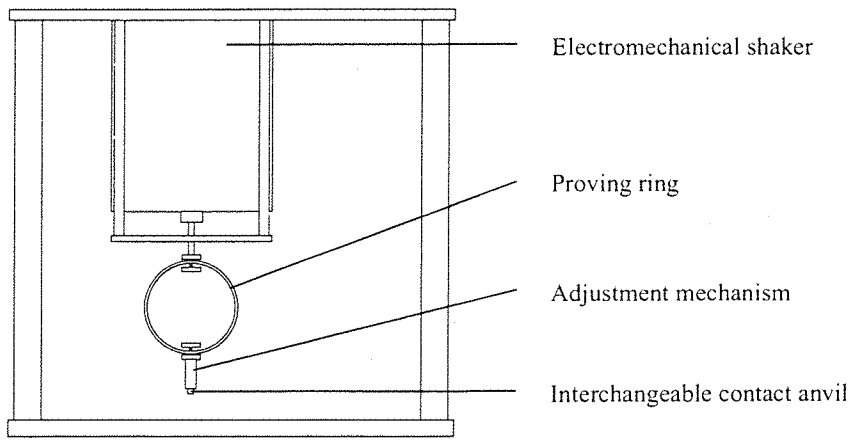


**Figure 3:7 Test rig: dynamic test configuration**

Oscillating load from electromechanical shaker transmitted to polymer sensor via proving ring and adjuster.

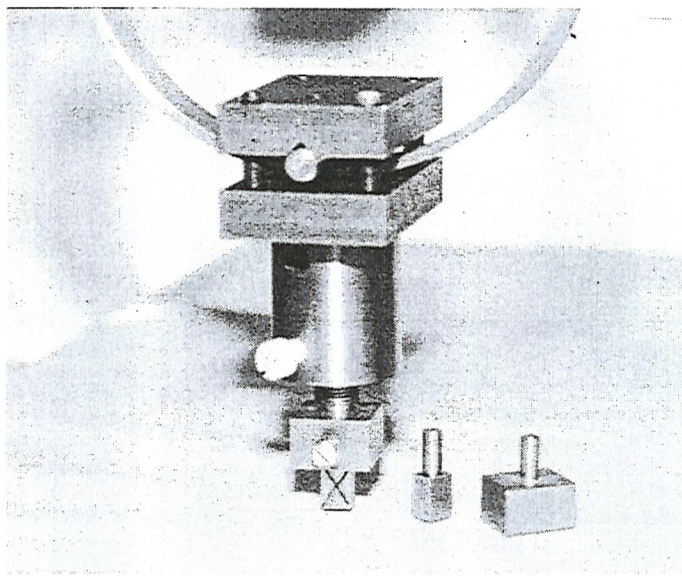

**Figure 3:8 Adjustment mechanism with anvils**

Screw thread adjuster allowed mechanism to be extended until anvil contacted the polymer surface. Anvil could be rotated to any position for correct alignment with selected sensor element.

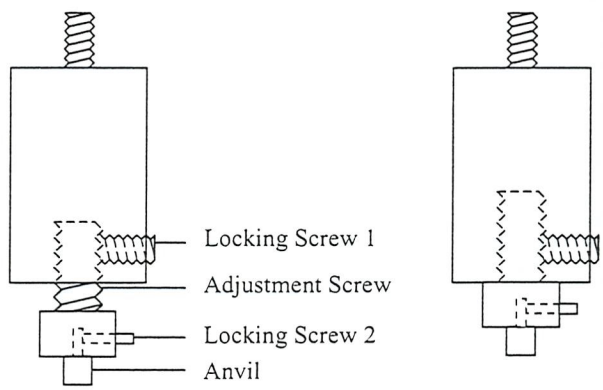


**Figure 3:9 Adjustment mechanism: schematic details**

Contact anvil in extended and retracted positions.

The basic rig, figure 3.4, consisted of a steel frame that could be configured in order to allow loading either with calibrated weights (static loading mode, figure 3.6), or via the electromechanical shaker (dynamic mode, figure 3.7).

In either configuration, the applied load was transmitted to the polymer sensor via an instrumented proving ring with an adjustment mechanism and a contact anvil, figure 3.5. Several anvils of different sizes were constructed. Each could be attached to the adjustment mechanism by a simple spigot, which allowed it to rotate freely about its vertical axis, figure 3.8. The screw adjustment mechanism, figure 3.9, allowed the position of the anvil to be vertically altered until it just made contact with the polymer sensor, at which point a small change in the output from the proving ring was observed. The anvil could also be rotated until the edges of its contact surface were aligned precisely with the borders of the polymer sensor element. After adjustment, the mechanism and anvil were secured in position by two locking screws.

From the review of the literature it had been determined that pressures to about 1.0 MPa can occur beneath the normal foot. This value was therefore used as a design parameter for components of the rig. The small anvil was designed with a contact surface equal to the active surface area of a single element (0.3 $cm^2$), while a larger anvil (1.95 $cm^2$), capable of simultaneously covering four adjacent sensor elements, was also constructed, figure 3.8. A force of about 200N was required to develop a pressure of 1.0 MPa beneath the large anvil, and this was a determinant for the selection of a reference transducer. Use of the small anvil produced contact pressures that easily exceed the test requirements.

The use of steel anvils offered the advantage that a rapidly oscillating force could be exerted on the polymer sensor to facilitate dynamic testing, however, some difficulties were subsequently encountered with this technique. In use, the large anvil, figure 3.8, covered four adjacent polymer sensor elements, figure 3.1, and was therefore located indirectly upon several of the small insulation pads which separate the conductive tracks, figure 3.2. This arrangement appeared to prevent the effective distribution of pressure over the sensing surface of the polymer elements, whose outputs remained minimal even under

substantial load. For this reason, use of the large anvil was abandoned. Furthermore, although the small anvil sat within the sensing area of a single polymer element, and was not impeded by the insulation pads, an elastomeric membrane (≈1.5 mm thick) was used to interface between the rigid surface of the anvil and the compliant surface of the sensor during all tests.

A strain gauged proving ring was selected as a reference transducer. This design was simple, robust, inexpensive, and the structural behaviour, which can be modelled as a special case of simple beam deflection [171], was predictable. A suitable proving ring would also act as a compliant structure for the transmission of the oscillating force signal, and could follow both static and dynamic loading events. The proving ring was constructed from mild steel and full details of its design are given in appendix 1. The dimensions of the ring were determined according to Castigliano's second theorem [172], such that a 200N load would produce 1000με of surface strain at the level of the horizontal diameter. One thousand microstrain is a conventional design parameter for the use of foil strain gauges and maximises the sensitivity in the desired range, while allowing a reasonable margin for overload without permanent distortion of the gauge.

### 3.5.1. Proving ring calibration and performance

While in use, the proving ring was subjected to compression loading conditions only, it was tested and calibrated in both compression and tension. This confirmed that the response was linear, predictable and reliable beyond the range necessary for the designated tests. Calibration in tension was achieved by sequentially suspending calibration weights from the lower adjustment mechanism. The compression tests were conducted with the ring in-situ as part of the rig. Weights were applied to the loading spindle and the output from the ring was recorded. The spindle was constrained to vertical motion by a low friction (PTFE) bearing and, during calibration, vertical motion was confirmed by means of a dial gauge. A set of 0.25 kg lead weights was manufactured, each being carefully adjusted against a laboratory weighing scale to ensure an error of <0.5%.

A calibration graph is shown in figure 3.10. For loads of upto 100N, in both tension and compression, the curve is essentially linear (non-linearity <1% full scale) with negligible hysteresis and excellent repeatability.
The following calibration factors were determined from the proving ring calibration graph:

| | |
|---|---|
| Load (kgf) | 416.5 mV $kgf^{-1}$ |
| Load (N) | 42.46 mV $N^{-1}$ |
| Pressure (0.3 $cm^2$ anvil) | 1.27 mV $kPa^{-1}$ |

### 3.5.2. Test rig performance

The performance of the test rig was evaluated. In the static configuration no particular problems were identified. However, in the dynamic mode two operating observations were made. At low frequency oscillations (<4 Hz), the armature of the electromechanical shaker exhibited poor amplitude control. Towards the end of each loading cycle, as the applied force approached zero, the armature would jolt and, at times, lose contact with the polymer array. This behaviour was heard as a chattering vibration from the rig and, although it was not always easy to see, the transient vibrations were confirmed by attaching a small accelerometer to the adjustment mechanism, figure 3.11. At higher frequencies (> 27 Hz), the armature again demonstrated erratic amplitude control. The manufacturers technical specifications indicated that a drop in performance was to be expected at frequencies close to DC (0 Hz). Similarly, the technical specifications indicated a change in the mode of operation, from constant displacement to constant thrust, at about 30 Hz. The slight restrictions in performance were therefore attributed to the characteristics of the electromechanical shaker, however, the actual working frequency range of 4 to 26 Hz was considered to be acceptable. When combined with the static tests, an overall range of 0 to 26 Hz was achieved, which was marginally short of the 30 Hz target.

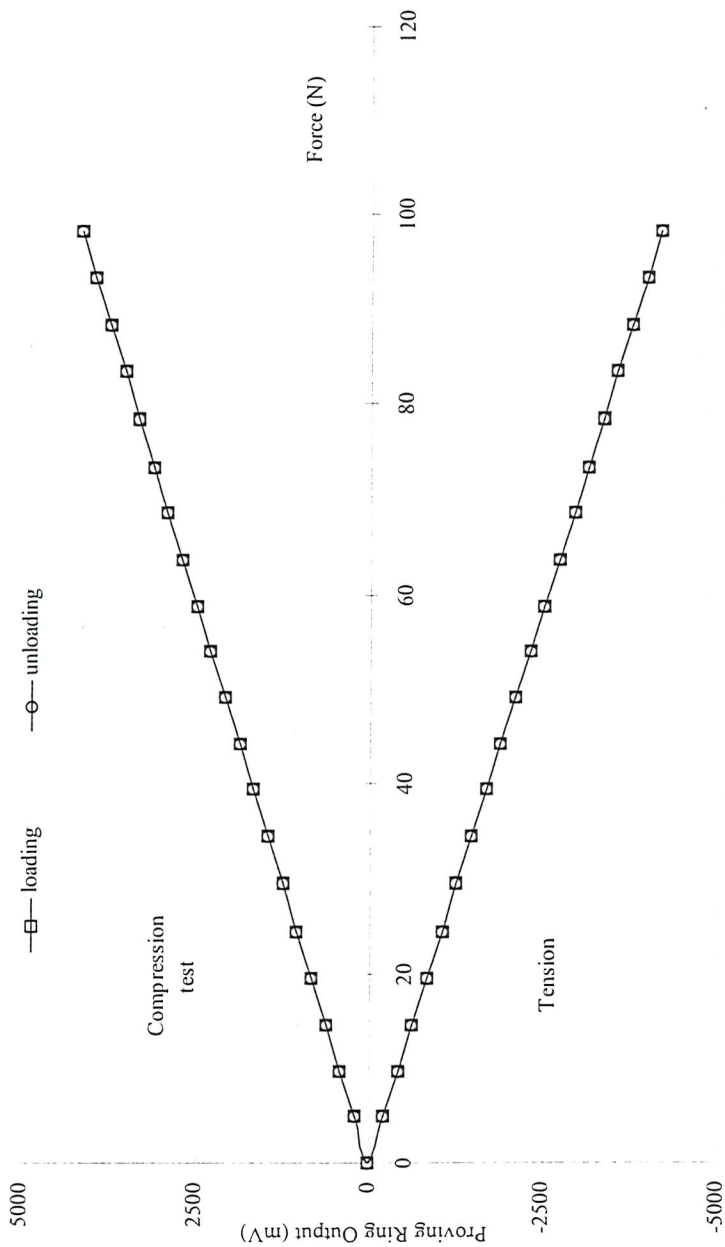


**Figure 3.10 Proving ring calibration**

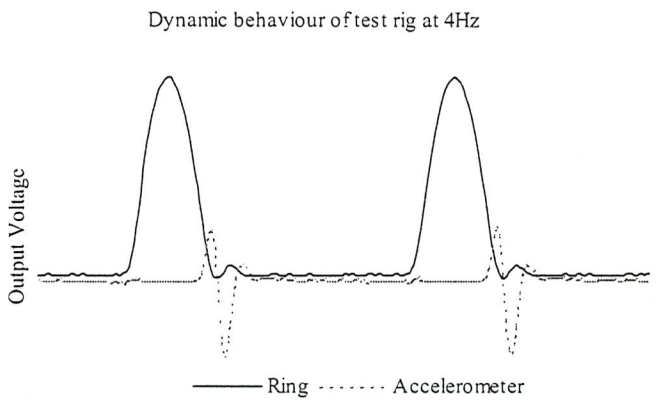


**Figure 3:11 Test rig dynamic behaviour**

Poor control of the shaker at low frequencies caused anvil lift and rig vibration, which was confirmed with an accelerometer.

## 3.6. Alignment template

A small template was constructed to aid alignment of the anvil with the polymer sensor element. The template was constructed from an 8x8 cm piece of thin (≈2 mm) clear acrylic plastic. Two orthogonally aligned pairs of parallel marker lines were scored into the undersurface of the template and stained with ink to make them easily visible. The four lines bordered a centrally positioned rectangular aperture that was dimensionally identical with the active surface area of a single sensor element. The aperture could accommodate the contact anvil closely and constrain it to vertical motion only. The template was aligned with the grid pattern on the surface of the polymer array using the reference lines and then temporarily held in position with adhesive tape while the anvil was located in the aperture.

## 3.7. Shear test rig

A separate test rig was designed and constructed so that the effect of shear force on the polymer sensor could be assessed, figure 3.12. This rig had to be capable of applying a stable vertical load in conjunction with a simultaneous shear force. The vertical load had to generate contact pressures approaching those

experienced beneath the foot in walking and the rig had to maintain its vertical stability while the shear force was applied. The need for stability indicated a design with a large base, however, a commensurably large contact area would have resulted in pressures well below the desired level. A compromise was achieved by producing a large rectangular frame with four small contact plates, one near each corner, to act as stress raisers. This method of concentrating the stress allowed representative contact pressures to be achieved with relatively low loads (20 kg). The loading weights could be stacked onto the frame without any apparent instability.

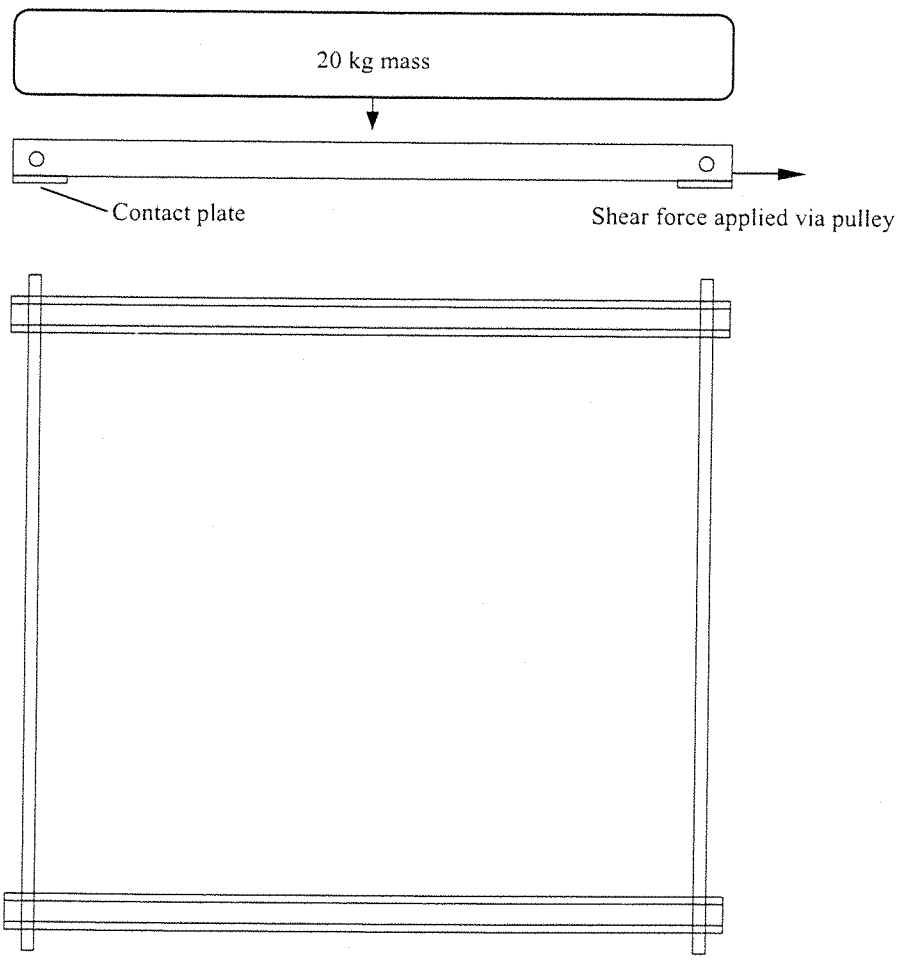


**Figure 3:12 Shear test rig**

(a) Side elevation illustrating method of applying normal and shear forces.
(b) Plan view. Distance between parallel sections could be adjusted on the connecting rods

The frame was constructed by joining two lengths of channel section aluminium with two pieces of threaded rod. The positions of the aluminium sections could be adjusted, along the two rods, so that they were parallel. The adjusting nuts were then locked into position to constrain the aluminium from any significant lateral displacement, although sufficient slack was left in the frame to ensure that each channel section could adjust independently to accommodate any unevenness over the surface of the pressure platform. The stress raisers took the form of small, thin aluminium plates (18x18x1.5 mm), and were adhered to the undersurface of each end of each aluminium section, figure 3.12. The frame was placed onto the surface of the polymer sensor membrane, vertically loaded by applying weights, and then a shear force exerted via a weighted pulley system.

### 3.8. Tiltable walkway

A wooden walkway was constructed in sections, the adjacent ends of which could interlock to improve stiffness. The entire walkway could be tilted such that the slope was transverse to the direction for walking, and this was referred to as a sideslope, figure 3.13. The walkway was hinged along one edge while the other was supported, at regular intervals, by pin-jointed steel struts. The struts were notched so that the walkway could be adjusted quickly and easily by locating the appropriate notch on a supporting bar. The geometry of the notches was such that the angle of slope could be adjusted in 2° increments from level upto a maximum of 8°. The walkway was seven metres long and 1 metre wide, and the pressure platform was mounted in a steel frame at the central point. The frame ensured that the upper surface of the pressure platform was accurately aligned with the surrounding walkway surface, and that the relative alignment was automatically maintained whenever the angle of slope was adjusted.

### 3.9. Planimeter

A cartographic planimeter was used to determine the area of some of the footprints. A planimeter is device that can determine the surface area of a two-dimensional surface by tracing the outline of the surface and applying an appropriate coefficient of proportionality. A calibration tool was available with

the planimeter to ensure that the appropriate coefficient of proportionality was applied.

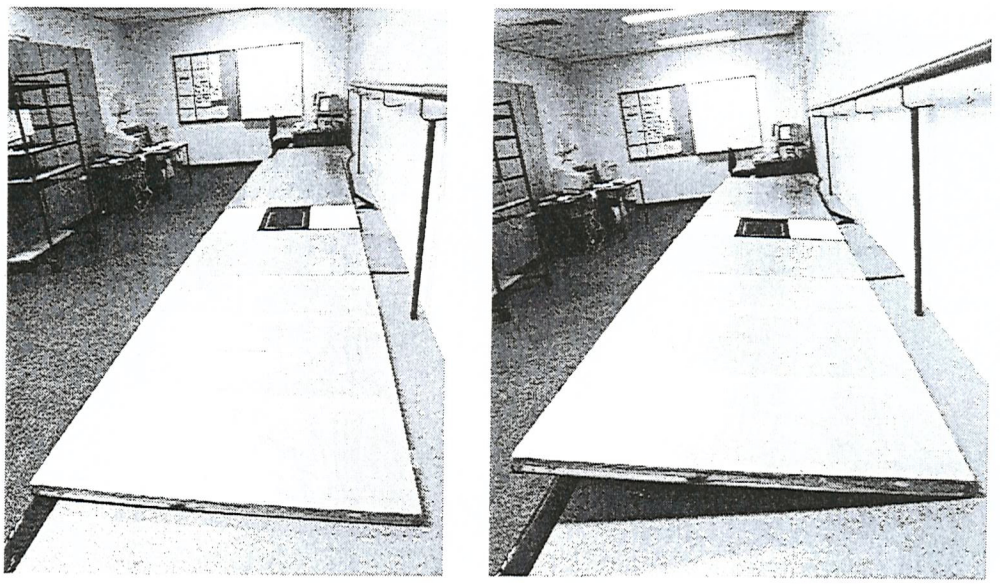

(a) (b)

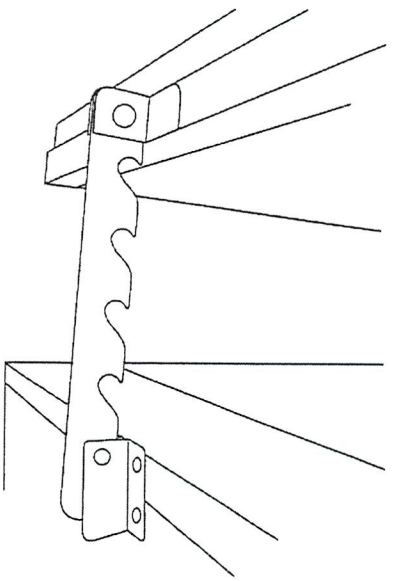

(c)

**Figure 3:13 Tiltable walkway**

(a) Walkway in level position, (b) walkway tilted at eight degrees, (c) detail of adjustment mechanism.

# 4. Methods

## 4.1. Introduction

The overall study consisted of four distinct investigations. For the first investigation a laboratory based evaluation of the performance of the conductive polymer sensors of the pressure platform was undertaken. In the second investigation, the performance of the platform was assessed, under a range of operational conditions, by comparing it with an alternative system. The third investigation used an analysis of footprints to determine the accuracy with which contact area could be measured with the pressure platform. Finally, in the fourth investigation, foot loading profiles were recorded for level and sideslope walking from a group of healthy young adults. Because of the clear distinctions between these investigations, the respective methods are dealt with separately. The methods are presented in the order indicated here.

## 4.2. Overview of polymer array test procedure

### 4.2.1. Selection of sample sensors

A sample of sensors was selected from the 2048 (64 rows x 32 columns) elements of the conductive polymer array. By excluding the two most peripheral columns and the four most peripheral rows, the sample was selected from the eighteen hundred central elements of the array. One sensor was randomly selected from each block of one hundred elements in the central region. Thus, a sample of eighteen sensors, representing the entire surface of the platform, was obtained.

### 4.2.2. Sensor alignment for testing

Two methods of alignment were trialed to evaluate the effect of positioning and repositioning on reliability. The aim with each method of alignment was to position the anvil precisely within the boundary of the contact area of one sensor element. The boundary of an element was clearly marked by the four adjacent conductive tracks, and these were easily visible through the transparent polymer membrane, figure 3.3.

#### 4.2.3. Visual alignment of anvil and sensor element

The first method, visual alignment, was a simple alignment by eye. The sensor array was positioned in the test rig and the contact mechanism was lowered until the anvil was just clear of the membrane surface (≈ 2 mm). The array was then manoeuvred until the sensor element appeared to be well aligned with the contact anvil, at which point the anvil was lowered and the relative alignment was subjectively assessed. If the alignment was thought to be unsatisfactory then the anvil was raised and the process was repeated. Once the alignment was judged to be satisfactory the array was clamped to the base of the test rig to prevent any displacement during testing.

#### 4.2.4. Template alignment of anvil and sensor element

The second method of positioning utilised an alignment template. This template was constructed from a 10 x 8 cm rectangle of 2 mm thick acrylic plastic sheet (Perspex). The template was placed onto the surface of the sensor array and positioned so that the marker lines registered with the conductive tracks of the polymer membrane. This ensured that the central aperture of the template was positioned precisely over a single element. Once the template was located accurately, it was temporarily fixed in place with adhesive tape. The sensor array and the attached template were then placed into the test rig and manoeuvred together until the anvil could slide smoothly through the template aperture. The array was then clamped to the test rig and the template was detached.

### 4.3. Static testing procedure for polymer array

Once the element had been correctly aligned and the array clamped firmly to the base of the test rig, the adjustment mechanism was extended until the anvil contacted the polymer membrane through a thin elastomeric sheet. This elastomeric sheet had been included with the platform by the manufacturer and was therefore retained throughout all of the tests. As contact occurred, the output from the proving ring transducer was observed to fluctuate slightly and, at this point, the adjustment mechanism and anvil were constrained by tightening the two locking screws. The initial contact pressure was kept to a minimum and was

always lower than the threshold pressure of the polymer sensor, the output of which registered no change.

Following the satisfactory adjustment of the loading mechanism, weights were added sequentially to the weight platform, with each weight being carefully located about the central spindle. Whenever a weight was added, the output from the polymer sensor was observed to change rapidly and then stabilise, at which time the output value was recorded. The sequence was repeated until the final weight had been applied and the maximum output recorded. The weights were then removed in the reverse order, recording the sensor output at each stage, until the output had returned to zero. The output from the proving ring was recorded each time a reading from the polymer sensor was obtained.

### 4.4. Dynamic testing procedure for polymer array

The polymer array was aligned and clamped to the test rig as in the static testing procedure, however, in contrast to the static tests, the adjustment mechanism was extended beyond the point of initial contact so that a pre-load was applied to the element. While the pre-load was being set, the anvil was unlocked so that it did not rotate with the adjustment mechanism but remained aligned with the polymer element. However, when the desired level of pre-load was reached, the locking screws of the adjustment mechanism were tightened so as to maintain both the alignment and the pre-load settings for the duration of the test.

Prior to pre-loading the sensor, the control amplifier for the electro-mechanical shaker was adjusted so that the frequency and power settings were both zeroed. Once the pre-load had been established, the frequency was increased gradually to the desired rate of oscillation. The power was subsequently increased until the required force amplitude, as determined from the output of the proving ring, was established. By following this method, an oscillating input force signal could be applied to the polymer sensor. A signal generator was used to produce the sinusoidal input signals feeding the control amplifier. When the dynamic test conditions had been established and the shaker armature was oscillating without producing vibration in the rig, the signals were recorded. Signals from both

transducers were low pass filtered with a cut-off at 50Hz, and sampled at 200 Hz. Analogue to digital conversion was at 8 bits.

The pre-load enabled the anvil to retain contact with the polymer sensor throughout the test and ensured that a smooth load-unload cycle was maintained within the constraints of the frequency:power envelope of the shaker. Without pre-load, the anvil lost contact with the sensor through one-half of the cycle, causing intermittent, poorly controlled impacts, and resulting in undesirable vibration through the rig. The impacts also had potential to damage the polymer membrane.

### 4.4.1. Signal analysis

The signals from the proving ring and the polymer sensor were analysed in both the time and frequency domains. The cross-correlation function was used as a measure of the similarity between the two signals [173] in the time domain. The frequency domain power spectra were compared in order to assess the linearity of the polymer sensor [174].

### 4.4.2. Cross correlation

The cross-correlation function, for a pair of stationary ergodic processes, can be defined as a time average:

$$R_{xy}(\tau) = \lim_{T\to\infty} \frac{1}{T} \int_0^T x(t)y(t+\tau)dt \qquad (173)$$

where x and y are the processes (records)
$\tau$ is the time shift between records
and T is the record length.

Since $T \neq \infty$, $R_{xy}(\tau)$ is estimated by

$$\frac{1}{T} \int_0^T x(t)y(t+\tau)dt$$

The normalised cross-correlation was used instead of $R_{xy}(\tau)$ since it scales the cross-correlation in terms of the root mean square values of the signals x(t) and y(t) [173]. The normalised cross-correlation is defined as:

$$r_{xy}(\tau) = \frac{R_{xy}(\tau)}{\sqrt{[R_{xx}(0)R_{yy}(0)]}} \qquad (173)$$

The analysis was undertaken using the xcorr (x, y, coeff) function in MATLAB. The coeff parameter normalises the sequence so that the autocorrelations at zero lag are identically 1.0, and the normalised cross-correlation is therefore expressed as a proportion of 1. If $R_{xy}(\tau)=0$ (in which case $r_{xy}(\tau)=0$) for all $\tau$, then the signals x(t) and y(t) are said to be uncorrelated. Normalised cross-correlations will therefore show values in the range zero to one, with one indicating perfect correlation.

### 4.4.3. Power spectral density

The power spectral density function was used to produce the power spectrum for each of the two signals. Each spectrum would contain frequencies in the range 0-100 Hz, the upper limit being half the sampling frequency (Nyquist frequency). From each spectrum, the power contained at any specified frequency could be determined as a proportion of the total spectral power. The characteristics of the proving ring signal (input spectrum) were compared with those of the polymer sensor signal (output spectrum), to assess the linearity of the polymer transducer. This assessment utilises the principle of sinusoidal fidelity exhibited by linear systems. For a linear system, sinusoidal wave input will generate sinusoidal wave output and both will have exactly the same frequency [174].

Since the transducer signals were discrete and periodic, the analytical approach was based on the Discrete Fourier Transform, and utilised a Fast Fourier Transform algorithm to generate the power spectra. The Fast Fourier Transform used 512 samples and rectangular windowing [174]. Signal analysis was undertaken with sinusoidal input signals between 4 and 26 Hz, and for amplitudes of about 280 and 500 kPa.

## 4.5. Shear testing procedure for both platforms

Shear tests were conducted with the pressure platform recessed firmly in a wooden surround to prevent displacement during testing. The platform remained connected to the host computer and all output data were derived from the system software. The aluminium test rig was placed on the upper surface of the platform and aligned squarely with the sensor matrix. The normal load was applied to the frame by a 20 kg mass that was lowered smoothly but quickly into position using a pulley system. A cable, connected to the front of the frame, followed a horizontal course to a pulley and then descended vertically to a shackle from which a second mass was suspended. This pulley system was used to generate the shear force. The shear force was applied once the normal load was in place.

Tests both with and without the shear were conducted. Six replicates of each loading condition were recorded, and the loading conditions were then altered for the subsequent test. The order of testing was; zero-shear, 25% shear, zero-shear, 50% shear, zero-shear. The frame was left in-situ throughout the entire procedure. Proportional values of shear indicate the relative magnitudes of the horizontal (shear) and vertical (normal) forces. Since vertical load was applied with a mass of 20 kg, 25% shear was achieved with 5 kg and 50% with 10 kg.

## 4.6. Comparison of pressure platform performance in operation

Analysis of results from the shear tests indicated that the polymer sensor pressure platform was sensitive to shear. To determine the impact that this characteristic would have on loading profiles of the foot, a comparison was undertaken with a second platform that used alternative transducer technology. A sub-group of nine individuals from the main cohort of volunteers was assessed with both pressure platforms. Data for both level and sideslope walking was obtained according to the protocol adopted for the main study of sideslope walking. A two factor general linear statistical model (GLM) was used to identify differences between the two systems for both level and sideslope walking conditions. All dependent variables were further examined using the Bland and Altman [175] method for assessing agreement between two measurement techniques.

## 4.7. Use of footprints for the measurement of contact area

Footprints were used to determine estimates of the foot-ground contact area. Ink footprints on paper templates and electronic footprint images from the pressure platform were obtained. The area contained by the ink footprint outline gave the most precise estimate of contact area and was used as a benchmark. By calculating the difference in area between the ink and electronic footprints, an indication of the measurement error of the pressure platform could be derived. While this method could establish the error of the measurements from the platform, it could not determine the relative influence of contributory factors such as spatial resolution. The effect of spatial resolution was therefore investigated separately to determine the smallest error that could be expected using 5x6 mm sensors. To achieve this, ink footprints were collected on imitations of the polymer array. The imitations were paper templates onto which a grid pattern, dimensionally identical to the sensor array, was printed. Estimates of contact area were derived by counting the ink stained rectangles of these latticed paper-templates, figure 4.1

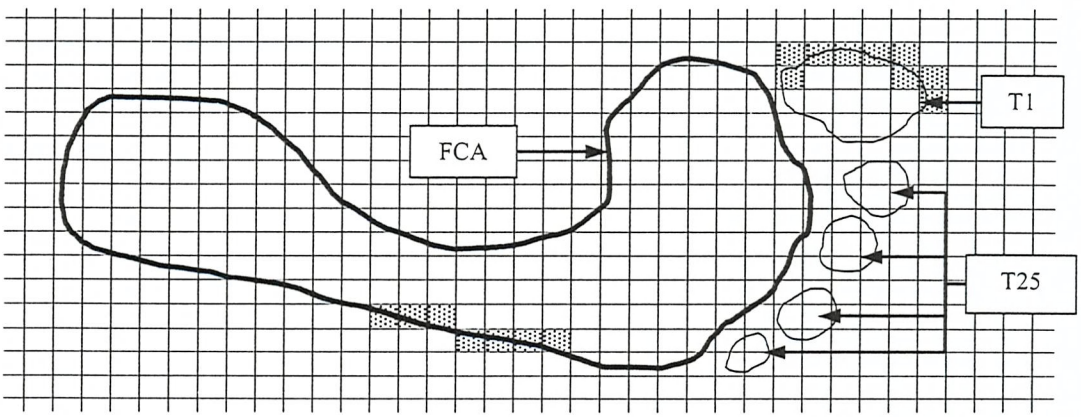


**Figure 4:1 Schematic representation of footprint on lattice template**

Ink footprints were obtained on latticed paper-templates as shown (grid not to scale). Contact areas were estimated using a planimeter to trace the outlines of the sole and the toes. Further estimates of contact areas were determined by counting the grid rectangles. One estimate included the full area of the peripheral elements, while the second method weighted their contribution by 50%. Examples of the peripheral elements are shaded. The foot contact area (FCA) excluded the toes and is indicated by the bold line. The contact area for each toe was derived separately, but the lesser toes (T25) are reported as a group. The total footprint area was the sum of FCA, hallux (T1) and the lesser toes (T25).

The use of templates avoided any possible confounding effect of sensor threshold. Estimates obtained from the latticed template were therefore considered definitive of the achievable accuracy for systems with this spatial resolution. A difference between the smallest achievable error by the templates and the actual error by the platform would indicate that the operational sensors or the system hardware were functioning at a sub-optimal level. The influence of transducer sensitivity on contact area measurement was investigated by gathering footprints from the pressure platform after the polymer array had been modified so that the sensor threshold could be adjusted. Change in contact area measurement with altered threshold was assessed using a repeated measures analysis of variance. Finally, the arch index was calculated for both electronic and ink footprints to determine any difference between the two methods.

### 4.7.1. Collection of footprints

The vinyl fabric cover of the pressure platform was removed and a latticed paper-template was placed on the surface of the sensor array. The paper template was centrally positioned and fixed in place with adhesive tape. Care was taken to ensure that the grid pattern on the template was aligned precisely with the grid of the underlying sensor array. The latticed templates were dimensionally identical to the platform sensors because they were produced from a lithographic film copy of the polymer array. The elastomeric membrane, incorporated into the platform by the manufacturer, was left in-situ.

The pressure platform was positioned flush with the surrounding surface and a foam rubber pad, moistened with water soluble ink, was placed in a shallow tray directly behind it. The volunteer inked their barefoot, then stepped slowly onto the paper covered platform, holding their left foot just clear of the ground. A support was available to aid their balance, and the entire manoeuvre was completed smoothly. The pressure platform was triggered automatically by the foot contact and data were collected for a period of about three seconds. When the footprint was retrieved, the border of the ink image was immediately outlined in pencil to ensure that any future distortion or spread of the ink could be ignored. If, during any trial, the subject was observed to sway excessively, or

if the ink footprint was found to be smudged then those trials were discarded. The footprint was considered representative of single limb static stance.

## 4.8. Estimation of contact areas from footprint images

Three procedures were used to obtain estimates of contact area; planimetric, electronic and grid-counting. The planimetric procedure gave a value for contact area based on the precise outline of the inked print. The electronic procedure gave an estimate from the platform as determined from the activated sensor elements. The grid-counting procedure derived an estimate from the ink stained rectangles on the latticed paper-template. For the purpose of contact area analysis, the sole of the foot was considered as a whole, the lesser toes were grouped together, and the first toe was measured separately. Descriptive statistics for the regions of the foot (T1, T25, FCA and total area, figure 4.1) were determined with each method.

### 4.8.1. Footprint area estimation: planimetric procedure

A planimeter was used to trace the outline of the ink footprint and an estimate of the area was obtained. The mean of three measurements was taken and this value was used for statistical purposes. Before use the planimeter was calibrated using the tool supplied by the manufacturer.

### 4.8.2. Footprint area estimation: latticed template procedure

Contact area was determined by counting the number of elements (rectangles) on the latticed template that were stained with ink, figure 4.1. Peripheral elements were counted as contributing in full (maximum-count, $C_{max}$) or weighted at fifty percent (weighted-count, $C_{wt}$). The two estimates of contact area, $C_{max}$ and $C_{wt}$, were compared with estimates obtained with the planimeter. The number of peripheral elements contributing to an estimate of area was derived as a proportion of the number of central elements (peripheral / central), and the resulting quotient was termed the peripheral element ratio (PER).

4.8.3. Footprint area estimation: electronic procedure

An estimate of contact area was derived from the pressure platform by counting the activated sensors indicated on the relevant regions of the Maximum Pressure image produced by the system software. Contact area was calculated as the product of the sensor count and the area of a single element.

## 4.9. Modification of the polymer array

Analysis of results from some early tests indicated that the sensor had a higher threshold than expected. This observation was constructive in devising a method of modifying the sensor so that the threshold could be adjusted while the sensing area remained unobstructed. In its standard form, the upper and lower membranes of the polymer sensor are separated by an air filled gap. Decrease in electrical resistance results when external pressure depresses the upper membrane sufficiently for it to contact the lower conductive substrate. When the internal air is displaced it can escape from the sensor through small vents at the margin of the array. By bonding a small bore cannula into one of the vents and sealing the others, the internal air could be extracted with a vacuum pump. The relatively low internal pressure deflected the sensor membrane in a similar way to an externally applied pressure. A vacuum control valve was used to regulate the internal pressure. The modified sensor was tested through a vacuum pressure range of 0-70 kPa. Profiles, indicating the deflection of the surface membrane of the polymer sensor, were recorded through the pressure range.

## 4.10. Arch index

The arch index (AI) was charted from inked footprints using the method described by Cavanagh and Rodgers[25]. Essentially, the long axis of the footprint was determined, and the foot contact area (FCA) was then subdivided into thirds. The planimeter was used to obtain measurements of the central third of the FCA and the entire FCA. The arch index from the footprint was calculated as AI =B/(A+B+C), figure 4.2. The arch index for the electronic footprint was derived in a similar way. However, in the electronic prints the border between two adjacent zones usually transected a number of sensor elements. Only fifty percent of the area of these transected elements was considered to contribute to

the central region. The area of the central region was therefore estimated from the total of the respective whole elements summed with half of the border elements.

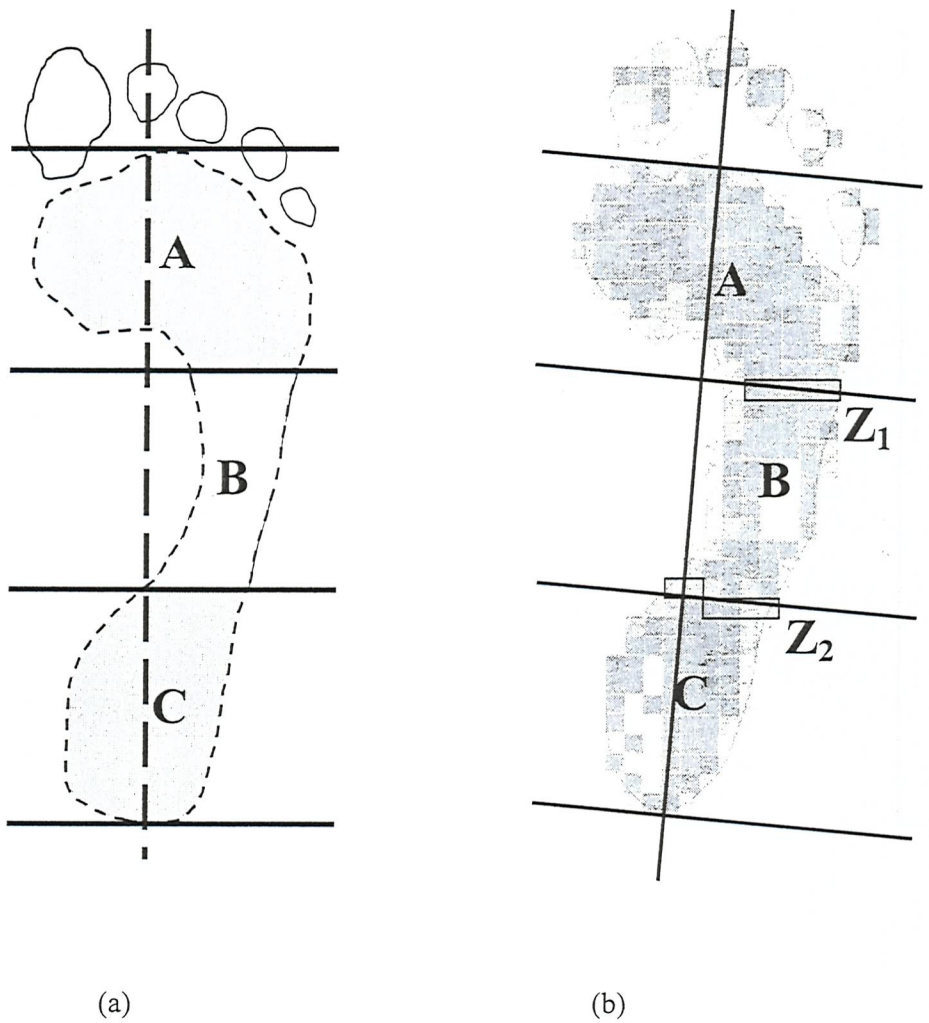


(a) (b)

**Figure 4:2 Arch index for ink and electronic prints**

The foot contact area (FCA) excluded the toes and is indicated by the hashed line (a). The arch indices were calculated as AI = B/(A+B+C), and the toes were excluded in each case. In the electronic print, the sensor elements which cross the boundaries at $Z_1$ and $Z_2$ influence the determination of the magnitude of areas A, B and C separately, but have no effect on the total area (A+B+C) as a whole.

## 4.11. Investigation of sideslope walking

### 4.11.1. Subject details

Thirty young healthy volunteers participated in the walkway study, fifteen males and fifteen females. The mean (sd) age, weight and height were, 23.9 (2.6) years, 69.3 (12.7) kg, and 176.1 (10.5) cm, respectively. Subjects were excluded from participation if they had a history of lower limb surgery, foot deformity, evidence of neuromuscular disease, difficulty with balance, or obviously restricted motion of the subtalar joint. Ethical clearance was obtained and, in compliance with the guidelines, all subjects received verbal and written information concerning the study (appendix 2). Informed consent was obtained before data collection occurred.

### 4.11.2. Inclined walkway protocol

During a familiarisation period, the subject was given an opportunity to walk along the inclined walkway, but the surface was returned to the level position for the initial data collection. The subject was positioned about three-and-a-half meters from the centre of the pressure platform, which was visible, and asked to walk to the far end of the walkway at their usual walking speed. The starting position was iteratively adjusted to ensure appropriate placement of their right foot on the pressure platform without any obvious need for targeting. Similar starting positions were established at each end of the walkway, so that walking trials could be conducted across the pressure platform in either direction. Data recording commenced once the subject appeared at ease and the stance phase duration for three consecutive trials varied less than 30 milliseconds [77].

The procedure was repeated for each angle of tilt, in ascending order to 8°, however, the starting positions were not altered when the incline was changed. Whenever the walkway was adjusted, the subject was given time to feel secure and, when their stance phase durations demonstrated consistency again, data collection then recommenced. The subject was encouraged to walk close to the mid-line of the walkway whenever it was tilted, so as to avoid any tendency to drift down the slope. By walking in each direction along the tilted walkway, the

right foot was placed either relatively high on the slope (the upslope position) or low on the slope (the downslope position), figure 1.1.

Trials were repeated if atypical foot placement, targeting, down-slope drift, or hesitation of the gait was observed. Twenty-seven data sets were recorded for the right foot of each subject, (3 replicates x (1 level, 4 upslope, and 4 downslope conditions)).

4.11.3. Footprint masking

The electronic footprints were masked (sub-divided graphically) to facilitate an analysis of the loading characteristics of six regions of the foot, figure 4.3. The six regions represented the heel, midfoot, first-metatarsal, central-metatarsals, fifth-metatarsal and first toe. Apart from their structural relevance, these six sites are probably those most often selected in contemporary foot pressure studies[79,93,94,99]. The length of the footprint, excluding the toes, was divided into three parts, representing the heel, midfoot and metatarsal regions. The number of rows of sensors indicated on the footprint determined the division and, when possible, the three parts were of equal length. For example, forty-five rows of sensors would be sub-divided into three regions (masks), each fifteen sensors in length. However, when the length was not exactly divisible by three, then the heel and metatarsal regions were always allocated equal lengths, and an adjustment was made to the midfoot region.

The metatarsal portion was further sub-divided, by width, into three parts, representing the first metatarsal, central metatarsals, and fifth metatarsal. This division was determined by the number of columns of sensors seen across the width of the metatarsal region of the footprint. Each of the five metatarsals was apportioned one-sixth of the total width, with the exception of the first metatarsal, which was apportioned two-sixths because of its relatively large size. Thus, the first metatarsal, central metatarsal and fifth metatarsal regions accounted for two-sixths, three-sixths, and one-sixth of the overall width, respectively.

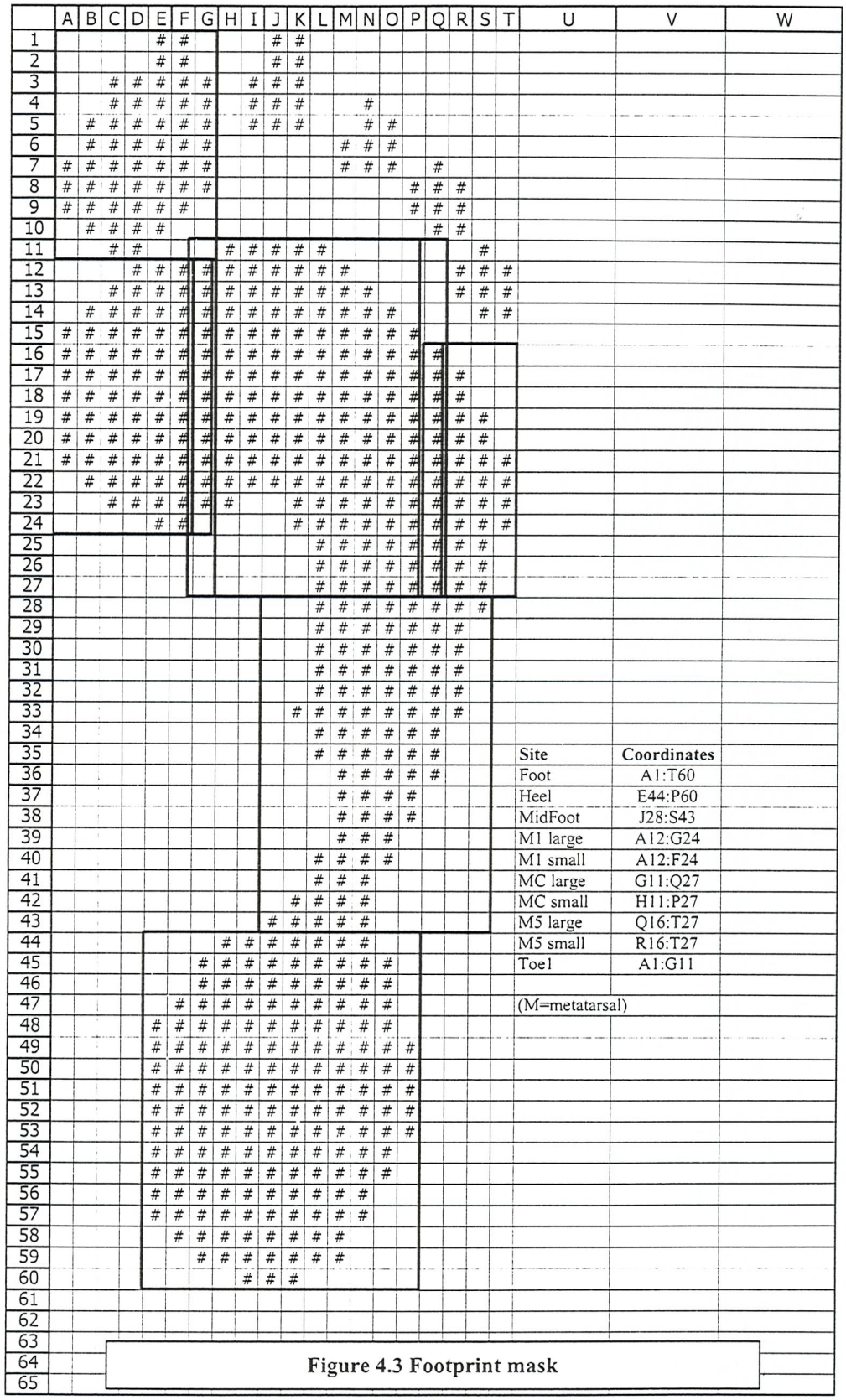

| Site | Coordinates |
|---|---|
| Foot | A1:T60 |
| Heel | E44:P60 |
| MidFoot | J28:S43 |
| M1 large | A12:G24 |
| M1 small | A12:F24 |
| MC large | G11:Q27 |
| MC small | H11:P27 |
| M5 large | Q16:T27 |
| M5 small | R16:T27 |
| Toe1 | A1:G11 |

(M=metatarsal)

**Figure 4.3 Footprint mask**

When the metatarsal width was exactly divisible by six, then the width of each metatarsal mask could be defined by an integer number of sensors. For example, a metatarsal region eighteen sensors wide would determine that the first, central and fifth masks would be exactly six, nine and three sensors wide, respectively. However, when the width was not exactly divisible by six, then two mask definitions for each metatarsal site were determined, one being the integer over-estimate and the other being the integer under-estimate. Therefore, for many footprints, two masks were defined for the first, central and fifth metatarsal sites (M1, Mc, M5 respectively). Final values for each site were then derived as the average of the under and over-estimates. This procedure ensured that the greatest error possible for the width definition of a metatarsal mask was approximately one-third the width of a single sensor, ie ≈1.7 mm. An example of width determination is given in table 4.1.

**Table 4:1 Error estimation for metatarsal masking technique**

The maximum masking error never exceeded one-third the width of a sensor when the width of a metatarsal sub-region was derived as an average of two estimates.

| Metatarsal width (N sensors) | N/6 | Under-estimate (U sensors) | Over-estimate (O sensors) | Average ((U+O)/2) | Error (U+O/2)-(N/6) |
|---|---|---|---|---|---|
| 18 | 3.00 | 0 | 0 | 3.0 | 0.00 |
| 19 | 3.17 | 3 | 4 | 3.5 | 0.33 |
| 20 | 3.33 | 3 | 4 | 3.5 | 0.17 |
| 21 | 3.50 | 3 | 4 | 3.5 | 0.00 |
| 22 | 3.67 | 3 | 4 | 3.5 | 0.17 |
| 23 | 3.83 | 3 | 4 | 3.5 | 0.33 |
| 24 | 4.00 | 0 | 0 | 4.0 | 0.00 |

The masking technique for an electronic footprint produced nine masks (Hl x1, MdFt x 1, M1 x 2, Mc x 2, M5 x 2, T1 x1), each defined by a pair of coordinates. The coordinate list was input to the analysis software at the time of processing, and outcome measures were then derived automatically for each mask. Where two masks represented a single region of the footprint, then averages of each pair of dependent variables were calculated.

### 4.11.4. Measurement of the foot placement angle

The angle of alignment of the foot on the pressure platform was referred to as the foot placement angle (FPA). It was derived from the electronic footprint image by drawing a tangent to the inner border of the footprint, along the edge of the heel and first metatarsal sites, and measuring the angle it made with the longitudinal axis of the platform.

### 4.11.5. Reduction and analysis of data from sideslope walking

The system software operating with the pressure platform lacked the facility to mask the footprint. Therefore, a commercial spreadsheet (Microsoft Excel) was customised to allow semi-automated analysis. The spreadsheet was adapted by developing a series of subroutines, figure 4.4 within the native programming language (Visual Basic). Using this approach, each footprint had to be masked individually, but the appropriate values of the dependent variables for each region were then extracted automatically

Data files were transferred in their entirety in ASCII format, using the export utility of the system software, and subsequently used within the spreadsheet. Data in the exported files were arranged as a series of consecutive blocks, or arrays, with each array containing the values gathered during one scan of the surface of the pressure platform. A second export format (maximum pressures format), produced a file with a single matrix of data containing the maximum values detected throughout the entire period of loading. The maximum pressure file was exported, and the matrix printed, to produce the electronic footprint from the pressure platform, figure 4.3. This footprint image was subsequently used to determine the appropriate masking coordinates for the step.

*(1) Setup*

Clears all working spreadsheet areas, inserts column headings and formulae, defines variables and sets constants etc.

*(2) Import Data*

Selects data-file containing sequential scans of data (each scan is formatted as a matrix of known dimensions).

*(3)Input Mask*

Inputs mask coordinates for regional division of footprint. Inputs matrix (scan) dimensions and number of scans in data file.

*(4) File Preparation*

Removes file header details, separators etc.

*(5) Import Matrix*

Copies leading matrix (scan) from data-file and imports it into the main calculation spreadsheet. Deletes copied matrix from data-file and increments all remaining data

*(6) Data Extraction*

Locates and extracts or calculates all required dependent variable data from each foot-site in accordance with mask ordinates.

*(7) Data Storage*

Outputs all selected data to a separate spreadsheet for storage.

*(8) Clear Mainsheet*

Clears main calculation spreadsheet in preparation for next matrix (scan).

*(9) Loop*

Repeats processes 5 to 9 until all scans in current data-file are processed.

**Figure 4:4 Data processing flow chart**

Shows main stages for the extraction and storage of the dependent variables obtained in accordance with the mask.

### 4.11.6. Software development and testing

The analysis software was developed on the basis of the outline shown in figure 4.4. A data file consisted of a series of arrays, each containing the data from one scan of the platform. Usually there were about forty arrays in a single file. The core of the program was structured as a loop that was conditioned to execute until all arrays had been processed sequentially. An array was selected, masked using the previously derived ordinates, dependent variables from each foot site were extracted and stored. The spreadsheet was then automatically cleared in preparation for the next array. The program was tested by processing data files from an Emed SF pressure platform and comparing the results to those obtained using the commercial analysis software. An abridged version of the analysis software, showing only the core modules and restricting the code to one site of the mask, is contained in appendix 3.

### 4.11.7. Statistical analysis of data for sideslope walking

A within subject repeated measures experimental design was adopted for the main study of sideslope walking. The central aim was to establish the effects of sideslope walking on load at selected sites of the foot. A general linear statistical model (GLM) with repeated measures was developed. Differences between the level and sideslope walking conditions for particular sites were not investigated until the assumptions supporting the model were met, and then contrasts were used to establish significance.

The general procedure for the analysis was as follows:

1. Each outcome variable was isolated and it was established whether the data were normally distributed. Non-normally distributed data were segregated and excluded from the main model.

2. A correlation matrix was produced for all normally distributed outcome variables, and all significant correlations were identified. If a correlate was considered to emulate or duplicate an alternative outcome variable then it was excluded from further analysis.

3. For each of the selected outcome variables, the site specific data sets that demonstrated normal distributions were grouped and a GLM univariate test was conducted. This revealed whether significant site-by-slope interaction occurred for that variable.

4. Within site GLM univariate tests were then conducted for each site where significant site-by-slope interaction had been confirmed. The F values and significance levels (p values) obtained from the site specific tests of the within subject contrasts were used as the criteria for statistical significance. All tests for significance compared the incline conditions with the level condition. No tests for significance between incline conditions were conducted.

In total, 810 trials (30 subjects x 3 steps x 9 inclines) were processed for the statistical analysis of eight outcome measures for six sites of the right foot. Details of the sites of the foot and the outcome measures are given in table 4.2.

**Table 4:2 Statistical analysis: dependent variables and foot sites for masking procedure**

| Foot sites | Magnitude variables | Timing variables |
|---|---|---|
| Heel | Peak pressure | Initial contact time |
| Midfoot | Average pressure | Duration of contact |
| First metatarsal | Contact area | Time to peak pressure |
| Central metatarsals | Peak force | Time to peak force |
| Fifth metatarsal | | |
| First toe | | |

### 4.11.8. Assessment of normal distribution for statistical analysis

Each dependent variable was tested against a list of criteria in order to assess whether the data could be considered to approximate to the normal distribution. The mean, standard deviation, median, minimum and maximum descriptive statistics were derived, as were the skewness and kurtosis coefficients, and the frequency histogram was plotted. The Kolmorgorov-Smirnov test for normality was also applied.

The initial assessment for normal distribution sought to fulfil the following criteria:

the mean and the median should be within 10% of each other,
the standard deviation should be less than, or equal to, half the mean,
the skewness and kurtosis coefficients should be within the range, -2 to 2,
the Kolmorgorov-Smirnov test should return a non significant result.

If all of the above criteria were met, then the data were considered to approximate the normal distribution and were included in the main statistical model. If some, but not all, of the criteria were met, then a subjective decision to include or exclude the data had to be made. For example, a data set may have fulfilled all of the criteria with the exception of the kurtosis coefficient, which may have exceeded the desired range or, alternatively, the standard deviation may have exceeded fifty percent of the mean. In the first case, the data could still have been considered as a reasonable approximation to the normal distribution, while in the latter instance the data would have been excluded.

For any particular variable-site combination (eg. peak pressure-first metatarsal), the rejection of some but not all of the nine condition data sets (slope angle) would have meant that the main hypothesis could not have been tested fully. Therefore, subjective acceptance of a data set that had failed to fulfil all of the selection criteria was enhanced in the event that the majority of the nine sets, for that variable-site combination, approximated the normal distribution.

# 5. Results

## 5.1. Introduction

Results are presented in four main sections, one section relating to each of the major investigations conducted as part of the overall study. The first section presents results relating to laboratory tests of the conductive polymer sensors. Performance data regarding responses to static, dynamic and shear loading conditions are reported. The findings from these tests informed the direction for a subsequent assessment of the platform under actual operating conditions. The results of this assessment are presented in the second section, a comparison of platforms. The third section presents results from an investigation of footprints that determined the accuracy with which the contact area of the sole of the foot could be measured. The influence of spatial resolution and transducer sensitivity is also presented here. Finally, results are presented from a study of level and sideslope walking. The final section includes the findings for temporal parameters, contact area, peak pressure and regional force. Descriptive statistics for the foot progression angle are included in the final section.

### 5.1.1. Rationale for the presentation of results in kilopascals

Although a force transducer was used as the reference for comparison with the polymer sensor output, the results of the tests are presented in terms of pressure (kPa). The average pressure was calculated as the product of the input force and the contact area of the anvil which, for the results presented here, was constant at 0.3 $cm^2$. The results therefore simply reflect the input force as derived from the reference transducer scaled by a constant of proportionality. This practice was necessary because the polymer sensors were sensitive to both force and area of contact independently [39,40] and, therefore, their output altered if a contact anvil of a different size was used. In addition, results expressed in kilopascals were attuned with the output format of the platform because the system software returned measurements in terms of pressure, reflecting the calibration method used by the manufacturer. Also, by using units of pressure, the test results could be interpreted with respect to the performance of the operational system and to the values obtained during the study of level and sideslope walking. Furthermore, they could be more readily compared with previous reports

regarding both sensor performance and clinical findings. Overall, this approach accords well with the convention recommended by Cavanagh *et al.* [31].

## 5.2. Test results for the polymer sensor

The polymer sensors were subjected to a series of tests to determine their responses to normal static loading, normal static loading with a simultaneously applied orthogonal shear, and dynamic loading. In addition, because of the obvious ease with which the sensor could be distorted, an attempt was made to determine the profile of the surface membrane in both the unloaded and loaded conditions.

### 5.2.1. Polymer membrane profile test results

Polymer sensors are constructed from two membranes and, when sufficient pressure is applied, the upper one deflects downwards to contact the lower. Because the polymer membranes are very thin and flexible, the contour of the deflection will vary across the surface of the sensor element. The least deflection occurred near the periphery of the element (where the membrane is elevated by underlying electrically conductive tracks and insulation pads, figures 3.1 to 3.3) and the greatest deflection occurred at the centre. Downward deflection, or hammocking, of the membrane was particularly obvious when the air was partially evacuated from the internal space of the sensor. Partial evacuation of the air produced a dimpled appearance across the surface of the pressure platform, figure 3.3. A surface profiling machine was used to trace the profiles of several sensor elements, and profiles were obtained both with and without a partial vacuum of the internal air space. By adjusting the pressure of the vacuum, the membrane deflection changed and the profiles altered. The profiles of two of the sensor elements are shown in figures 5.1 and 5.2.

Without vacuum adjustment, the upper membrane of the sensor appeared slack and sagged slightly, but this was insufficient for it to make contact with the lower substrate. When a low pressure vacuum was applied (≈10 to 20 kPa), the upper membrane hammocked noticeably and a parabolic profile resulted.

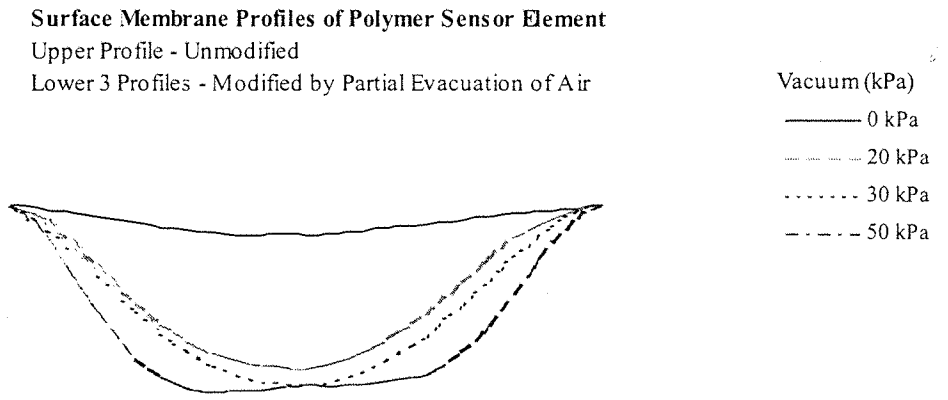


**Figure 5:1 Polymer membrane profile: symmetrical**

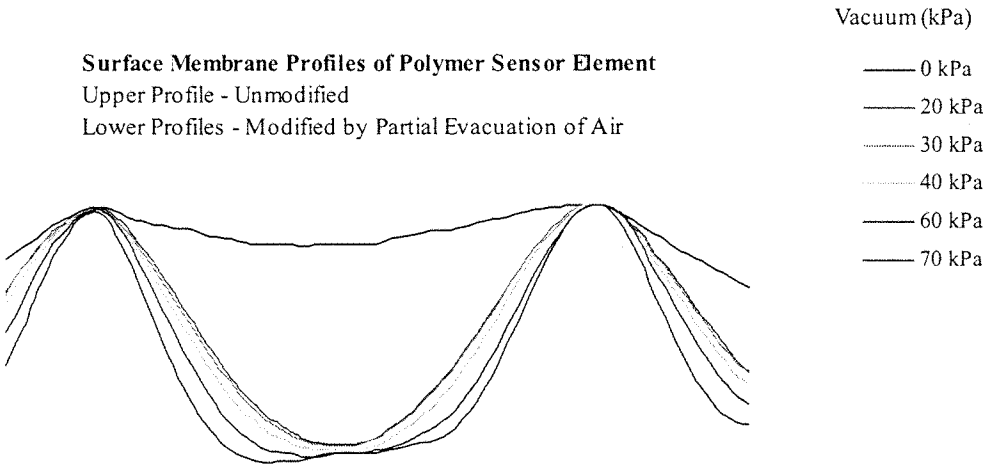


**Figure 5:2 Polymer membrane profile: asymmetrical**

The vacuum caused a simultaneous deflection of the membrane over all sensor elements of the platform and this took up the slack giving the top surface a slightly tense but dimpled appearance. The hammocking of the membrane progressed as the vacuum was increased, until a maximum downward deflection was reached, figure 5.1. This was assumed to be the point at which the upper membrane contacted the lower substrate. The profile continued to alter with the vacuum until the membrane contour flattened noticeably, distorting the parabola and producing a dish-shaped depression, figure 5.1.

In some elements, the flattening of the membrane beyond the point of initial contact was symmetrical and the profile developed a relatively even central region, figure 5.1. However, in other elements the profile became asymmetric and uneven, figure 5.2. If the cause of the irregular contour had been within the upper membrane, it is thought likely that the distortion would have appeared in the profiles for relatively low pressures. It was concluded, therefore, that the distortion of some profiles was due to unevenness of the substrate on the lower membrane.

### 5.2.2. General response to static loading

The results from the static tests were obtained by step loading the sensor elements using the main test rig. Descriptive statistics derived from the sample of eighteen sensors are reported, but examples from individual elements have been used for illustrative purposes. A typical test result is shown in figure 5.3. In this example, the simultaneously acquired output from the proving-ring has been included for comparison. The polymer sensor was subjected to a single load-unload cycle, by step loading to a maximum pressure of about 2.0 MPa. The polymer sensor was neither preconditioned nor modified in any way, and the elastomeric cover, fitted to the platform by the manufacturer, was left in-situ over the sensor surface.

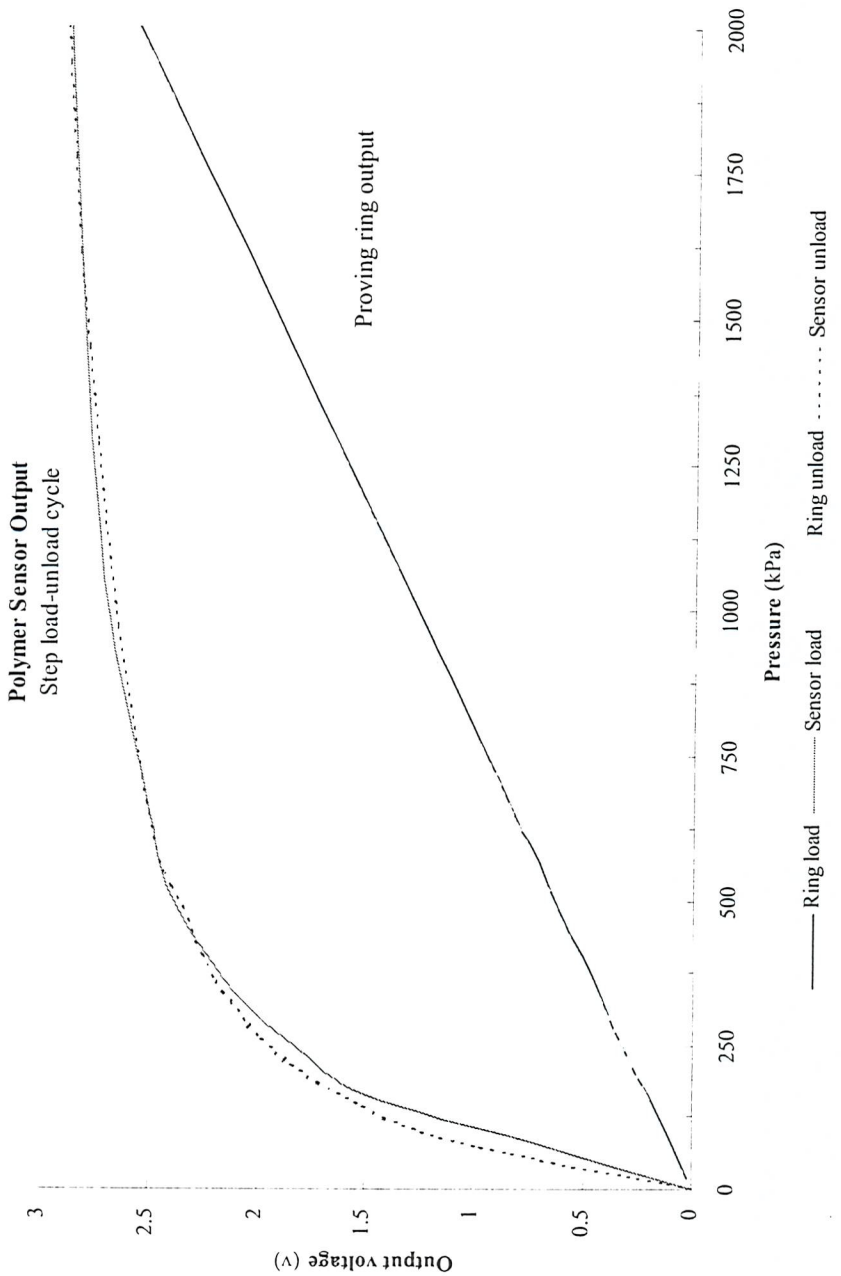


**Figure 5.3 Polymer sensor static loading graph**

The initial part of the loading curve of the polymer sensor, to about 200 kPa, was fairly linear. This zone varied between sensor elements but in general was estimated to cover a range of 250 to 300 kPa. In one case, however, it was observed to extend to almost 400 kPa. A second zone where the sensor output was noticeably curvilinear followed the initial rise. This zone extended upto about 800 or 1000 kPa, depending on the element. Beyond 1000 kPa the profile became relatively linear again. One or two sensors near the periphery of the sensing area of the pressure platform were subjected to deliberate overloads in excess of 3.5 MPa. They demonstrated no apparent difference from other elements, while confirming that beyond 1000 kPa the output plateaued. The unloading curve followed the general shape of the loading curve, although the two tended to separate slightly in the pressure region below about 500 kPa. The unloading curve usually appeared to be smoother than the equivalent loading curve.

In comparison with the polymer sensor, the reference transducer output was observed to be highly linear throughout all tests, figure 5.3.

### 5.2.3. Within sensor variation and effects of positioning

An assessment of the effects of repositioning the polymer sensor relative to the reference transducer was undertaken by moving and repositioning the sensor element between tests. The results of the tests were compared to a control situation where repeated tests were conducted without altering the position of the sensor. The tests without repositioning were used to derive values for the within sensor repeatability.

The average effects of repositioning between subsequent loading tests are demonstrated, along with the control results, in figure 5.4. With the polymer sensor left in-situ between tests, the maximum coefficient of variation (cv) was about 8.0% and occurred at the lowest test pressure of 80 kPa. For pressures above about 150 kPa, the cv remained below 5.0%. When the polymer sensor was moved and repositioned using the alignment template, then the maximum cv increased to almost 12.0%, and this was again observed at the lowest test

pressure. The cv for template positioning fell to ≈6.0% for pressures of about 165 kPa and remained below 5.0% for pressures above 250 kPa.

When the polymer sensor was repositioned without the use of any alignment device and the relative position to the reference transducer was judged visually, then the maximum cv increased to 22.0%. For the visual alignment method, a cv of less than 5.0% was not achieved until the sensor was subjected to pressures in excess of 400 kPa.

In comparison to these results, the reference transducer demonstrated a maximum cv of 1.0%, occurring at the 80 and 160 kPa pressure levels, and this reduced to about 0.5% for pressures of 250 kPa and above.

The coefficients of variation derived from measurements obtained during unloading, revealed a similar pattern to those of loading but were generally smaller. Overall, the maximum cv for unloading was 4.0%. The within sensor coefficients of variation derived from five test cycles of each of the eighteen sample sensors for both loading and unloading are shown in figure 5.5, and in table 5.1. Both the coefficients of variation and the standard deviations were greater for loading than unloading, and these differences are clearly demonstrated in the single sensor example of figures 5.6 and 5.7.

**Table 5:1 Within sensor coefficients of variation (cv%)**

| | Loading | Unloading |
|---|---|---|
| Mean | 2.21 | 0.92 |
| StDev | 0.66 | 0.12 |
| Min | 0.38 | 0.15 |
| Max | 8.47 | 4.03 |

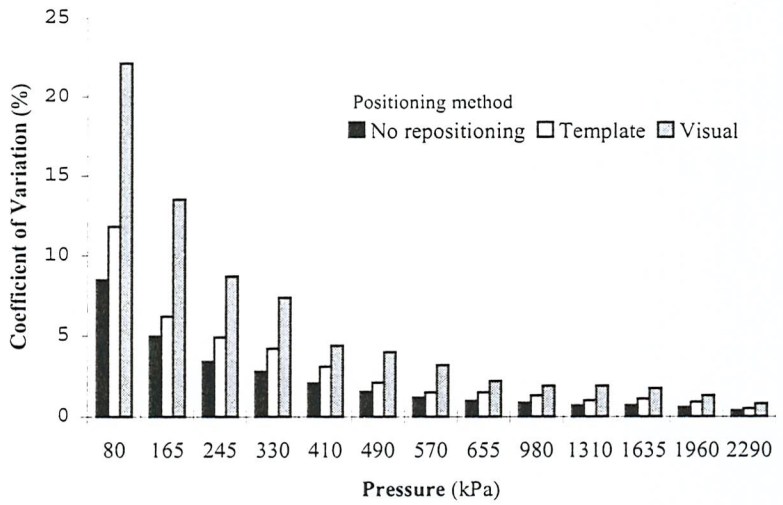


**Figure 5:4 Sensor repositioning effects**

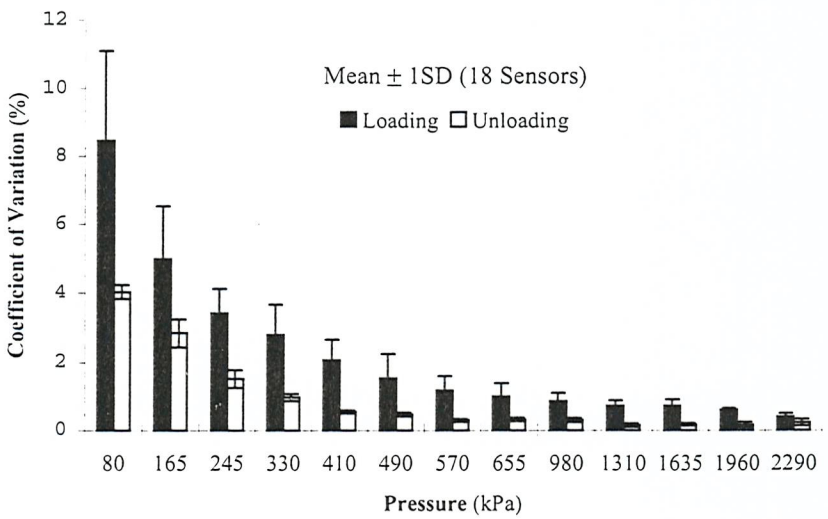


**Figure 5:5 Within sensor variation**

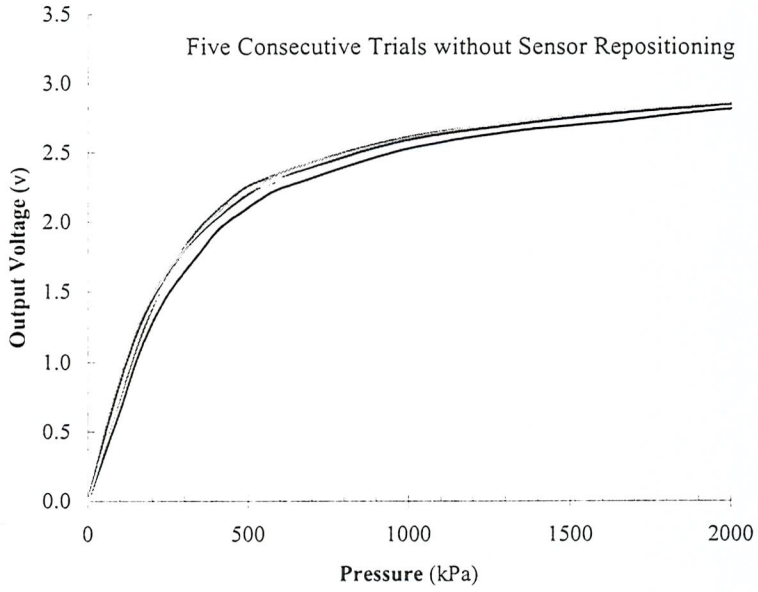


**Figure 5:6 Polymer element response to repeated loading**

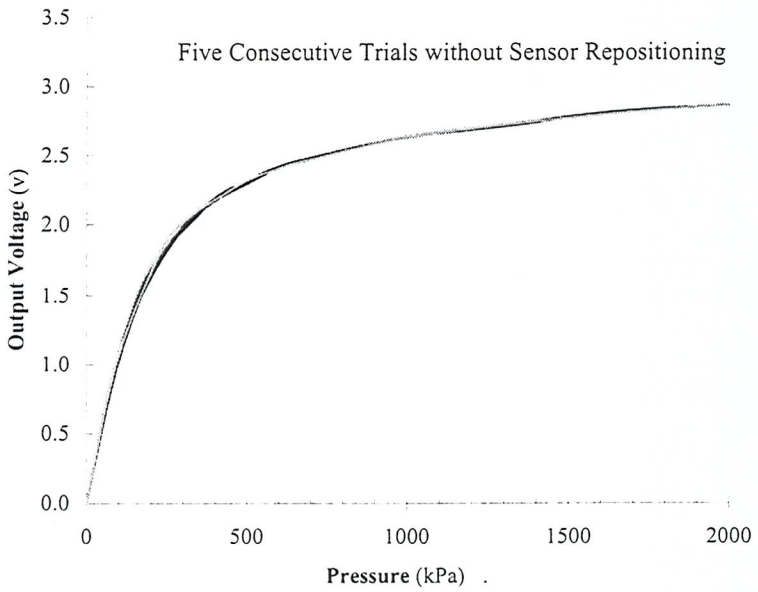


**Figure 5:7 Polymer element response to repeated unloading**

### 5.2.4. Between sensor variation

Having established the response characteristics of individual sensor elements, it was possible to determine an estimate of the between sensor variation over the sensing area of the pressure platform. The between sensor coefficients of variation are given in table 5.2, and figure 5.8. The maximum cv was ≈18.0% and occurred for loading at the lowest test pressure level. The coefficients of variation for loading remained above 10.0% for pressures below 300 kPa and only approached 5.0% for pressures above 1 MPa. The between sensor variation for the unloading condition was essentially the same as for loading although the variation was, in general, slightly less.

**Table 5:2 Between sensor coefficients of variation (cv%)**

| | Loading | Unloading |
|---|---|---|
| Mean | 8.34 | 7.56 |
| StDev | 4.03 | 2.92 |
| Min | 4.97 | 5.03 |
| Max | 18.18 | 15.28 |

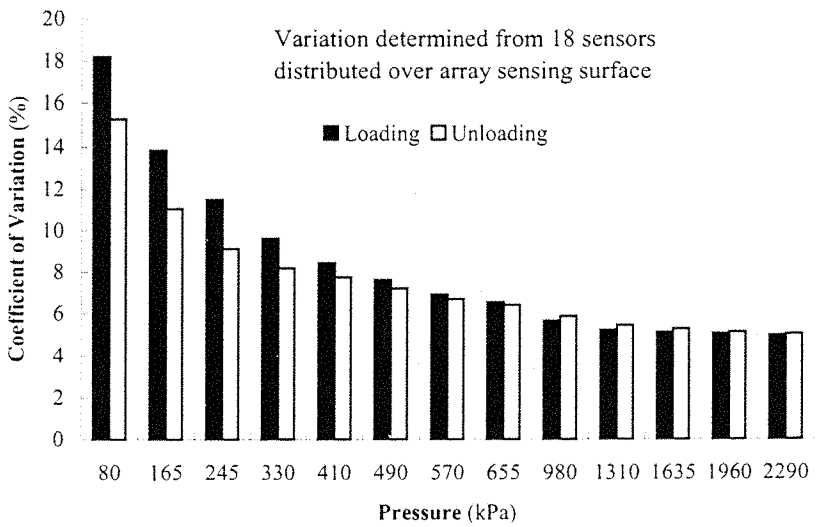


**Figure 5:8 Between sensor variation**

### 5.2.5. Threshold sensitivity

The threshold sensitivity was defined as the level of applied pressure at which the polymer sensor output voltage changed from zero. One sensor, representing 5.5% of the sample, registered an output at 8 kPa, while sixteen sensors (89%) were activated by pressure of ≈20 kPa. The two remaining sensors from the sample were not triggered until a threshold pressure of 35 kPa was reached.

### 5.2.6. Hysteresis

For the purpose of evaluation, the hysteresis was defined as the difference between the load-unload curves, at each level of applied pressure, and was expressed as a percentage of the full-scale output (FSO). The FSO in these tests was ≈2.2MPa. The means (± 1 standard deviation) of the values derived from the eighteen sample elements are displayed in figure 5.9. In the pressure range above 350 kPa the hysteresis was <5.0% FSO. For pressure over ≈800 kPa hysteresis was less than 1.0% FSO. However, for the pressures below 350 kPa, the hysteresis averaged 9.4% FSO. For the eighteen sample elements, the mean value for hysteresis, derived across all pressures, was 4.0%.

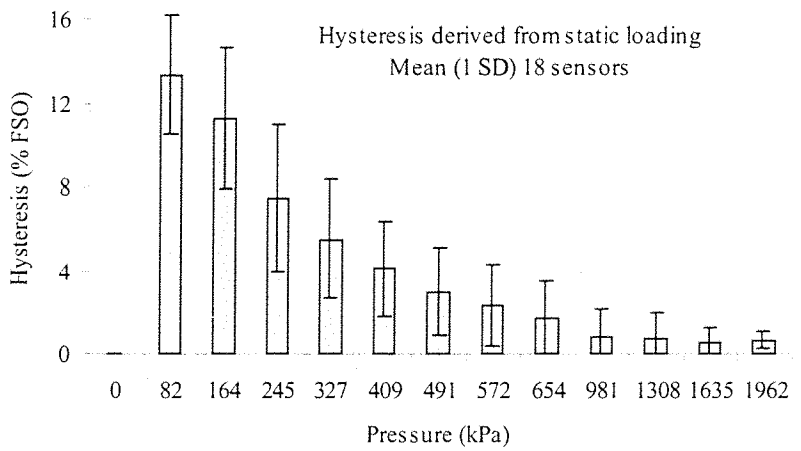


**Figure 5:9 Polymer sensor hysteresis**

### 5.2.7. Results for dynamic tests

The electromechanical shaker was bolted firmly to the top plate of the test rig for all dynamic tests. The tests were conducted for frequencies in the range 4-26 Hz, and at two levels of amplitude. The lower amplitude incorporated tests that reached pressures of between 200 and 300 kPa, while the higher amplitude was tested with pressures between 400 and 500 kPa.

### 5.2.8. Cross-correlation signal analysis

Correlation coefficients, obtained by cross-correlation of the reference and polymer signals, are reported in table 5.3. While the coefficients are indicative of correlation when lag was effectively zero, a residual lag (≈0.005s), induced by alternate sampling of the two signals, was present. The mean cross-correlation coefficient for the low amplitude test range was ≈0.89, while that for higher amplitudes was ≈0.87. The lowest coefficients occurred at the 4 Hz test condition (0.81 and 0.83, low and high range respectively). The highest correlations were at 12 Hz (0.92) for the low pressure range, and 18 Hz (0.91) for the high pressure range.

**Table 5:3 Cross-correlation coefficients**

| Test frequencies in upper row with derived correlations for respective amplitudes shown below. | | | | | | | | | | | | |
|---|---|---|---|---|---|---|---|---|---|---|---|---|
| Frequency (Hz) | 4 | 6 | 8 | 10 | 12 | 14 | 16 | 18 | 20 | 22 | 24 | 26 |
| Low range (2-300 kPa) | .81 | .89 | .88 | .88 | .92 | .91 | .91 | .91 | .91 | .90 | .91 | .89 |
| High range (4-500 kPa) | .83 | .85 | .86 | .89 | .89 | .88 | .84 | .91 | .88 | .89 | .86 | .86 |

### 5.2.9. Power spectral density analysis

Power spectra for the reference and polymer signals were produced for each of the test conditions. From each power spectrum, the fundamental frequency was identified and the power contained within it was determined as a proportion of the total spectral power. The magnitude of the power of the fundamental frequency of the polymer sensor was then derived as a percentage of the corresponding part of the appropriate reference signal. The results are shown graphically in figure 5.10.

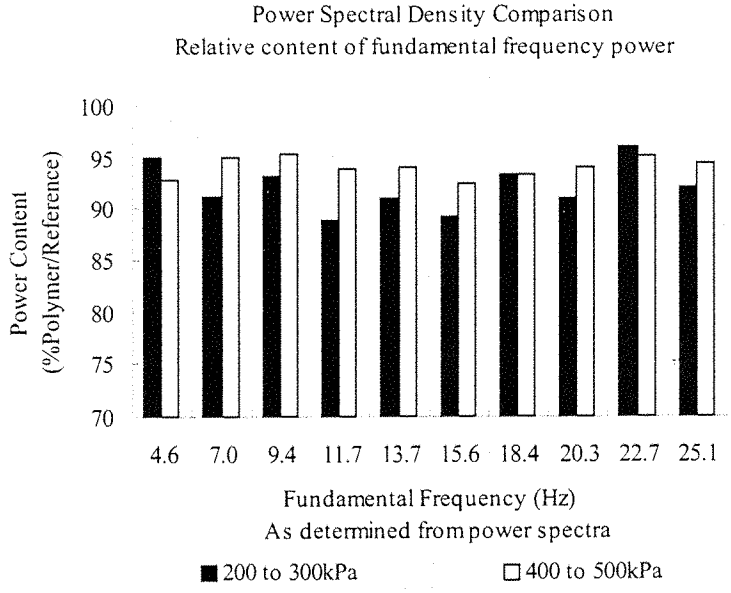


**Figure 5:10 Power spectral density comparisons**

Shows the relative power contained in the same portion of each of the two power spectra, with the polymer content expressed as a percentage of the reference content.

On average, the polymer sensor returned 92.2% of the fundamental frequency power in the low amplitude test range, and 94.0% in the high amplitude range. Across all test conditions, the minimum return was 88.8% (11.7 Hz, low range), and the maximum was 96.1% (22.7 Hz, low range). The fundamental frequencies, as identified for each pair of signals, were coincidental in all cases.

### 5.2.10. Effects of vacuum modification on polymer sensor dynamics

The application of a partial vacuum to the polymer sensor during dynamic loading produced a positive offset to the baseline of the output signal, indicating that the amplitude of the signal was constrained by the vacuum. The effect of partial evacuation of the polymer sensor on signal dynamics was assessed by cross-correlation and power spectral analysis. None of the tests revealed any substantial changes from the results obtained from the unmodified sensor.

### 5.2.11. Shear test results

Results for the shear tests for both platforms are presented, table 5.4. The initial test was conducted without shear. In subsequent tests, shear force was applied at either 25% or 50% of the normal force, as indicated in the table. Six replicates for each measurement condition were obtained. A general linear model with repeated measures revealed statistically significant differences between loading conditions for the polymer sensor platform ($F_{2,4}$=38.4, p=0.026) but not for the capacitive platform ($F_{2,4}$=2.75, p=0.284).

**Table 5:4 Shear test results for both platforms**

Contact pressures (kPa), for normal loading with and without shear. (zero indicates no shear, subscripts $_{(1)}$ indicate order of tests, % indicates relative shear, * indicates significant diff).

| | Shear | Zero$_1$ | 25% | Zero $_2$ | 50% | Zero $_3$ |
|---|---|---|---|---|---|---|
| Resistive polymer | Mean | 103.9 | 133.0* | 142.5* | 137.8* | 135.0* |
| | StDev | 2.16 | 7.21 | 10.01 | 8.73 | 7.33 |
| Capacitive elastomer | Mean | 137.8 | 135.2 | 136.2 | 134.1 | 134.4 |
| | StDev | 2.62 | 2.47 | 2.62 | 3.46 | 2.43 |

## 5.3. Comparison of platforms

The polymer sensor platform was compared with a second platform that utilised capacitive sensors. In contrast to the polymer sensor platform, the second platform had not demonstrated significant sensitivity to shear. Data for level and sideslope walking was collected for both machines. Initially, the data were analysed for differences using univariate two factor general linear models with repeated measures. Results are presented in table 5.5. Additional results, based on the Bland and Altman [175] method for assessing agreement between two clinical measurement techniques, are presented in tables 5.6 to 5.14. In the following tables, P1 refers to the polymer sensor pressure platform, P2 refers to the capacitive sensor pressure platform.

**Table 5:5 Initial statistical results for comparison of platforms**

| | Machine | | Machine x Slope | |
|---|---|---|---|---|
| | $F_{(3,6)}$ value | p value | $F_{(48,294)}$ value | p value |
| Area | 8.73 | 0.052 | 2.02 | <0.001 |
| Pressure | 1.89 | 0.322 | 1.87 | 0.001 |
| Force | 2.34 | 0.259 | 3.2 | <0.001 |
| ICT* | 4.98 | 0.073 | 1.39 | 0.066 |
| Dur | 6.61 | 0.075 | 1.49 | 0.043 |
| TPP | 5.54 | 0.094 | 1.32 | 0.086 |
| TPF | 5.10 | 0.087 | 1.11 | 0.079 |

ICT = initial contact time, Dur = duration of contact,
TPP = time to peak pressure, TPF = time to peak force,
*For ICT the F values are based on $F_{4,5}$ and $F_{40,320}$ because heel site was excluded from analysis.

**Table 5:6 Level walking bias values for temporal parameters**

All values expressed as a percentage of the stance phase.

| | ICT | | Dur | | TPP | | TPP | |
|---|---|---|---|---|---|---|---|---|
| | P1 | P2 | P1 | P2 | P1 | P2 | P1 | P2 |
| Mean | 11.3 | 11.2 | 72.4 | 74.2 | 55.5 | 57.5 | 57.4 | 59.2 |
| St Dev | 7.94 | 7.83 | 14.4 | 12.3 | 22.3 | 21.2 | 26.1 | 24 |
| Bias | -0.1 | | -1.9 | | -2 | | -1.8 | |
| 95% CI (upper) | -2.2 | | -5.9 | | -6.2 | | -5.9 | |
| 95% CI (lower) | 2.13 | | 2.17 | | 2.15 | | 2.22 | |

P1 = polymer sensor pressure platform, P2 = capacitive sensor pressure platform.

**Table 5:7 Level walking bias values for non-temporal parameters**

| | Area ($cm^2$) | | Pressure (kPa) | | Force (N) | |
|---|---|---|---|---|---|---|
| | P1 | P2 | P1 | P2 | P1 | P2 |
| Mean | 16.6 | 18.2 | 319 | 303 | 240 | 239 |
| St Dev | 9.62 | 10.2 | 130 | 148 | 198 | 194 |
| Bias | -1.6 | | 16.2 | | 1.17 | |
| 95% CI (upper) | 0.13 | | 70.2 | | 41.3 | |
| 95% CI (lower) | -3.3 | | -38 | | -39 | |

P1 = polymer sensor pressure platform, P2 = capacitive sensor pressure platform.

**Table 5:8 Sideslope walking bias values for initial contact time (ICT)**

| All values indicated as a percentage of the stance phase time. | | | | | | | | | | | | |
|---|---|---|---|---|---|---|---|---|---|---|---|---|
| | Hl | | MdFt | | M1 | | Mc | | M5 | | T1 | |
| | P1 | P2 | P1 | P2 | P1 | P2 | P1 | P2 | P1 | P2 | P1 | P2 |
| | 7.3 | 7.36 | 12.7 | 11.9 | 6.49 | 6.64 | 6.7 | 7.13 | 28.2 | 23.7 | | |
| Mean | 7.3 | | 12.3 | | 6.6 | | 6.9 | | 26.0 | | | |
| Bias | -0.1 | | 0.83 | | -0.1 | | -0.4 | | 3.5 | | | |
| 95% $CI_{up}$ | 1.38 | | 2.81 | | 1.23 | | 1.08 | | 13.2 | | | |
| 95% $CI_{low}$ | -1.5 | | -1.2 | | -1.5 | | -1.9 | | -4.2 | | | |
| P1 = polymer sensor pressure platform, P2 = capacitive sensor pressure platform. | | | | | | | | | | | | |

**Table 5:9 Sideslope walking bias values for duration of contact (DUR)**

| All values indicated as a percentage of the stance phase time. | | | | | | | | | | | | |
|---|---|---|---|---|---|---|---|---|---|---|---|---|
| | Hl | | MdFt | | M1 | | Mc | | M5 | | T1 | |
| | P1 | P2 | P1 | P2 | P1 | P2 | P1 | P2 | P1 | P2 | P1 | P2 |
| | 54.2 | 57.5 | 60.5 | 63.6 | 80.3 | 81.2 | 87.7 | 87.2 | 79.8 | 80.3 | 70.5 | 74.9 |
| Mean | 55.9 | | 62.1 | | 80.8 | | 87.5 | | 80.1 | | 72.7 | |
| Bias | -3.3 | | -3.1 | | -0.9 | | 0.52 | | -0.5 | | -4.4 | |
| 95% $CI_{up}$ | -0.3 | | 1.47 | | 1.44 | | 2.3 | | 2.47 | | 4.02 | |
| 95% $CI_{low}$ | -6.3 | | -7.7 | | -3.3 | | -1.3 | | -3.5 | | -13 | |
| P1 = polymer sensor pressure platform, P2 = capacitive sensor pressure platform. | | | | | | | | | | | | |

**Table 5:10 Sideslope walking bias values for time to peak pressure (TPP)**

| All values indicated as a percentage of the stance phase time. | | | | | | | | | | | | |
|---|---|---|---|---|---|---|---|---|---|---|---|---|
| | Hl | | MdFt | | M1 | | Mc | | M5 | | T1 | |
| | P1 | P2 | P1 | P2 | P1 | P2 | P1 | P2 | P1 | P2 | P1 | P2 |
| | 16.6 | 17.3 | 38.5 | 39.2 | 73.5 | 73.1 | 81.3 | 80.1 | 60.6 | 61.6 | 78.5 | 77.6 |
| Mean | 17.0 | | 38.9 | | 73.3 | | 80.7 | | 61.1 | | 78.1 | |
| Bias | -0.8 | | -0.7 | | 0.35 | | 1.28 | | -1 | | 0.94 | |
| 95% $CI_{up}$ | 2.87 | | 9.83 | | 6.37 | | 3.54 | | 5.63 | | 3.15 | |
| 95% $CI_{low}$ | -4.4 | | -11 | | -5.7 | | -1 | | -7.7 | | -1.3 | |
| P1 = polymer sensor pressure platform, P2 = capacitive sensor pressure platform. | | | | | | | | | | | | |

**Table 5:11 Sideslope walking bias values for time to peak force (TPF)**

| All values indicated as a percentage of the stance phase time. | | | | | | | | | | | | |
|---|---|---|---|---|---|---|---|---|---|---|---|---|
| | Hl | | MdFt | | M1 | | Mc | | M5 | | T1 | |
| | P1 | P2 | P1 | P2 | P1 | P2 | P1 | P2 | P1 | P2 | P1 | P2 |
| | 21 | 20.5 | 40.3 | 40.7 | 67.7 | 68.1 | 68.9 | 73 | 58.1 | 58.8 | 81.7 | 79.8 |
| Mean | 20.8 | | 40.5 | | 67.9 | | 71.0 | | 58.5 | | 80.8 | |
| Bias | 0.44 | | -0.5 | | -0.4 | | -4.2 | | -0.6 | | 1.9 | |
| 95% $CI_{up}$ | 2.42 | | 5.5 | | 5.54 | | 1.51 | | 6.95 | | 4.01 | |
| 95% $CI_{low}$ | -1.5 | | -6.4 | | -6.4 | | -9.8 | | -8.2 | | -0.2 | |
| P1 = polymer sensor pressure platform, P2 = capacitive sensor pressure platform. | | | | | | | | | | | | |

**Table 5:12 Sideslope walking bias values for contact area ($cm^2$)**

| | Hl | | MdFt | | M1 | | Mc | | M5 | | T1 | |
|---|---|---|---|---|---|---|---|---|---|---|---|---|
| | P1 | P2 | P1 | P2 | P1 | P2 | P1 | P2 | P1 | P2 | P1 | P2 |
| | 29 | 31.1 | 17.3 | 19.8 | 12.8 | 13.2 | 27.4 | 28.2 | 5.24 | 5.85 | 8.87 | 9.5 |
| Mean | 30.1 | | 18.6 | | 13.0 | | 27.8 | | 5.5 | | 9.2 | |
| Bias | -2.3 | | -2.5 | | -0.4 | | -0.8 | | -0.6 | | -0.6 | |
| 95% $CI_{up}$ | -0.8 | | 0.08 | | 0.61 | | 0.84 | | 0.29 | | 0.25 | |
| 95% $CI_{low}$ | -3.5 | | -5 | | -1.4 | | -2.4 | | -1.5 | | -1.5 | |

P1 = polymer sensor pressure platform, P2 = capacitive sensor pressure platform.

**Table 5:13 Sideslope walking bias values for pressure (kPa)**

| | Hl | | MdFt | | M1 | | Mc | | M5 | | T1 | |
|---|---|---|---|---|---|---|---|---|---|---|---|---|
| | P1 | P2 | P1 | P2 | P1 | P2 | P1 | P2 | P1 | P2 | P1 | P2 |
| | 376 | 349 | 130 | 90.6 | 314 | 321 | 434 | 410 | 258 | 240 | 413 | 517 |
| Mean | 362 | | 110 | | 318 | | 422 | | 249 | | 465 | |
| Bias | 26.5 | | 39.7 | | -6.5 | | 24 | | 18 | | -104 | |
| 95% $CI_{up}$ | 68.9 | | 66.4 | | 101 | | 76.5 | | 88.5 | | 13.5 | |
| 95% $CI_{low}$ | -16 | | 12.9 | | -114 | | -29 | | -52 | | -222 | |

P1 = polymer sensor pressure platform, P2 = capacitive sensor pressure platform.

**Table 5:14 Sideslope walking bias values for force (N)**

| | Hl | | MdFt | | M1 | | Mc | | M5 | | T1 | |
|---|---|---|---|---|---|---|---|---|---|---|---|---|
| | P1 | P2 | P1 | P2 | P1 | P2 | P1 | P2 | P1 | P2 | P1 | P2 |
| | 535 | 531 | 96.3 | 88.4 | 164 | 166 | 487 | 443 | 63.5 | 55.3 | 138 | 147 |
| Mean | 533 | | 92.4 | | 165 | | 465 | | 59.4 | | 142.5 | |
| Bias | 4.38 | | 7.93 | | -2.1 | | 43.7 | | 8.27 | | -9.3 | |
| 95% $CI_{up}$ | 60.9 | | 41.2 | | 42 | | 97.2 | | 24.5 | | 18.7 | |
| 95% $CI_{low}$ | -52 | | -25 | | -46 | | -9.8 | | -8 | | -37 | |

P1 = polymer sensor pressure platform, P2 = capacitive sensor pressure platform.

### 5.3.1. Bland and Altman plots

The Bland and Altman method plots the average of a pair of values from the two platforms against the difference between the pair. When the agreement between the two measurement techniques is good then the data are spread evenly above and below the horizontal axis of the plot, across the full measurement range. The initial contact time data, derived from the six foot sites, are presented in figure 5.11. For the measurement range (0-35 % stance phase), the data are evenly distributed and the agreement is good. In this example, the bias would therefore be close to zero. Figures 5.12 and 5.13 illustrate examples of poor agreement.

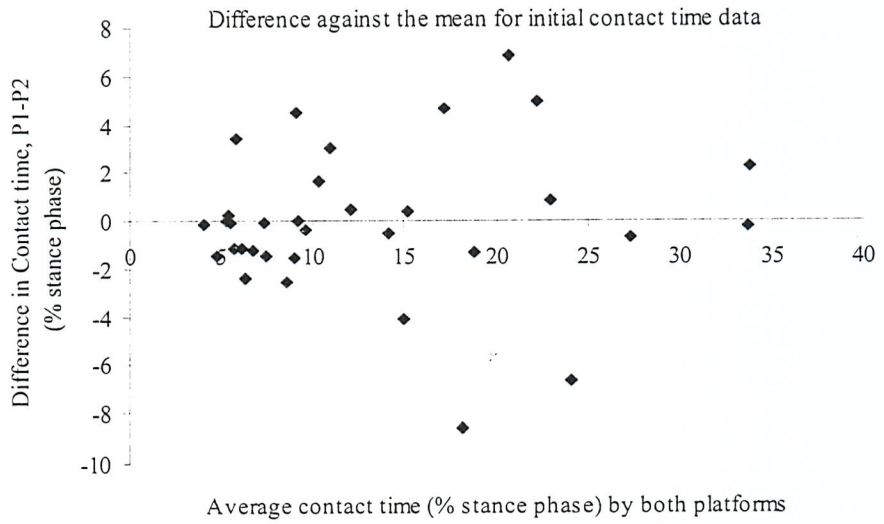


**Figure 5:11 Bland and Altman plot of Initial Contact Time data**

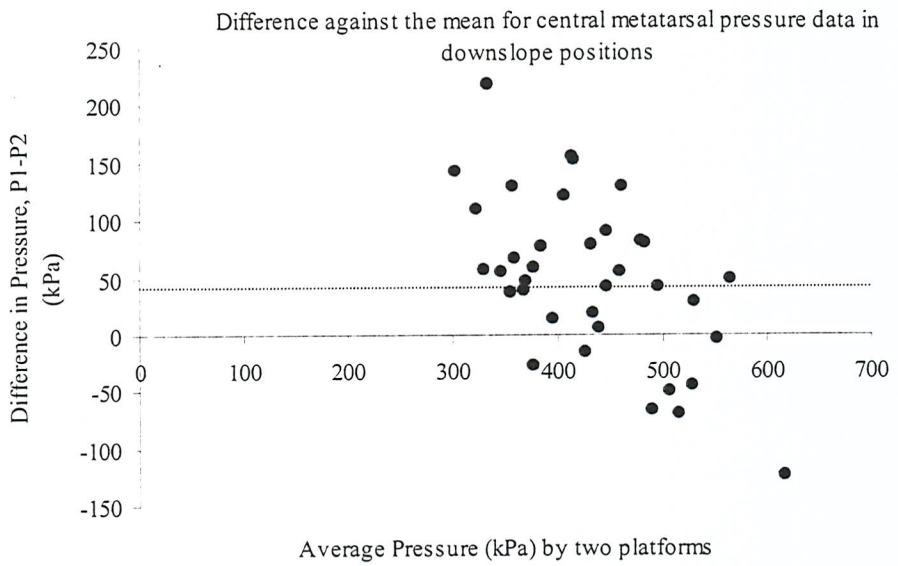


**Figure 5:12 Central metatarsal pressure discrepancy for sideslope walking**

For sideslope walking, pressures for the central metatarsal site differed significantly between the two platforms. In the downslope positions, values from the polymer sensor system exceeded those from the capacitive system by an average of about 50 kPa, as indicated by the bias line.

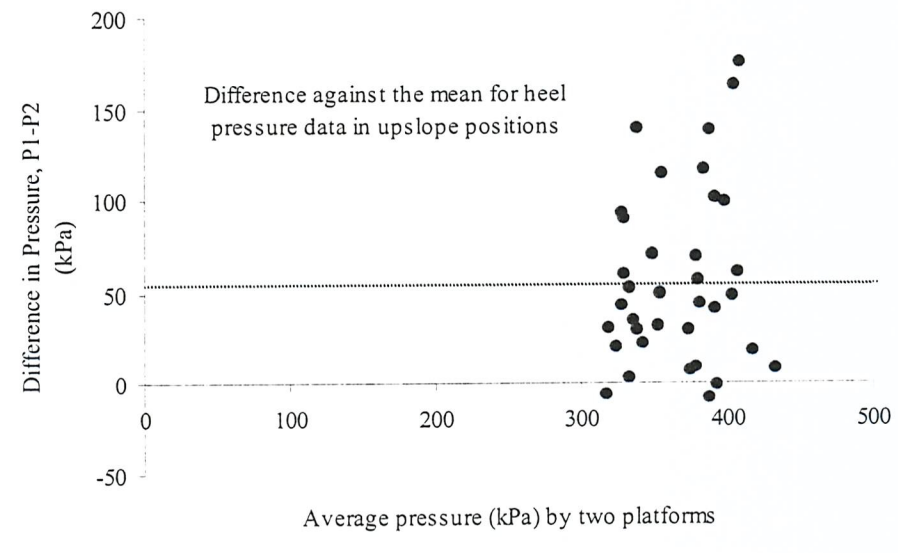


**Figure 5:13 Heel pressure discrepancy for sideslope walking**

For sideslope walking, pressures for the heel site differed significantly between the two platforms. In the upslope positions, values from the polymer sensor system exceeded those from the capacitive system by an average of about 57 kPa, as indicated by the bias line.

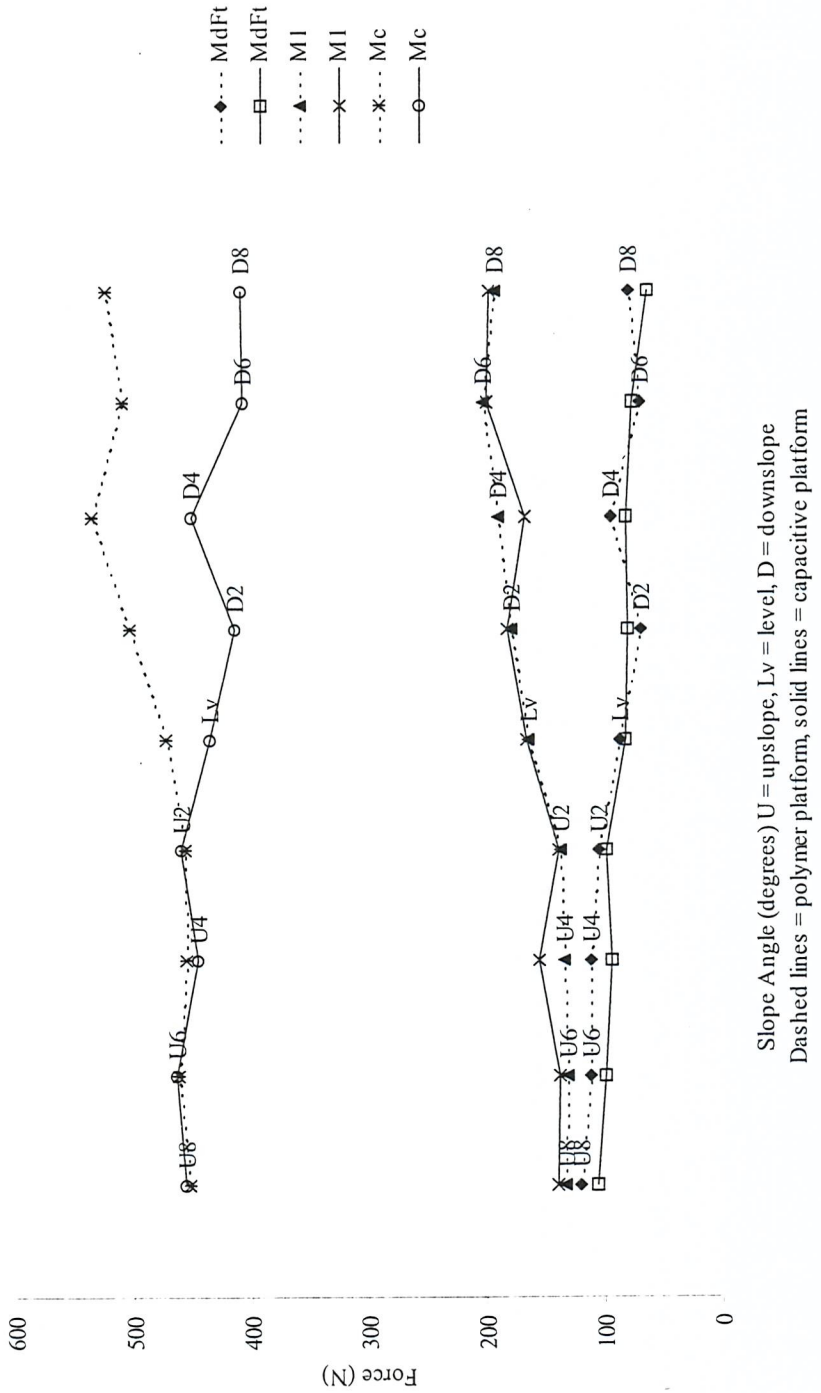


**Figure 5.14 Regional force profiles from two platforms (Mc, M1, MdFt)**

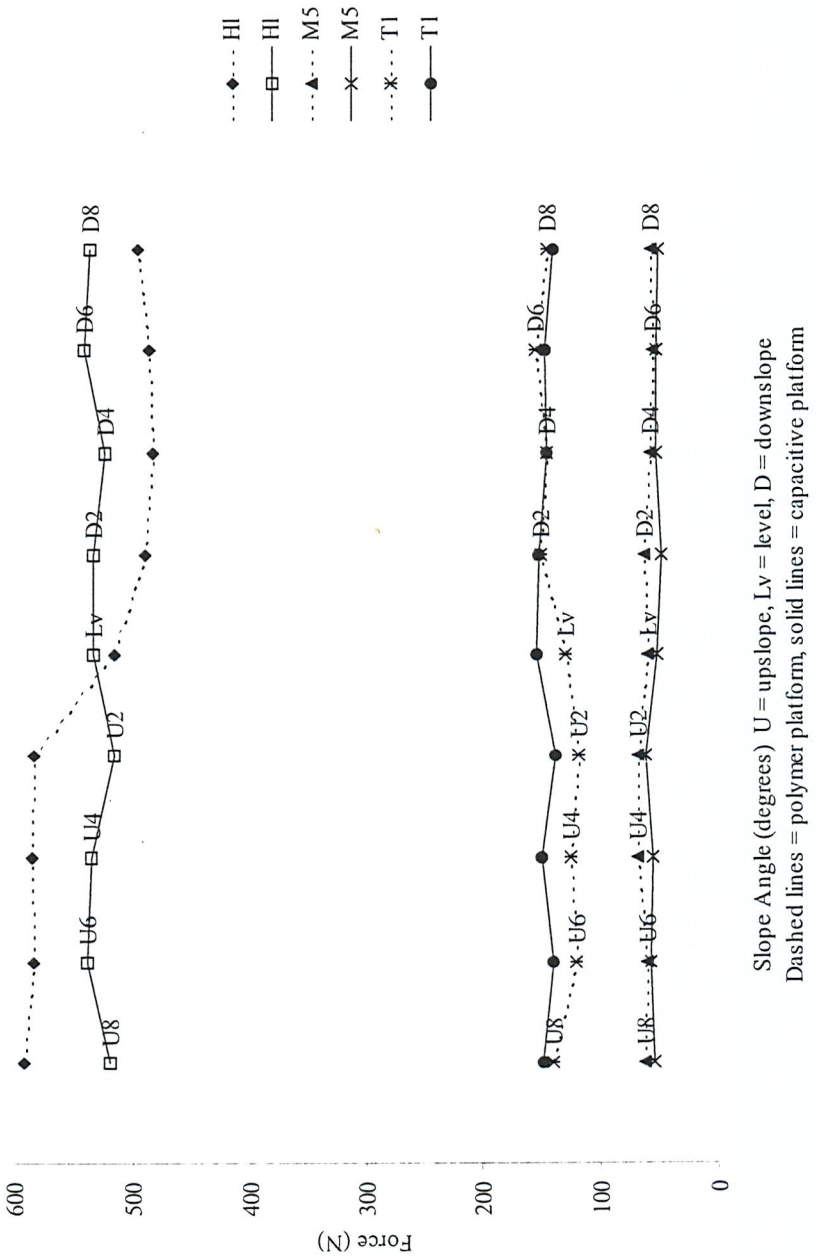


**Figure 5.15 Regional force profiles from two platforms (Hl, M5, T1)**

## 5.4. Footprint contact area results

Contact area was measured by tracing the outline of ink footprints with a planimeter. Additional estimates of contact area were derived by counting the ink stained elements of a latticed template that was dimensionally identical to the sensor array of the platform. Estimates obtained from the lattice template were weighted according to the contribution of peripheral elements. Full contribution by peripheral elements is indicated as $C_{max}$, while fifty percent weighting is indicated as $C_{wt}$. To assess the influence of sensor threshold, tests were conducted with the array in its standard form and while it was subjected to a partial vacuum.

Contact areas were derived for the FCA, T1, T25, and the entire foot. The foot contact area (FCA) was defined as the whole footprint minus the toe region, and this parameter is reported in all cases unless specified otherwise. Where appropriate, assumptions of normality were assessed via Kolmorgorov-Smirnov goodness of fit tests. Tests of significance were conducted at a significance level of $\alpha$=0.05.

### 5.4.1. Contact area measurement: pressure platform versus ink footprints

The statistical significance of differences between FCA as estimated by the alternative methods was assessed using paired t-tests. Table 5.15 presents the descriptive statistics for the foot contact area and arch index as derived from both ink and electronic footprints. The pressure platform significantly underestimated the foot contact area (79.3 ± 8.9 $cm^2$) when compared with the ink footprints (92.4 ± 10.0 $cm^2$); ($df=15$, $t=11.094$, $p<0.001$). On average the underestimation was about 14%. The arch index derived from the pressure platform (0.220 ± 0.001) was significantly smaller ($t=7.01$, $p<0.001$) than that obtained from the ink prints (0.231 ± 0.002). Table 5.16 demonstrates the correlation matrix for the arch index derived from inked and electronic footprints and their respective discrepancy scores. Significant positive correlations were noted between inked and electronic footprints with respect to both FCA ($r=0.88$, $p<0.001$) and AI ($r=0.965$, $p<0.001$). The arch index derived

from the ink prints was negatively correlated to the discrepancy in foot contact area (r=-0.796, P<0.001), table 5.16.

**Table 5:15 Footprint statistics**

Descriptive statistics, t and p value for the foot contact area (FCA) and arch index (AI) obtained from ink and electronic footprints.

| | Ink Footprint | | Electronic Footprint | | | |
|---|---|---|---|---|---|---|
| | Mean | SD | Mean | SD | t | P |
| FCA | 92.4 | 10.0 | 79.3 | 8.9 | 11.09 | .001 |
| AI | 0.231 | 0.002 | 0.220 | 0.001 | 7.01 | .001 |

**Table 5:16 Footprint correlations**

Correlation matrix for arch index and discrepancy scores derived from both inked and electronic footprints. * Indicates statistical significance (p<.05)

| Ink Measures | Electronic Measures | | Discrepancy Scores | |
|---|---|---|---|---|
| | Foot Contact Area | Arch Index | Foot Contact Area | Arch Index |
| Foot Contact Area | 0.880* | 0.024 | 0.451 | -0.046 |
| Arch Index | 0.436 | 0.965* | -0.796* | 0.286 |

5.4.2. Contact area measurement: template methods versus ink footprints

Statistical significance was tested using a general linear model with repeat measures. In total, 112 footprint images (16 subjects x 7 prints) were analysed. For contact area estimates, a significant interaction between method and site was found ($F_{6,191}$=617.9, p<0.05). Table 5.17 presents the mean and standard deviation of the contact area estimates for each site. The foot contact area (FCA) as determined by planimetry (91.20 ±9.4 $cm^2$) was significantly different from both the $C_{wt}$ estimate (89.10 ±9.29 $cm^2$), and the $C_{max}$ estimate (101.60 ±10.19 $cm^2$). For the hallux (T1) and lesser toe (T25) sites, the $C_{max}$ estimates differed significantly from those obtained by planimetry, while the $C_{wt}$ estimates did not. Estimates of total contact area derived from both count based methods differed significantly from their planimetric equivalent, table 5.17.

Discrepancy scores for contact area estimates are presented in table 5.17. The $C_{wt}$ estimates were approximately 2% less than the planimetric equivalents, with the exception of the lesser toe site (T25), which was overestimated on average by 8.8%. In comparison, the $C_{max}$ estimates gave consistently greater

discrepancy scores for the FCA (≈11%), the hallux (≈30%) and the lesser toes (≈78%).

The peripheral element ratio was the ratio of peripheral to central elements within a region. The mean peripheral element ratios (PER) are presented in table 5.18, along with the size of each site. On average, the contact area of a lesser toe was less than 2% of the FCA. The large PER for the lesser toes demonstrates that, in this region, there were about four peripheral elements for each central element.

Evaluation of the within subject variability, table 5.19, revealed that there was no statistically significant difference between methods for the FCA, the total contact area or the hallux. However, in comparison with planimetry, the lesser toe site was significantly less variable when estimated by both count based methods ($F_{6,191}$=4.51, $p<0.05$).

**Table 5:17 Footprint contact areas by different methods**

Mean and standard deviation (SD) for contact areas ($cm^2$) determined by planimetric and grid-count methods. Discrepancy scores (DS) determined as percentage difference from planimetric mean.

| | Planimetric | | $C_{wt}$ | | | $C_{max}$ | | |
|---|---|---|---|---|---|---|---|---|
| | Mean | SD | Mean | SD | DS | Mean | SD | DS |
| FCA | 91.20 | 9.40 | 89.10* | 9.29 | 2.30[a] | 101.60*# | 10.19 | 11.40[b] |
| T1 | 7.45 | 1.69 | 7.30 | 1.43 | 2.01[a] | 9.68*# | 1.93 | 29.93[b] |
| T25 | 6.24 | 1.62 | 6.79 | 1.65 | 8.81[b] | 11.13*# | 2.53 | 78.37[b] |
| Total Area | 104.89 | 11.02 | 103.20* | 10.53 | 1.61[a] | 122.41*# | 12.30 | 16.70[b] |

FCA = foot contact area, T1 = hallux, T25 = lesser toes.
Significant difference ($p<0.05$); * indicates comparison with planimeter, # indicates comparison with $C_{wt}$.
[a] indicates underestimation of planimetric measurement,
[b] indicates overestimation of planimetric measurement.

**Table 5:18 Peripheral element ratios and discrepancy scores**

Mean planimetric size ($cm^2$), peripheral element ratio (PER), and discrepancy score (DS) for each foot site. PER derived as peripheral:central elements.

| | Size | PER | DS ($C_{wt}$) |
|---|---|---|---|
| Total Area | 104.9 | 0.460 | 1.61 |
| FCA | 91.2 | 0.328 | 2.3 |
| T1 | 7.4 | 0.994 | 2.01 |
| T25 | 1.6 | 4.102 | 8.81 |

**Table 5:19 Footprint variablity (cv)**

Mean within subject coefficients of variation (cv) determined from seven measurements by planimetric and grid-count methods and expressed as a percentage.
* indicates significant difference ($p<0.05$) from planimetric mean.

| | Planimetric | $C_{wt}$ | $C_{max}$ |
|---|---|---|---|
| Variable | CV | CV | CV |
| FCA | 2.69 | 2.99 | 2.96 |
| T1 | 16.74 | 15.72 | 15.88 |
| T25 | 18.32 | 15.31* | 14.81* |
| Total Area | 3.33 | 3.32 | 3.42 |

### 5.4.3. Contact area measurement: template methods versus pressure platform

Tests were conducted with the array in its standard form and with six levels of pre-load vacuum. Statistical significance was tested using a repeated measures analysis of variance with Student-Newman-Keuls post hoc. Analysis revealed a statistically significant difference between the estimates of FCA obtained simultaneously using the platform and the template methods ($df=90$, $F=105.36$, $p<0.0001$). The post hoc comparisons revealed that underestimation of area by the pressure platform occurred for each of the seven test situations. However, when the internal pressure of the polymer sensor was adjusted, the estimates of area measured by the platform significantly increased ($df=90$, $F=5.03$, $p=0.0002$). Post hoc analysis revealed that the increases were associated with a partial vacuum ≥50 kPa. The modification of the polymer sensor had no effect on the estimates of area obtained from the lattice templates.

The average underestimation of area by the platform was 9.8% across all trials. The underestimation reduced to an average of 7.7% in those trials where the partial vacuum resulted in significantly increased measurements of area. While the area measurements from the platform increased significantly when the polymer sensor was subjected to vacuum pressures of 50kPa and above, the estimates remained below those obtained from the template.

### 5.4.4. Summary of foot contact area measurement results

In comparison with ink prints, the template method resulted in an underestimation of ≈2.8% of the FCA. This magnitude of error is determined by the spatial resolution of the platform and will be present regardless of other factors that may influence measurements of contact area. In contrast to the small error from the latticed template, the pressure platform underestimated the FCA by about 14% when compared with the ink footprint. Since approximately 3% of this underestimation could be attributed to the restricted spatial resolution, it was concluded that the remaining 11% was due to factors within the pressure measurement system. With the application of the vacuum pre-load, the system error of 11% was reduced to about 7%. This suggests that some (≈4%), but not all, of the error associated with contact area measurement was the effect of the transducer threshold level. The remaining error (≈7%) may be due to a threshold imposed by the system electronics or the software. The error associated with measurements of area from this platform has immediate clinical implications (appendix IV). The findings also indicate that there is a need for platforms with enhanced spatial resolution for increased accuracy of contact area measurement of the lesser toe region (appendix IV).

## 5.5. Results for level and sideslope walking

### 5.5.1. Foot placement angle results

The foot placement angle (FPA), which is the angle of alignment of the foot relative to the line of progression of walking, was estimated from the electronic footprints. The angle was determined by comparing a line along the medial edge of the footprint image with the longitudinal axis of the sensor matrix. If the reference line of the foot was angled out from the line of progression then the FPA was positive and the alignment was referred to as out-toe. If angled inwards, then the FPA was negative and the alignment was referred to as in-toe.

The mean (sd) FPA for level, upslope and downslope foot placements were 0.7° (4.4°), 1.8° (4.12°) and 0.75° (4.75°) respectively. On average, therefore, the FPA increased slightly (≈ 1.1°), becoming more out-toe in the upslope

condition, but did not alter in the downslope condition. However, there was considerable variation between individuals.

For level walking, the within subject mean values revealed that thirteen subjects (43.3%) had an out-toe FPA (mean = 2.8°), thirteen (43.3%) had an in-toe FPA (mean = 4.5°), and four (13.3%) were parallel with the platform.

To determined whether the FPA changed when walking on a sideslope, the within subject differences between level and slope walking were calculated for each incline. In the upslope conditions, seven subjects decreased their FPA, twenty-two demonstrated an increase, and one showed no change. In the downslope conditions, by comparison, twelve subjects increased their FPA, fourteen demonstrated a decrease, and four showed no change. Overall, changes in the FPA averaged about 2°.

The subjects were sub-classified according to the changes that they exhibited during the up and downslope walking conditions, table 5.20. When subjects demonstrated a positive change in their FPA for one direction of slope and a negative change for the opposite slope, they were classified as having a bidirectional response. If, however, they showed the same type of change (either positive or negative) for both slope orientations, they were classified as having a unidirectional response. A third group of subjects demonstrated a change in their FPA for one slope condition, either upslope or downslope, only. Eight subjects (26.7%) exhibited a bidirectional response; seven of these out-toed on the upslope and in-toed on the downslope, while the eighth showed the opposite response. Seventeen subjects (56.7%) exhibited a unidirectional response, twelve out-toed for both slope conditions, while five in-toed. Finally, five subjects (16.7%) demonstrated a change in their FPA for only one of the two slope orientations. Four of the five out-toed for the upslope, while one out-toed on the downslope.

**Table 5:20 Change in foot placement angle (FPA) with sideslope walking**

| Group | Change on BOTH slopes Bidirectional (Direction of change dependent on slope) | | Unidirectional (Direction of change same for both slopes) | | Change on ONE slope | |
|---|---|---|---|---|---|---|
| Number in group | 8 | | 17 | | 5 | |
| Number in sub-group | 7 | 1 | 12 | 5 | 4 | 1 |
| Upslope change | +ve (out-toe) | -ve (in-toe) | +ve (out-toe) | -ve (in-toe) | +ve (out-toe) | No change |
| Downslope change | -ve (in-toe) | +ve (out-toe) | +ve (out-toe) | -ve in-toe | No change | +ve (out-toe) |

## 5.5.2. Statistical analysis for the walkway study

A multivariate analysis of variance test statistic could not be produced because of insufficient residual degrees of freedom. However, multivariate tests (Wilks' Lambada) of within-subjects effects for site-by-slope interactions were derived. Ideally, to obtain the multivariate statistics, all data relating to the outcome variables (contact area etc) would be simultaneously analysed in a single model. Software limitations, however, restricted this approach such that data had to be assigned to one of three sub-groups for the initial analysis. The grouping was arbitrary and, along with the resulting statistics, is shown in table 5.21. Since the multivariate tests revealed highly significant within-subject effects without marginal results, and this study was concerned only with the within-subjects effects for site-by-slope interactions, no further multivariate tests were conducted.

**Table 5:21 GLM statistics for Site-by-Slope interactions**

| | | | |
|---|---|---|---|
| Multivariate Tests of Within-Subjects Effects (Wilks' Lambada) | | | |
| | Analysis Group * | F | Sig |
| | Group 1 | $F_{120,\ 6960}=26.6$ | $p<0.001$ |
| | Group 2 | $F_{120,\ 6960}=22.9$ | $p<0.001$ |
| | Group 3 | $F_{120,\ 6960}=28.9$ | $p<0.001$ |
| Univariate Tests of Within-Subjects Effects (Greenhouse-Geisser) | | | |
| | Group Reference # | F | Sig |
| Area | 3 | $F_{11.8,\ 685.3}=135.0$ | $p<0.001$ |
| Force | 3 | $F_{11.1,\ 645.5}=95.9$ | $p<0.001$ |
| Peak Pressure | 1 | $F_{9.0,\ 522.4}=25.9$ | $p<0.001$ |
| Average Pressure | 2 | $F_{12.3,\ 714.9}=15.2$ | $p<0.001$ |
| Force Initial Contact Time | 3 | $F_{6.6,\ 380.5}=79.1$ | $p<0.001$ |
| Force Duration | 1 | $F_{9.5,\ 551.9}=24.2$ | $p<0.001$ |
| Time to Peak Force | 2 | $F_{10.3,\ 599.7}=67.0$ | $p<0.001$ |
| Time to Peak Pressure | 1 | $F_{11.5,\ 667.5}=12.6$ | $p<0.001$ |

F indicates F statistic shown with respective degrees of freedom, Sig indicates level of statistical significance with respective p value. The grouping of the outcome variables is indicated by their respective group reference number #. For example, variables with a group reference number of 1 were clustered for simultaneous processing within the first analysis group *.

Conservative (Greenhouse-Geisser) univariate tests of within-subjects effects for site-by-slope interactions are also shown in table 5.21. These indicated that statistically significant site-by-slope interactions occurred for each dependent variable. Therefore, tests of within-subjects contrasts were conducted for each variable to identify the slope angles where significant differences from the level walking condition occurred.

### 5.5.3. Contact area results for level and sideslope walking

The means and standard deviations for the measurements of contact area are given in table 5.22. The influence of the angle of incline on the contact area for each site is shown in figure 5.16. Change between either level and upslope, or level and downslope is presented as a percentage of the level value, and is the average change over the four respective incline conditions.

**Table 5:22 Contact area ($cm^2$) results for sideslope walking**

Mean values (upper row) and standard deviations (lower row) for each site of the foot (* indicates a significant difference from the level condition, U indicates upslope, D indicates downslope, Lv indicates level).

| Incline | U8° | U6° | U4° | U2° | Lv | D2° | D4° | D6° | D8° |
|---|---|---|---|---|---|---|---|---|---|
| Heel | 28.1 | 28.9* | 29.0* | 28.8* | 28.4 | 28.7 | 28.3 | 28.4 | 28.4 |
| | 3.8 | 3.9 | 4.2 | 4.2 | 4.3 | 4.3 | 5.0 | 4.4 | 4.6 |
| Midfoot | 20.4* | 19.4 | 19.8* | 19.9* | 18.6 | 17.6* | 17.5* | 17.9 | 16.9* |
| | 6.6 | 7.1 | 6.6 | 6.8 | 6.9 | 6.6 | 7.0 | 6.1 | 6.5 |
| Met 1 | 12.4* | 12.2* | 12.2* | 12.4* | 13.0 | 13.1 | 12.8* | 12.7* | 12.9 |
| | 2.1 | 2.3 | 2.0 | 2.1 | 1.9 | 2.2 | 1.8 | 2.1 | 1.6 |
| Met Cen | 26.0* | 26.1 | 26.5 | 26.6 | 26.6 | 26.9 | 27.3* | 27.1 | 26.5 |
| | 4.4 | 4.1 | 4.1 | 4.2 | 4.3 | 3.8 | 3.6 | 3.4 | 3.6 |
| Met 5 | 5.3* | 5.3 | 5.4 | 5.6 | 5.5 | 5.3 | 5.3 | 5.3 | 5.5 |
| | 0.9 | 1.0 | 1.1 | 2.0 | 1.0 | 1.1 | 0.9 | 1.1 | 1.1 |
| Toe 1 | 8.7 | 8.5 | 8.5 | 8.3 | 8.5 | 8.7* | 8.7 | 8.7 | 8.4 |
| | 2.1 | 1.8 | 1.7 | 1.8 | 1.3 | 1.2 | 1.4 | 1.4 | 1.4 |

Although all sites within the foot demonstrated some significant differences, only the heel, midfoot and first metatarsal showed consistent changes. The contact area of the heel increased slightly (average =1.1%) in the upslope conditions but did not change on the downslopes. The midfoot showed the greatest changes of any site, with an average increase of 6.7% on the upslope and an average decrease of 6.2% on the downslope, an overall change of almost 13%. Although the first metatarsal showed changes in both slope conditions, the upslope decrease of 5.6% was more substantial than the downslope decrease of 1.4%. No other site demonstrated an average change of greater than 1.6%.

## 5.5.4. Arch index results for level and sideslope walking

Results for the arch index determined for both level and sideslope walking are presented in table 5.23.

**Table 5:23Arch index (AI) results for level and sideslope walking**

% Diff = Difference from level index, U = upslope, D = downslope.

| | U8° | U6° | U4° | U2° | Lv | D2° | D4° | D6° | D8° |
|---|---|---|---|---|---|---|---|---|---|
| AI | .221 | .210 | .213 | .213 | .202 | .192 | .192 | .196 | .187 |
| % Diff | 9.4 | 3.9 | 5.5 | 5.5 | 0 | 4.9 | 5.0 | 3.0 | 7.4 |

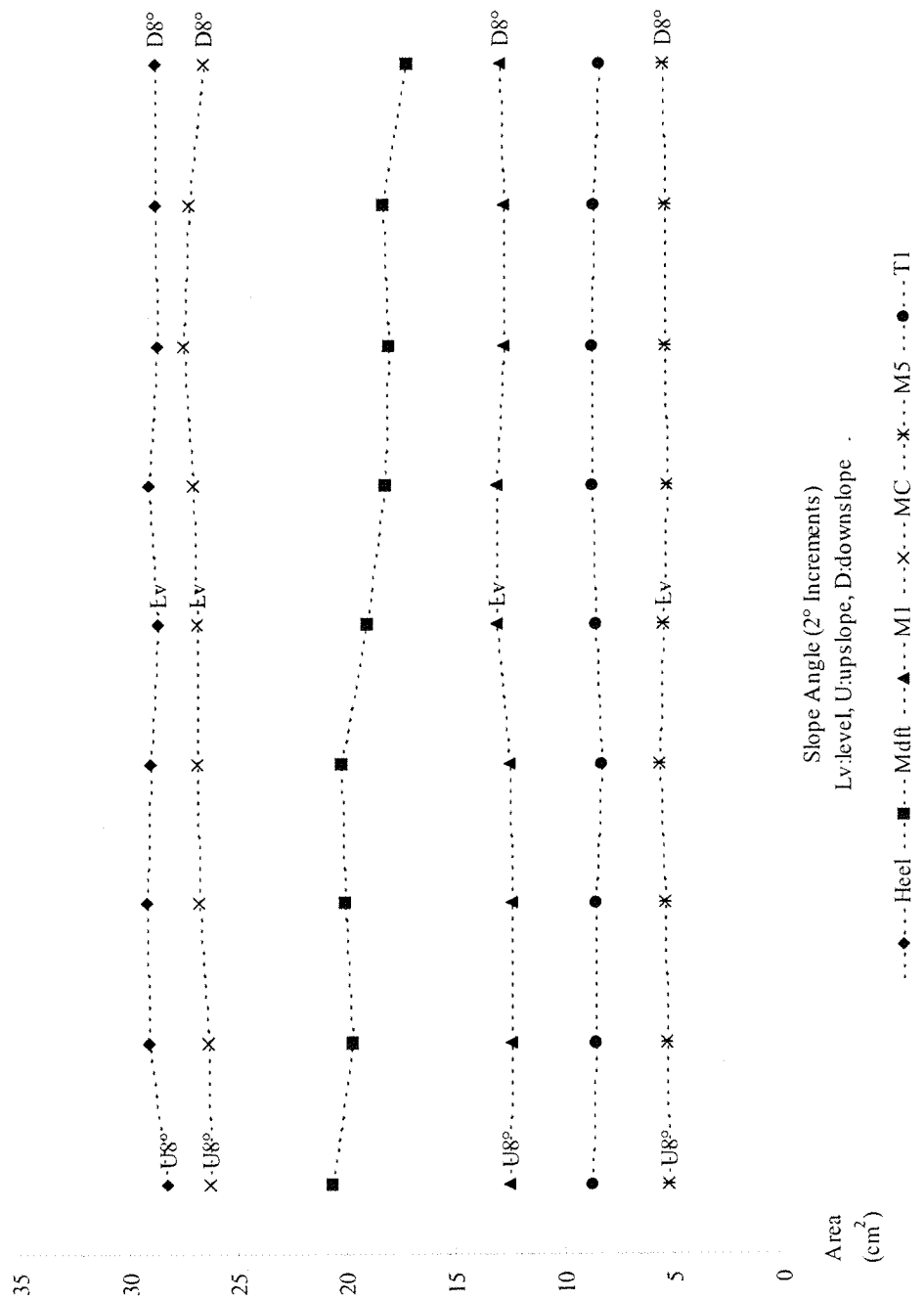


**Figure 5.16 Influence of sideslope on contact area**

## 5.5.5. Peak pressure results for level and sideslope walking

The means and standard deviations for the measurements of peak pressure are given in table 5.24. The influence of the angle of incline on peak pressure for each site is shown if figure 5.17.

**Table 5:24 Peak pressure (kPa) results for sideslope walking**

Mean values (upper row) and standard deviations (lower row) for each site of the foot (* indicates a significant difference from the level condition, U indicates upslope, D indicates downslope, Lv indicates level).

| Incline | U8° | U6° | U4° | U2° | Lv | D2° | D4° | D6° | D8° |
|---|---|---|---|---|---|---|---|---|---|
| Heel | 379.5* | 375.4 | 374.0 | 377.3 | 365.1 | 353.7* | 361.4 | 372.1 | 372.4 |
| | 55.9 | 56.8 | 54.4 | 51.3 | 63.9 | 55.7 | 69.2 | 75.3 | 73.7 |
| Midfoot | 141.0* | 134.9* | 141.0* | 132.1* | 114.2 | 113.7 | 120.1 | 118.1 | 117.0 |
| | 50.9 | 49.5 | 53.0 | 51.7 | 39.3 | 38.7 | 40.4 | 37.6 | 47.3 |
| Met 1 | 286.8* | 284.3* | 297.1* | 284.1* | 350.5 | 380.6* | 385.7* | 408.4* | 381.4* |
| | 117.0 | 139.9 | 137.3 | 108.8 | 148.2 | 169.2 | 169.3 | 127.3 | 154.7 |
| Met Cen | 414.9 | 409.1 | 407.9 | 417.6 | 413.3 | 423.4 | 430.8* | 438.3* | 433.8* |
| | 88.7 | 63.7 | 70.9 | 80.0 | 72.7 | 85.9 | 97.5 | 115.3 | 83.1 |
| Met 5 | 292.2* | 270.8* | 269.5* | 254.5* | 234.5 | 229.5 | 237.0 | 227.5 | 242.7 |
| | 125.7 | 97.2 | 105.0 | 78.1 | 89.2 | 80.0 | 81.5 | 71.7 | 79.4 |
| Toe 1 | 402.2 | 394.7* | 394.5* | 389.1* | 443.3 | 468.7* | 436.4 | 451.0 | 419.2 |
| | 214.8 | 216.4 | 193.2 | 204.5 | 222.3 | 214.7 | 206.1 | 220.8 | 197.4 |

The peak pressures, in the upslope conditions, significantly increased at the midfoot and fifth metatarsal sites (+20.2% and +15.9%, respectively), but decreased at the first metatarsal and first toe (-17.8% and -10.9%, respectively). In the downslope conditions, peak pressures increased beneath the central and first metatarsals (+4.4% and +11.0%, respectively). Statistically significant differences for the central metatarsals occurred for slopes of 4° and greater only. The first metatarsal was the only site that demonstrated consistently significant changes throughout the entire range of up and downslope conditions.

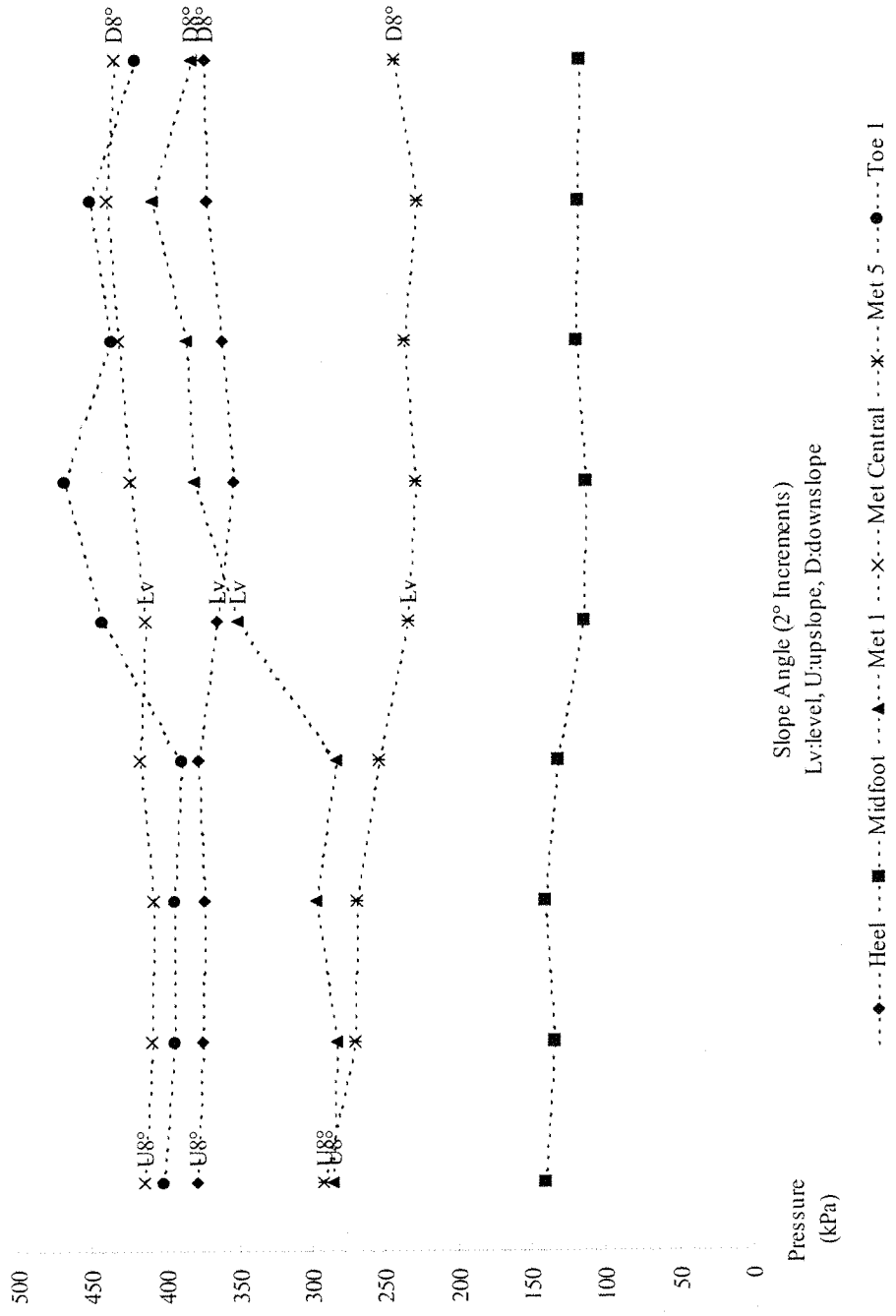


**Figure 5.17 Influence of sideslope on peak pressure**

### 5.5.6. Regional force results for level and sideslope walking

The means and standard deviations for the measurements of peak force are given in table 5.25. The fifth metatarsal was the only site that did not show some statistically significant change in peak force, although a mean increase of +3.9% was recorded for the upslope conditions. The influence of the angle of incline on peak force for each site is shown if figure 5.18.

**Table 5:25 Force (N) results for sideslope walking**

Mean values (upper row) and standard deviations (lower row) for each site of the foot (* indicates a significant difference from the level condition, U indicates upslope, D indicates downslope, Lv indicates level).

| Incline | U8° | U6° | U4° | U2° | Lv | D2° | D4° | D6° | D8° |
|---|---|---|---|---|---|---|---|---|---|
| Heel | 555.1* | 561.5* | 555.4* | 552.8* | 504.2 | 490.1 | 483.2* | 491.3 | 495.2 |
| | 82.3 | 95.7 | 91.6 | 92.8 | 101.2 | 91.9 | 107.8 | 104.8 | 104.6 |
| Midfoot | 130.5* | 121.7* | 124.7* | 119.3* | 94.5 | 90.4 | 94.7 | 94.4 | 91.0 |
| | 75.1 | 75.6 | 72.6 | 68.5 | 58.5 | 59.3 | 63.7 | 62.0 | 64.7 |
| Met 1 | 135.6* | 136.1* | 139.9* | 137.4* | 175.6 | 189.5* | 191.0* | 196.1* | 197.4* |
| | 55.4 | 55.8 | 48.5 | 47.7 | 58.1 | 53.1 | 60.6 | 54.3 | 64.7 |
| Met Cen | 445.0 | 447.2 | 446.0 | 443.2 | 450.4 | 467.7* | 477.7* | 468.0 | 474.1* |
| | 100.6 | 96.4 | 95.5 | 98.1 | 108.8 | 123.1 | 123.9 | 110.6 | 129.6 |
| Met 5 | 62.3 | 60.9 | 62.2 | 62.9 | 59.7 | 57.9 | 57.8 | 60.0 | 62.5 |
| | 18.0 | 19.0 | 20.2 | 30.1 | 22.0 | 21.0 | 18.7 | 20.5 | 22.9 |
| Toe 1 | 125.8 | 119.1* | 122.2* | 116.5* | 132.5 | 142.0* | 139.3* | 138.8 | 129.3 |
| | 49.4 | 52.1 | 46.1 | 49.9 | 48.9 | 46.0 | 48.5 | 51.9 | 54.8 |

The heel and midfoot sites responded similarly, demonstrating increased force in the upslope conditions (+10.3% and +31.2%, respectively) but little change on the downslopes. The force on the central metatarsals increased (+4.8%) in the downslope conditions without significantly changing on the upslopes, the exact opposite of the heel and midfoot.

Unlike all other sites, the first metatarsal and first toe demonstrated statistically significant differences in both the up and downslope conditions when compared with level walking. However, the magnitude of the changes was greater and more consistent for the first metatarsal (+10.2%) than for the first toe (+3.7%). In addition, these two sites were the only ones to show significant reductions in peak force. The reductions occurred in the upslope conditions and resulted in mean differences of -21.9% (first metatarsal) and -8.8% (first toe).

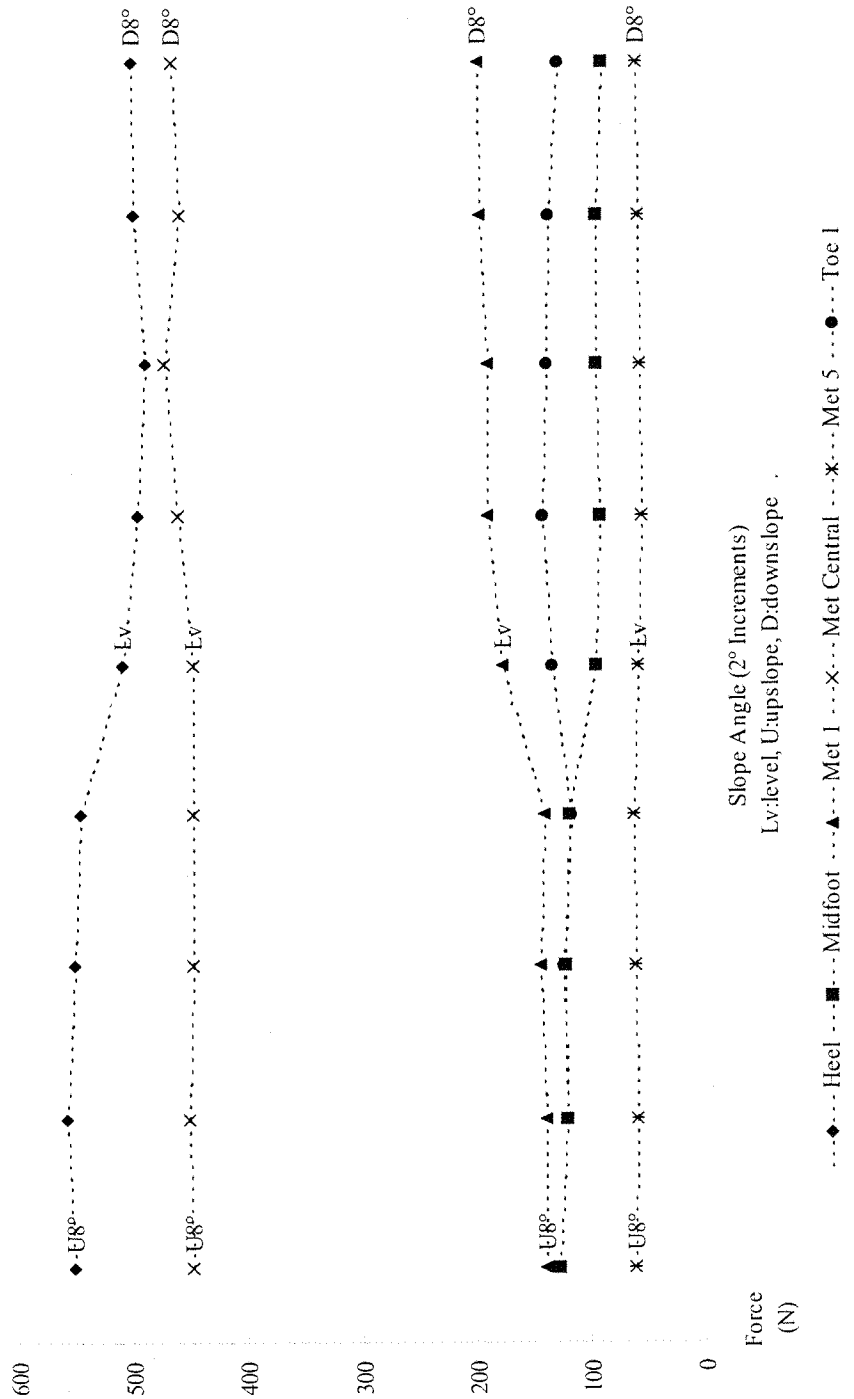


**Figure 5.18 Influence of sideslope on regional force**

### 5.5.7. Temporal parameters and the stance phase time

Four temporal parameters of the gait cycle were measured and analysed to reveal the within site timing responses to changes of slope angle. The parameters were, initial contact time (ICT), contact duration (CD), time to peak force (TPF) and time to peak pressure (TPP). Each of these was expressed as a percentage of the stance phase time. The stance phase time was defined as that period when the foot, or part of the foot, was in contact with the supporting surface. It was returned directly from the pressure platform as a function of the number of recorded scans for each test.

The means (±sd) for the overall stance phase times were 774ms (±43), 802ms (±54) and 779ms (±58), for the level, upslope and downslope conditions respectively. The upslope time was, on average, 28ms longer than the time for level walking; an increase of 3.6%. There was also an increase for the downslope conditions but this was only 0.6%. Level walking showed the most consistency in stance phase time, with a coefficient of variation (cv) of 5.6%, while the cv for upslope and downslope were 6.7% and 7.4% respectively. In the downslope trials the cv increased progressively with the angle of slope, with a maximum of 8.4% at 8°. Analysis of variance, however, revealed that the differences between any of the nine conditions were not statistically significant ($df_{8,261}$ F=1.62, p=0.12).

### 5.5.8. Initial contact time for level and sideslope walking

The initial contact time (ICT) was measured with respect to the time of initial contact of the foot as a whole and expressed as a percentage of the stance phase of gait. The heel was always the first region to contact the ground and its ICT was, therefore, zero by definition. The means and standard deviations for the ICT are given in table 5.26. The influence of the angle of incline on ICT for each site is shown in figure 5.19.

**Table 5:26 Initial contact time (% stance phase) results for sideslope walking**

Mean values (upper row) and standard deviations (lower row) for each site of the foot (* indicates a significant difference from the level condition, U indicates upslope, D indicates downslope, Lv indicates level).

| Incline | U8° | U6° | U4° | U2° | Lv | D2° | D4° | D6° | D8° |
|---|---|---|---|---|---|---|---|---|---|
| Heel | 0.0 | 0.0 | 0.0 | 0.0 | 0.0 | 0.0 | 0.0 | 0.0 | 0.0 |
| | 0.0 | 0.0 | 0.0 | 0.0 | 0.0 | 0.0 | 0.0 | 0.0 | 0.0 |
| Midfoot | 8.1 | 8.5* | 8.2 | 8.2 | 7.7 | 7.5 | 7.3 | 6.9* | 7.3 |
| | 2.7 | 5.5 | 3.3 | 4.0 | 3.4 | 2.3 | 2.6 | 2.1 | 2.0 |
| Met 1 | 14.6* | 15.0* | 14.6* | 14.9* | 12.4 | 11.6* | 11.3* | 11.3* | 11.4* |
| | 4.6 | 6.6 | 4.0 | 4.5 | 3.9 | 3.0 | 3.1 | 3.5 | 3.4 |
| Met Cen | 7.4 | 7.4* | 7.4* | 7.6* | 6.9 | 6.5 | 6.2* | 6.4* | 6.7 |
| | 2.3 | 1.9 | 2.2 | 2.1 | 2.1 | 1.7 | 1.8 | 1.9 | 1.8 |
| Met 5 | 7.4 | 7.6 | 7.6 | 7.9* | 7.2 | 7.2 | 7.0 | 7.1 | 7.9* |
| | 2.5 | 2.1 | 2.5 | 2.4 | 2.0 | 2.1 | 2.0 | 2.2 | 2.4 |
| Toe 1 | 29.4 | 29.5 | 32.6 | 32.8 | 31.2 | 25.9* | 27.2* | 29.1 | 28.6* |
| | 14.1 | 14.1 | 13.5 | 14.5 | 13.2 | 12.0 | 12.7 | 14.7 | 14.2 |

In the upslope conditions, all sites, except the first toe, contacted later in the stance phase when compared with level walking. Overall, the delayed contacts demonstrated mean differences of 5% to 8% with respect to their level values. The first metatarsal, however, demonstrated a mean upslope ICT difference of 19.4% with statistical significance for all four upslope angles. The central metatarsals also showed a fairly consistent delay, with statistical significance at three of the four upslopes, although the average delay was only 8.2% for this site.

In the downslope conditions, the ICT were earlier for all sites except the fifth metatarsal, producing an overall mean difference of about -5.9% in comparison with level walking. Again, the first metatarsal demonstrated statistical significance for all four inclines, although the downslope mean difference was only -7.8%. The central metatarsals had an average difference of -6.3% with statistical significance for only two inclines. The ICT for the first toe followed the trend for the other sites in the downslope conditions but its responses varied in the upslope conditions, being later on the 2° and 4° slopes but earlier on the 6° and 8° slopes.

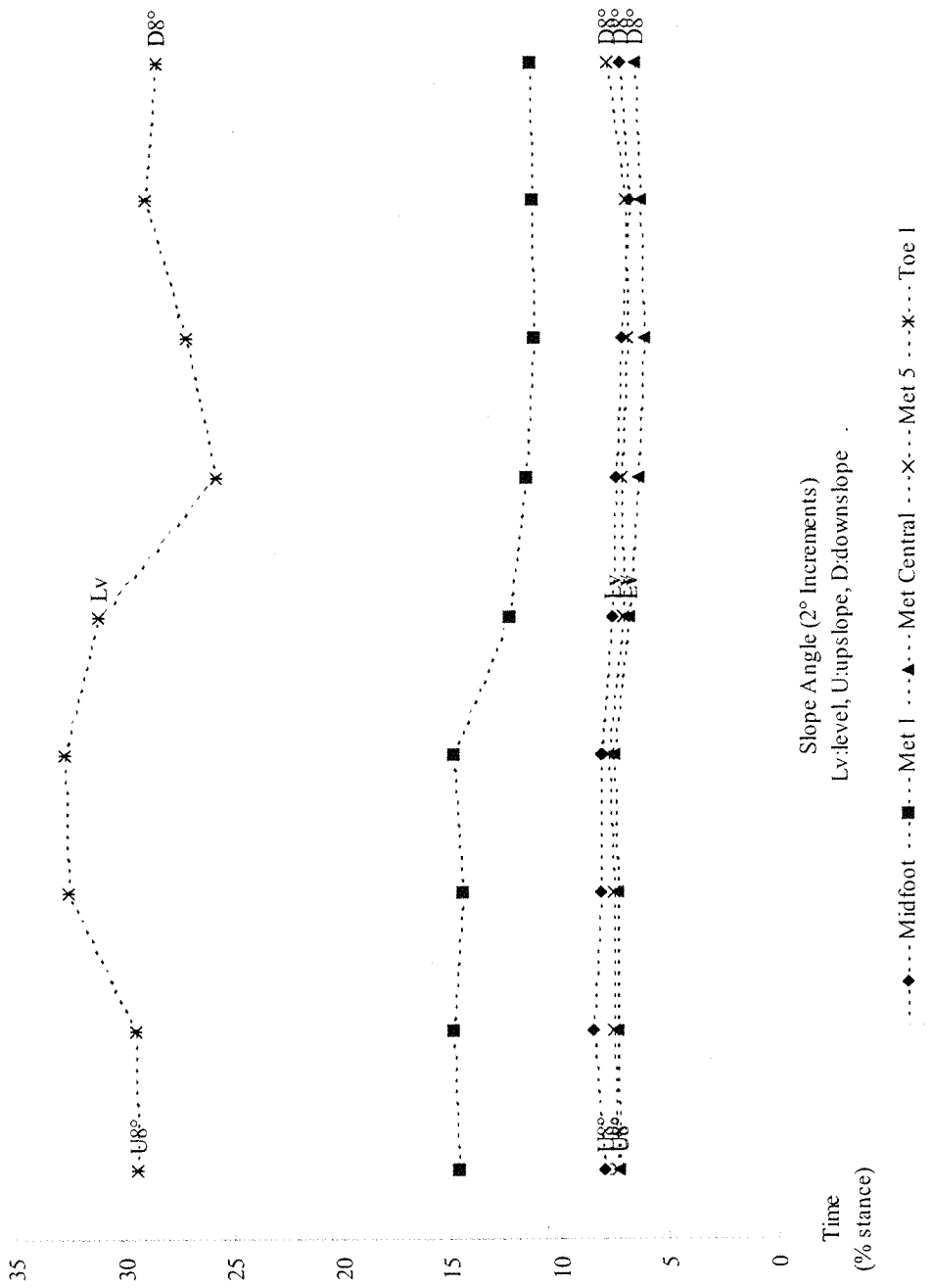


**Figure 5.19 Influence of sideslope on initial contact time**

### 5.5.9. Contact duration for level and sideslope walking

For each foot site, the contact duration (CD) was considered as the period from initial ground contact until loss of contact, and expressed as a percentage of the contact duration for the whole foot (ie. the stance phase). The means and standard deviations for the CD are given in table 5.27. The influence of the angle of incline on CD for each site is shown if figure 5.20.

**Table 5:27 Contact duration (% stance phase) results for sideslope walking**

Mean values (upper row) and standard deviations (lower row) for each site of the foot (* indicates a significant difference from the level condition, U indicates upslope, D indicates downslope, Lv indicates level).

| Incline | U8° | U6° | U4° | U2° | Lv | D2° | D4° | D6° | D8° |
|---|---|---|---|---|---|---|---|---|---|
| Heel | 58.2 | 58.5* | 57.7 | 57.3 | 57.1 | 55.5* | 54.3* | 54.7* | 55.6* |
| | 8.4 | 7.4 | 8.2 | 7.8 | 8.5 | 8.9 | 9.1 | 8.9 | 8.9 |
| Midfoot | 66.1* | 65.7* | 64.1 | 63.6 | 63.1 | 61.3* | 61.4* | 62.1 | 61.6* |
| | 8.6 | 10.0 | 11.1 | 9.4 | 9.2 | 10.0 | 9.9 | 8.6 | 10.0 |
| Met 1 | 79.0* | 78.2* | 78.6* | 78.2* | 81.0 | 82.1* | 82.0* | 81.6 | 82.2* |
| | 5.1 | 9.5 | 3.7 | 5.0 | 4.7 | 3.7 | 3.9 | 4.5 | 3.7 |
| Met Cen | 87.2 | 87.2* | 86.7* | 86.6* | 87.9 | 88.0 | 88.4 | 88.2 | 87.9 |
| | 2.9 | 2.6 | 2.7 | 3.0 | 2.9 | 2.8 | 2.7 | 2.8 | 2.7 |
| Met 5 | 81.6* | 81.1 | 80.7 | 80.5 | 80.6 | 80.1 | 79.9 | 80.0 | 79.3* |
| | 3.9 | 3.5 | 4.2 | 4.1 | 4.2 | 4.6 | 4.6 | 5.3 | 4.0 |
| Toe 1 | 69.5 | 69.1 | 66.3 | 65.8 | 66.6 | 72.6* | 71.7* | 70.0* | 70.3* |
| | 14.1 | 14.7 | 13.4 | 14.7 | 13.9 | 12.4 | 12.9 | 14.7 | 14.5 |

In the upslope conditions, the heel and midfoot both demonstrated increases in contact duration (+1.5% and +2.8%, respectively) although statistical significance occurred only for the 6° and 8° slopes. In contrast with these sites, the CD of the first and central metatarsal were reduced (-3.0% and -1.1%, respectively), the reductions being statistically significant for almost all slope angles. The CD in the downslope conditions decreased at the heel (-3.6%) and the midfoot (-2.4%) and increased at the first metatarsal (+1.2%), but did not change for the central and fifth metatarsals. The first toe showed the largest mean difference from level walking (+6.8%), with statistically significant increases for all downslope conditions, although no significant differences were seen for the upslopes.

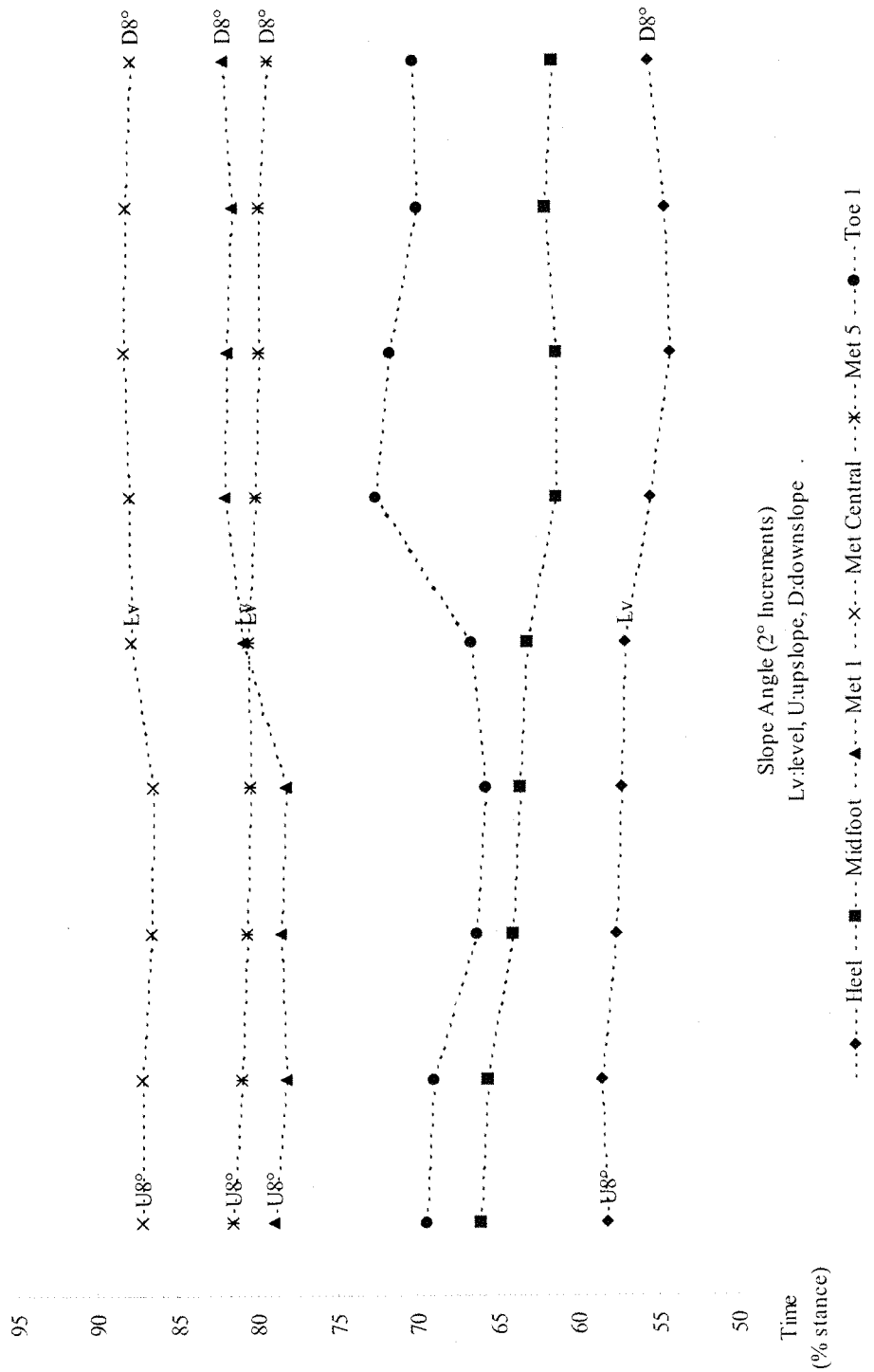


**Figure 5.20 Influence of sideslope on contact duration**

5.5.10. Time to peak force and time to peak pressure

The time to peak force (TPF) was defined as the period from the initial contact of the foot as a whole until the occurrence of the maximum force at a particular site. Maximum force was determined by the sum of the loads across all sensors within the site, figure 1.9. The time to peak pressure (TPP) was similarly defined but was determined by the occurrence of the maximum pressure at a single sensor within a site. The means and standard deviations for the TPF and the TPP are given in tables 5.28 and 5.29. The pattern of upslope and downslope responses observed in the timing of peak forces and peak pressures were essentially the same and are therefore considered together.

In the upslope conditions, the heel, midfoot and first metatarsal all showed significant delays in the TPF with mean differences of +5.7%, +5.1% and +2.7%, respectively. Although the central metatarsals, fifth metatarsal and first toe also demonstrated increases in TPF, these were not usually statistically significant. Generally, in the downslope conditions, the TPF was decreased and loading therefore occurred relatively earlier. The first metatarsal, however, was an exception and showed an increase of +2.5%, with statistical significance for the 6° and 8° slopes. This result is unusual since an increase in the TPF was also recorded in the upslope conditions.

The overall pattern of the upslope and downslope responses for the TPP parameter was essentially the same as that for the TPF. However, the actual timings were different and a phase shift between the two was observed for particular sites, figure 5.21. In the heel and midfoot the TPP was shorter than the TPF and peak pressures occurred earlier than peak forces, whereas, this order was reversed for the metatarsal sites where the peak pressures occurred after the peak forces. The delays of the TPP in comparison with the TPF at the first, central and fifth metatarsals were about 5%, 9% and 4%, respectively. At the first toe, however, peak pressure occurred about 2.0% earlier than peak force.

**Table 5:28 Time to peak force (% stance phase) results for sideslope walking**

Mean values (upper row) and standard deviations (lower row) for each site of the foot (* indicates a significant difference from the level condition, U indicates upslope, D indicates downslope, Lv indicates level).

| Incline | U8° | U6° | U4° | U2° | Lv | D2° | D4° | D6° | D8° |
|---|---|---|---|---|---|---|---|---|---|
| Heel | 22.3* | 22.2* | 22.2* | 21.7* | 20.9 | 20.5 | 19.8* | 19.7* | 20.7 |
| | 3.6 | 2.9 | 2.7 | 3.1 | 3.1 | 2.8 | 3.6 | 2.7 | 2.9 |
| Midfoot | 42.8* | 44.1* | 42.3 | 40.3 | 40.3 | 38.2* | 37.6* | 36.1* | 34.9* |
| | 9.4 | 10.5 | 9.2 | 9.8 | 9.5 | 9.4 | 10.3 | 8.3 | 12.0 |
| Met 1 | 70.0* | 69.5* | 70.1* | 67.9 | 67.6 | 68.0 | 68.4 | 70.9* | 69.6 |
| | 6.2 | 5.8 | 7.3 | 8.8 | 8.7 | 9.6 | 10.8 | 5.8 | 9.5 |
| Met Cen | 73.1 | 73.2* | 72.4 | 72.5 | 72.2 | 68.9* | 69.9* | 67.5* | 69.8* |
| | 5.4 | 5.4 | 4.9 | 5.5 | 5.2 | 8.4 | 7.5 | 9.5 | 8.6 |
| Met 5 | 63.8* | 62.4 | 62.2 | 62.1 | 60.8 | 58.0* | 57.4* | 58.2* | 58.0 |
| | 10.7 | 11.6 | 10.6 | 11.7 | 11.4 | 13.3 | 15.6 | 12.7 | 16.6 |
| Toe 1 | 81.1 | 81.6 | 81.7 | 81.7 | 81.3 | 81.3 | 81.2 | 81.1 | 80.3* |
| | 4.4 | 3.7 | 4.1 | 4.5 | 3.7 | 3.5 | 3.8 | 4.4 | 4.6 |

**Table 5:29 Time to peak pressure (% stance phase) results for sideslope walking**

Mean values (upper row) and standard deviations (lower row) for each site of the foot (* indicates a significant difference from the level condition, U indicates upslope, D indicates downslope, Lv indicates level).

| Incline | U8° | U6° | U4° | U2° | Lv | D2° | D4° | D6° | D8° |
|---|---|---|---|---|---|---|---|---|---|
| Heel | 18.6* | 18.3* | 17.2 | 16.5 | 16.5 | 16.6 | 16.7 | 16.5 | 17.4 |
| | 5.7 | 5.2 | 5.2 | 5.6 | 5.4 | 5.4 | 4.6 | 4.5 | 5.4 |
| Midfoot | 38.7 | 42.8* | 38.4 | 36.7 | 36.7 | 35.6 | 35.6 | 31.9* | 34.7 |
| | 13.1 | 14.0 | 11.8 | 13.4 | 11.7 | 12.1 | 12.6 | 9.8 | 13.5 |
| Met 1 | 73.6 | 73.7 | 73.9 | 73.2 | 73.3 | 74.6* | 75.0* | 75.6* | 75.0 |
| | 6.1 | 6.0 | 6.2 | 7.7 | 7.0 | 6.1 | 7.0 | 6.7 | 6.4 |
| Met Cen | 80.8 | 80.5 | 80.2 | 80.7 | 80.8 | 80.9 | 81.2 | 80.5 | 81.1 |
| | 3.8 | 3.3 | 3.5 | 3.7 | 3.4 | 4.3 | 4.3 | 5.0 | 4.5 |
| Met 5 | 66.5* | 65.8 | 66.2* | 66.0 | 64.7 | 61.0* | 61.0* | 61.7* | 60.1* |
| | 9.2 | 10.4 | 9.9 | 10.3 | 9.3 | 13.6 | 14.5 | 13.0 | 16.4 |
| Toe 1 | 79.2 | 79.2 | 79.2 | 79.5 | 79.3 | 78.9 | 78.0* | 78.3* | 77.5* |
| | 4.9 | 4.6 | 4.8 | 5.7 | 4.1 | 4.8 | 4.1 | 4.7 | 4.8 |

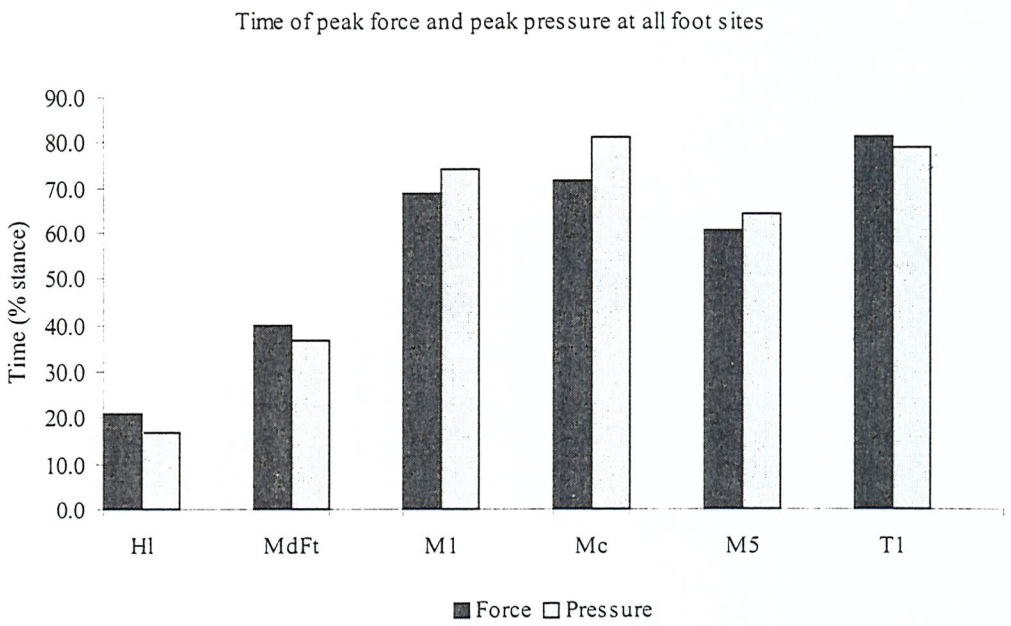


**Figure 5:21 Comparison of peak times for force and pressure**

At the heel and midfoot sites peak pressure preceded peak force. At the metatarsal sites peak pressure occurred later than peak force. The same trend was seen in both level and sideslope walking conditions. The averages for all walking conditions are presented.

# 6. Discussion

## 6.1. Introduction

This investigation aimed to determine alterations in regional load, contact area and pressure on the sole of the normal foot during sideslope walking. An important objective was to establish a method that could be incorporated into future investigations, and to gain an understanding of the factors that might impact on the reliability of such a method. The initial work included a detailed evaluation of a pressure measurement system based on conductive polymer technology. Undesirable characteristics in the polymer sensors, particularly sensitivity to shear, necessitated additional investigation with an alternative pressure measurement system using capacitive sensors. The results from a comparative study of the two systems identified the likely impact of the anomalous behaviour of the polymer sensors, and the findings of the study are interpreted accordingly.

## 6.2. Conductive polymer sensors

In accordance with the initial objectives of this study, the characteristics of the elements of the polymer array have been established and similarities with discrete polymer sensors of the same type have been determined. Dynamic characteristics, which have not been described previously, were established within the limits of the investigation. Importantly, the deflection behaviour of the upper membrane of the sensor has been described in detail for the first time. Finally, the accuracy of measurement of the contact area of the sole of the foot by means of electronic footprints was determined.

### 6.2.1. Sensor membrane behaviour in response to a decreased internal pressure

By modifying the polymer sensor so that the internal air could be evacuated, the deflection behaviour of the upper membrane was observed and recorded. Prior to the application of the vacuum, the upper membrane sagged slightly so that the central point of the surface was lower than its periphery. In the modified sensor, as the air was withdrawn the sag increased and the membrane developed a smooth, concave depression that appeared parabolic. Eventually, the central part

of the upper membrane contacted the lower substrate and the previously curvilinear profile developed a flattened central portion. As more air was withdrawn the flattened portion of the membrane enlarged, suggesting that the contact area between the upper membrane and the lower substrate had increased, figures 5.1 to 5.2. Partial evacuation demonstrated that the upper membrane usually contacted the lower substrate when the vacuum pressure was about 20 to 30 kPa. This observation strengthens the finding that the threshold sensitivity for 90% of the elements was 20 kPa, while the remainder triggered at 35 kPa. The contact region enlarged progressively until the maximum vacuum pressure of about 70 kPa was applied, by which time the upper membrane appeared to be approaching a position of almost full contact with the lower substrate. With high levels of vacuum, the profiles demonstrated that the upper membrane had to deflect steeply at the periphery of the sensor where it was separated from the lower substrate by the intervening insulation elements, figure 3.2. Therefore the arrangement of the conductive tracks and insulation elements in a polymer sensor array appears to influence the deflection behaviour of the upper membrane. This arrangement is likely to cause an edge effect phenomenon for elements in polymer arrays, similar to that reported by Hedman [39] for discrete polymer sensors. While the same basic pattern of deflection was seen for all of the tests where air was evacuated from the sensor, it became apparent that the region of contact was more even and geometrically regular for some elements than for others, figures 5.1 and 5.2. Since the decrease in the electrical resistance of these sensors has been shown to be a function of the area of contact [39,40,43], local irregularities could account for some of the between sensor variation that was found across the array, table 5.2 and figure 5.8.

A partial vacuum ensured that an even pressure was exerted over the entire surface of the membrane, and this accounted for the smooth, symmetrical profiles that appeared prior to contact with the lower substrate at about 30 kPa. During mechanical testing, however, the deflection and contact behaviour of the upper membrane would be expected to be different beneath the unyielding surface of the anvil that was used for the step loading tests even though a compliant elastomer was placed at the interface. Therefore, the inflexibility of the mechanical indenter may have increased the within sensor variation recorded

for the step loading tests, figure5.5. In contrast, the soft tissues of the sole of the foot may act as a compliant interface and minimise the distortion of the sensor membrane but this cannot be guaranteed especially in the presence of bony prominences or callused skin. It is possible, therefore, that the sensor would be subjected to non-uniform pressure distribution across its active surface [100,101], and this could distort the membrane. For these reasons, the response of the sensor would be less predictable in its working environment than under controlled test conditions. This may account in part for the observations of Pax *et al.* [43], who reported that force sensing resistors responded consistently to pressures applied over areas greater than or equal to the sensing area, but inconsistently when the pressure was applied to an area smaller than the sensing area. Following the initial contact between the upper and lower membranes, the propagation of the contact region could be irregular, especially for elements with an uneven substrate.

For sensors with such a flexible surface, therefore, the position of the initial contact point between the upper membrane and the lower substrate, and the subsequent spread of the contact region is likely to vary. The variation will be most significant with eccentric loading conditions but should reduce once the membrane has fully contacted the underlying substrate.

In summary, it is proposed that some of the within sensor variation may be due to unpredictable behaviour of the upper membrane, especially at low pressures before contact over the full sensing area has been established. Asymmetrical distortion of the membrane is likely to occur with uneven load distribution and the position of the centroid of the load on the sensing surface. The initial point of contact between the upper membrane and the lower substrate may alter, and this could induce variation especially in instances where the substrate is uneven.

### 6.2.2. Performance of the polymer sensor elements

The polymer elements tested in this study revealed similar performance characteristics to those of discrete polymer sensors, table 2.7. The elements demonstrated a non linear output in response to increasing pressure, such that

their sensitivity changed through their useful range. At low pressures, upto about 200 kPa, the elements were very sensitive and demonstrated relatively large changes in output voltage for correspondingly small changes in pressure. For pressures between 200 and 800 kPa, the sensors demonstrated a gradual but continuous decrease in sensitivity, while from about 800 kPa the sensitivity became relatively constant once more. The elements were approximately twenty times more sensitive to pressure change in their low region (<200 kPa) than in their high region (>800 kPa). The findings of non linearity and pressure dependent sensitivity are in accord with those reported previously for discrete polymer sensors [39-42,44]

Healthy young adults, such as the volunteers for this study, have mean peak foot pressures of between about 200 and 600 kPa, tables 2.1 and 2.3, and measurement of these would utilise the central region of the polymer sensor response range, figure 5.3. Having a coefficient of variation (cv) ≈2 to 4%, this region offered a reasonable compromise between repeatability and amplitude resolution. From this perspective the sensor is reasonably well suited to the measurement of foot pressures. However, in the low pressure region the cv ≈8%, and measurements from low pressure sites of the foot, such as the midfoot (≈60 kPa, table 2.3), would therefore be less reliable even though the amplitude resolution in this region is acceptable. Furthermore, many of the sensors at the periphery of the foot would be expected to be lightly loaded and measurements from these areas would also be expected to be less reliable. For pressures greater than 600 kPa, the cv was small (≤1%) and measurements were therefore more repeatable. However, because the sensor output tended to plateau, the amplitude resolution in this pressure range was less than that at the low and mid-pressure regions. Therefore, the sensor would be less able to discriminate between pressure levels above about 600 kPa.

The within sensor variation, determined from the step loading tests, revealed mean coefficients of variation for loading and unloading as 2.2% and 0.9% respectively. However, the variation was observed to be a function of the applied pressure, such that the repeatability was least for the low pressures, figure 5.5.

The greatest within sensor cv was ≈8.5% and occurred in the loading tests for pressures of ≈80 kPa; the initial loading pressure. The within sensor variation for discrete polymer sensors [40,41,44], has been reported as about 7%. and the previous findings are, therefore, in agreement with the maximum value of 8.5% found in this study. In addition to supporting the findings of earlier work, this investigation has identified that within sensor variation is greatest at low pressures, reducing to less than 5% for pressures above 150 kPa.

Measurement repeatability was shown to worsen when an element was moved and subsequently repositioned between tests, figure 5.4. When the element was repositioned and the alignment judged by eye, then the maximum cv increased substantially to 22%, whereas the use of an alignment template produced a maximum cv of 12%. For all of these tests a small anvil, with a contact area marginally less than the active area of the element, was used. However, a small error in the placement of the anvil positioned it directly above one of the nodes where the underlying conductive tracks and insulation elements intersected, figure 3.2. When the anvil was positioned over a node the sensor response to loading diminished noticeably. The alignment template was designed specifically to ensure that the anvil was positioned central to the sensing area of the element so as to avoid the nodes at each corner. Hedman [39], reported that discrete polymer sensors exhibited substantial edge effects, and found reductions in sensor output similar to those observed during these tests, but reduced the problem by using a rubber coated metal plunger to apply loads. Furthermore, while the discrete sensors showed almost no variation from one cycle to the next when loaded repeatedly, the initial load resistances varied by about 10% after repositioning. The variation of 10% is in close agreement with the cv of 12% achieved in this study where template realignment was used to minimise the influence of edge effects. The results from this study suggest that edge effects are as influential on the individual elements of an array as they are on discrete polymer sensors. Although it was not ultimately necessary to retest individual elements in this study, it was shown that correct alignment between the test rig and the sensor is essential for maximum consistency. Reasonable estimates of within sensor variation can only be achieved by using an alignment template if

the sensor is moved between tests. While edge effects can clearly cause a decrease in the repeatability of the measurements, they do not account for all of the within sensor variation. The behaviour of the sensor membrane, or other unidentified factors, may explain the additional variation.

The within sensor variation for the loading and unloading parts of the test cycles showed a similar overall pattern, figure 5.5. However, the behaviour of the polymer sensor was more consistent for unloading than for loading, figures 5.6 and 5.7. The reasons for this observation are unclear, although one possible explanation is that an internal restoring force has a more uniform effect on the sensor membrane than an externally applied loading force. In addition, cohesive forces within the sensor may restrain the upper membrane and stabilise or smooth its return to the position of equilibrium. Unfortunately, none of the previous studies regarding discrete polymer sensors have segregated the unloading curve for separate evaluation and there are, therefore, no comparable findings within the literature.

All of the tested sensor elements demonstrated the same general pattern of response but the output magnitudes varied. The mean between sensor variation across the surface of the platform was ≈8.3%, with a maximum of ≈18% occurring with low pressure measurements. No comparable values are available from the literature. The variation measured over the surface of the platform emphasises the need for a method of calibration that produces individual tables for all of the elements within the array[158]. The calibration method adopted by the manufacturer [159,160] utilises a material testing machine and a fluid filled bladder in an attempt to ensure uniform pressure distribution to groups of elements which are simultaneously calibrated.

Inspection of the load-unload graphs reveals the presence of hysteresis within the polymer sensors, figure 5.3. The mean value for hysteresis derived from all test results was 4.0% full scale output (FSO), while the maximum was approximately 12% FSO. For measurements obtained in the pressure range below 350 kPa, the hysteresis averaged 9.4% FSO. The results from the previous

studies of discrete polymer sensors are reported to be between 5 and 8% FSO, table 2.7, and therefore appear marginally less than those reported here. Factors that influence the time dependent characteristics of polymer sensors have been investigated previously [154,162] The findings from these studies must be examined with caution, however, because the designs of the sensors differed substantially from the polymer array investigated here, as did the materials used for their construction[149,150]. The hysteresis of polymer sensors of the type used for this study (Interlink FSR™) has consistently been reported to be about 5 to 8% FSO. In comparison, hysteresis for the most common alternative polymer sensor (Fscan ™) is 21%, greater by a factor of about three. The results from the Fscan ™ tests indicate that the duration of the loading is more influential on viscoelastic behaviour than the cyclical nature of the loading itself. In previous studies of discrete Interlink FSR™ sensors [39-42,44] the hysteresis was determined from dynamic loading cycles of short duration whereas, in this study, the sensors were step-loaded and the overall loading period typically lasted several minutes. The longer period of loading may therefore account for the marginally greater hysteresis found in this study when compared with the results from studies of discrete Interlink FSR™ sensors.

Potentially, hysteresis can have two effects on the sensor performance. First, if the calibration was determined from the loading curve then there will be some inaccuracy associated with the unloading portion of the output signal. Second, the hysteresis will distort the dynamic signal. It was anticipated at the start of the study that the behaviour of the polymer elements would be similar to that of discrete polymer sensors and, since the previous literature concerning discrete sensors [39-42,44] indicated both non-linearity and hysteresis, a suitable method of dynamic analysis was required. The elements of the polymer array were therefore tested dynamically and the resulting signals subjected to cross-correlation and power spectral density analysis. The cross-correlation function was selected because it is a well known time-domain analysis technique giving a measure of the similarity between two waveforms [173]. Power spectral density analysis was selected as an appropriate frequency domain technique. Using the principle of sinusoidal fidelity, it can identify substantial non-linearity, since a

sinusoidal input to a linear system will generate a sinusoidal output of exactly the same frequency [174].

Cross-correlations for the polymer sensors are presented in table 5.3. The mean normalised cross-correlation coefficients were 0.89 and 0.87 for the low and high amplitude test ranges, respectively. In both the low and high amplitude ranges, the lowest correlations were found for the tests at 4 Hz. At the 4 Hz frequency the electromechanical shaker was just able to follow the signal from the control amplifier and simultaneously ensure that the anvil maintained continuous contact with the polymer array. The input signal at 4 Hz was, therefore, the least sinusoidal of all the test conditions but correlation coefficients of 0.81 and 0.83 (low and high ranges, respectively) were achieved. High correlation coefficients were maintained throughout the test range indicating that, within these frequency-amplitude boundaries, the signal morphologies from the two transducers were similar, and the polymer sensor had the ability to follow the input signal. Analysis of the power spectra demonstrated that, for each test, the output signal retained the exact frequency of the input signal. Furthermore, the relative power content of the fundamental frequency for the two signals did not change substantially throughout the test range. On average, the polymer sensor returned over 90% of the relative power of the input signal, at the fundamental frequency, figure 5.10.

The results from the tests indicate that the dynamic behaviour of the polymer sensor remains reasonably consistent for input signals upto about 26 Hz. Since most of the power in the signals associated with normal walking is within this bandwidth the polymer sensors are useful for the measurement of walking foot pressures. However, it remains unknown as to whether the sensors are capable of following the high frequency transients that can occur when either the heel or metatarsals strike the ground. Furthermore, the results do not necessarily suggest that the sensor will behave as a linear system [174]. The dynamic tests were confined to the initial regions of the polymer loading curve, with maximum amplitudes of about 500 kPa. Since the polymer sensor output had a tendency to plateau as the pressure increased, figure 5.3, it would be anticipated that tests at higher pressures could reveal changes in the dynamic amplitude. It would be

anticipated that this could reduce the relative power in the power spectra for high pressure signals.

Shear sensitivity characteristics of polymer sensors have not been described fully in the literature. Hedman [39], conducted a detailed investigation into the properties of discrete polymer sensors similar to those used for this study, and commented that the sensor did "not register shear forces". Unfortunately, no supporting evidence for this statement was presented. Nicolopoulos *et al.*[176], hold a contradictory view, asserting that the output of the discrete sensors can alter substantially when they are subjected to shear, and cite the additional work of Zahednejad to support their claim. The methods used to determine these results were not fully described, although it appears that the sensors were tested at low pressures (75 kPa). Shear sensitivity was considered particularly relevant to the current study because of the likely increase in shear force when walking on an inclined surface, and it was important that this issue be clarified.

The polymer sensor elements of the array were therefore tested to determine the sensitivity to shear. The tests were conducted with a vertical load that produced contact pressures more representative of those beneath a normal foot (≈120 kPa). A shear force was applied after the vertical load was established producing shear to vertical force ratios of 0.25 and 0.5 which indicate relative shears of 25 and 50% respectively. These are representative of the loading conditions that would be expected for level and incline walking on slopes of upto ≈18°, as reported by Harper [16] for uphill walking. It was considered, therefore, that the shear exerted during these tests would equal or exceed those likely to occur on an 8° incline such as the one used for the study of sideslope walking.

Tests were conducted sequentially beginning with vertical load only. The test sequence then alternated between loading conditions where shear was either present or absent. The results, in the order of testing, are presented in table 5.4. For the polymer sensor, all of the tests differed significantly in comparison with the initial non-shear condition. The results suggest that shear does influence the sensor output, elevating it in comparison to its original level by an average of

about30 kPa (≈30% increase). Once this change had occurred, the new output level appeared to be maintained even when the shear component of force was removed. The fact that the results from the first non-shear test differed from the subsequent second and third non-shear tests may indicate that the sensor had undergone some form of conditioning. Previous studies have shown that polymer sensors can exhibit time dependent behaviour when subjected to repetitive cyclical loading [154,162], and it has been postulated that this may result in a combination of recoverable (rapid viscoelastic) and irrecoverable (slow creep) components [154]. Since these phenomena are reported to be primarily influenced by the duration of loading, evidence of their effects should have become more noticeable as the tests progressed. However, this was not the case. Furthermore, in comparison with later measurements, the six replicate measurements that were recorded for the first non-shear condition were reasonably consistent. None of the tests revealed obvious signs of creep. Although it appears that the sensor may have undergone some form of conditioning, the underlying process remains unclear. However, the evidence indicates that the most significant changes in output are brought about by the initial shear.

It must be concluded from these findings that a rise in sensor output might indicate either a local escalation in pressure or the presence of some coexistent shear. While it is believed that shear contributes to tissue damage on the sole of the foot and that knowledge of its presence is therefore beneficial [177], the inability to differentiate between pressure intensification and substantial coexistent shear is less than optimal. In an attempt to clarify the effect that this particular characteristic of polymer sensor behaviour may have on measurements of foot loading, a pressure platform utilising a different transducer was sought so that comparative tests could be undertaken. An Emed SF platform, incorporating capacitive sensors constructed from an elastomeric substrate, was subsequently obtained and its sensors tested using the same method used for the polymer tests. The results for the shear tests for the second platform are presented in table 5.4. There were no significant differences between any of the test conditions for the capacitive sensors. However, the

sensors did demonstrate a slight drop in output of about 4 kPa (≈2.5%) between the start and end of the tests, suggesting that they may also be affected by pre-conditioning although to a lesser extent. The within sensor repeatability remained approximately constant throughout the tests (<4 kPa), in stark contrast to the polymer sensor results. This was taken as an indication of the stability and reliability of the capacitive sensors. While the capacitive sensor platform had almost identical spatial resolution and sampling frequency as the polymer sensor platform, it did not exhibit the same sensitivity to shear. It was concluded therefore that the capacitive sensors would be suitable for investigating load distribution beneath the foot during sideslope walking. Furthermore, these results indicated that a comparative study of the two platforms would be beneficial. By analysing data for both level and sideslope walking in order to identify differences between the two systems, additional insight into the loading profiles could be gained, and the actual effects on the polymer sensors could be determined

### 6.3. Comparison of Platforms

The polymer sensor exhibited a peculiar response when subjected to shear. Shear force, applied in combination with normal force, caused the sensor output values to increase. However, the elevated output reappeared in the subsequent tests when only the normal force was applied, table 5.4. Shear may therefore bring about some conditioning of the sensor and this could result in the elevation of subsequent output values even if shear is absent. Regardless of this possibility, the output from the sensor alters when shear is present. In an effort to determine the implications of these findings, a pressure platform using alternative sensor technology was borrowed, tested for shear effects, and a comparative walking trial was conducted. The test protocol used for the trial was identical to the one subsequently used in the main study of sideslope walking. Data were collected from nine subjects for all level and sideslope incline conditions, and for both foot placement orientations (upslope and downslope).

The presence of significant differences between the two platforms was initially sought using a two factor general linear statistical model with repeated

measures. The results are given in table 5.5. The temporal parameters (initial contact time, duration of force, time to peak pressure and time to peak force) were not significantly different between machines, table 5.5. Neither were peak pressures and regional forces, table 5.5. Differences in contact area were, however, statistically borderline, table 5.5. For pressure, while pooled values in the general linear model did not demonstrate differences overall, examination of the interactions (machine x slope) indicated that the platforms had returned significantly different results for certain sideslope walking conditions, table 5.5. Regional force data produced a pattern of results similar to that of the pressure data. All parameters were therefore re-examined using the Bland and Altman [176] method for assessing agreement between two clinical measurement techniques. Furthermore, the data for level walking was isolated from the sideslope data and each were examined separately.

Estimates of bias, indicating the level of agreement between the two platforms, were determined for all parameters. Small bias values are indicative of close agreement. For level walking, bias for each of the four temporal parameters was ≤2% of the stance time, table 5.6. A Bland and Altman plot of the initial contact time data is presented in figure 5.11. In this example the data are equally spread above and below the horizontal axis, across the measurement range, and the bias is therefore close to zero. Contact area measurements demonstrated a bias of 1.6 $cm^2$ with the polymer sensor platform returning generally smaller values, table 5.7. The bias for peak pressure was ≈16 kPa, while that for force was ≈1N, table 5.7. Therefore, agreement between the two machines for level walking appeared reasonable, with the exception of the differences identified for contact area. For sideslope walking there was a greater quantity of data available, in comparison with level walking, because of the eight slope conditions (4 gradients x 2 orientations). These data were pooled to enable assessment of effects at each foot site. Subsequently, data for each site were separated according to orientation (upslope versus downslope) and explored to identify atypical patterns of bias.

Temporal parameter differences remained essentially unaltered for sideslope walking, tables 5.8 to 5.11. The overall average bias for the temporal parameters during sideslope walking was <1% of the stance phase. The largest bias estimates were recorded for the initial contact time for the first toe (3.5% stance phase), and the duration times for the heel (-3.3% stance phase) and midfoot (3.1% stance phase). Bias estimates for contact area measurements from sideslope walking were similar to those for level walking, table 5.12. Larger bias estimates generally occurred at the larger foot sites of the heel (-2.3 $cm^2$) and midfoot (-2.5 $cm^2$), but the central metatarsal region (-0.8 $cm^2$) was an exception to this observation, table 5.12. Since footprint studies conducted earlier in the investigation demonstrated that the polymer array selectively excluded sensors from peripheral and low pressure regions, it may be speculated that the difference in the bias estimates for these sites was due to the proportionally greater peripheries at the heel and midfoot. Because the first and fifth metatarsal sites border it, the central metatarsal site has a smaller periphery, figure 4.3. All other sites demonstrated small bias estimates. Furthermore, slope orientation had no apparent effect on contact area measurement.

Estimates of peak pressure bias for sideslope walking differed considerably between sites, table 5.13. The average bias across all sites approximated zero, but this was distorted by the large bias at the first toe site (-104 kPa). For the remaining five sites the bias averaged ≈20 kPa. For the heel and the central metatarsal sites the bias altered markedly according to slope orientation. In the downslope position the central metatarsal bias increased to almost 50kPa, figure 5.12. In the upslope position the heel bias increased to almost 60kPa, figure 5.13. Similar effects were not discernible for the other sites. The first metatarsal demonstrated the smallest bias. Regional force measurements revealed similar patterns to those for peak pressures. In the downslope position the central metatarsal bias increased to ≈89N, while for the upslope orientation the heel bias was ≈59N. For particular foot sites, therefore, the bias estimates for pressure and force indicate that measurements from the two platforms disagree. The effects of the disagreements are discernible in the regional force profiles, figures 5.14 and 5.15. The heel and central metatarsal sites demonstrate striking differences

between platforms. At the other sites differences are less obvious although some divergence is apparent for the first toe site (T1). Agreement appears best at the midfoot (MdFt) and first metatarsal (M1) sites, with both pressure platforms demonstrating the same trend of altered loading with sideslope walking.

While a full investigation of the transducer characteristics of the second platform was not possible, it is considered that the observed measurement anomaly could be due to the shear sensitivity of the polymer sensors. This explanation could account particularly well for the notable effects recorded at the heel and central metatarsal sites when the platform was inclined from the level. Shear forces, measured with force plates, have been described previously. For level walking, the fore-aft shear component of the ground reaction force peaks at 15-20% body weight, and is directed backwards against the foot in the first half of the stance period and forwards in the second half. The mediolateral component peaks at about 5% body weight and acts medially on the foot for nearly the entire stance phase [178-180]. For downhill walking, the fore-aft shear force can increase significantly and, in contrast to level walking, it is directed backwards against the foot for almost the entire stance phase [16,18,19]. For uphill walking, fore-aft shear is directed forwards against the foot for the entire stance phase [16]. The distribution of shear force on the sole of the foot, as detected by discrete sensors, has also been reported. For healthy young adults, regional shear generally appears to be greatest beneath the central metatarsals [177,181] and the first toe [181,182]. The magnitude of shear reported for the first metatarsal differs between authors but this inconsistency may be a reflection of the effects of factors such as walking speed, age or disease [183]. There is agreement that sheer on the heel is less than that on the central metatarsals but the shear stress-time integral may be largest at this site [177,181-183].

It is possible therefore that the polymer sensor will be influenced during both level and non-level walking since substantial shear forces act at the sole during both activities. Effects on the polymer sensor could be amplified during sideslope walking if the shear increases or its direction changes as happens when walking uphill or downhill. Furthermore, shear effects appear to be site dependent and this could account in part for the strong response observed in the

central metatarsal region. While the effect at the heel may be related to the large shear stress-time integral previously observed for this site, it may alternatively be associated with alteration of the mediolateral shear. Sideways oscillations of the centre of mass of the body occur during level walking as load is transferred from foot to foot [184]. For sideslope walking, greater effort may be required to displace the centre of mass sideways in the upslope direction. An augmented shear force, acting on the foot in the upslope direction, would therefore be required as load is transferred from the forefoot of the downslope foot to the heel of the upslope foot. This strategy could maximise shear at the central metatarsals, first toe and heel in a manner that would account precisely for the anomalies observed in loading patterns recorded by the two platforms. Further investigation of regional shear forces in sideslope walking is, however, required before definitive conclusions can be established.

This work indicated that the polymer sensor platform could be used to determine temporal parameters of foot loading for both level and sideslope walking. Contact area measurement was also possible although the returned values would underestimate the actual magnitudes. Systematic underestimation, however, is not problematic in a within subject experimental design of the type used to investigate sideslope walking. Measurements of peak pressure and regional force obtained with the polymer sensor platform must be interpreted with caution. For normal level walking anomalous effects do not appear to predominate and the values show reasonable agreement with those of the other platform. In sideslope walking, increases observed at the heel (Hl) and central metatarsal (Mc) sites do not appear to reflect increases in the normal component of the ground reaction force and should not be interpreted as such. Although the effects do not manifest as clearly at other sites, the first toe (T1) and fifth metatarsal (M5) show some similar signs and should be regarded with uncertainty until further evidence is available. However, results from the midfoot (MdFt) and first metatarsal (M1) sites demonstrated similar loading patterns to those revealed by the alternative pressure platform and, for this reason, they are considered to reflect actual changes of the regional normal force.

## 6.4. Use of the platform for the measurement of contact area

The use of pressure platforms to measure the contact area of footprints has received only superficial attention in the literature. Footprints, however, can be used for a variety of purposes including the classification of foot type according to arch index [25]. Pressure platforms offer an efficient method for collecting footprints but the accuracy of the electronic images, and their similarity to traditional ink prints, has not be determined. Since one objective of this study was to measure the contact area of the foot and to determine whether it changed when walking on the sideslope, it was necessary to quantify the reliability and accuracy of these measurements. The accuracy of contact area measurements obtained from the pressure platform was determined by comparing its electronic images with simultaneously acquired ink footprints. The ink footprints, being high resolution images, were considered to represent an optimal standard and were used as a benchmark. Contact area was measured by tracing the outline of the ink footprint with a planimeter. By calculating the difference between the planimetric and the electronic measurements, an indication of the error of contact area measurements from the pressure platform could be derived. While this method could establish the error of the measurements from the platform, it could not determine the relative influence of contributory factors such as spatial resolution and sensor threshold. The effect of spatial resolution was therefore investigated separately to predict the minimum error that could be expected from pressure platforms incorporating sensors of 5x6 millimetres. Any difference between the smallest achievable error and the actual error would be indicative that the platform sensors or the system hardware were operating at a sub-optimal level. To determine the minimum error, estimates of contact area were derived by counting the ink stained elements of a latticed template that was dimensionally identical to the sensor array of the platform, figure 4.1. Estimates obtained from the lattice template were therefore considered definitive of the achievable accuracy for systems with this spatial resolution.

### 6.4.1. Lattice template versus ink footprint

Contact area was determined by counting the number of elements (rectangles) on the latticed template that were stained with ink, figure 4.1. Peripheral

elements were counted as contributing in full (maximum-count, $C_{max}$) or weighted at fifty percent (weighted-count, $C_{wt}$). The two estimates of contact area, $C_{max}$ and $C_{wt}$, were compared with estimates obtained with the planimeter. The number of peripheral elements contributing to an estimate of area was derived as a proportion of the number of central elements (peripheral / central), and the resulting quotient was termed the peripheral element ratio (PER). Descriptive statistics for four regions (T1, T25, FCA and total area, figure 4.1) were determined with each method, table 5.17.

By adjusting for the partial loading of peripheral elements using the weighted count method ($C_{wt}$), the total area, FCA and the area of the hallux (T1) could all be estimated to within 3% of their planimetric equivalents, table 5.17. The error associated with the lesser toe region (T25), however, was considerably greater and averaged almost 9%. Interestingly, with the weighted-count method ($C_{wt}$), the FCA and T1 areas were underestimated while the lesser toe area was overestimated. Thus, on average, when the areas for the three discrete sites were summed, the magnitude of the error associated with the lesser toes was hidden and the estimate of the total contact area was falsely optimised.

In contrast to the $C_{wt}$ estimates, the $C_{max}$ estimates were consistently larger than the planimetric equivalents. $C_{max}$ estimation caused the error for the total area to increase from 2% to about 17%, and similar increases were observed for each of the three discrete sites of the foot. While sites with peripheral element ratios (PER) below 1.0 demonstrated consistently small (<3%) discrepancy scores, table 5.18, the lesser toes had a PER of approximately 4.0 and a substantially greater error (DS ≈9%). The noticeable increase in the error for the lesser toe site suggests that there may be a critical size, possibly indicated by a PER >1.0, below which the error will increase substantially. These findings indicate that the elements at the periphery of the image can be highly influential and, therefore, the processes by which they are detected and quantified are of particular importance.

The weighted-count ($C_{wt}$) method was deliberately selected to avoid the extreme estimate of the maximum-count method. It is considered that a weighted-count method could be implemented in operational platforms by using appropriate software to distinguish the peripheral elements from the central elements and weight them appropriately. The $C_{wt}$ method had the additional advantage over $C_{max}$ estimation in that it gave a reasonable compromise between over and underestimations, and thereby kept all errors close to zero. Thus, if the 2% underestimates for the FCA and T1 were adjusted to zero, then the 9% overestimate for the lesser toes would increase to 11%. The weighted-count method appears to offer potential advantage over the alternative maximum-count.

It is particularly important that the FCA is portrayed accurately because it is used as the basis for the majority of footprint indices. The best estimate of FCA, derived using the $C_{wt}$ method, was within 2.3% of the respective planimetric value. This is a small difference and unlikely to be clinically significant. However, when using the $C_{max}$ method, the error in the FCA increased to almost 12%. Pressure platforms of this spatial resolution could therefore offer a useful alternative to the traditional ink printing approach. The accuracy of the FCA measurement should however be determined for the operational platform.

Referring to pressure platform characteristics, Hughes *et al.*[185], stated that "good [spatial] resolution is needed to pick out the small areas under the toes", and selected an optical pedobarograph for that reason. Unfortunately, no values for contact areas or error levels were reported, although they did indicate that the "great toe presents about double the area of any of the lesser toes". Further, it was argued that the low spatial resolution of some measurement systems was responsible for the discrepancies that had been reported with respect to the proportional loading of the hallux. The planimetric measurements reported here demonstrate that the hallux has a contact area that is more than three times the average contact area of a lesser toe, table 5.17. This difference in size may account, in part, for the small errors (≈2%) in the hallux estimates compared with the larger errors (≈9%) in the lesser toe estimates, table 5.17. Therefore,

while estimates of hallux loading (T1) obtained from these pressure platforms may be of reasonable accuracy, estimates of loading for the lesser toes may not.

Coefficients of variation (cv) for the FCA, table 5.19, demonstrated that within subject variability was less than 2.7% when determined from seven images. However, reliable FCA measurements (cv≈2.9%), were derived using only three prints, and three or four footprints may therefore be considered adequate for this purpose. In contrast, both the hallux and lesser toe measurements demonstrated substantial variability, with coefficients of variation averaging about 16%. The stance posture used for the collection of the footprints may explain the difference between the cv for FCA and that for the toes, since the toes demonstrate their most consistent function during dynamic activities, such as walking [74], but are only active intermittently when standing [104]. The ability of the planimeter to follow the small intricate outlines of the lesser toes probably accounts for the statistically greater cv demonstrated at this site in comparison with the count based methods.

In this experiment, paper templates were used in preference to an operational pressure platform in order to avoid the influence of any indeterminate performance by sensors or the associated monitoring system. Hidden performance characteristics, such as high threshold, would have confounded the results. In the operational platform the sensors could act as high-pass filters and only those elements where the threshold is exceeded will register in the image. If sensor threshold were negligibly low, then this type of platform could overestimate contact areas, as demonstrated by the $C_{max}$ estimates. If sensor threshold is relatively high, however, then elements exposed to low pressure would be excluded and underestimation of contact area will occur. The actual level of accuracy of the operational platform would be expected to be between the upper and lower estimates, and the error associated with the FCA would therefore be between 2 and 12%.

### 6.4.2. Electronic versus ink footprint

The actual accuracy of measurements from the pressure platform was derived from the electronic footprint images obtained during this experiment. The pressure platform consistently underestimated the foot contact area by an average of 13.2 $cm^2$, (≈14%). The negative correlation between the discrepancy score for foot contact area and the ink arch index suggests that the difference in area between the two techniques is dependent on foot shape, table 5.16. Higher arched feet with low arch indices yielded greater errors within electronic prints. Consequently, the electronic prints cannot be regarded as accurate facsimiles of inked prints. Similarly, electronic prints produced a small but statistically significant reduction (≈5%) in the arch index. A uniform reduction in size of the electronic footprint, reflecting a magnification error, would have had no effect on a ratio parameter such as the arch index. Consequently, the electronic footprints seem to be distorted by a preferential loss of area from the middle third of the print. Since the electronic footprints were distorted, the arch index derived from them is not interchangeable with that from inked footprints and, values for electronic parameters should not be interpreted with respect to reference values derived from inked prints [186]. The preferential loss of information from the middle part of the print occurred in a region of relatively low pressure [79,93,94], and it may be speculated that this was a result of high sensor threshold. Sensor threshold may be an important factor in determining electronic footprint fidelity and sensors with a low threshold may allow an ink footprint to be imitated with greater accuracy.

### 6.4.3. Lattice template versus pressure platform

Because the comparison between the electronic images of the pressure platform and the reference ink prints indicated that sensor threshold may have been unduly high, a series of tests in which a variable pre-load could be applied to the polymer array were conducted. By using a vacuum pump to partially evacuate the array, the upper membrane was pre-set in a slightly deflected position as if an external load had been applied to it. The upper surface of the platform, however, remained unobstructed, and both ink and electronic footprints could be collected using the standard method.

The tests revealed that the pressure platform underestimated the FCA by ≈9.8% when averaged across all trials. For vacuum pressures of about 50 kPa and above, the underestimation significantly reduced to ≈7.7%. These results indicated that the accuracy of the FCA measurement may be improved by 2 to 3% by physically adjusting the sensor. However, a relative underestimation of about 7.7% remained.

### 6.4.4. Summary of contact area measurement findings

The pressure platform systematically underestimated the contact area. There was a preferential loss of area from regions of low pressure. The midfoot was the most substantially affected region, but loss also occurred at the periphery of the footprint. Because investigation indicated that feet with a small arch index (high arch) are prone to a greater measurement error than feet with a large index, this platform may be unsuitable for the identification of differences between individuals. Neither this phenomenon nor the systematic underestimation that was also observed, however, would be prohibitive to an investigation of within subject effects. It was concluded therefore that the platform could be used for the measurement of contact area during sideslope walking, although the resulting values would underestimate actual values. The arch index derived from the pressure platform was significantly different from that obtained using the ink footprints, and if used should not be interpreted with respected to the conventional literature. For contact area, measurement repeatability can be reliably achieved (cv<3%) from three footprint images.

The results of this study are applicable to platforms of this spatial resolution in general. Contact area measurements can be determined quite simply and give some indication of the performance of a pressure platform system. Where errors greater than those predicted are discovered then the performance of the sensors or of the system as a whole should be evaluated. Accurate measurement of contact area is restricted to particular regions of the foot, dependent on their relative size. It is probable that contact area of the lesser toes will be erroneously estimated with platforms of this spatial resolution regardless of the methods used

to adjust the contribution made by peripheral sensors. When estimates of contact area have a large error then the associated estimate of regional force may also be erroneous.

## 6.5. Summary of sensor discussion

The polymer sensor platform had a mixture of desirable and undesirable performance characteristics. The large sensing area and reasonable spatial resolution allowed the whole foot to be investigated with subsequent analysis of separate anatomical regions of interest. A study of the normal unshod foot serves as a benchmark reference and can be used for ongoing comparative investigations. The surface area of the platform was large enough to accommodate an adult foot without undue targeting, while the individual sensor elements were small enough to secure reasonable estimates of peak pressures [100,101]. The overall surface area (450 mm x 200), element size (5 x 6 mm) and sampling rate (50 Hz) of the platform were adequate for the purposes of this study.

The reduced sensitivity of the sensor at higher loads makes the differentiation of high pressure measurements more difficult and the accuracy of pressures above 600 to 800 kPa may be questionable. Similarly, the accuracy of low pressure measurements of about 70 kPa and below, may also be questionable because of the relatively high within sensor variation at low loads. However, both the within sensor variation and the amplitude resolution were acceptable for the range of the majority of the measurements (250 to 600 kPa), expected with normal healthy adults, such as those used in the study.

Hysteresis was also an undesirable characteristic and could induce some degree of error in the dynamic signal. The results from the dynamic tests, however, demonstrated that the polymer sensor reproduced the input signal with an acceptable level of fidelity and no degradation was observed within the experimental range. It is not known whether the high frequency transient components of the ground reaction force would be adequately reproduced, but this was not a significant restriction for this study and, furthermore, these

harmonics contribute relatively little power to the signal. The polymer sensors were found to be sensitive to shear at normal foot pressure levels. Because of this characteristic, a comparative study was undertaken with a second pressure platform having similar features but utilising sensors that exhibited no significant sensitivity to shear. The comparative study indicated that pressure and force estimates for the heel and central metatarsal sites are influenced strongly during conditions of sideslope walking. These estimates should not be considered as reflecting normal force. It is speculated that the estimates for these two sites are more reflective of the combined normal and shear forces.

## 6.6. Sideslope walking

### 6.6.1. Foot placement angle or angle of gait

In this study, the foot progression angle was defined as the angle formed by the medial border of the footprint and the longitudinal axis of the pressure platform. It is common in gait studies, however, for the term angle of gait to be used to indicate the relative in-toe or out-toe angle that the foot adopts during walking. The FPA was therefore adjusted to enable comparison with the angle of gait findings reported in the literature. When determining the angle of gait, reference is made to the long axis of the foot which is usually defined as the bisecting line between the medial and lateral tangents to the footprint [187]. Since the angle between the two tangents averages about 19°, the long axis of the foot will be displaced ≈9.5° from the medial tangent. The FPA was therefore adjusted to approximate the angle of gait by adding 9.5°.

The mean (sd) adjusted FPA for level walking was 10.2° (±4.4°), and the coefficient of variation was 43.1%. Previous studies have reported the angle of gait for level walking as ranging from 7.8° to 13.9° [188-191]. Averaged figures from previous studies give values of 9.6° (±3.8°), and a coefficient of variation of 45.3%. The adjusted FPA for level walking therefore shows good agreement with previous angle of gait values for young healthy adults. The mean adjusted FPA for the upslope (11.3° ±4.8°) and downslope (10.3° ±4.6°) conditions demonstrated similar levels of variation, with coefficients of variation of 42.5%

and 44.7%, respectively. This suggests that the angle of gait was as consistent for sideslope walking as for level walking.

While the mean values for the FPA indicate a slight increase in the angle of gait for the upslope placement but no change for the downslope placement, considerable diversity was observed on an individual basis, table 5.20. Some subjects adjusted their FPA for both the up and down slope conditions. In a unidirectional group, the direction in which the FPA changed was consistent, either increasing or decreasing, regardless of the slope orientation. In a bidirectional group, the direction in which the FPA changed varied with the orientation of the slope, increasing for one orientation but decreasing for the other. The majority of subjects (n=25, 83%) altered their FPA for both slope orientations, while the remainder changed their FPA for only one of the slope conditions. For upslope placement of the foot, 23 subjects (≈77%) demonstrated an increase in their FPA, while 6 (20%) decreased and 1 (≈3%) showed no change. For downslope placement of the foot, 14 subjects (≈47%) demonstrated an increase in their FPA, while 12 (40%) decreased and 4 (≈13%) showed no change. This analysis suggests that the majority of individuals increase the angle of gait of their upslope foot, and therefore tend to out-toe. However, for downslope placement it appears that increases and decreases of the FPA are about equally distributed. These observations raise two issues, the first concerns the possible reasons for adjustments to the FPA when walking on side slopes, while the second concerns the underlying mechanisms for adjustment.

Studies of walking uphill and downhill have suggested that individuals may adjust their walking style for reasons of safety or security. Sun *et al.* [52], concluded that a reduction in step length may be a mechanism to reduce the friction demand at heel strike when walking downhill since this was the most likely time for dangerous slips to occur. In addition to alterations of step length, Simpson *et al.* [6] reported that subjects also adjusted their trunk inclination when walking downhill and either leaned back into the slope of forward away from the slope. Subjects who leaned back shortened their step length, walked more slowly and decreased the impact pressures beneath their heels. This strategy is

suggestive of a cautious method of descent. However some individuals leaned forward, walked more quickly, increased their step length and demonstrated greater impact pressures. The different strategies may indicate preferred methods for descending slopes, based on levels of confidence with respect to postural control, balance and coordination. Simpson *et al.* [6], concluded that the gait adjustments for downhill walking were complex but required sagittal plane kinematic adjustments at several levels including the knee, hip and trunk.

The muscle activity patterns recorded for incline walking suggest that the lower limb is managed as a unit [54], with both proximal and distal muscles being recruited, although the distal muscles appear more tightly controlled. The tight control of the distal muscles may indicate that the need to stabilise the knee and ankle joints is greater for slope walking than level walking [53]. It has also been suggested that a need for enhanced stability of the joints of the foot is the reason for the amplified and prolonged activity of the intrinsic muscles of the foot when walking uphill and downhill [55]. While these findings relate specifically to walking uphill or downhill, the principles of functional adjustment and increased motor control apply equally to walking on a sideslope. Change of the angle of gait during sideslope walking may therefore reflect some underlying requirement to maximise safety and enhance security. In this case it would be anticipated that the FPA would need to increase for stability to improve. In contrast however, the FPA frequently decreased indicating there may be other demands impacting on the gait pattern. It is possible that the FPA could be additionally influenced, however, because of demands for positional change placed on the foot tilt mechanisms by the gradient of the sideslope. While foot tilt in up and downhill walking occurs mainly at the ankle [10], accommodation for a sideslope is more likely to occur within the foot at the subtalar joint [22,23].

A change of the gait angle could therefore accompany the subtalar tilt that occurs when walking on a sideslope because the foot bones are constrained to undergo simultaneous transverse plane realignment [14,67-69]. The orientation of the subtalar joint axis dictates that the FPA should increase when the subtalar joint pronates and decrease when it supinates. Kitaoka *et al.* [23], demonstrated that rearfoot eversion, an indicator of subtalar pronation, is likely to occur when the

foot is placed in the upslope position. From these observations, it would be predicted that the FPA would increase on the upslope. Conversely, in the downslope position the FPA would be predicted to decrease because of accompanying rearfoot inversion [23]. In addition to influences from the rearfoot, the forefoot could also contribute to the angle of gait. The forefoot is known to be capable of independent transverse plane motion, and is partially free from the constraints imposed by rearfoot motion [14,67-69]. In running, Freychat *et al.*[67] found that adduction of the forefoot correlated with the vertical load on the foot, and observed that in this configuration the foot appeared relatively stiff. Viale *et al.* [68], also considered that an adducted forefoot increased the stiffness of the foot while abduction accompanied flexibility, and concluded that the configuration of the foot influenced the compliance of the leg. Motion at the joints of the foot may therefore influence the angle of gait while simultaneously trying to satisfy demands for stability, security, compliance and adaptation to the angle of the underlying slope.

During single support, balance is maintained by a combination of manoeuvres at the joints of the ipsilateral foot and hip[20,61,62]. The foot tilts and the hip adducts or abducts to assist control of frontal plane balance. However, tilt of the weightbearing foot is accompanied by simultaneous rotation of the leg because of the constraints imposed by the tarsal mechanism and the ankle joint [14]. Function of the hip and the rearfoot are therefore intimately connected and, in consequence, the hip may also be linked with the FPA. External rotation of the hip could increase the FPA, causing more out-toe, while internal hip rotation could reduce the gait angle. Furthermore, the mechanisms at the hip and the foot could enhance their overall effect by collaborating, or one could nullify the effect of the other. Independent or combined actions by the hip and the foot could therefore account for the variety of changes recorded for the FPA.

In summary, gait accommodations have been reported previously for both uphill and downhill walking. Changes in the angle of gait recorded in this investigation are indicative of accommodative strategies similar in principle to those identified during sagittal plane studies of gait. The FPA can be influenced by a variety of factors including alterations at the hip or within the foot, and these

could be either pro-active or reactive with regards to events that occur in gait. Pronation at the subtalar joint would abduct the foot and increase the gait angle while simultaneously tilting the foot into an everted position. This could account for the higher frequency of out-toe adjustment in upslope orientations. In the downslope orientation a preferred option is less obvious. The changes observed in the FPA during sideslope walking indicate that this method may be fruitful for future investigation of the factors influencing the angle of gait.

### 6.6.2. Peak pressures during sideslope walking

The peak pressure results from the level walking trials of this study compare well with the those from previous studies of healthy young adults obtained using pressure measurement systems with similar characteristics [93,79,105]. For sideslope walking, estimates from the heel and central metatarsal sites appear to be distorted because of the sensitivity of the sensor to shear force. These sites are, therefore, not discussed in detail.

Clinically, peak pressures are considered to be particularly important. For some decades, retrospective studies have linked abnormally high foot pressures with plantar ulceration [32,33,192]. More recently, prospective research has confirmed that elevated plantar pressure is a significant risk factor for soft tissue breakdown and ulcer development [193]. Since foot ulceration is one of the most common causes of limb loss, its prevention and treatment has become a principal objective in the management of the diabetic patient [194]. As a consequence of the perceived gravity of this problem, considerable resources have been devoted to try to identify those factors that promote abnormally elevated pressures beneath the feet[2]. Many functional features have been investigated in an attempt to identify the key predictive factors of peak pressure[2]. Investigators have scrutinised physical characteristics, anthropometric data, passive range of joint motion, radiographic measurements of skeletal alignment, soft tissue properties, stride parameters, three-dimensional foot kinematics, and electromyography of the leg muscles [2]. From all of these investigations, foot structure and function generally accounts for only about 50%

of the variance in peak pressure, although this figure does alter considerably from site to site within the foot [2].

While these findings provide valuable insight into the interplay between many features, and are therefore important, it is surprising that a stronger link between structure and function of the foot and peak pressure variance has not been demonstrated. A possible reason for this disappointing outcome could be the persistent use of an experimental protocol that only investigates a single functional activity. Studies continue to measure pressures for straight level walking only. As a functional task, straight level walking is relatively undemanding and, for this reason, a full range of foot function may not be brought into play. In contrast to this, activities of daily living often necessitate more demanding locomotor tasks. Even with level walking, complex tasks such as turning have been shown to increase peak pressures [195]. In the same way, studies of up and downhill walking have revealed changes, despite the disparity between findings from different researchers [8]. The current study is the first known investigation of foot loading during sideslope walking and the unorthodox approach has revealed a distinct pattern of peak pressure changes. The findings further justify a move away from the conventional experimental protocol.

Changes in peak pressure were found to be dependent on foot site and sideslope orientation (upslope versus downslope), table 5.24. In the downslope orientation both the first and central metatarsal sites demonstrated significant increases, although the mean increase for the first metatarsal (≈11%) was more than twice that for the central metatarsals (≈4%). Furthermore, the increases at the central metatarsals occurred only when the incline was equal to or greater than 4° whereas the first metatarsal showed significant changes at 2° of sideslope. These findings suggest that the first metatarsal may be the site most sensitive to changes in the angle of sideslope. This might be a reflection of its capacity for independent motion. With upslope positioning of the foot, significant increases in peak pressure occurred at the midfoot (≈20%) and the fifth metatarsal (≈16%) sites. Regardless of the site, elevated pressures recorded at these sites have

implications for individuals with poor tissue vitality who are predisposed to cutaneous injury. The findings are particularly relevant to issues of preventative care.

Prevention of ulceration minimises the overall risk for individuals by avoidance of more serious outcomes such as amputation. Prevention also substantially reduces the financial burden on the health services. For these reasons considerable emphasis is placed on the development of foot pressure screening programs for individuals with diabetes. For a screening program to be implemented some reference criterion must be used to differentiate individuals who are at risk from those who are not. Several attempts have been made to determine the critical threshold pressure that would identify diabetics who have a high risk of ulceration. Boulton *et al.* [192], proposed that a pressure of about 1000 kPa represented an appropriate demarcation, while limits of 500 kPa [196] and 700 kPa [194] have been recommended subsequently. Regardless of the selected threshold level, the screening process will be ineffective if the pressure values indicated during the examination are not representative of the actual pressures that occur in routine daily activities. Since sideslope pressures exceed those for level walking, conventional screening may fail to identify some at risk individuals, especially those who retain an active outdoors lifestyle. To overcome this flaw, the screening procedure could be enhanced to include tests of sideslope walking. However, an extension of the screening procedure would increase the burden on the patient and this would be undesirable. Furthermore, the use of a test that is likely to directly elevate pressures and potentially bring about unseen tissue trauma is ethically questionable, especially if an alternative option exists. A more realistic option would be to apply a compensation factor, or added margin of safety, to pressure values obtained for level gait. The results of this study suggest that appropriate adjustment of the threshold value would depend on foot site. For example, peak pressure beneath the first and fifth metatarsals would require allowances of about 11% and 16%, respectively. The potential benefit of compensatory adjustments at these sites would also seem to be indicated by the fact that about 35% to 40% of plantar ulcers occur beneath the first and fifth metatarsal heads [193].

It has been estimated that 50% to 80% of all lower limb amputations in Europe and the USA occur in adults with diabetes, and that these are often the sequel to foot ulceration. Within this diabetic group there is a high rate of repeat salvage amputation, amputation of the contralateral leg, and death soon after amputation. Even when reasonable recuperation and rehabilitation follow amputation, there often remains a significant demise in the amputee's level of independence, resulting in an increased need for extended health care. The financial cost associated with these outcomes is immense, and the impact on individual quality of life immeasurable. Any factors that may lead to an improvement in the prevention or management of ulcerations are therefore desirable. The findings from this study suggest that an improvement in diabetic foot care may be possible and an investigation of sideslope walking with an appropriate diabetic cohort is therefore required. It may be speculated that an investigation of sideslope walking in chronic diabetics would demonstrate more substantial pressure increases because of the limited joint mobility [197] that often accompanies the disease.

While pressures were generally observed to increase with sideslope walking, the first metatarsal and first toe demonstrated decreased peak pressures (17.8% and 10.9%, respectively) when the foot was in the upslope position. Although this is irrelevant to screening, it could be pertinent where pressure reduction is an objective of treatment. Placing an appropriate wedge in the shoe might induce a reduction of load at these sites. Therapeutic wedging may be successful with small wedges since pressure reductions were significant for small sideslope angles (2°). Further investigation is necessary before a definitive conclusion can be drawn.

### 6.6.3. Regional forces during sideslope walking

The magnitudes of the level walking forces from this study show close agreement to results obtained with a similar measurement system [38,79]. The results also correspond closely to those obtained from a force measurement system of lower spatial resolution [35,88,106,198]. With respect to maximum regional forces, the heel demonstrated an increase in upslope positions, while the central

metatarsals showed increases for downslope positions. These findings, however, are thought to be indicative of the anomalous behaviour of the polymer sensor rather than actual alterations in normal load. These sites are not, therefore, discussed in detail. The first metatarsal and first toe, unlike other sites, demonstrated significant differences for both the up and downslope orientations, although the magnitudes of the changes were greater and more consistent for the first metatarsal. The loads at the first metatarsal and first toe increased when the foot was in downslope positions, but decreased when the foot was in upslope positions, table 5.25.

The ground reaction forces of gait vary with walking speed [87]. While walking speed was not measured, the stance phase duration, which is inversely proportional to walking speed [87,93], was recorded. The mean stance phase time in the upslope position was approximately 28 ms (3.6%) longer than that for level walking, while the downslope time showed a difference of 5 ms (<1%). If differences in walking speed were the primary cause of the loading changes recorded in this investigation, then forces should have been unaffected when the foot was in the downslope position and shown a tendency to decrease in the upslope position. In stark contrast to this, however, when the foot was in the downslope position significant changes, both increases and decreases, occurred. Furthermore, with upslope positioning some sites demonstrated significantly increased loading. The speed induced pressure and force changes previously reported by Hughes *et al.* [89] and Rosenbaum *et al.* [87] were associated with changes in the stance phase duration of approximately 28% and 19% respectively. Furthermore, the altered loading patterns they observed with speed changes were clearly different from those found in this study. Fast walking caused simultaneous increases in force on both the heel and the forefoot [87,89], but this was not observed for sideslope walking. It is considered unlikely, therefore, that the load changes are primarily the result of alterations in the walking speed.

Force has more relevance to the mechanical behaviour of the foot [94] and the dynamics of gait than peak pressure. For level walking, Hayafune *et al.* [34] found that maximum force on the first metatarsal occurred during the push-off period of stance, when it usually accepted about 29% of body weight. A change in

maximum force may therefore indicate an altered demand for active propulsion. However, although Hayafune *et al.* [34] emphasised the magnitude of force at the first metatarsal during the push-off phase of gait, its function may extend beyond simple load bearing. Matsusaka [64] reported that the lower leg muscles may contribute to the medio-lateral balance of walking, and that activity of the peroneus longus muscle can assist in controlling the medial inclination of the tibia while simultaneously influencing first metatarsal activity. This suggests that the first metatarsal could play an important role in facilitating the smooth cyclical transfer of load in the medio-lateral direction during walking. Since a sideslope is likely to have most effect on medio-lateral body balance, medio-lateral transfer of body weight, from one foot to the next, would be influenced more than antero-posterior transfer. Involvement of the first metatarsal in medio-lateral load transfer might therefore explain why force at the first metatarsal changed for all slopes. Furthermore, medial transfer of body weight from the upslope foot to the lower downslope foot could be assisted by gravity, which would account for the decreased force beneath the first metatarsal. Movement in the opposite direction would be against gravity and could explain the increased force recorded for this site when the foot was placed downslope.

### 6.6.4. Contact area of the foot and arch index during sideslope walking

Footprinting techniques [25,199-202] are among the most commonly used methods for categorising feet. Footprints are simple to obtain, inexpensive, have a strong visual impact and provide a permanent record for future use. The footprint is a visual representation of both the shape [203] and contact area of the sole of the foot [25]. Footprints are usually charted geometrically to produce parameters such as the Chippaux-Smirak index and the Footprint Angle [203]. The diversity of footprint methods that have been proposed for the classification of foot-types is, in itself, an indication that a simple, objective and quantitative measure remains elusive. The arch index, however, is the most frequently cited parameter and is deemed by some to facilitate reliable classification of feet according to arch height [25,27-29].

Recent opinions differ regarding the dependability of the arch index. Hawes *et al.*[203] were unable to predict medial arch height from footprints obtained during stance and concluded that the indices were indicators of footprint shape only. McPoil and Cornwall [204] found that medial arch height was predictive of only 27% of the contact area of dynamic footprints, concluding that their clinical usefulness is limited. In contrast, McCrory *et al.*[28] reported that approximately 50% of the variance in medial arch height could be explained by measurement of the arch index. They asserted that the strength of the relationship was partly dependent on precise radiographic measurement of arch height. Despite this assertion, Shiang *et al.* [29] similarly found the arch index to account for approximately 50% of the variance in arch height when they measured it with an external gauge.

While those studies used the index as an indicator of foot structure, there is evidence that it may be alternatively associated with function. Cavanagh and Rodgers [25] reported variability of the index with standing, walking and running. And later, Hamill *et al.* [26] found a significant difference between standing and walking even though the response seemed to be erratic and unpredictable. In view of the possible link with function rather than structure, contact area and arch index were investigated to ascertain if their behaviour is more defined during sideslope walking than it is during level walking.

It was found that the pressure platform measurement system systematically underestimated contact area, with a preferential loss from regions of low pressure, table 5.15. The midfoot was the most substantially affected region, but loss also occurred at the periphery of the footprint. The arch index derived from the pressure platform was significantly different from that obtained using ink footprints, table 5.15. While arch indices could be derived from the pressure platform data they were not interchangeable with those from the ink prints. This does not prohibit their use, but the findings must be interpreted cautiously with respected to the conventional reference values derived from ink footprints.

The mean arch indices for both level and slope walking are reported in table 5.23. The index demonstrated an approximately linear change across the range

of sideslope angles, with the smallest index (0.187) occurring for the steepest downslope condition and the largest (0.221) for the steepest upslope condition. The changes were statistically significant for all slope conditions with the exception of the 6° gradient in both the upslope and downslope orientations. Interpretation of these results with respect to the general conclusions of McCrory *et al.*[28] and Shiang *et al.*[29] would suggest that the arches of normal feet adjust during sideslope walking. In the downslope orientation the smaller indices would be indicative of a raised arch, while in the upslope orientation the larger indices suggest that the arch lowered. The changes that occurred for the 6° slopes approached but did not reach statistical significance. This may simply be a reflection of a sample size effect but alternatively it could be indicative of an incline dependent change in foot function. For incline angles of 2° and 4° the arch index demonstrated a mean change of about 5% in comparison to level walking. For the 6° inclines the difference reduced to 3 to 4% but then increased for the 8° inclines to exceed 7% for the downslope and 9% for the upslope. While a 6° incline may therefore represent a transition point between alternative gait strategies, perhaps similar in principle to that postulated by Bojsen-Moller [205], such an inference must remain tentative until complementary kinematic studies are undertaken.

The arch index expresses the area of the central one-third of the footprint as a proportion of the area of the whole footprint less the toes so as to facilitate comparison between feet of different sizes. However, while the parameter is intended to reflect alterations in the contact area of the midfoot, the arch index could change as a result of contact area change at other sites. Contact areas were therefore assessed on a regional basis. The heel, midfoot and first metatarsal sites were the only ones to show consistent statistically significant changes in contact area, table 5.22, figure 5.16.

The heel demonstrated a small increase on the upslope but did not change on the downslope. The increase averaged 0.28 $cm^2$, which was approximately 1% of the area of the heel in level walking, and is about the size of a single sensor. While this change is small, it occurred for upslope walking only and may therefore indicate that the heel response alters according to the orientation of the

slope. Kitaoka *et al.* [23] established that the heel utilised a greater range of frontal plane motion in the upslope position, while Wright *et al.* [22] demonstrated that the motion was offset according to the orientation of the sideslope. Asymmetrical tilt of the heel could influence its contact area, particularly if the local force is offset from the heel centre and the soft tissues are distorted and bulge accordingly. Regardless of the cause, it is considered unlikely that this small change will impact on the arch index or be clinically significant.

The first metatarsal showed some statistically significant changes in both slope conditions. In the downslope orientation the contact area decreased by an average of approximately 0.13 $cm^2$ which was less than the size of a single sensor and was attributed to random error. In the upslope orientation a mean decrease of 0.73 $cm^2$ was recorded, approximating 5.6% of the area of the first metatarsal for level walking. However, the upslope alteration was accompanied by decreased loading of the metatarsal and associated with a lateral shift of load in the forefoot, table 5.25.

The midfoot region demonstrated statistically significant changes of contact area for both slope orientations during sideslope walking. The area was observed to increase or decrease progressively as the angle of incline altered. In the downslope position the contact area decreased by an average of 1.1 $cm^2$, approximating 6% of the area of the midfoot for level walking. In the upslope position the area increased on average by 1.3 $cm^2$ ($\approx$7% level contact area). The pattern of change observed for the contact area of the midfoot closely paralleled that of the arch index, indicating that the midfoot may predominate in determining the arch index. Area changes at the heel and first metatarsal were individually small and, because the heel area increased while the metatarsal area decreased, the net average change of approximately 0.4 $cm^2$ appeared insignificant (<0.5% of foot contact area). Furthermore, the changes only occurred when the foot was in the upslope position.

While both Hamill *et al.* [26], and Cavanagh and Rodgers [25] reported that the arch index altered in an inconsistent manner during level gait, the average response

with sideslope walking is clearly systematic, table 5.23. In general, when the foot was positioned upslope the index increased suggesting that the foot underwent some flattening, while the decreased values for the downslope position may be indicative of arch raising. Hamill *et al.* [26] postulated that the arch would deform in response to increased loading but, while the regional load in the midfoot did increase significantly when the foot was in the upslope position no equivalent decrease was found on the downslope, table 5.25. For sideslope walking, foot tilt with accompanying readjustment of the tarsal mechanism would better explain the observed changes in the arch index. In the upslope position the foot would tilt into eversion to enable the sole to remain parallel with the support surface [23]. Eversion tilt brings about a lowering of the arch as the tarsal mechanism readjusts, and this would accord with the increased indices recorded in the upslope position. The opposite would occur for the downslope position, raising the arch and resulting in decreased indices. Hamill *et al.* [26] additionally demonstrated a significant relationship between the mobility of the first metatarsal and the arch index, and proposed that its flexibility was a sign of ligamentous laxity which would contribute to flattening of the foot. However, motion of the first metatarsal is believed to accompany tarsal mechanism readjustment in the weight bearing foot, and this could also account for Hamill's findings. Furthermore, simultaneous adjustment of the first metatarsal could explain the change in the contact area recorded at this site in the upslope position.

It is concluded that the contact area of the midfoot is the major determinant of the arch index parameter, and that systematic changes in the arch index indicate that normal feet alter their form during sideslope walking. Adjustments by the tarsal mechanism could explain these observations, and the joints of the foot might therefore be implicated in gait adaptation to non-level terrain. Kinematic investigation of the foot in sideslope walking is indicated.

### 6.6.5. Temporal adjustments during sideslope walking

The mean (sd) of the stance phase times for the level, upslope and downslope conditions were 774 (±43), 802(±54) and 779 (±58) ms, respectively. On

average the upslope times were 3.6% greater than those for level walking but differences were not statistically significant between the conditions. Since stance phase duration is approximately inversely proportional to walking speed, the increased duration of the stance phase in the upslope condition may be an indication that a slight slowing occurred [89,93]. If speed varies during sideslope walking, it might be predicted to decrease in the upslope direction but increase in the downslope direction. However, there was no concomitant decrease in the downslope stance phase time. For reasons of security individuals may retard their progress in the downslope direction, thereby controlling their speed, and this may account for the absence of change in the stance phase time. Similar gait strategies have been shown previously for downhill walking [6].

Analysis of the initial contact times indicates that contact with the support surface was delayed for most of the foot sites when the foot was in the upslope position, table 5.26. These results demonstrate that, after heel strike, foot contact progresses more slowly than for level walking and this further supports the idea of a general slowing of events in the upslope condition. On average, contacts were delayed by about five to eight percent of the respective initial contact times for level walking. The first metatarsal demonstrated the largest contact delay, being more than twice that at any other site. Since the first metatarsal has its own range of motion and can be independently dorsiflexed, the delay in contact may be indicative of extended activity in the tibialis anterior muscle. Interestingly, while contact by the first metatarsal was significantly delayed, first toe contact was not. For the downslope condition, contacts occurred earlier by an average of about six percent of the respective initial contact times for level walking. Swift contact with the support surface would allow the downslope limb to participate in retarding the progress of the body and would optimise safety, and therefore accords well with the absence of change in stance phase duration for the downslope foot.

In general, changes in the duration of loading were relatively small and reflected the changes that were observed in the initial contact times, table 5.27. Significant changes in loading duration occurred at several sites and were usually dependent on the slope orientation. On average, sites of the foot

demonstrated changes of about 1% or 2% of the respective level walking contact periods. For the first metatarsal in the upslope position the duration of contact decreased by ≈3.0%, which reflects the slightly more delayed onset of load for that site. These findings suggest that, for the majority of sites, the proportional duration of contact remains relatively unaffected by a change in slope. However, the first toe demonstrated a larger change with an increased duration of ≈7% in the downslope condition.

For most sites of the foot, the time at which force peaked generally reflected the change in the initial contact time and, like the other temporal parameters, altered according to the orientation of the slope. Thus, when initial contact was delayed then the time to peak force was also delayed by approximately the same period. The first metatarsal was an interesting exception to this generality. In the upslope condition it followed the general pattern for other sites. Initial contact was delayed by about 20 ms and the time to peak force was delayed by about the same amount. However, on the downslopes although initial contact occurred marginally earlier, the time to peak force was actually delayed by about 20 ms. The first metatarsal was the only site within the foot that demonstrated these findings, and this behaviour is not easily explained. Despite the changes brought about by the demands of the sloped surface, the first metatarsal may possibly function in a way that minimises any change in the timing of the peak force event. This response could occur if first metatarsal loading is closely synchronised with some other event in the gait cycle, especially one external to the foot. The double support period, when load is being transferred from one foot to the next, may be worthy of investigation in this respect. It could not be examined in this study because of the limitations imposed when using a single pressure platform.

While it was found that the instant of peak force and the instant of peak pressure were close, and that the relationship between them was maintained throughout the range of slope conditions, the two events were not synchronous, figure 5.21. At the heel and midfoot sites the instant of peak pressure preceded the instant of peak force. However, at all of the sites in the forefoot the instant of peak

pressure followed the instant of peak force. For the forefoot sites, the peaks for both force and pressure occur after the heel has lifted. The contact area is therefore reducing while the regional force is increasing and this may lead to the delayed propagation of peak pressures. In the heel, the contact area is increasing with force and the peak pressures may occur before the contact area has reached its maximum. These finding demonstrate that while closely similar force and pressure should not be considered as precisely interchangeable. The time to peak pressure was in exact agreement with the value reported by Kelly *et al.* [206].

The slight difference of about 4% between the level and upslope stance phase times raises a previously unreported dilemma concerning gait studies of this type. Because the speed of walking can influence many gait parameters, including plantar pressures, some investigators recommend that walking speed is controlled. However, by controlling walking speed and imposing a speed that may be different to the usual speed for an individual, greater variation can be induced in the measured parameters, suggesting that the gait is less stable. Consequently, some investigators prefer not to control walking speed but to monitor the stance phase duration as an indicator of speed. When walking speed is controlled, it is often determined as an average over a known distance, usually the zone incorporating the pressure platform. Under such circumstances, for this study, a walking speed averaged over a single stride would fail to indicate the apparent asymmetry between the left and right steps contained within the stride. For this reason, the stance phase time may be a more useful measure than the average walking speed.

# 7. Conclusions

The performance characteristics of individual elements of the polymer array are similar to those reported previously for discrete sensors of the same type (Interlink FSR$^{TM}$), table 2.7. The sensor output was non-linear, mean within-sensor variation ≈3% (maximum 8%), mean hysteresis ≈9% (maximum 13%), pressure threshold sensitivity ≈35 kPa, and mean between-sensor variation ≈8% (maximum 18%) over the surface of the platform. The dynamic behaviour of polymer sensors has not been reported previously but was reliable to 26Hz.

The polymer sensor was found to be sensitive to shear. Although this has been asserted previously, no work had been undertaken to assess the impact of this characteristic on foot pressure measurements. Comparison with a capacitive sensor platform of similar characteristics indicated that foot loading profiles may be significantly influenced by this feature. While further investigation is required to confirm a provisional conclusion that the anomalous behaviour was due to shear, the findings must raise doubt regarding the reliability of previous foot pressure studies utilising polymer sensor technology. Future investigations should incorporate a method of verification, or interpret findings with respect to both normal and shear force.

The polymer sensor pressure platform systematically underestimated the contact area of the footprint. Error in contact area measurement may be attributed in part to an effect of spatial resolution, however, the error in measurements from the platform exceeded this level. Selective loss of contact area was influenced partly by the threshold of the sensor, but this did not account for the entire error. It must therefore be concluded that an additional factor, such as an electronically imposed threshold, must be active. Systematic underestimation of contact area is not prohibitive to a within subject investigation. Pressure platforms of comparable spatial resolution to that used in this investigation are unlikely to return reliable estimates for the contact area of the lesser toes. A higher spatial resolution is required for this purpose.

The electronic footprint images were different from simultaneously acquired ink footprints. Geometrically derived parameters, such as the arch index, may therefore be distorted and should not be used to group feet according to classifications based on studies of ink footprints. The arch index derived from the pressure platform, however, demonstrated a systematic change with sideslope walking. The index increased with upslope placement of the foot and decreased with downslope placement of the foot. The systematic change of the arch index may support the contention that it is linked with foot function, and indicates that further investigation is justified. Furthermore, the arch index was found to reflect changes in the midfoot region of the footprint, rather than at other sites. For within subject investigations, therefore, the contact area of the midfoot may be used as a substitute for the arch index.

The loading profiles for sideslope walking differ from those of level walking. The differences were dependent on both the orientation of the slope (upslope versus downslope) and foot site. The first metatarsal demonstrated the most notable pattern of change. For this site, loading decreased when the foot was placed upslope and increased when the foot was placed downslope. The increased pressures recorded from some sites of the foot indicate than an immediate reassessment of current methods of determining the risk status of individuals with poor tissue viability or sensory deficiency is required. A repeat study with a diabetic cohort is warranted.

The hypotheses of the investigation (section 1.1.1) should not be rejected. A method for the investigation of sideslope walking has been developed, and potentially problematic factors have been identified. Further investigations utilising the method are indicated.

## 8. References

1. Lord M, Reynolds DP, Hughes JR. *Foot pressure measurement: A review of clinical findings.* J Biomed Eng 1986; 8, 283-294.

2. Morag E, Cavanagh PR. *Structural and functional predictors of regional peak pressures under the foot during walking.* J Biomech 1997; 32, 359-370.

3. Alexander IJ, Chao EY, Johnson KA. *The assessment of dynamic foot to ground contact forces and plantar pressure distribution: A review of the evolution of current techniques and clinical applications.* Foot Ankle Int 1990; 11, 152-167.

4. Lord M. *Foot pressure measurement: A review of methodology.* J Biomed Eng 1981; 3, 91-99.

5. Kastenbauer T, Sokol G, Irsigler K. *The effects of walking uphill or downhill on dynamic plantar foot pressure in diabetic patients.* Foot 1995; 5, 199-201

6. Simpson KJ, Jiang P, Shewokis PA, Odum S, Reeves KT. *Kinematic and plantar pressure adjustments to downhill gradients during gait.* Gait Posture 1993; 1, 172-179.

7. Milani TL, Hennig E. *Pressure distribution patterns inside of a running shoe during uphill and downhill running.* Proceedings of the XIIth International Congress on Biomechanics. CA: UCLA. 1989, 306-307.

8. Grampp J, Wilson J, Kernozeck T. *The plantar loading variations to uphill and downhill gradients during treadmill walking.* Foot Ankle Int 2000; 21,3,227-231.

9. Engsberg JR, Allinger TL. *A function of the talocalcaneal joint during running support.* Foot Ankle Int 1990; 11, 2, 93-96.

10. Wall JC, Nottrodt JW, Chateris J. *The effects of uphill and downhill walking on pelvic oscillations in the transverse plane.* Ergonomics 1981; 24, 10, 807-816.

11. Huson A. Biomechanics of the tarsal mechanism. *A key function of the normal human foot.* J Am Podiatr Med Assoc 2000; 90, 3, 12-17.

12. Vogler HW, Bojsen-Moller F. *Tarsal functions movements and stabilisation mechanisms in foot ankle and leg performance.* J Am Podiatr Med Assoc 2000; 90, 3, 112-125.

13. Sarrafian SK. *Functional characteristics of the foot and plantar aponeurosis under tibiotalar loading.* Foot Ankle Int 1987; 8, 1, 4-18.

14. Olerud C, Rosendahl Y. *Torsion-transmitting properties of the hind foot.* Clin Orthop Rel Res 1987; 214, 285-294.

15. Root ML, Orien WP, Weed JH. *Normal and abnormal function of the foot* Volume 2, 1977 Clinical Biomechanics, Los Angeles.

16. Harper FC, Warlow WJ, Clarke BL. *The forces applied to the floor by the foot in walking. II Walking on a slope.* National Building Studies Research Paper 32, HMSO, London. 1967.

17. Kawamura K, Tokuhiro A, Takechi H. *Gait analysis of slope walking: a study on step length, stride width, time factors and deviation in the centre of pressure.* Acta Med Okayama 1991; 45, 3, 179-184.

18. Kuster M, Sakurai S, Wood GA. *Kinematic and kinetic comparison of downhill and level walking.* Clinical Biomech 1995; 10, 2, 79-84.

19. Redfern MS, DiPasquale J. *Biomechanics of descending ramps.* Gait Posture 1997; 6, 119-125.

20. Hoogvliet P, van Duyl WA, de Bakker JV, Mulder PGH, Stam HJ. *A model for the relationship between the displacement of the ankle and centre of pressure in the frontal plane, during one leg stance.* Gait Posture 1997; 6, 39-49.

21. Jones RL. The human foot. *An experimental study of its mechanics and the role of its muscles and ligaments in the support of the arch.* Am J Anat 1941; 68, 1, 1-39.

22. Wright DG, Desai SM, Henderson WH. *Action of the subtalar and ankle joint complex during the stance phase of walking.* J Bone Joint Surg 1964; 46A, 2, 361-382.

23. Kitaoka HB, Winkenheiser MA, Shaughnessy J, Kai-Nan A. *Gait abnormalities following resection of talocalcaneal coalition.* J Bone Joint Surg 1997; 79-A, 3, 369-374.

24. Tranberg R, Karlsson D. The relative skin movement of the foot: a 2-D roentgen photogrammetry study. Linical Biomech. 1998; 13, 1, 71-76.

25. Cavanagh PR, Rodgers MM. The arch index: *A useful measure from footprints.* J Biomech 1987; 20, 5, 547-551.

26. Hamill J, Bates BT, Knutzen KM, Kirkpatrick GM. *Relationship between selected static and dynamic lower extremity measures.* Clinical Biomech 1989; 4, 4, 217-225.

27. Chu WC, Lee SH, Chu W, Wang TJ, Lee MC. *The use of arch index to characterise arch height: A digital image processing approach.* IEEE Trans Biomed Eng 1995; 42, 11, 1088-1092.

28. McCrory JL, Young MJ, Boulton AJM, Cavanagh PR. *Arch index as a predictor of arch height.* Foot 1997; 7, 79-81.

29. Shiang TY, Lee SH, Chu WC. *Evaluating different footprint parameters as a predictor of arch height.* IEEE Eng Med Biol 1998; Nov, 62-66.

30. Nyska M, McCabe C, Linge K, Laing P, Klenerman L. *Effect of the shoe on the plantar foot pressures.* Acta Orthop Scand 1995; 66, 1, 53-56.

31. Cavanagh PR, Hewitt FG, Perry JE. *In-shoe plantar pressure measurement: a review.* Foot. 1992; 2, 185-194.

32 Stokes IAF, Faris IB, Hutton WC. *The neuropathic ulcer and loads on the foot in diabetic patients.* Acta Orthop Scand. 1975, 46, 839-847.

33 Cterctecko GC, Dhanendran M, Hutton WC. *Vertical forces acting on the feet of diabetic patients with neuropathic ulceration.* Br J Surg. 1981, 68, 608-614.

34. Hayafune N, Hayafune Y, Jacob HAC. *Pressure and force distribution characteristics under the normal foot during the push-off phase in gait.* Foot. 1999; 9, 88-92.

35. Dhanendran M, Hutton WC, Paker Y. *A quantitative assessment of normal and pathological foot function.* Eng Med 1979; 8, 2, 69-74.

36. Stokes IAF, Hutton WC, Stott JRR, Lowe LW. *Forces under the hallux valgus foot before and after surgery.* Clin Orthop 1979; 142, 64-72.79.

37. Willson JD, Kernozek TW. *Plantar loading with fatigue.* Med Sci Sports Exerc 1999; 31, 12, 1828-1833.

38. Wearing SC, Urry SR, Smeathers JE. *Ground reaction forces at discrete sites of the foot derived from pressure plate measurements.* Foot Ankle Int 2001, 22, 8, 653-661.

39. Hedman TP. *A new transducer for facet force measurement in the lumbar spine: benchmark and in vitro test results.* J Biomech 1992; 25, 1, 69-80.

40. Maalej N, Bhat S, Zhu H, Webster JG, Tompkins WJ, Wertsch JJ, Bach-y-Rita P. *A conductive polymer pressure sensor.* IEEE Eng in Med & Biol Soc. 10th Int Conf. 1988; 770-771.

41. Maalej N, Webster JG, Tompkins WJ, Wertsch JJ. *A conductive polymer pressure sensor array.* IEEE Eng in Med & Biol Soc. 11th Ann Int Conf. 1989; 1116-1117.

42. Knudson DV, White SC. *Forces on the hand in the tennis forehand drive: Application of force sensing resistors.* Int J Sport Biomech 1989; 5, 324-331.

43. Pax RA, Webster JG, Radwin RG. *A conductive polymer sensor for the measurement of palmar pressures.* IEEE Eng in Med & Biol Soc. 11th Ann Int Conf. 1989; 1483-1484.

44. Wertsch JJ, Webster J, Tompkins WJ. *A portable insole plantar pressure measurement system.* J Rehab Res & Dev. 1992; 29, 13-18.

45. Cobb J, Claremont DJ. *Transducers for foot pressure measurement: survey of recent developments.* Med & Biol Eng & Comput 1995, 33, 525-532.

46. Abu-Faraj ZO, Harris GF, Chang AH, Shereff MJ. *Evaluation of a rehabilitative pedorthotic: plantar pressure alterations with scaphoid pad application.* IEEE Trans Biomed Eng 1996; 4, 4, 328-336.

47. Abu-Faraj ZO, Harris GF, Abler JH, Wertsch JJ, Smith PA. *A Holter-type microprocessor-based rehabilitation instrument for acquisition and storage of plantar pressure data in children with cerebral palsy.* IEEE Trans Rehabil Eng 1996; 4, 33-37.

48. Abu-Faraj ZO, Harris GF, Abler JH, Wertsch JJ. *A Holter-type microprocessor-based rehabilitation instrument for acquisition and storage of plantar pressure data.* J Rehabil Res Dev 1997; 34, 187-194.

49. Urry S. *Plantar pressure-measurement sensors.* Meas Sci Technol 1999; 10, R16-R32.

50. Harrington C, Zagari MJ, Corea J, Klitenic J. *A cost analysis of diabetic lower extremity ulcers.* Diabetes Care 2000; 23, 9, 1333-1338.

51. Menz HB. *Alternative techniques for the clinical assessment of foot pronation.* J Am Podiatr Med Assoc 1998; 88, 3, 119-129.

52. Sun J, Walters M, Svensson N, Lloyd D. *The influence of surface slope on human gait characteristics: a study of urban pedestrians walking on an inclined surface.* Ergonomics 1996; 39,4, 677-692.

53. Tokuhiro A, Nagashima H, Takechi H. *Electromyographic kinesiology of lower extremity muscles during slope walking.* Arch Phys Med Rehabil 1985; 66, 610-613.

54. Patla A. *Effects of walking on various inclines on EMG patterns of lower limb muscles in humans.* Human Movement Sci 1986; 5, 345-357.

55. Mann RA, Inman VT. *Phasic activity of the intrinsic muscles of the foot.* J Bone Joint Surg 1964; 46-A, 3, 469-481.

56. Zhao Y, Upadhyaya SK, Kaminaka MS. *Foot-ground forces on sloping ground when lifting.* Ergonomics 1987; 30, 12, 1671-1687.

57. Gehlsen GM, Stewart LB, Van Nelson C, Bratz JS. *Knee kinematics: the effects of running on cambers.* Med Sci Sports Exerc 1989; 21, 4, 463-466.

58. Koles ZJ, Castelein RD. *The relationship beyween body sway and foot pressure in normal man.* J Med Eng Tech 1980; 4, 6, 279-285.

59. Horak FB, Nashner LM. *Central programming of postural movements: adaptation to altered support-surface configurations.* J Neurophysiol 1986; 55, 6, 1369-1381.

60. Winter DA. *Sagittal plane balance of posture in human walking.* IEEE Eng Med 1987; Sept, 8-11.

61. Tropp H, Odernick P. *Postural control in single-limb stance.* J Orthop Res 1988; 6, 833-839.

62. Gauffin H, Arebald M, Tropp H. *Three-dimensional analysis of the talocrural and subtalar loints in single-limb stance.* Clinical Biomech 1993; 8, 307-314.

63. Mackinnon CD, Winter DA. *Control of whole body balance in the frontal plane during human walking.* J Biomech 1993; 26, 6, 633-644.

64. Matsusaka N. *Control of the mediolateral-balance in walking.* Acta Orthop Scand 1986; 57, 555-559.

65. Hoogvliet P, van Duyl WA, de Bakker JV, Mulder PGH, Stam HJ. *Variations in foot breadth: effect on aspects of postural control during one-leg stance.* Arch Phys Med Rehabil 1997; 78, 284-289.

66. Stacoff A, Kaelin X, Stuessi E, Segesser B. *The torsion of the foot in running.* Int J Sport Biomech 1989; 5, 375-389.

67. Freychat P, Belli A, Carret JP, Lacour JR. *Relationship between rearfoot and forefoot orientation and ground reaction forces during running.* Med Sci Sports Exerc 1996; 28, 2, 225-232.

68. Viale F, Dalleau G, Freychat P, Lacour JR, Belli A. *Leg stifness and foot orientations during running.* Foot Ankle Int 1998; 19, 11, 761-765.

69. Freychat PF, Belli A, Carret JP, Lacour JR. *Rearfoot and forefoot alignment during running.* Proceedings of the XIVth International Congress on Biomechanics. Paris. 1993; 424-425.

70. Rietdyk S, Patla AE, Winter DA, Ishac MG, Little CE *Balance recovery from medio-lateral pertubations of the upper body during standing.* J Biomech 1999; 32, 1149-1158.

71. Akhlaghi F, Daw J, Pepper M, Potter M. *In-shoe step-to-step pressure variations.* Foot. 1994; 4, 62-68.

72. Robertson K, Delbridge L. *A comparison and classification of forefoot pressures in young and middle aged adults using a pedobarograph.* Chiropodist 1985; 40, 62-69.

73. Toshiaki T, Nobuya H, Masashi N, Toshikazu I, Shuichi I, Tohru I. *Analysis of toe pressures under the foot while dynamic standing on one foot in healthy subjects.* JOSPT 1996; 23, 3, 188-193.

74. Mann RA, Poppen NK, O'Konski M. *Amputation of the great toe: a clinical and biomechanical study.* Clin Orthop Rel Res 1987; 226, 192-205.

75. Steindler A. *The supinatory compensatory torsion of the forefoot in pes valgus.* J Bone Joint Surg 1929; 11, 272-276.

76. Olerud C. *The pronation capacity of the foot: its consequences for axial deformity after tibial shaft fractures.* Arch Orthop Trauma Surg 1985; 104, 303-306.

77. Meyers-Rice B, Sugars L, McPoil T, Cornwall MW. *Comparison of three methods for obtaining plantar pressures in nonpathologic subjects.* J Am Podiatr Med Assn 1994; 84, 10, 499-504.

78. Harrison AJ, Folland JP. *Investigation of gait protocols for plantar pressure measurement of non-pathological subjects using a dynamic pedobarograph.* Gait Posture. 1995; 6, 50-55.

79. Wearing SC, Urry S, Smeathers JE, Battistutta D. *A comparison of gait initiation and termination methods for obtaining plantar foot pressures.* Gait Posture 1999; 10, 255-263.

80. Nicholson DE, Armstrong PF, MacWilliams BA, Terry S, Porter J, Miller ML. *The effects of velocity, step initiation and a visible platform on plantar pressures of healthy children (abstract).* Gait Posture. 1998; 7, 146.

81. Patla AE, Adkin A, Martin C, Holden R, Prentice S. *Characteristics of voluntary visual sampling of the environment during locomotion over different terrains.* Experimental Brain Research 1996; 112, 513-522.

82. Patla AE, Robinson C, Samways M, Armstrong CJ. *Visual control of step length during overground locomotion: task specific modulation of the locomotor synergy.* J Experimental Psychology: Human perception and performance 1989; 15, 603-617.

83. Grabiner MD, Feuerbach JW, Lundin TM, Davis BL. *Visual guidance to force plates does not influence ground reaction force variability.* J Biomech 1995; 28, 1115-1117.

84. Martin PE, Marsh AP. *Step length and frequency effects on ground reaction forces during walking.* J Biomech 1992; 25, 1237-1239.

85. Wearing SC, Urry S, Smeathers JE. *The effect of visual targeting on ground reaction force and temperospatial parameters of gait.* Clinical Biomech 2000; 15, 583-591.

86. Hirokawa S. *Normal gait characteristics under temporal and distance constraints.* J Biomed Eng 1989; 11, 449-456.

87. Andriacchi TP, Ogle JA, Galante JO. *Walking speed as a basis for normal and abnormal gait measurements.* J Biomech 1977; 10, 261-268.

88. Stott JRR, Hutton WC, Stokes IAF. *Forces under the foot.* J Bone Joint Surg. 1973; 55-B, 2, 335-344.

89. Hughes J, Pratt L, Linge K, Clark P, Klenerman L. *Reliability of pressure measurements: the EMED F system.* Clin Biomech 1991; 6, 1, 14-18.

90. Zhu H, Wertsch JJ, Harris GF, Alba H. *Walking cadence effect on plantar pressures.* Arch Phys Med Rehabil 1995; 76, 1000-1005.

91. Drillis R. *Objective recording and biomechanics of pathological gait.* Annals NY Acad Sci 1958; 74, 86-109.

92. Zhu H, Wertsch JJ, Harris GF, Loftsgaarden JD, Price MB. *Foot pressure distribution during walking and shuffling.* Arch Phys Med Rehabil 1991; 72, 390-397.

93. Rosenbaum D, Hautmann S, Gold M, Claes L. *Effects of walking speed on plantar pressure patterns and hindfoot angular motion.* Gait Posture. 1994; 2, 3, 191-197.

94. Hennig EM, Rosenbaum D. *Pressure distribution patterns under the feet of children in comparison with adults.* Foot Ankle 1991; 11, 5, 306-311.

95. Maruyama H, Nagasaki H. *Temporal variability in the phase durations during treadmill walking.* Human Movement Science 1992; 11, 335-348.

96. Stehr M, Dietz HG, Morlock MM. *Clinical application of pressure distribution measurements during full gait.* European J Phys Med Rehab 1992; 2, S35.

97:59. Holmes GB, Timmerman L, Willits NH. *Practical considerations for the use of the pedobarograph.* Foot Ankle 1991; 12, 2, 105-108.

98:60. Gross TS, Bunch RP. *Measurement of discrete vertical in-shoe stress with piezoelectric transducers.* J Biomed Eng 1988; 10, 261-265.

99. Kernozeck TW, LaMott EE, Dankisak MJ. *Reliability of an in-shoe pressure measurement system during treadmill walking.* Foot Ankle 1996; 17, 4, 204-209.

100. Davis BL, Cothren RM, Quesada P, Hanson SB, Perry JE. *Frequency content of normal and diabetic plantar pressure profiles: implications for the selection of transducer sizes.* J Biomech 1996; 29, 7, 979-983.

101. Lord M. *Spatial resolution in plantar pressure measurement.* Med Eng Phys 1997; 19, 2, 140-144.

102. Betts RP, Franks CI, Duckworth T, Burke J. *Static and dynamic foot-pressure measurements in clinical orthopaedics.* J Med Biol Eng Computing. 1980; 18, 674-684.

103. Duckworth T, Betts RP, Franks CI, Burke MD. *The measurement of pressures under the foot.* Foot Ankle 1982; 3, 3, 130-141.

104. Cavanagh RP, Rodgers MM, Liboshi A. *Pressure distribution under symptom-free feet during barefoot standing.* Foot Ankle 1987; 7, 262-276.

105. Bennett PJ, Duplock LR. *Pressure distribution beneath the human foot.* J Am Podiatr Med Assoc 1993; 83, 674-678.

106. Hutton WC, Dhanendran M. *A study of the distribution of load under the normal foot during walking.* Int Orthop 1979; 3, 153-157.

107. Soames RW. *Foot pressure patterns during gait.* J Biomed Eng 1985; 7, 120-126.

108. Schaff PS, Cavanagh PR. *Shoes for the insensitive foot: the effect of a rocker bottom shoe modification on plantar pressure distribution.* Foot Ankle. 1990; 11, 3, 129-140.

109. Bransby-Zachary MAP, Stother IG, Wilkinson RW. *Peak pressures in the forefoot.* J Bone Joint Surg 1990; 72-B, 4, 718-721.

110. Rodgers MM *Pressure distribution in Mortons' foot structure.* Med Sci Sports Exerc 1989; 21, 23-28.

111. Rattanaprasert U, Smith R, Sullivan M, Gilleard W. *Three-dimensional kinematics of the forefoot rearfoot and leg without function of the tibialis posterior in comparison with normals during stance phase of walking.* Clin Biomech 1999; 14, 14-23.

112. Elftman H. *A cinematic study of the distribution of pressure in the human foot.* Anat Rec 1934; 59, 481-491.

113. Harris RI, Beath T. *Army Foot Survey.* National Research Council of Canada, Ottawa. 1947.

114. Miura M, Miyashita M, Matsui H, Sodeyama H.
*Photographic method of analysing the pressure distribution of the foot against the ground.* In: Nelson RC, Morehouse CA ed. Biomechanics IV. Baltimore: University Park Press 1974; 482-487.

115. Aritomi H, Morita M, Yonemoto K. *A simple method of measuring the footsole pressure in normal subjects using prescale pressure-detecting sheets.* J Biomech 1983; 16, 157-163.

116. Grieve DW, Rashdi T. *Pressures under normal feet in standing and walking as measured by foil pedobarography.* Ann Rheum Dis 1984; 43, 816-818.

117. Chodera J. Pedobaragragh - *Apparatus for visual display of pressures beneath contacting surfaces of irregular shapes.* CZS Patent No 10451430D. 1960.

118. Betts RP, Duckworth T. *A device for measuring plantar foot pressures under the sole of the foot.* Eng Med 1978; 7, 4, 223-228.

119. Betts RP, Duckworth T, Austin IG, Crocker SP, Moore S. *Critical light reflection at a plastic/glass interface and its application to foot pressure measurement.* J Med Eng Tech 1980; 4, 136-142.

120. Betts RP. *A simple grey-scale to colour converter.* J Med Eng Technol. 1979; 3, 31-34.

121. Arcan M, Brull A. *A fundamental characteristic of the human body and foot, the foot-ground pressure pattern.* J Biomech 1976; 9, 453-457.

122. Simkin A. *The dynamic vertical force distribution during level walking under normal and rheumatic feet.* Rheumatology and Rehabilitation 1981; 20, 88-97.

123. Simkin A, Stokes IAF. *Characterisation of the dynamic vertical force distribution under the foot.* Med Biol Eng & Comp 1982; 20, 12-18.

124. Cavanagh PR, Michiyoshi Ae. *A technique for the display of pressure distribution beneath the foot.* J Biomech 1980; 13, 69-75.

125. Arcan M, Brull MA. *An experimental approach to the contact problems between flexible and rigid bodies.* Mechanics Res Commun 1980; 7, 151-157.

126. Dhanendran M, Hutton WC, Paker Y. *The distribution of force under the human foot - an on-line measuring system.* Measurement and Control 1978; 261-264.

127. Manley MT, Solomon E. *The clinical assessment of the normal and abnormal foot during locomotion.* Prosthet Orthot Int 1979; 3, 103-110.

128. Stokes IAF, Stott JRR, Hutton WC. *Force distribution under the foot: A dynamic measuring system.* Biomed Eng 1974; 140-143.

129. Arvikar R, Seirig A. *Pressure distribution under the foot during static activities.* Eng in Med 1980; 2, 99-103.

130. Nicol K, Hennig EM. *Measurement of pressure distribution by means of a flexible, large surface mat.* In: Asmussen E, Jorgensen K ed. Biomechanics VI-A. Baltimore: University Park Press 1978; 374-380.

131. Hennig EM, Nicol K. *Registration methods for time-dependent pressure measurements with mats working as capacitors.* In: Asmussen E, Jorgensen K ed. Biomechanics VI-A. Baltimore: University Park Press 1978; 361-376.

132. Nicol K, Preiss R, Albert H. *Capacitance type force measuring system - methods and applications.* In: Morecki A, Fidelus K, Kedzior K, Wit A ed. Biomechanics VII-A. Baltimore: University Park Press 1981; 553-557.

133. Gerber, H. *A system for measuring dynamic pressure distribution under the human foot.* J Biomech 1982; 15, 225-227.

134. Aisslinger U, Preiss R, Nicol K. *Device for high resolution force distribution measurement.* In: Morecki A, Fidelus K, Kedzior K, Wit A ed. Biomechanics VII-A. Baltimore: University Park Press 1981; 548-552.

135. Cavanagh PR, Rodgers MM. *Pressure distribution underneath the human foot.* In: Perren SM, Schneider E ed. Biomechanics: Current interdisciplinary research. Boston: Martinus Nijhoff 1984; 85-95.

136. Janssen M, de Lange A, Bisschoff M. *Footsole pressure during walking.* Eur Soc of Biomech. 7th meeting.Aarhus, Denmark 1990; 33.

137. Mittlemeier Th, Fassler M, Lob G, Mutschler W, Bauer G. *Analysis of gait asymmetry in normals by dynamic pedography.* Eur Soc of Biomech. 7th meeting, Aarhus, Denmark 1990; 36.

138. Samnegard E, Turan I, Lanshammar H. *Postoperative pressure under the rheumatic feet.* J Foot Surg 1990; 29, 593-594.

139. Cavanagh PR, Hennig EM, Rodgers MM, Sanderson DJ. *The measurement of pressure distribution on the plantar surface of diabetic feet.* In: Whittle M, Harris D, ed. Biomechanical Measurement in Orthopaedic Practice. Oxford: Clarendon Press 1985; 159-166.

140. Plank MJ, Potter M. *The pattern of forefoot pressure distribution in hallux valgus.* Foot 1995; 5, 8-14.

141. Corrigan JP, Moore DP, Stephens MM. *Effect of heel height on forefoot loading.* Foot Ankle 1993; 14, 148-152.

142. Kaliszer M, O'Flanagan S, McCormack B, Mulhall J, Heavey A, Shehan J. *Setting the baseline parameters for clinical assessment of foot to ground contact using the Musgrave pressure plate system.* J Biomed Eng 1989; 11, 30-34

143. James WV, Orr JF, Huddleston T. *A load cell system in foot pressure analysis.* Eng in Med 1982; 11, 121-122.

144. Peruchon E, Jullian JM, Rabischong P. *Wearable unrestraining footprint analysis system. Applications to human gait study.* Med & Biol Eng & Comp 1989; 27, 557-565.

145. Chandrasekaran HJ. *On the Measurement of Average Foot Pressure and Ground Reactions During Walking.* Mech Design 1980; 102, 683-687.

146. Draganich LF, Andriachi TP, Strongwater AM, Galante JO. *Electronic measurement of instantaneous foot-floor contact patterns during gait* J Biomech 1980; 13, 875-880.

147. Macellari V, Giacomozzi C. *Multistep pressure platform as a stand alone system for gait analysis.* Med & Biol Eng & Comput 1996; 34, 299-304.1996

148. Giacomozzi C, Macellari V. *Piezo-dynamometric platform for a more complete analysis of foot-to-floor interaction.* IEEE Trans Rehabil Eng 1997; 5, 322-330.

149. PCT Patent: Publication No WO 91/09289 *Flexible tactile sensor for measuring foot pressure distribution and for gaskets.* 27 June 1991.

150. United States Patent: No 4,994,783 *Electronic device fabrication on non-conductive substrate.* 19 Feb 1991.

151. Rose NE, Feiwell LA, Cracchiolo A. *A method for measuring foot pressures using a high resolution, computerized insole sensor: The effect of heel wedges on plantar pressure distribution and centre of force.* Foot Ankle 1992; 13, 263-270.

152. Mueller M, Sinacore DR, Hoogstrate S, Daly L. *Hip and ankle walking strategies: effect on peak pressures and implications for neuropathic ulceration.* Arch Phys Med Rehabil 1994; 75, 1196-1200.

153. Mueller M. *Use of an in-shoe pressure measurement system in the management of patients with neuropathic ulcers or metatarsalgia.* JOSPT 1995; 21, 6, 328-336.

154. Pitie DL, Ison K, Edmonds ME, Lord M. *Time-dependent behaviour of a force-sensitive resistor plantar pressure measurement insole.* Proc Instn Mech Engrs. Part H, J Eng in Med 1996; 210, 121-125.

155. Zhu H, Wertsch JJ, Harris GF, Alba H, Price MB. *Sensate and insensate in-shoe plantar pressures.* Arch Phys Med Rehabil 1993; 74, 1362-1368.

156. Chang AH, Abu-Faraj ZU, Harris GF, Nery J. *Multistep measurement of plantar pressure alterations using metatarsal pads.* Foot Ankle 1994; 15, 12, 654-660.

157. Wertsch JJ, Frank LW, Zhu H, Price MB, Harris GF, Alba HM. *Plantar pressures with total contact casting.* J Rehabil Res Dev 1995; 32, 3, 205-209.

158. Ledoux WR, Song J, Hillstrom HJ, Secord D, Kugler F. *The static accuracy and repeatability of the Musgrave Footprint pressure plate system.* (Abstract). Gait Posture. 1995; 3, 93.

159. Orthotic Research & Locomotor Assessment Unit, Robert Jones & Agnes Hunt Orthopaedic Hospital, Oswestry, UK. *Annual Report* 1988; 14, 71-73.

160. Orthotic Research & Locomotor Assessment Unit, Robert Jones & Agnes Hunt Orthopaedic Hospital, Oswestry, UK. *Annual Report* 1990; 16, 33-38.

161. Borton DC, Stephens MM. *Basal metatarsal osteotomy for hallux valgus.* J Bone Joint Surg 1994; 76-B, 2, 204-209.

162. Woodburn J, Helliwell PS. *Observations on the F-Scan in-shoe pressure measuring system.* Clin Biomech 1996; 11, 301-304.

163. Mueller MJ, Strube MJ. *Generalizability of in-shoe peak pressure measures using the F-Scan system.* Clin Biomech 1996; 11, 3, 159-164.

164. Nicolopoulos CS, Anderson EG, Solomindis SE, Giamondis PV. *Evaluation of the gait analysis Fscan pressure system: clinical tool or toy?* Foot 2000; 10, 124-130.

165. Brown M, Rudicel S, Esquenazi A. *Measurement of dynamic pressures at the shoe-foot interface during normal walking with various foot orthoses using the Fscan system.* Foot Ankle. 1996; 17, 152-156.

166. Ahroni JH, Boyko EJ, Forsberg R. *Reliability of F-Scan In-shoe measurements of plantar pressure.* Foot Ankle. 1998; 19, 10, 668-673.

167. Antonsson EK, Mann RW. *The frequency content of gait.* J Biomech 1985; 18, 39-47

168. Archarya KR, Harris GF, Riedel SA, Kazarian L. *Force magnitude and spectral frequency content of heel strike during gait.* IEEE Eng Med & Biol 11th Ann Int Conf 1989; 826-827.

169. Nevill AJ, Pepper MG, Whiting M *In-shoe foot pressure measurement system utilising piezoelectric film transducers.* Med & Biol Eng & Comp 1995; 33, 76-81.

170. Zhu H, Harris GF, Wertsch JJ, Tompkins WJ, Webster JG. *A microprocessor based data acquisition system for measuring plantar pressures from ambulatory subjects.* IEEE Trans Biomed Eng 1991; 38, 7, 710-714.

171. Roark RJ, Young WC. 1989 *Roark's formulas for stress and strain.* 6th edition, McGraw Hill, London.

172. Benham PP, Warnock FV. 1984 *Mechanics of Solids and Structures* (ISBN 0 273 361910). Castigliano's Second Theorem (pp199).

173. Turner JD. *Instrumentation for engineers.* 1988 Macmillan Education (ISBN 0-333-47295-0).

174. Smith SW. *The scientist and engineer's guide to digital signal processing.*1997. California Technical Publishing (ISBN 0-9660176-4-1).

175 Bland JM, Altman DG. *Statistical methods for assessing agreement between two methods of clinical measurement.* Lancet 1986; Feb, 307-310.

176 Nicolopoulos CS, Solomonidis S, Anderson EG, Black JA. *In-shoe plantar pressure measurements for the diagnosis of different foot pathologies using FSR technology.* Foot Pressure Interest Group (UK) Newsletter 1996, 19-24.

177 Lord M, Hosein R. A study of in-shoe plantar shear in patients with diabetic neuropathy. 2000; 15, 278-283.

178 Giakas G, Baltzopoulos V. *Time and frequency domain analysis of ground reaction forces during walking: an investigation of variability and symmetry.* Gait Posture. 1997; 5; 189-197.

179 Chao EY, Laughman RK, Schneider E, Stauffer RN. *Normative data of knee joint motion and ground reaction forces in adult level walking.* J Biomechanics. 1983; 16, 229-233.

180 Gronquist R, Roine J, Jarvinen E, Korhonen E. *An apparatus and method for determining the slip resistance of shoes and floors by simulation of human foot motions.* Ergonomics. 1989; 32, 979-995.

181 Laing P, Deogan H, Cogley D, Crerand S, Hammond P, Klenerman L. *The development of the low profile Liverpool shear transducer.* Clin Phys Physiol Meas 1992; 13, 2, 115-124.

182 Lebar AM, Harris GF, Wertsch J, Zhu H. *An optoelectronic plantar "shear" sensing transducer: design validation and preliminary subject tests.* IEEE Trans Rehabil Eng 1996; 4, 4, 310-319.

183 Hosein R, Lord M. *A study of in-shoe plantar shear in normals.* Clin Biomech 2000; 15, 46-53.

184 Saunders JB, Inman VT, Eberhart HD. *The major determinants in normal and pathological gait.* J Bone Joint Surg 1953; 35A, 3, 543-558.

185 Hughes J, Clark P, Klenerman L. *The importance of the toes in walking.* J Bone Joint Surg 1990; 72B, 245-251.

186 Urry SR, Wearing SC. *A comparison of footprint indexes calculated from ink and electronic footprints.* J Am Podiatr Med Assoc 2001; 91, 4, 203-209.

187 University of Strathclyde, Bioengineering Unit. *Terminology CEC Programme AIM Project A-2002 CAMARC II.* University of Strathclyde Bioengineering Unit. UK. 1994, 12-16.

188 Macellari V, Giacomozzi C, Saggini R. *Spatial-temporal parameters of gait: reference data and a statistical method for normality assessment.* Gait & Posture. 1999, 10, 171-181.

189 Stolze H, Kuhtz-Buschbeck JP, Mondwurf C, Johnk K, Friege L. *Retest reliability of spatiotemporal gait parameters in children and adults.* Gait & Posture. 1998, 7, 125-130.

190 Opara C, Levangie PK, Nelson DL. *Effects of selected assistive devices on normal distance gait characteristics.* Phys Thera. 1985, 65, 8, 1188-1191.

191 Boenig D. *Evaluation of a clinical method of gait analysis.* Phys Thera. 1977, 57, 7, 795-798.

192 Boulton AJM, Hardisty CA, Betts RP. *Dynamic foot pressure and other studies as diagnostic and management aids in diabetic neuropathy.* Diabetes Care. 1983, 6, 26-33.

193 Veves A, Murray HJ, Young MJ, Boulton AJM. *The risk of foot ulceration in diabetic patients with high foot pressure: a prospective study.* Diabetologia. 1992, 35, 660-663.

194 Armstrong DG, Peters EJG, Athanasiou KA, Lavery L. *Is there a critical level of plantar foot pressure to identify patients at risk for neuropathic foot ulceration.* J Foot & Ankle Surgery. 1998, 37, 4, 303-307.

195 Lundeen S, Lundquist K, Cornwall MW, McPoil TG. *Plantar pressures during level walking compared with other ambulatory activities.* Foot & Ankle. 1994, 15, 6, 324-328.

196 Cavanagh PR, Ulbrecht JS. *Clinical plantar pressure measurement in diabetes: rationale and methodology.* The Foot. 1994, 4, 123-135.

197 Fernando DJS, Masson EA, Veves A, Boulton AJM. *Relationship of limited joint mobility to abnormal foot pressures and diabetic ulceration.* Diabetes Care. 1991, 14, 8-11.

198 Hutton WC, Dhanendran M. *The mechanics of normal and hallux valgus feet - a quantitative study.* Clinic Orthopaedics and Related Research. 1981, 157, 7-13.

199 Rose GK, Welton EA, Marshall T. *The diagnosis of flatfoot in the child.* J Bone Joint Surg 1985; 67B, 71-78.

200 Volpon JB. *Footprint analysis during the growth period.* J Paediatr Orthoped 1994; 14, 83-85.

201 Forriol F, Pascual J. *Footprint analysis between three and seventeen years of age.* Foot Ankle 1990; 11, 101-104.

202 Welton EA. *The Harris and Beath footprint: interpretation and clinical value.* Foot Ankle 1992; 13, 462-468.

203 Hawes MR, Nachbauer W, Sovak D. *Footprint parameters as a measure of arch height.* Foot Ankle 1992; 13: 22-26.

204 McPoil TG, Cornwall MW. *Use of medial longitudinal arch height to predict plantar surface contact area during walking (Abstract).* J Orthop Sports Phys Ther 2000; 30, A29-30.

205 Bojsen-Moller F. *Calcaneo-cuboid joint stability of the longitudinal arch of the foot at high and low gear push off.* J Anat 1979; 129, 165-176.

206 Kelly VE, Mueller MJ, Sinacore DR. *Timing of peak plantar pressure during the stance phase of walking.* J Amer Podiatr Med Assoc. 2000, 90, 1, 18-23.

# 9. **Appendix I** Proving ring design

**Design of the proving ring**

The design details for the proving ring transducer are given in figures A1 and A2 and the accompanying formulae over the following pages. The ring formulae were based on the following assumptions:

- The ring is of uniform cross section
- It is of such large radius in comparison with its radial thickness that the deflection theory for straight beams is applicable (R > 10 x thickness).
- It is nowhere stressed beyond its elastic limit.
- It is not so severely deformed as to lose its essentially circular shape.
- Its deflection is due primarily to bending with no axial stress or transverse shear deformation.

The notation used in the diagrams and formulae are given in the following table.

Notation used in proving ring design formulae and diagrams.

| Symbol | Definition | SI units |
|---|---|---|
| e | normal strain at the surface | - |
| s | normal stress | - |
| W | load applied | N |
| R | radius of ring to neutral plane | m |
| y | distance from neutral plane | m |
| a | width of ring | m |
| b | thickness of ring | m |
| I | second moment of area | - |
| M | bending moment | - |
| E | modulus of elasticity | $Nm^{-2}$ |

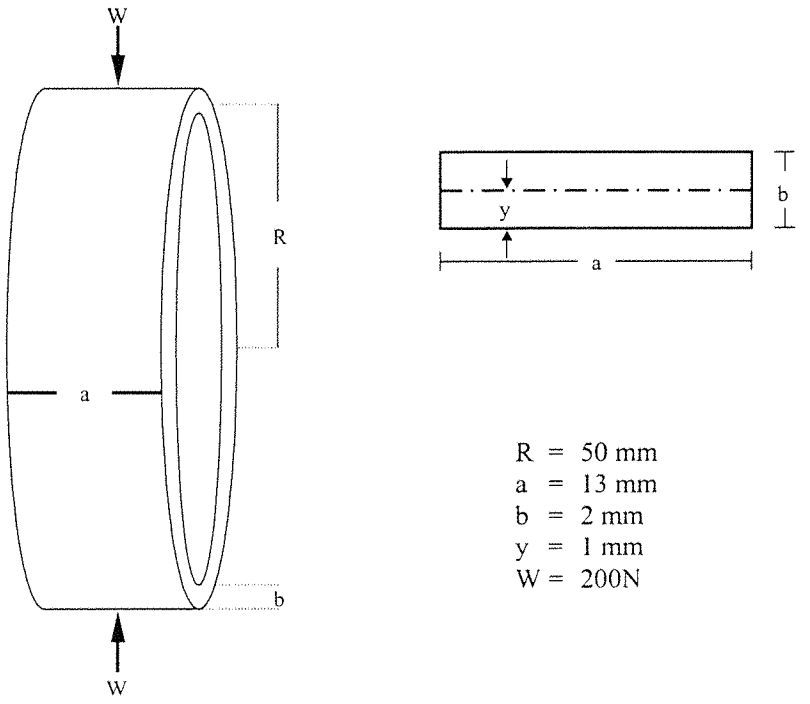


**Figure A1 Proving ring dimensions.**

Main image shows general dimensions, radius = 50 mm. Inset shows cross-section through the ring wall, with the neutral plane indicated at the midpoint.

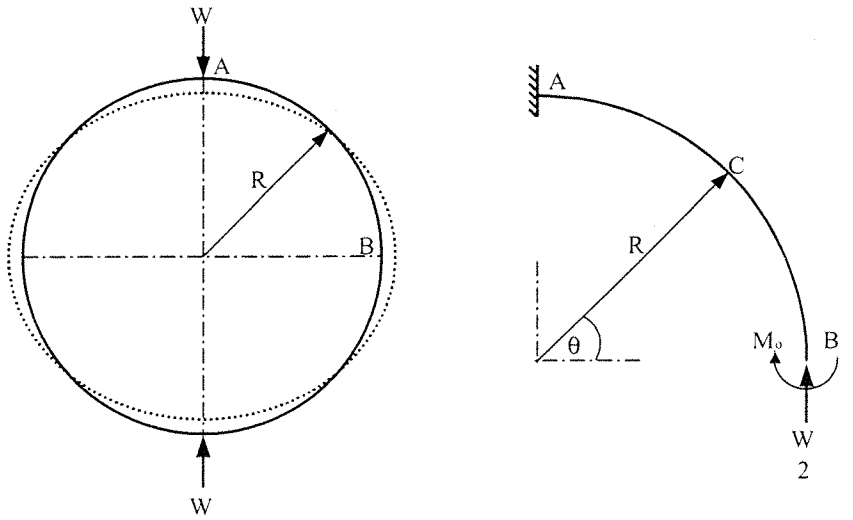


**Figure A2 Deflection of proving ring under load.**

Surface strain derived for point c, in accordance with Castigliano's second theorem.

(Referring to figure A2, point c is the horizontal diameter when cosθ=0)

Where, $M_C$ = Bending moment at point c

$$Mc = WR\left(\frac{1}{2}\cos\theta - \frac{1}{\pi}\right) \qquad \text{(A.1)}$$

and

$$\frac{M}{I} = \frac{\sigma}{y} = \frac{E}{R} \qquad \text{(A.2)}$$

To find the normal strain ε

$$\varepsilon = \frac{\sigma}{E} \qquad \text{(A.3)}$$

from equation A.2

$$M = \frac{I\sigma}{y}$$

and from equation A.3

$$\sigma = E\varepsilon$$

$$\therefore M = \frac{IE\varepsilon}{y}$$

by substitution into equation A.1

$$\frac{IE\varepsilon}{y} = WR\left(\frac{1}{2}\cos\theta - \frac{1}{\pi}\right)$$

thus,

$$\varepsilon = \frac{WRy}{IE}\left(\frac{1}{2}\cos\theta - \frac{1}{\pi}\right) \qquad \text{(A.4)}$$

Second moment of area for the proving ring section

(referring to figure A1, cross-section through the proving ring wall)

$$I = \frac{ab^3}{12}$$

If the surface strain is required then

$$y = \frac{b}{2}$$

By substitution into equation A.4

$$\varepsilon = \frac{WRy}{IE}\left(\frac{1}{2}\cos\theta - \frac{1}{\pi}\right)$$

$$= \frac{WR\left(b/2\right)}{\left(ab^3/12\right)E}\left(\frac{1}{2}\cos\theta - \frac{1}{\pi}\right)$$

$$= \frac{6WR}{ab^2E}\left(\frac{1}{2}\cos\theta - \frac{1}{\pi}\right) \qquad \text{(A.5)}$$

Referring to figure A2, the surface strain at the horizontal diameter for a rectangular section ring where $\theta = 0°$, $\cos\theta = 1$,

$$\varepsilon = \frac{6WR}{ab^2E}\left(\frac{1}{2} - \frac{1}{\pi}\right)$$

Then

$$\varepsilon = \frac{6WR}{ab^2E}\left(\frac{1}{2} - \frac{1}{\pi}\right)$$

$$= \frac{6 \times 200 \times 50 \times 10^{-3}}{13 \times 10^{-3} \times \left(2 \times 10^{-3}\right)^2 \times 210 \times 10^9}\left(\frac{1}{2} - \frac{1}{\pi}\right)$$

$\therefore \varepsilon = 998 \times 10^{-6}$ Thus, a 200N load will give approximately 1000με

Natural frequency of the proving ring

Although the design was optimised for sensitivity, it was also necessary to consider the dynamic characteristics of the ring-anvil combination in order to ensure that its natural frequency would be removed from the desired test frequency of 30 Hz. A simple spring-mass model was adopted in order to obtain an estimate of the natural frequency for vertical oscillations.

The natural frequency was determined from,

$$f_n = \frac{1}{2\pi}\sqrt{\frac{k}{m}}$$

it was necessary, therefore, to establish an estimate for *k*, the spring stiffness, and this was achieved by calculating the deflection of the ring. A closed circular ring may be regarded as a statically indeterminate beam and analysed as such by the use of Castigliano's first theorem. In this way, the deflection of the ring under load may be estimated, figure A2.

$$D_H = \frac{WR^3}{EI}\left(\frac{2}{\pi} - \frac{1}{2}\right)$$

Where $D_H$ = horizontal diameter change

For a mild steel proving ring with the dimensions given in figure A1,

$$D_H = \frac{200 \times \left(50 \times 10^{-3}\right)^3}{210 \times 10^9 \times 8.67 \times 10^{-12}}\left(\frac{2}{\pi} - \frac{1}{2}\right)$$

$$= 1.88 \times 10^{-3} \text{ m}$$

Therefore, the ring will deflect approximately 2 mm under a load of 200N.

Considering the ring as a linear spring [171], an estimate of stiffness $k$ was derived.

Spring stiffness,

$$k = \frac{F_2 - F_1}{e_2 - e_1}$$

$$= \frac{200 - 0}{1.88 \times 10^{-3} - 0}$$

$$\approx 107 \text{ kNm}^{-1}$$

Natural frequency (Hz)

$$f_n = \frac{1}{2\pi}\sqrt{\frac{k}{m}}$$

$$\approx \frac{1}{2\pi}\sqrt{\frac{107\times10^{3}}{150\times10^{-3}}}$$

$$\approx 134 \text{ Hz}$$

The first estimate of the natural frequency (≈134 Hz) is considerably removed from the chosen test frequency of 30 Hz, being 4-5 orders of magnitude greater. However, the mass of the spring would be an influencing factor and a second estimate was derived on the assumption that half of the mass of the spring would contribute to the overall mass of the system. In this case the natural frequency was estimated as 80 Hz and was still well removed from the test frequency.

Instrumentation of the proving ring

Four foil strain gauges (type: RS 308-102), with a gauge factor of 2.1, were bonded to the ring; two along the central line of the inner surface and two more similarly positioned on the outer surface. All four gauges were centrally located about the horizontal diameter. The gauges were incorporated into a full Wheatstone bridge resistive circuit to maximise the sensitivity to strain while minimising the sensitivity to temperature variation. The selected gauges were temperature compensated for mild steel (coefficient of expansion 10.8 x $10^{-6}/^{o}C$). Amplification was through a purpose designed, low noise, low drift linear strain gauge amplifier (model: RS 308-815). All interconnecting leads were screened, as was the amplifier casing, to minimise electrical interference, and a full-length compensation lead was included.

# 10. Appendix II Documentation

(Informed consent and volunteers information)

**UNIVERSITY RESEARCH ETHICS COMMITTEE**

Mr Stephen Urry
School of Public Health
QUT Kelvin Grove

8 September, 1997

Dear Mr Urry

I wish to advise that the University Research Ethics Committee has granted ethical approval for the human experimentation proposed in the project "The influence of slope angle on pressure distribution beneath the human foot" (Ref No QUT 1271H). This approval is subject to amendments to the consent form and information package, as indicated on the attached copy.

Please provide me with the revisions/additional information outlined above by 23 September 1997. Failure to submit this information by the date specified will result in withdrawal of approval for the project.

This approval is valid for the duration of the project or three years, whichever is earlier, commencing from 29 October 1997.

Please note the following conditions of approval:

- any departure from the protocol detailed in your application must be reported immediately to the Committee;
- you are required to advise the Secretary if any complaints are made, or expressions of concern raised, in relation to the project;
- you are required to report on the progress of the approved project at least annually, or at intervals determined by the Committee. The Committee may also choose to conduct a random audit of your research;
- where a minor change to an approved protocol is proposed, you are required to submit a request for approval of this change in writing to the Secretary. Minor changes will be assessed on a case by case basis and interim approval may be granted subject to ratification at the next meeting of the Committee; and
- major changes to any approved protocol require a new application to be submitted and approved by the University Research Ethics Committee.

Yours sincerely

**Gary Allen**
Secretary, University Research Ethics Committee
QUT Secretariat
Telephone: (07) 3864 2902
Facsimile: (07) 3864 1818
Email:gx.allen@qut.edu.au

cc Assoc Prof Donald E Stewart, School of Public Health, QUT Kelvin Grove

\falcon\1997comm\be\merge\condhum.sep

# Consent Form for Participation in a Foot Pressure Study

**Chief Investigator:** Stephen URRY, School of Public Health (Podiatry)
3864 5649 (office), 3864 5652 (reception), 3864 5628 (fax)

**Project Title:** The influence of slope angle on pressure distribution beneath the human foot.

Thank you for considering to participate in this research project.

This project is part of some research being undertaken by myself, Stephen Urry, a lecturer at QUT, as part of my PhD degree. The project hopes to show that high pressures can occur under a foot whenever someone walks over a sloping surface. High pressures can cause many painful foot conditions and, if this work is successful, then it will be possible to undertake similar studies in order to improve the care of patients.

If you agree to participate then you will be asked to walk barefoot along a short walkway (about ten steps) while the pressure is automatically measured beneath your feet - you will be unaware of the measurement. Once the pressures have been recorded you will be asked to stand clear of the walkway while it is adjusted. The walkway will be tilted sideways a very small amount (2°) and you will then be asked to walk along it again. This entire routine will be repeated three more times, until the walkway is tilted 8°, and will take about half an hour.

Before you are allowed on the walkway I will quickly check your balance and co-ordination. This is important because, although the tilt is very small, there could be a possibility of stumbling especially if you have balance problems. The walkway is tilted towards a hand rail so that you can reach for some support if you need to, it will also prevent any major fall. I will watch and advise you through the entire session and you may decide to stop at any stage if you wish. If you decide not to continue you may still return to the Podiatry clinic at any time in the future without comment orpenalty.

All records from this study will be kept in strict confidence. No personal information about you will be released. You may ask questions about the project at any stage. Furthermore, if you have any concerns about the ethical conduct of this project, you can also contact the QUT Ethics Committee ( 3864 2902 ) if you wish. You may have feedback about the general findings from the project once it has been completed, if you want to know the outcomes.

Thank you for taking the time to read this information and, hopefully, agreeing to take part in the study.

## Consent Form for Participation in a Foot Pressure Study

**Chief Investigator:** Stephen URRY, School of Public Health (Podiatry)
3864 5649 (office), 3864 5652 (reception), 3864 5628 (fax)

**Project Title:** The influence of slope angle on pressure distribution beneath the human foot.

1. I have had the purpose of the study explained to me;
2. I have had my questions in relation to the study answered;
3. I understand the risks involved in this study;
4. I understand that I am free to withdraw at any time without comment or penalty;
5. I understand that all records will be kept in the strictest confidence; and
6. I am willing to participate in the study.

**Signatures:**

..... .....
Chief investigator Date

..... .....
Participant Date

**NB** A signed copy of this statement should be kept by the participant.

# 11. **Appendix III** Program listing

Program listing (abridged) written in Visual Basic for Microsoft Excel (97-SR2) spreadsheet.

```
'*******************************************************************************
'                              DoFileTest()
'This module formats three spreadsheets within a workbook (RawDataSheet, MainSheet and ResultSheet).
'Each sheet is cleared of all data and then columns and rows are labeled appropriately. Parts of the
'MainSheet are reserved for storage of the addresses of anatomical regions when the mask ordinates are
'input. On completion of the set-up, the user is prompted to paste the data file into the RawDataSheet for
'analysis.
'*******************************************************************************
Sub DoFileTest()
   SetUpSheets
   ImportRawData
End Sub
Sub ImportRawData()
   Sheets("RawData").Select
   MsgBox ("Select data file for analysis then cut and paste into RawDataSheet")
   Range("A1").Select
End Sub

'*******************************************************************************
'                              CrunchData()
'This module processes the datafile by transferring a single scan from the RawDataSheet to the MainSheet
'where the appropriate parameters are extracted or computed and temporarily stored. When all parameters
'from the single scan are available, they are transferred to the ResultSheet for storage. The procedure
'GetArray repeats the extraction for each consecutive scan (upto Max_Scans) in the export file. At the start
'of the module, the appropriate masking coordinates are input to define the anatomical regions.
'*******************************************************************************
Dim Array_Row_Size
Dim Array_Col_Size
Dim Max_Scans
Dim Scan_Size As Object
  Sub CrunchData()
   GetValues
   Areas
   ClearOut Array_Row_Size, Array_Col_Size, Max_Scans
   GetArray Array_Row_Size, Array_Col_Size, Max_Scans
   Summary_Results
End Sub

'*******************************************************************************
'                              GetValues()
'This procedure prompts for input of the number of rows and columns as determined by the size
'of the footprint. It also requests the number of scans contained in the export data file.
'*******************************************************************************
Sub GetValues()
   Sheets("RawData").Select
   Array_Row_Size = Application.InputBox(Prompt:="How many ROWS of DATA in each scan?",
                                         Type:=1)
   Array_Col_Size = Application.InputBox(Prompt:="How many COLUMNS of DATA in each scan?",
                                         Type:=1)
   Max_Scans = Application.InputBox(Prompt:="How many SCANS of data?", Type:=1
End Sub

'*******************************************************************************
'                              Areas()
'This procedure prompts for the ordinates of each of the regions defined by the mask. The addresses are then
'stored on the MainSheet for use by other procedures.
'*******************************************************************************
Sub Areas()
Dim countup As Integer
Dim HL As String                                    Repeat for other sites
Dim Heel As Object
Sheets("MainSheet").Select

Set Heel = Application.InputBox(Prompt:="Heel? eg. A1:F17", Type:=8)
```

```
Let HL = Heel.Address(rowAbsolute:=False, columnAbsolute:=False)
Cells(86, 3).Value = HL
Cells(87, 3).Value = Heel.Column                                    Repeat for other sites
Cells(88, 3).Value = Heel.Columns(Heel.Columns.Count).Column
Cells(89, 3).Value = Heel.Row
Cells(90, 3).Value = Heel.Rows(Heel.Rows.Count).Row
Cells(77, 3).Formula = "=SUM(" & HL & ")"
Cells(79, 3).Formula = "=MAX(" & HL & ")"
End Sub

*******************************************************************************************
                                        ClearOut()
This procedure removes the extraneous material (separaters) from the export data file.
*******************************************************************************************
Sub ClearOut(Array_Row_Size, Array_Col_Size, Max_Scans)
Dim Row_Num
Dim Scan_Num
Dim ClearOut_Count
   Sheets("RawData").Select
   Range(Cells(1, 1), Cells(6, Array_Col_Size)).Delete (xlUp)
   For ClearOut_Count = 1 To (Max_Scans - 1)
   Let Row_Num = (ClearOut_Count * Array_Row_Size + 1)
   Range(Cells(Row_Num, 1), Cells(Row_Num + 3, Array_Col_Size)).Delete (xlUp)
   Next ClearOut_Count
   Range("A1").Select
End Sub

*******************************************************************************************
                                        GetArray()
This procedure cuts one scan from the export data file, pastes it into the MainSheet, and extracts output
values.The procedure loops until all scans (Max_Scans) are processed.
*******************************************************************************************
Sub GetArray(Array_Row_Size, Array_Col_Size, Max_Scans)
Dim Scan_Num
Dim Row_Num
Dim Col_Num
Dim Counter
Dim Total_Force

Dim Heel_F As String                                                Repeat for other sites

   Let Counter = 0
   For Scan_Num = 1 To Max_Scans

         'This loop selects one scan of data from the RawData file. The regions are defined according to
the      mask coordinates The procedure then derives the following parameters:
         'Contact area (derived from "Calculate_Areas" procedure)
         'Force (as sum of values in each region)
          'Peak Pressure (as maximum value in each region)

   Sheets("RawData").Select
   ActiveSheet.Range(Cells(1, 1), Cells(Array_Row_Size, Array_Col_Size)).Copy
   Sheets("MainSheet").Select
   Range("A1").Select
   ActiveSheet.Paste
   Sheets("RawData").Select
   ActiveSheet.Range(Cells(1, 1), Cells(Array_Row_Size, Array_Col_Size)).Delete (xlUp)
   Calculate_Areas
   Worksheets(2).Cells(4 + Scan_Num, 1).Value = Scan_Num

   Let Heel_Force = Cells(81, 3)                                    Repeat for other sites
   Worksheets(2).Cells(4 + Scan_Num, 16).Value = Heel_Force
   Worksheets(2).Cells(4 + Scan_Num, 30).Value = Worksheets(1).Cells(82, 3)
   Worksheets(2).Cells(4 + Scan_Num, 44).Value = Worksheets(1).Cells(76, 3)

   Let Counter = Counter + 1
   Next Scan_Num
```

```
  Sheets("ResultSheet").Select
End Sub

**********************************************************************************
                        Calculate_Areas()
'This procedure determines the area of contact for each region. The variable countup, returns a count of all
non-zero (ie. active) cells within the appropriate part of the mask. The contact area is then determined as
the product countup * Sensor_Area
**********************************************************************************
Sub Calculate_Areas()
Sheets("MainSheet").Select
  Dim Sensor_Area
  Let Sensor_Area = 0.3

  Let Hl_A = Cells(86, 3)                                    Repeat for other sites
  Set Hl_V = Range(Hl_A)

  Application.Calculation = xlManual
  Let countup = 0

    For Each C In Hl_V                                       Repeat for other sites
    If C.Value > 0 Then
    Let countup = countup + 1
    End If
    Next
  Cells(76, 3).Value = countup * Sensor_Area

   Worksheets("MainSheet").Calculate
   Application.Calculation = xlAutomatic
End Sub

**********************************************************************************
                        Summary_Results()
This is a data reduction module. The ResultSheet data are processed initially to derive average pressure
values for each region. The summary values, for statistical use, are copied automatically for archiving.
**********************************************************************************

**********************************************************************************
                        Average_Pressure()
This procedure uses the ResultSheet data to calculate the average pressure for each region. The average
pressure is derived from the force and contact area values on a scan by scan basis.
**********************************************************************************
Sub Average_Pressure()
Dim Col1
Dim Col2
Dim Col_Out_Put
Dim Row
Dim Force_Val
Dim Area_Val
Dim Av_Pressure

Sheets("ResultSheet").Select
Let Col1 = 0
Let Col2 = 0
Let Col_Out_Put = 0
Let Col1 = 16
Let Col2 = 44
Let Col_Out_Put = 58
For Row = 5 To 50
Let Force_Val = Cells(Row, Col1)
Let Area_Val = Cells(Row, Col2)
  If Area_Val > 0 Then
    Let Av_Pressure = (Force_Val / Area_Val)
    Cells(Row, Col_Out_Put).Value = Av_Pressure
    Else
    Cells(Row, Col_Out_Put).Value = 0
  End If
```

```
Next Row
End Sub

*******************************************************************************************
                                    Timing_Parameters()
'This is a data reduction module. The ResultSheet data are processed to derive timing parameter values for
each region. The summary values, for statistical use, are copied automatically for archiving.
*******************************************************************************************
Dim Max_Scans
Dim Column_num
Sub Timing_Parameters()
Let Row_Num = 5
   Max_Scans = Application.InputBox(Prompt:="How many SCANS of data?", Type:=1)
   Application.ScreenUpdating = False
   For Column_num = 15 To 27
      Initial_contact
      Contact_duration
      Time_to_Peak_val
   Next Column_num
   For Column_num = 29 To 41
      Time_to_Peak_val
   Next Column_num
   Application.ScreenUpdating = True
   Get_Times
End Sub


*******************************************************************************************
                                    Initial_contact()
'This procedure loops until the first non-zero value is identified. The respective scan is used to calculate the
time of initial contact as a percentage of the stance phase (Max_Scans).
*******************************************************************************************
Sub Initial_contact()
   Let I_C_Time = 0
   Let Local_counter = 0
   Let Set_flag = 0
   Let Get_values = 0
   Let Row_Num = 5
   Do
   Let Get_values = Cells(Row_Num, Column_num)
   Let Row_Num = Row_Num + 1
   If Get_values > 0 Then
   I_C_Time = ((Row_Num - 6) / Max_Scans * 100)
   Cells(55, Column_num).Value = I_C_Time
   Set_flag = 1
   Else I_C_Time = 0
   End If
   Loop Until Set_flag = 1
End Sub

*******************************************************************************************
                                    Contact_duration()
'This procedure counts the non-zero values and calculates the duration of loading as a percentage of the
stance phase (Max_Scans).
*******************************************************************************************
Sub Contact_duration()
   Let Cont_dur_time = 0
   Let Local_counter = 0
   Let Get_value = 0
   Let Row_Num = 5
   For Row_Num = 5 To (Max_Scans + 4)
   Let Get_value = Cells(Row_Num, Column_num)
   If Get_value > 0 Then
   Local_counter = Local_counter + 1
   End If

   Next Row_Num
```

```
   Cont_dur_time = (Local_counter / Max_Scans * 100)
   Cells(56, Column_num).Value = Cont_dur_time
End Sub

*******************************************************************************************
                                    Time_to_Peak_val()
'This procedure identifies the first occurence of a maximum value by using a moving baseline as a
reference, and calculates the time of the peak as a percentage of the stance phase (Max_Scans).
*******************************************************************************************
Sub Time_to_Peak_val()
   Let Peak_val_time = 0
   Let Temp_num = 0
   Let Get_value = 0
   Let Base_line = 0
   Let Row_Num = 5
   For Row_Num = 5 To (Max_Scans + 4)
   Let Get_value = Cells(Row_Num, Column_num)
   If Get_value > Base_line Then
   Let Temp_num = Row_Num
   Let Base_line = Get_value
   End If
   Next Row_Num
   Peak_val_time = ((Temp_num - 4.5) / Max_Scans * 100)
   Cells(57, Column_num).Value = Peak_val_time
End Sub
```

# 12. **Appendix IV** Publications

The following published papers were included in the bound thesis. These have not been digitised due to copyright restrictions, but their doi are provided.

Urry, S., 1999. Plantar pressure-measurement sensors. Measurement Science and Technology, 10(1), pp.R16–R32. Available at: http://dx.doi.org/10.1088/0957-0233/10/1/017.

Urry, S.R. & Wearing, S.C., 2001. A Comparison of Footprint Indexes Calculated from Ink and Electronic Footprints. Journal of the American Podiatric Medical Association, 91(4), pp.203–209. Available at: http://dx.doi.org/10.7547/87507315-91-4-203.

Urry, S.R. & Wearing, S.C., 2001. The accuracy of footprint contact area measurements: relevance to the design and performance of pressure platforms. The Foot, 11(3), pp.151–157. Available at: http://dx.doi.org/10.1054/foot.2001.0684.